

**On the role of
sugar compartmentation and stachyose
synthesis in symplastic
phloem loading**

Dissertation
zur Erlangung des Doktorgrades
der Mathematisch-Naturwissenschaftlichen Fakultäten
der Georg-August-Universität zu Göttingen

Vorgelegt von
Olga Vladimirovna Voitsekhovskaja
aus St.-Petersburg, Rußland

Göttingen 2001

D7

Referentin: PD Dr. Gertrud Lohaus

Koreferent: Prof. Dr. Hans-Walter Heldt

Tag der mündlichen Prüfung: 30.01.2002

Content

1. Introduction	1
1.1. Types of companion cells in minor vein phloem.....	2
1.2. Symplastic (dis)continuity between mesophyll and phloem	3
1.3. Apoplastic phloem loading mode.....	4
1.4. Symplastic phloem loading mode	5
1.5. Relationship between companion cell types and the types of translocated sugars	7
1.6. The polymerization trap model and the role of stachyose synthesis in symplastic phloem loading.....	10
1.7. The aim of this thesis and the choice and characterization of model plants.	12
1.7.1. The aim of this thesis	12
1.7.2. Phloem sap composition and characterization of minor vein anatomy in two related species, <i>Alonsoa meridionalis</i> and <i>Asarina barclaiana</i>	12
1.7.3. Choice of the model plants	15
2. Materials and Methods	17
2.1. Materials	17
2.1.1. Biochemicals	17
2.1.2. Enzymes used in molecular biology	18
2.1.3. Kits	18
2.2. Growth conditions	19
2.2.1. Plants	19
2.2.2. Bacteria	20
2.2.3. Plasmids	22
2.3. Extraction of metabolites	23
2.3.1. Chloroform:methanol extraction	23
2.3.2. Isolation of galactinol and antirrhinoside from plant material	24
2.3.2.1. Preparative isolation of galactinol	24
2.3.2.2. Preparative isolation and confirmation of the chemical structure of antirrhinoside.....	25
2.4. Extraction of apoplastic sap (intercellular washing fluid)	26
2.5. Determination of enzyme activities	26
2.5.1. Glucose-6-phosphate dehydrogenase (G6PDH)	27
2.5.2. NADP-dependent Glyceraldehyde 3-phosphate dehydrogenase (GAPDH)	27
2.5.3. Phosphoenolpyruvate carboxylase (PEPCx)	28
2.5.4. α-Mannosidase	28
2.5.5. Malate dehydrogenase	28

2.5.6 Stachyose synthase activity assays.....	29
2.5.6.1 Establishment of the <i>AmSTS</i> activity assay using leaves of <i>Alonsoa</i>	29
2.5.6.2 <i>AmSTS</i> activity assay in protein extracts of <i>E. coli</i> BL21 (DE3) (pET*/STS)	30
2.6 Non-aqueous fractionation of leaves	30
2.6.1. Preparation of leaf material.....	30
2.6.2. Non-aqueous fractionation of leaf tissue in a density gradient.....	30
2.6.3. Determination of the activities of marker enzymes in the gradient fractions.....	32
2.6.4. Determination of metabolite concentrations in the gradient fractions	32
2.6.5. Calculation of the subcellular distribution of metabolites	32
2.6.6. Determination of the chlorophyll:protein ratio.....	33
2.7. Protein determination	34
2.8. Sugar analysis	34
2.8.1. HPLC.....	34
2.8.2. Enzymatic measurements of glucose, fructose and sucrose	35
2.9. Determination of the osmolality of the leaf sap	36
2.10. Analyses in single cell sap	36
2.10.1. Single cell sampling.....	36
2.10.2. Osmolality of single cell sap	37
2.10.3. Sugar concentrations in single cell sap.....	37
2.11. Inhibition of phloem translocation	39
2.12. Study of sugar uptake from the apoplast in vivo.....	39
2.12.1. Feeding experiments	39
2.12.2. Gas and H ₂ O exchange measurements.....	40
2.12.3. Recordings of pH- and membrane potential changes.....	40
2.13. Electron microscopy and determination of partial volumina of subcellular compartments.....	41
2.14. Light microscopy.....	43
2.15. Isolation of total RNA and genomic DNA from plant tissues	45
2.15.1. Isolation of RNA from <i>Asarina</i> and <i>Alonsoa</i>	45
2.15.2. Isolation of genomic DNA from <i>Alonsoa</i>	46
2.15.3. Isolation of DNA from <i>Arabidopsis thaliana</i> F1 transformants	46
2.16. Plasmid DNA isolation from bacteria	47
2.16.1. Isolation of plasmid DNA from <i>E. coli</i> (miniprep and maxiprep).....	47
2.16.1.1. Plasmid DNA miniprep isolation using a triton boiling protocol	48
2.16.1.2. Plasmid DNA miniprep isolation with the Qiagen Miniprep Kit	48
2.16.1.3. Plasmid DNA maxiprep isolation with E.Z.N.A. Plasmid Miniprep Kit.....	48
2.16.2. Isolation of plasmid DNA from <i>Agrobacterium tumefaciens</i>	49
2.17. Determination of RNA and DNA concentration by spectrophotometry .	49
2.18. Purification and precipitation of DNA and RNA.....	50
2.19. Agarose gel electrophoresis of DNA and RNA	50

2.19.1. Separation of DNA	50
2.19.2. DNA gel blots (Southern blots).....	51
2.19.3. Separation of RNA	52
2.19.4. RNA gel blot (Northern blot).....	53
2.19.5. Hybridization of DNA and RNA gel blots.....	54
2.19.5.1. Labelling of probes.....	54
2.19.5.2. Hybridization and washing of blots.....	54
2.20. Gene cloning	55
2.20.1. Elution of DNA fragments from agarose gels	56
2.20.2. Filling of 5' overhanging ends with Klenow polymerase.....	56
2.20.3. Ligation.....	56
2.20.4. Preparation of competent cells of <i>E. coli</i> strains DH5 α and BL21 (DE3).....	56
2.20.4.1. Competent cells of DH5 α	57
2.20.4.2. Competent cells of BL21 (DE3).....	58
2.20.5. Transformation of <i>E. coli</i>	58
2.20.6. Bacterial glycerol cultures	59
2.21. Amplification of DNA by the polymerase chain reaction (PCR).....	59
2.21.1. Design of specific and degenerate primers.....	59
2.21.2. cDNA synthesis and Rapid Amplification of cDNA Ends (RACE)	60
2.21.2.1. cDNA synthesis	60
2.21.2.2. 3' RACE	61
2.21.2.3. 5' RACE	61
2.21.3. Amplification and cloning of the <i>AmSTS</i> full length cDNA	63
2.21.4. Amplification of a promoter fragment by Genome Walker DNA walking.....	63
2.21.5. Colony PCR.....	64
2.22. Expression of <i>AmSTS</i> in <i>E. coli</i> using pET expression system	65
2.22.1. Transformation of <i>E. coli</i> BL21 (DE3)	65
2.22.2. Induction of the expression of the transgene using IPTG.....	65
2.23. SDS - PAGE.....	66
2.23.1. Protein extraction from <i>E. coli</i> cells.....	66
2.23.2. SDS-Polyacrylamide gel electrophoresis	66
2.23.3. Coomassie staining of the gels	67
2.24. Promoter-GUS fusions in transgenic plants.....	68
2.24.1. Preparation of competent <i>Agrobacterium tumefaciens</i> GV3101 cells	68
2.24.2. Transformation of <i>Agrobacterium tumefaciens</i> by electroporation	68
2.24.3. Transformation of <i>Arabidopsis thaliana</i> with <i>Agrobacterium tumefaciens</i>	69
2.24.4. Qualitative GUS assay.....	69
2.24.4.1. Staining of rosette leaves from F1 plants	69
2.24.4.2. Infiltration of seedlings to induce GUS expression.....	70
2.25. in situ RNA hybridization of thin paraffin sections of <i>Alonsoa</i>	70
2.25.1. Preparation of the RNA probes.....	70

2.25.1.1. Construction and linearization of plasmids.....	70
2.25.1.2. <i>In vitro</i> transcription	71
2.25.1.3. Hydrolysis	72
2.25.2. Prehybridization.....	72
2.25.3. Hybridization.....	73
2.25.4. Washing	75
2.25.5. Detection	75
2.26. DNA sequencing	77
2.27. DNA and amino acid sequence analysis	78
3. Results	79
3.1. Compartmentation of phloem-translocated carbohydrates in leaves and within mesophyll cells in <i>Alonsoa meridionalis</i> and <i>Asarina barclaiana</i>	79
3.1.1. Leaves of <i>Alonsoa</i> and <i>Asarina</i> contain different types of soluble carbohydrates	79
3.1.2. Subcellular compartmentation of carbohydrates	80
3.1.2.1. Distribution of carbohydrates between the subcellular compartments of mesophyll cells.....	80
3.1.2.2. Estimation of the volumes of subcellular compartments of mesophyll cells in <i>Alonsoa</i> and <i>Asarina</i>	83
3.1.2.3. Sugar contents and concentrations in subcellular compartments of mesophyll cells in <i>Alonsoa</i> and <i>Asarina</i>	85
3.1.3. Concentrations of sucrose, glucose and fructose in mesophyll cells measured by single cell sampling technique agree well with the non-aqueous fractionation data.....	88
3.1.4. Epidermal concentrations of sucrose and hexoses in <i>Alonsoa</i> and <i>Asarina</i> were similar to those in mesophyll cells	89
3.1.5. Soluble carbohydrates in <i>Alonsoa</i> and <i>Asarina</i> essentially contributed to the osmolality of the cytosol in mesophyll cells.....	91
3.1.6. Levels of phloem-translocated carbohydrates other than raffinose and stachyose increased in the leaves with blocked translocation	92
3.2. Sugar concentrations in the apoplast of leaves in putative symplastic and apoplastic phloem loaders	94
3.2.1. Diurnal levels of the translocated carbohydrates in the apoplast	94
3.2.2. Levels of the translocated carbohydrates in the apoplast increased in apoplastic but not in symplastic phloem loaders when phloem translocation was blocked.....	95
3.2.3. Uptake of sugars including non-metabolizable isomers fed exogenously into the apoplast was driven by proton-motive force in both symplastic and apoplastic phloem loaders.....	100
3.3. Characterization of <i>AmSTS</i> , a stachyose synthase from <i>Alonsoa meridionalis</i>	108
3.3.1. Cloning of cDNA fragments of <i>Alonsoa meridionalis</i> raffinose synthase and stachyose synthase	108
3.3.2. The full length cDNA of stachyose synthase from <i>Alonsoa</i> (<i>AmSTS</i>) was cloned	109

3.3.3. Stachyose synthase activity assay with protein extracts of <i>Alonsoa meridionalis</i> leaves and of <i>E. coli</i> cells containing an expression vector carrying the <i>AmSTS</i> ORF	111
3.3.3.1. Stachyose synthase activity assay using leaves of <i>Alonsoa</i>	111
3.3.3.2. The induction of <i>AmSTS</i> expression did not function in <i>E. coli</i> cells.....	111
3.3.4. <i>AmSTS</i> is encoded by a small gene family containing most probably two members	115
3.3.5. Localization of <i>AmSTS</i> mRNA in leaves of <i>Alonsoa meridionalis</i> by in situ RNA hybridization: <i>AmSTS</i> expression is confined to intermediary cells....	117
3.3.6. Expression of <i>AmSTS</i> promoter-<i>GUS</i> fusion constructs in <i>Arabidopsis</i>....	120
3.3.6.1. Cloning of the <i>AmSTS</i> promoter.....	120
3.3.6.2. Promoter- <i>GUS</i> fusion constructs and 5' uORF	120
3.3.6.3. The <i>AmSTS</i> promoter directed <i>GUS</i> activity in minor veins in transgenic F1 lines of <i>Arabidopsis</i> containing either <i>AmSTS</i> promoter- <i>GUS</i> fusion construct.....	120
3.3.6.4. <i>GUS</i> activity was also found in the vascular tissue of sepals and siliques of F2 plants.....	124
3.3.6.5. The expression of the <i>AmSTS</i> promoter- <i>GUS</i> fusion was strongly enhanced by sucrose and glucose in <i>Arabidopsis</i>	124
4. Discussion	129
4.1. Subcellular compartmentation of carbohydrates and estimation of phloem:mesophyll concentration ratios: implications for the phloem loading mode of different carbohydrates in <i>Asarina</i> and <i>Alonsoa</i>	129
4.1.1. Subcellular distributions of carbohydrates in the symplastic phloem loader <i>Alonsoa meridionalis</i> do not differ from those in apoplastic phloem loaders.....	129
4.1.2. Concentration ratios between the cytoplasm of mesophyll cells and the phloem sap indicate the presence of an active loading step for sucrose and antirrhinoside, the major transported carbohydrates in <i>Asarina</i>	132
4.1.3. Concentration ratios between the cytoplasm of mesophyll cells and the phloem sap indicate that the minor transported sugars, mannitol in <i>Asarina</i> and sucrose in <i>Alonsoa</i> , may be symplastically loaded into the phloem.....	133
4.2. Inhibition of the export of sugars from the leaves results in the re-compartmentation of translocated carbohydrates in leaves of <i>Asarina</i> and <i>Alonsoa</i>	135
4.3. Apoplastic compartmentation of translocated sugars in symplastic and apoplastic phloem loaders	137
4.3.1. Inhibition of phloem translocation leads to the accumulation of sucrose in the apoplast of leaves in apoplastic, but not in symplastic phloem loaders	137
4.3.2. The exchange of sucrose, raffinose and stachyose through plasma membrane in both symplastic and apoplastic phloem loaders is not limited by the lack of specific transporters	138
4.3.3. The non-metabolizable sucrose isomers palatinose and turanose can be taken up from the apoplast into the leaf cells in a proton motive force-dependent manner	142

4.3.4. Sugar exchange between apoplast and phloem is limited in symplastic but not in apoplastic phloem loaders	143
4.4. Molecular characterization of <i>AmSTS</i> , a stachyose synthase from the symplastic phloem loader <i>Alonsoa meridionalis</i>	143
4.4.1. <i>AmSTS</i> is expressed in intermediary cells of <i>Alonsoa meridionalis</i>	143
4.4.2. The <i>AmSTS</i> promoter directs <i>GUS</i> expression into the phloem in <i>Arabidopsis</i>	144
4.4.3. Preliminary results indicate that the <i>AmSTS</i> promoter is inducible by sugars but also by osmotically active solutes.....	147
4.5. Reformulation of the model of symplastic phloem loading.....	148
5. Summary.....	153
6. Abbreviations	155
7. References.....	159

1. INTRODUCTION

In leaves of higher plants, photosynthesis results in the production of carbohydrates from carbon dioxide and water. For the most part they are converted into carbon and nitrogen compounds destined to be exported from the leaves to other plant organs. The development of the whole plant, its flowering and seed production completely depend on this transport from source leaves to sink organs such as meristems, young leaves, flowers, fruits, roots and storage organs. At most stages of the plant life, mature leaves are the only carbon source organs. In dicotyledonous plants, the source function is established in leaves during the sink-source transition which occurs within some hours or days (Turgeon and Webb, 1973, 1975). During this process, the terminal phloem becomes functional and starts collecting assimilates and loading them into the conducting route of the phloem. The process by which the major translocated substances are selectively and actively delivered to the sieve tubes in the source region prior to translocation has been termed phloem loading (Geiger, 1975). The long-distance assimilate transport is driven by the osmotic potential between source and sink organs which draws the water flux into the phloem (Münch, 1930).

The elementary functional unit of the phloem tissue is sieve element-companion cell (SE-CC) complex. These two cells derive from the division of one initial cell. During this division, plasmodesmal connections between the daughter cells are formed and retained later on. After the division, the daughter cells differentiate into SE and CC, respectively. Mature sieve elements are devoid of nuclei and of the apparatus for protein synthesis, and possess an extremely developed stacked smooth endoplasmic reticulum, abundant mitochondria and plastids of different types but no chloroplasts. Companion cells retain the nucleus and the apparatus for protein synthesis. Their further characteristics depend on their specific differentiation. The most specialized part of the leaf phloem is present in “minor veins” (Esau,

1967). Minor veins are the very endings of the vein network which are in close contact with mesophyll cells (approximately 20 - 40 mesophyll cells per minor vein; Gamalei, 1990) and, like most veins, typically include both xylem and phloem elements. Minor veins represent as much as 95% of the whole length of the leaf conducting tissue (Gamalei, 1990). The phloem part of the minor veins consists of SE-CC complexes which are mostly specialized for collecting and loading assimilates into the phloem. This specialization has led to the appearance of several types of companion cells which can be found in minor veins only. Because structure is a key to function, the understanding of their structure is important when the mechanisms of phloem loading will be discussed.

1.1. Types of companion cells in minor vein phloem

The ultrastructure of companion cells in minor veins has been studied in more than one thousand species of dicotyledonous plants (Esau, 1967; Gunning and Pate, 1969; Pate and Gunning, 1969; Fisher, 1986; Gamalei, 1990; Batashev and Gamalei, 1996; Batashev, 1997). The following types of companion cells were described: intermediary cells (IC), transfer cells (TC) and ordinary cells (OC; Table 1.1).

Table 1.1. Characterization of the three ultrastructural types of companion cells found in minor veins of leaves of dicotyledonous plants. IC, intermediary cells; TC, transfer cells; OC, ordinary cells.

	<i>IC</i>	<i>TC</i>	<i>OC</i>
<i>cytoplasm</i>	dense	dense	dense
<i>mitochondria</i>	abundant	abundant	abundant
<i>characteristics of endomembrane system</i>	highly developed smooth ER with many small "cisterns"	a single large vacuole	a single large vacuole
<i>plastids</i>	leucoplasts, no starch accumulation	chloroplasts, able to accumulate starch	leucoplasts or chloroplasts
<i>interface with mesophyll</i>	highly developed branched plasmodesmata in plasmodesmal fields	highly developed cell wall ingrowths with no or very few plasmodesmata	single plasmodesmata
<i>taxon specificity (examples)</i>	Buddlejaceae Cucurbitaceae Lamiaceae Oleaceae Scrophulariaceae	Asteraceae Boraginaceae Campanulaceae Fabaceae Scrophulariaceae	Betulaceae Brassicaceae Chenopodiaceae Solanaceae Scrophulariaceae
<i>ecological specificity</i>	plants families representing mostly vines and trees from warm areas	herbaceous plants able to inhabitate cold and temperate regions	plants spread over many climate zones and life forms; the only type found in plants from very extreme biotopes (arid zones, solontschaks)*

*Gamalei and Sjutkina, 1999

Two unique features of IC are the presence of a highly developed smooth ER and the abundance of branched plasmodesmata organized in plasmodesmal fields which connect IC to the mesophyll cells of the bundle sheath. These plasmodesmata are secondary, i.e. they are not the remainder of cell division but appear later, during the establishment of the source function of the leaf.

The distinct feature of TC is the presence of numerous cell wall ingrowths consisting of hemicellulose, which are formed just when intensive transport starts. These cells typically possess extremely few or no plasmodesmal connections with mesophyll cells.

OC are less specialized than the two other cell types described above. They are present not only in minor veins but also in veins of higher orders. Plants whose minor veins contain IC or TC also have OC in their larger veins. OC also can occur in minor veins together with IC or TC. However, in a large group of plants they are the only companion cell type found in the phloem of minor veins. They possess neither plasmodesmal fields nor cell wall ingrowths, although single plasmodesmal connections with mesophyll cells are always present.

On the basis of these three types of companion cells, ultrastructural variations are possible and altogether 14 subtypes have been described thus far (Batashev, 1997). The type of companion cells has turned out to be specific for a plant species and for a plant family, with rare exceptions. For instance, in Scrophulariaceae, all three types of companion cells are found.

1.2. Symplastic (dis)continuity between mesophyll and phloem

An important basic feature for the classification of companion cells is the abundance of plasmodesmata at the companion cell/mesophyll interface. As shown in Figure 1.1 (data are taken from Gamalei, 1995), this feature is gradually changing between two extremes which correspond to IC and TC, respectively.

This has important consequences for the assimilate transfer from the mesophyll into the phloem. In companion cells where plasmodesmata are absent (TC), sugars have to enter the apoplast before they can be taken up into the phloem. This apoplastic pathway also exists in plants with IC but here, the highly developed plasmodesmata provide an additional route, entirely symplastic, for sugar transfer from mesophyll cells into the companion cells and further into the sieve elements. This led to the proposal that in dicotyledonous plants, two mechanisms of assimilate loading into the phloem exist: an apoplastic one and a symplastic one. However, as shown in Figure 1.1, the boundary between “pure” apoplastic and “pure” symplastic phloem loaders cannot be set precisely. The only exception are species with TC

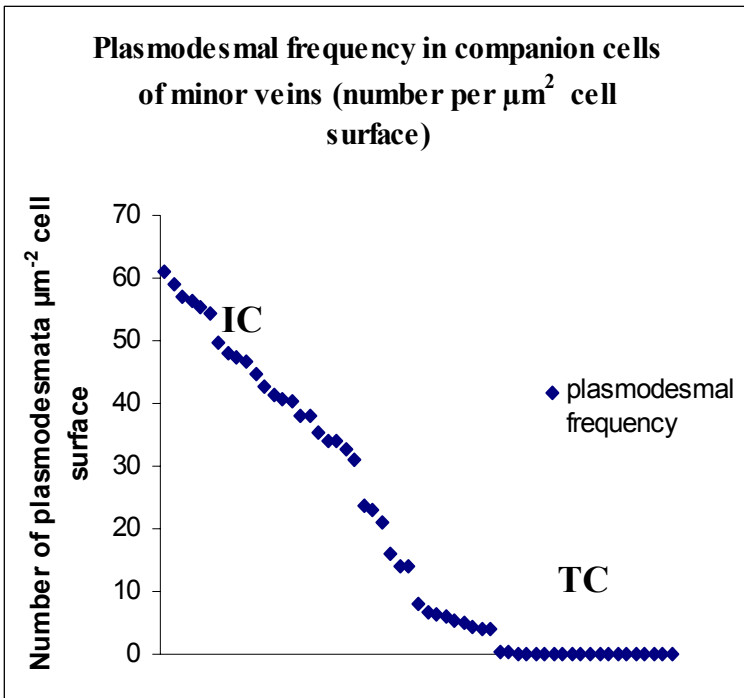


Figure 1.1. Plasmodesmal frequencies between mesophyll bundle sheath cells and companion cells as determined in 60 species selected from 34 families of dicotyledonous plants (data taken from Gamalei, 1995).

and, therefore, a lack of symplastic connections between mesophyll and phloem, which represent pure apoplastic phloem loaders.

1.3. Apoplastic phloem loading mode

A short summary of the model of apoplastic phloem loading is given in Figure 1.2.

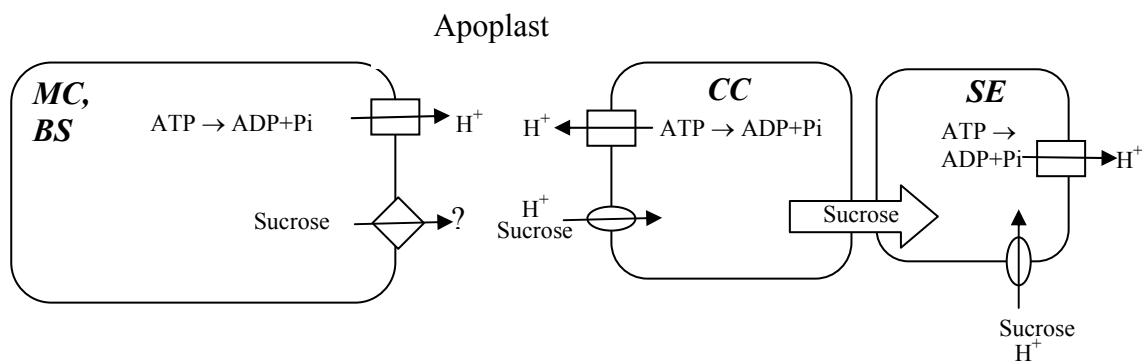


Figure 1.2. Apoplastic phloem loading. H^+ /sucrose-symporters are shown as ellipses and plasma membrane H^+ -ATPases as squares. Sucrose exporters from mesophyll cells and bundle sheath cells, which may or may not be identical with H^+ /sucrose-symporters, are shown as diamonds. Sucrose transfer between CC-SE via plasmodesmata is indicated by a white arrow. **MC**, Mesophyll cell; **BS**, bundle sheath cell; **CC**, companion cell; **SE**, sieve element.

In apoplastic phloem loading, assimilates have to pass through at least two membranes: the plasmalemma of mesophyll cells and the plasma membrane of companion cells or sieve elements. The transmembrane transfer occurs via sugar transporter proteins

which are specific for certain sugars. This requires that the variety of plant carbohydrates are converted to just one or a few transport forms. In most plant species, the dominant transport sugar is sucrose. Sucrose transporters have been found in many plants and seem to be ubiquitous (Lemoine, 2000). They translocate sucrose together with a proton using the proton motive force (PMF; $PMF = 0,059 \Delta pH + \Delta \Psi$) as an energy source for the transfer against a sucrose concentration gradient (Giaquinta, 1980). Evidence for the crucial role of sucrose transporters for apoplastic phloem loading was obtained in a study of transgenic potato plants expressing a sucrose transporter antisense construct (Riesmeier et al., 1994). This study has confirmed the theory of apoplastic phloem loading in general. However, a lot of information about the regulation of apoplastic phloem loading is still missing. For instance, knowledge on the mechanism of sugar export from mesophyll cells into the apoplast and its regulation is scarce (Lemoine et al., 1996; Schulz et al., 1998).

1.4. Symplastic phloem loading mode

Although in plants with IC in minor veins both apoplastic and symplastic routes are considered to participate in phloem loading (e.g. Kursanov, 1984), the latter is assumed to dominate. This is implied because of the extremely developed plasmodesmata at the mesophyll/phloem interface of these plants. Evidence that the loading of assimilates into the phloem in plants with IC occurs differently from those with OC or TC has been obtained in studies on partitioning of ^{14}C -labelled assimilates (Turgeon and Gowan, 1992; Flora and Madore, 1993, 1996), dynamics of sugar uptake and release from the apoplast (Madore and Webb, 1981; Schmitz et al., 1987; Turgeon and Wimmers, 1988) and ultrastructural changes (Gamalei et al., 1994; Gamalei and Pakhomova, 2000). However, the exact mechanism has not yet been revealed. According to the organization of plasmodesmata, there are two possible channels for the symplastic transfer of assimilates, the cytosolic sleeve and the endoplasmic reticulum (Figure 1.3, insert). Two models are depicted in Figure 1.3.

The traffic of viruses through plasmodesmata occurs via the cytosolic sleeve (see e.g. Ghoshroy et al., 1997). This has led to the conclusion that sugar transport should also occur through the cytosolic continuum between two types of cells, although no direct evidence is available. Contrarily, a role of the ER desmotubule in assimilate transfer and in water transport has been suggested by several studies (Gamalei, 1994; Gamalei et al., 1994, 2000; Zhang and Tyerman, 1997; Blackman and Overall, 2001) including some with fluorescent dyes (Cantrill et al., 1999, 2001). However, direct evidence for sugar transport via the ER is also missing.

In most studied plants, sugar concentrations in the phloem are higher than in other tissues. They are in the molar range (Ohshima et al., 1999; Lohaus and Fischer, 2001 and references therein). The exact phloem concentrations are known only for a few species with IC (Moing et al., 1997; Knop et al., 2001) but the data available suggest that phloem concentrations are equally high in these plants as in apoplastic phloem loaders. Thus, also in

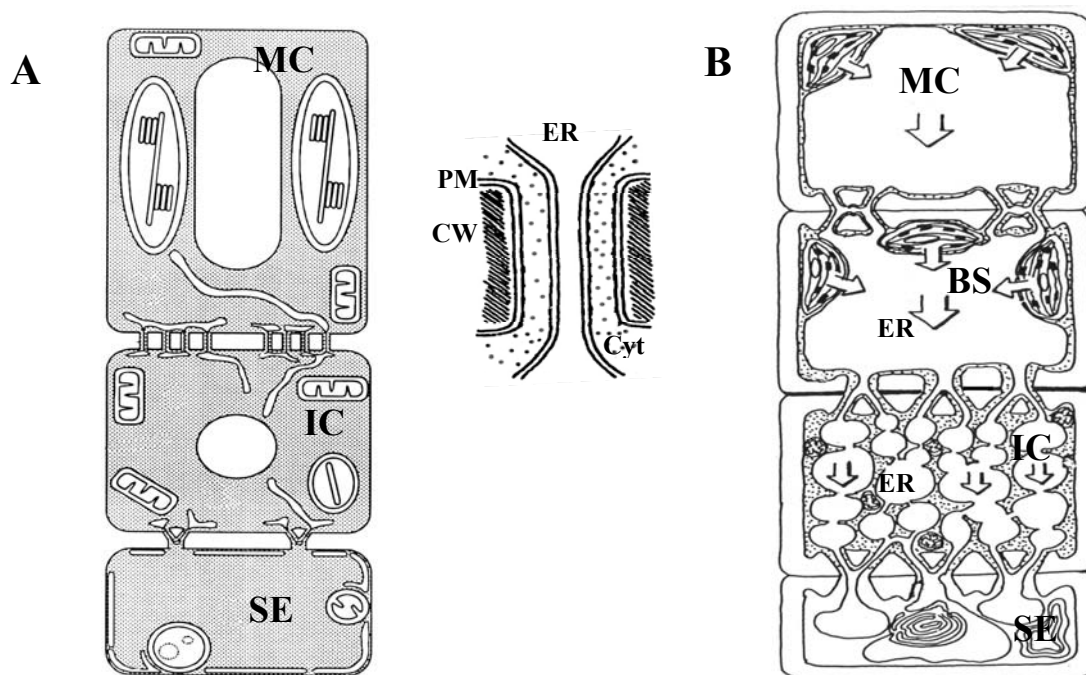


Figure 1.3. Two contemporary models of symplastic phloem loading. **A**, Schulz (1997); **B**, Gamalei (1994). **A**, assimilates move along the cytosol of the mesophyll cell through the cytosolic sleeve of plasmodesmata into the IC and further into the SE where they are moving in the cytosol; **B**, assimilates move from the vacuoles of mesophyll cells through the endoplasmic reticulum (ER) spreading from cell to cell into the IC and further into the SE whose lumen corresponds to ER lumen. **MC**, mesophyll cell; **BS**, bundle sheath cell; **IC**, intermediary cell; **SE**, sieve element. The insert shows a scheme of a plasmodesma. **CW**, cell wall; **Cyt**, cytoplasm; **PM**, plasmalemma. The cytosolic sleeve is the region between ER and PM.

symplastic phloem loaders sugar movement from sites of lower concentration (mesophyll cells) to sites with higher concentration (phloem) has to take place.

Several questions have to be answered before a complete model of symplastic phloem loading can be established. (1) Which mechanism enables the plant to keep up the sugar concentration gradient between mesophyll and phloem? (2) Which compartment, cytosolic sleeve or ER lumen, is involved in sugar transfer? (3) How is the distribution of assimilate flux between symplastic and apoplastic routes regulated in plants with IC? (4) Is there a connection between the structure of companion cells and the types of sugars transported? (5) Why have plasmodesmata between mesophyll and companion cells been retained in several

groups of plants during evolution? What has prevented a complete switch to apoplastic phloem loading in many plant species? (6) Are there other functions of plasmodesmata on the mesophyll/companion cell boundary than phloem loading?

1.5. Relationship between companion cell types and the types of translocated sugars

The phloem sap composition is specific for plant families (Zimmermann and Ziegler, 1975). Comparison of these data with the minor vein anatomy has revealed a relationship between types of companion cells and types of transported sugars (Gamalei, 1984; Turgeon et al., 1993; Flora and Madore, 1993, 1996). Plants with abundant symplastic connections between mesophyll and phloem translocate a large spectrum of organic compounds including sucrose, raffinose family oligosaccharides (RFOs, Figure 1.4), sugar alcohols and glucosamines. Plants with scarce or absent symplastic connections translocate almost exclusively sucrose.

Plants fall into three classes with regard to percentage of RFOs in the phloem sap (Gamalei, 1984). In the first group, RFOs are absolutely predominating, in the second group, RFOs are completely absent and in the third group, RFOs are minor components (<25%) of the phloem sap carbohydrates. The first group represents plants with IC, the second group consists of plants with OC and TC, whereas the third group includes plants with OC as well as plants with abundant plasmodesmata not organized in plasmodesmal fields. The latter type is the type 1-2a in Gamalei's classification, and the companion cells of these plants are considered as intermediates between IC and OC (Gamalei, 1995).

As revealed by studies of F. Keller and coworkers on *Ajuga reptans*, a Lamiaceae with IC (Bachmann et al., 1994; Bachmann and Keller, 1995; Büchi et al., 1998), RFOs in leaves occur also in vacuoles of mesophyll cells and can play a role in carbon storage and cold resistance in addition to their transport function. Importantly, two different isoforms of galactinol synthase were found in this species, one expressed in mesophyll cells and another one in IC (Sprenger and Keller, 2000). Because galactinol is a precursor for the synthesis of all RFOs, this finding implies that there are two pathways for RFO synthesis in *Ajuga*, one in the mesophyll and another in IC. Are there plants with only one, transport-independent RFO synthesis pathway present in leaves? The answer to this question would require a simultaneous study of RFO contents in leaves and in phloem sap in a large number of plant species from different families. Some information can be obtained from exhaustive studies on the occurrence of RFOs in leaves (Senser and Kandler, 1967) and on phloem sap composition

(Zimmermann and Ziegler, 1975). In Table 1.2, a comparison is made that includes data on the companion cell type taken from Gamalei (1990).

Figure 1.4. Biosynthesis of raffinose and stachyose. Raffinose family oligosaccharides are α -galactosylated derivatives of sucrose which differ in the number of galactosyl moieties (n). Galactinol (1L-1-O-(α -D-galactosyl)-*myo*-Inositol) serves as a donor of galactosyl moiety in the reactions of raffinose and stachyose synthesis. Galactinol is synthesized by galactinol synthase (UDP-galactose:*myo*-Inositol galactosyltransferase, EC 2.4.1.123) from UDP-galactose and *myo*-inositol. The first member of RFOs, the raffinose ($n=1$) is synthesized via galactosylation of sucrose by raffinose synthase (galactinol:sucrose 6- α -D-galactosyltransferase, EC 2.4.1.82; **RS**). The second member of RFOs, stachyose is formed via galactosylation of raffinose by stachyose synthase (galactinol:raffinose 6- α -D-galactosyltransferase, 2.4.1.67; **STS**). Further extensions of the chain of galactosyls lead to formation of other members of RFO (not shown).

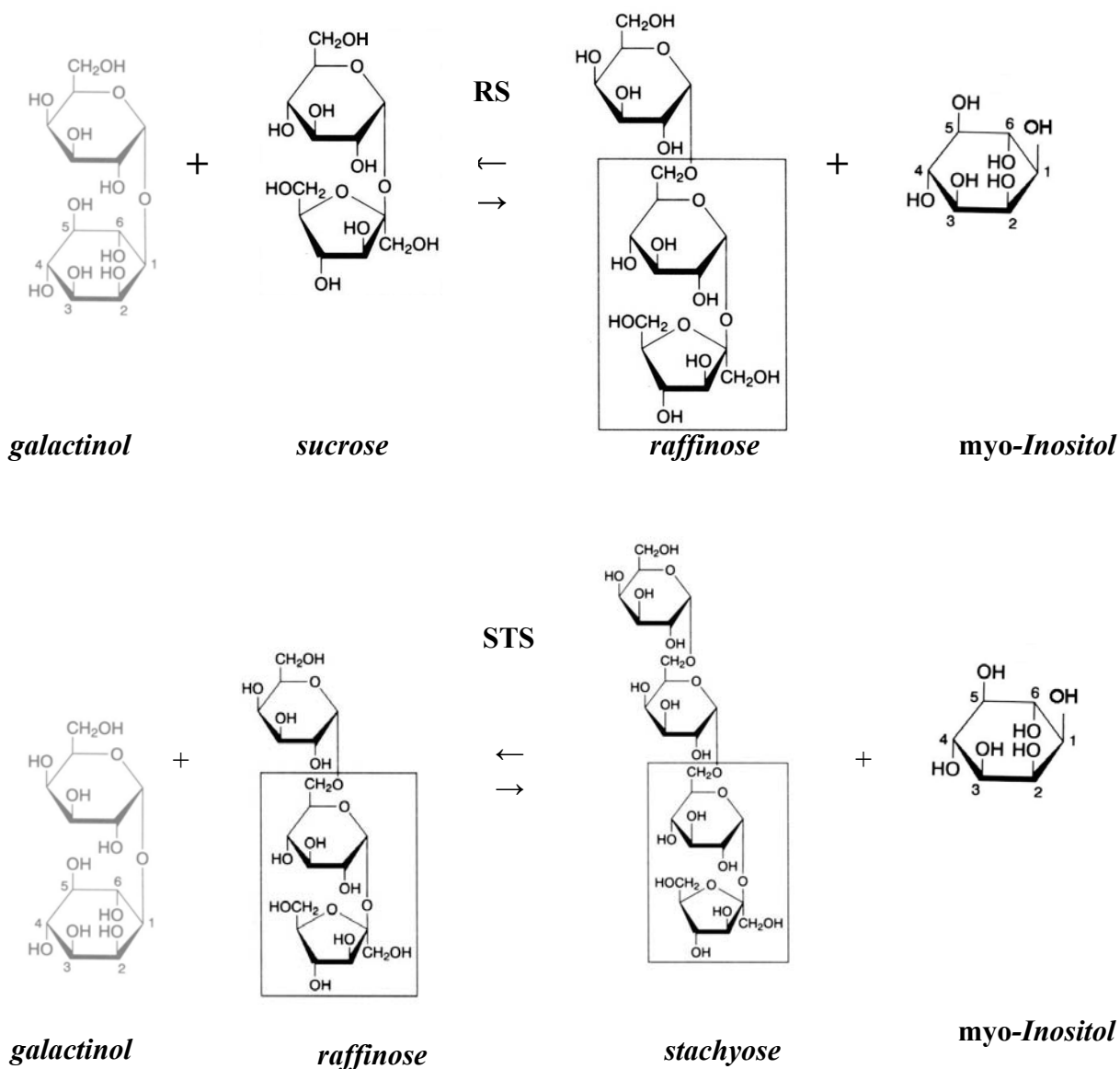


Table 1.2. Comparison of companion cell types and presence of RFOs in leaves and in phloem sap of several plant families/species. For some families/genera where a number of species have been studied, this number is indicated in parentheses. Abbreviations: raf, raffinose; sta, stachyose; tr, found in trace amounts.

Plant family	Companion cell type in minor veins ^{2, 10}	Galactinol and raffinose in leaves ^{1, 3, 4, 9, 10}	Stachyose in leaves ^{9, 10}	RFOs in phloem sap ^{1, 3, 5-8, 10-12}
Bignoniaceae: <i>Catalpa bignonioides</i>	IC	+	+	+
Buddlejaceae: <i>Buddleja davidii</i>	“	+	+	+
Celastraceae (4)	“	+	+	+
Cucurbitaceae (5)	“	+	+	+
Lamiaceae (2)	“	+	+	+
Oleaceae (2)	“	+	+	+
Onagraceae (3)	“	+	+	+
Verbenaceae: <i>Verbena hybrida</i>	“	+	+	+
Apiaceae: <i>Petroselinum crispum</i>	OC	no	no	no
Araliaceae: <i>Hedera helix</i>	“	+	no	tr raf
Brassicaceae: <i>Arabidopsis thaliana</i> (ecotype Columbia)	“	+	no	tr raf
Chenopodiaceae (4)	“	no	no	no
Rosaceae (4)	“	+	no/ tr	no/tr raf sta
Solanaceae (2)	OC, TC	no	no	no
Violaceae (2)	OC	+	tr	?
Asteraceae (2)	TC/?	no/tr	no	no/tr raf
Boraginaceae(3)	TC	no	no	no
Fabaceae (10)	“	no	no	no
Scrophulariaceae: <i>Alonsoa</i> (2)	IC	+	+	+
<i>Verbascum longifolium</i>	“	+	+	+
<i>Mimulus cardinalis</i>	“	+	+	+
<i>Rhodochiton atrosargineum</i>	IC+TC	+	+	+
<i>Asarina</i> (2)	OC+TC, IC+TC	+	+	tr raf sta
<i>Digitalis grandiflora</i>	OC	+	no	tr raf
<i>Cymbalaria muralis</i>	TC	+	no	tr raf
<i>Linaria maroccana</i>	TC	galactinol	no	no

¹⁻¹¹ Data from: (1) Flora and Madore, 1996; (2) Gamalei, 1990; (3) Haritatos et al., 2000a; (4) Hoffmann-Thoma et al., 2001; (5) Knop et al., 2001; (6) Lohaus et al., 1994; (7) Hendrix, 1982; (8) Riens et al., 1991; (9) Senser and Kandler, 1967; (10) Turgeon et al., 1993; (11) Winzer et al., 1996; (12) Zimmermann and Ziegler, 1975.

As shown in Table 1.2, stachyose and a precursor of its synthesis, raffinose, are always present and transported in leaves which contain IC. Stachyose is absent, with two exceptions, from leaves with OC in minor veins. However, raffinose is often present in these leaves, and, when present, is always transported. In leaves with exclusively TC in minor veins, neither RFOs nor galactinol could be detected (Senser and Kandler, 1967), with the exceptions of *Artemisia* (Asteraceae) and *Cymbalaria* (Scrophulariaceae) which were found to translocate trace amounts of raffinose (Zimmermann and Ziegler, 1975; Turgeon et al., 1993). It seems

that in leaves, the “primary” function of RFOs is in transport. Leaves which have lost the ability to synthesize RFOs for transport, do not produce them for other purposes. The ability to synthesize RFOs in leaves also seems to correlate with the development of symplastic connections between mesophyll and phloem (IC>>>OC>TC).

In all plants studied thus far, RFOs occur in germinating seeds (Peterbauer and Richter, 2001). This indicates that RFO synthesis certainly has other important functions in the plant organism apart from phloem translocation.

1.6. The polymerization trap model and the role of stachyose synthesis in symplastic phloem loading

One model to explain the mechanism of symplastic phloem loading was proposed by Turgeon (1991). According to this model, the precursors of RFO synthesis, galactinol and sucrose, diffuse from the mesophyll into IC via plasmodesmata following their concentration gradient. In the IC, they serve as substrates for the synthesis of raffinose and stachyose. The tetrasaccharide stachyose has a size of ca. 0.6 kDa. The size exclusion limit (SEL) of plasmodesmata in the IC/mesophyll interface was estimated to be about 0.7 – 0.8 kDa (Wolf et al., 1989; Robards and Lucas, 1990). Therefore, stachyose should not be able to diffuse back into mesophyll via plasmodesmata. It is supposed to be “trapped” in the IC and to be able to diffuse only into the sieve elements because the SEL of plasmodesmata of CC-SE complexes is estimated as > 3 kDa (Wolf et al., 1989; Robards and Lucas, 1990). Thus, stachyose synthesis and its phloem loading are mechanistically linked in this so-called “polymerization trap” model (Turgeon, 1991).

The polymerization trap model has been supported by experimental evidence with regard to the localization of stachyose synthesis in intermediary cells (Holthaus and Schmitz, 1991b). Although the synthesis of stachyose can occur in mesophyll cells of some plants that store RFOs in leaves, the existence of two isoforms of galactinol synthase specific for either mesophyll or IC (Sprenger and Keller, 2000) suggests that also in these plants a distinct IC-specific isoform of stachyose synthase exists. Galactinol synthesis could be shown to occur in IC (Sprenger and Keller, 2000) so that it does not need to be imported from mesophyll cells as the polymerization trap model postulates.

The occurrence of stachyose synthesis in IC has been confirmed by immunolocalization of the protein in *Cucurbita pepo* (Holthaus and Schmitz, 1991b). The biochemical specialization of IC for stachyose synthesis temporally correlates with the structural specialization of these cells, i.e., the development of ER and of plasmodesmal fields because all these features are established in IC at the same time, namely during the sink-

source transition of leaves (Turgeon and Webb, 1975; Gamalei, 1990). The exact mechanism underlying this relationship remains to be unravelled.

However, some observations indicate that the part of the model regarding the diffusion barrier for stachyose is too much simplified. For one, the polymerization trap model gives no explanation for the symplastic loading of molecules even smaller than sucrose and galactinol, like sugar alcohols, which also occurs in plants with IC (e.g. Flora and Madore, 1993, 1996; Häfliger et al., 1999). Also, it was shown that the SEL of plasmodesmata can be increased due to the action of certain endogenous and viral movement proteins (Waigmann et al., 1994; Kragler et al., 2000; Xoconostle-Cázares et al., 2000). According to the polymerization trap model, sucrose should enter IC via the cytosolic sleeve. The synthesis of stachyose and galactinol is also considered to occur in the cytosol because the pH optima of stachyose and galactinol synthases match the cytosolic conditions (Keller and Pharr, 1996). Therefore, the enlargement of the cytosolic sleeve of plasmodesmata should favour sugar diffusion from the IC to mesophyll cells due to the sugar concentration gradient. However, this was not observed when the cytosolic sleeve was enlarged by the action of cucumber mosaic virus (CMV) movement proteins (Shalitin and Wolf, 2000). In this experiment, infection of melons by CMV led to an increase of the phloem sucrose concentration but did not affect the concentration of stachyose in the phloem. The translocation rate was enhanced in infected melon, although the opposite would be expected if the increase in SEL would have led to destruction of the loading mechanism and diffusion of sucrose back into mesophyll following the increased concentration gradient (Shalitin and Wolf, 2000). Obviously, the diffusion of sugars through the cytosolic sleeve was not facilitated by the enlargement of plasmodesmal SEL in melon. At the same time, in transgenic tobacco plants, the diffusion of fluorescent dyes via plasmodesmata was enhanced due to the action of the CMV protein when the dyes were introduced into the cytosol (Vaquero et al., 1994).

A powerful tool for the further study of this relationship can be obtained by the investigation of the regulation of genes encoding enzymes involved in stachyose synthesis. Up to now, no information on the regulation of stachyose synthase expression is available. However, two recent investigations can provide a basis for such studies. The first full length cDNA clone of a stachyose synthase from seeds of *Vigna angularis* was obtained by Peterbauer et al. (1999) and the expression of the *VaSTS* cDNA in Baculovirus expression system has confirmed its biochemical function. Second, the promoter of galactinol synthase fused to the β -glucuronidase (*GUS*) reporter gene in *Arabidopsis thaliana* was shown to direct *GUS* expression into companion cells (Haritatos et al., 2000b). A serious challenge for this

approach is the absence of a well-established transformation procedure for a plant species with IC in minor veins. The only species which so far has been successfully transformed is *Cucumis melo* (Guis et al., 2000)

1.7. The aim of this thesis and the choice and characterization of model plants.

1.7.1. The aim of this thesis

This study was focused on several aspects of symplastic phloem loading. When a comparison with the apoplastic phloem loading mode was necessary, some aspects of the apoplastic transfer of sugars were also investigated. The following points had to be studied:

1. Subcellular distribution of various translocated carbohydrates in mesophyll cells of plants with different types of companion cells in minor veins.
2. Estimation of concentration gradients between the cytoplasm of mesophyll cells and the phloem for various translocated carbohydrates in plants with different types of companion cells in minor veins.
3. The participation of the apoplast in phloem loading in plants with IC in minor veins and, therefore, a high potential for symplastic phloem loading, and comparison with apoplastic phloem loaders.
4. Isolation of a full length cDNA of a stachyose synthase from leaves of a symplastic phloem loader.
5. Analysis of the expression pattern of stachyose synthase gene(s) *in situ*.
6. Isolation of the promoter of a stachyose synthase gene and construction of transgenic *Arabidopsis thaliana* plants expressing the GUS reporter gene under control of this promoter.

1.7.2. Phloem sap composition and characterization of minor vein anatomy in two related species, *Alonsoa meridionalis* and *Asarina barclaiana*

The choice of the model plant species was based on the following required characteristics:

(1) To make conclusions about the concentration barriers for symplastic transport, the composition and the concentrations of carbohydrates in the phloem sap should be known precisely;

(2) The minor vein anatomy and the companion cell type should be characterized.



Figure 1.5. *Alonsoa meridionalis* (A) and *Asarina barclaiana* (B).

The limiting factors are data on the exact concentrations of the phloem sap carbohydrates. Such data can only be obtained by the laser aphid stylet technique, and species that can be investigated by this method are scarce. Two Scrophulariaceae, *Alonsoa meridionalis* and *Asarina barclaiana* (Figures 1.5 A and B), have been studied and data on their phloem sap composition and concentrations are available (Knop, 1998; Table 1.3).

Table 1.3. Phloem sap concentrations determined in *Alonsoa meridionalis* and *Asarina barclaiana* (Knop, 1998; n=9).

	<i>Alonsoa meridionalis</i>		<i>Asarina barclaiana</i>	
	mM	% of total carbon transported	mM	% of total carbon transported
<i>sucrose</i>	174 ± 85	20.8	963 ± 280	47.9
<i>hexoses</i>	+		+	
<i>galactose</i>	1 ± 2	0.1	12 ± 9	0.6
<i>galactinol</i>	2 ± 3	0.2	10 ± 20	0.5
<i>myo-inositol</i>	12 ± 4	1.4	2 ± 2	0.1
<i>raffinose</i>	249 ± 51	29.7	29 ± 9	1.4
<i>stachyose</i>	397 ± 68	47.3	54 ± 17	2.7
<i>mannitol</i>	+		136 ± 101	6.8
<i>antirrhinoside</i> *	not detected		786 ± 136	39.1
sum	839 ± 177	100	2008 ± 400	100

* data added from this thesis (2.3.2)

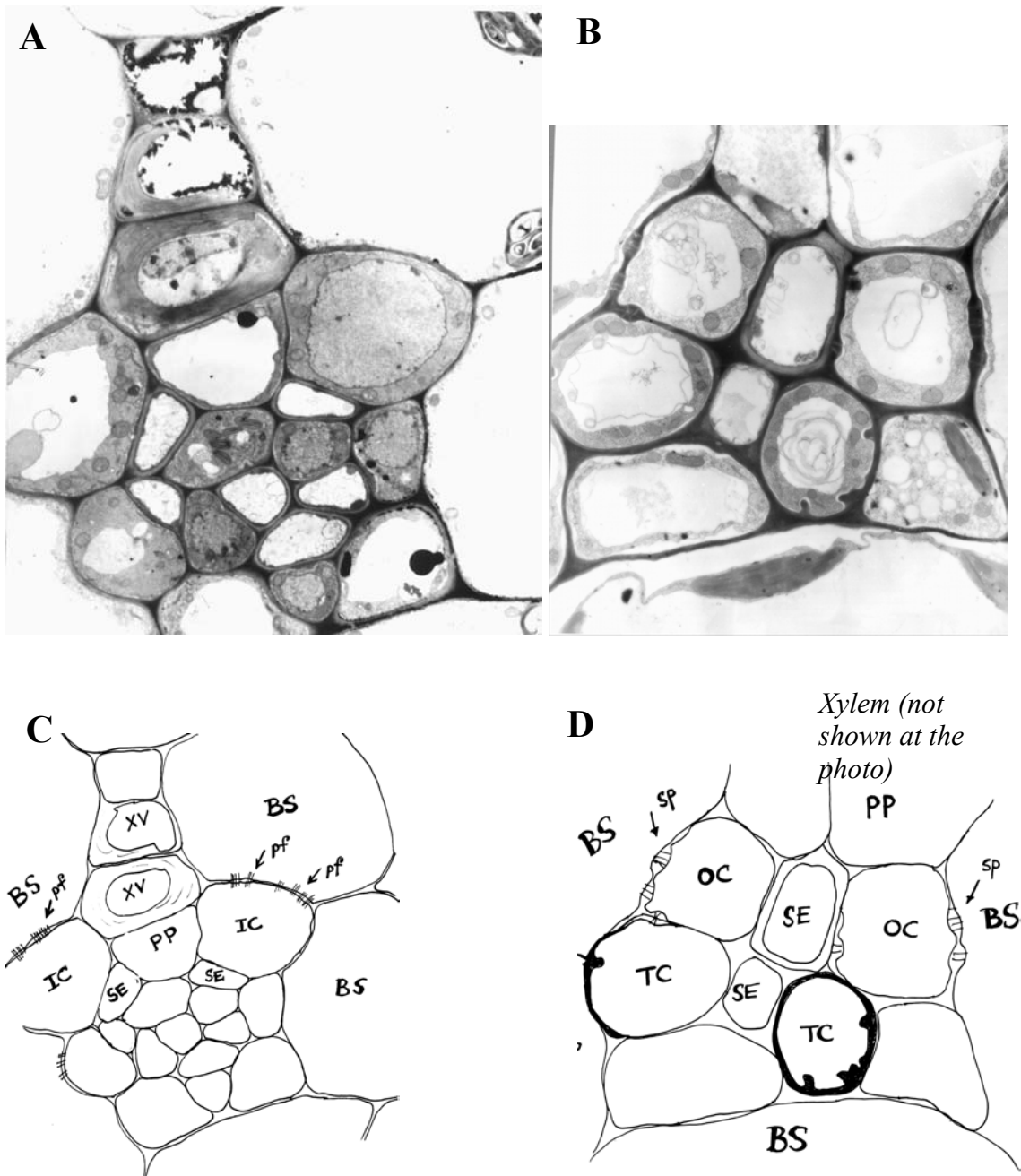


Figure 1.6. The minor vein anatomy of *Alonsoa meridionalis* and *Asarina barclaiana* as studied by electron microscopy. **A**, a minor vein of *Alonsoa meridionalis*; **B**, a minor vein of *Asarina barclaiana*; **C**, schematic picture of A with the indication of cell types; **D**, schematic picture of B with the indication of cell types. XV, xylem vessel; PP, phloem parenchyma, IC, intermediary cell; SE, sieve element; BS, bundle sheath; TC, transfer cell; OC, ordinary cell; pf, plasmodesmal field; sp, single plasmodesma.

As shown in Table 1.3, both plants translocate stachyose and raffinose. RFOs are predominating in the phloem sap of *Alonsoa* but are only minor components in *Asarina*. Contrarily, sucrose is the main translocated sugar in *Asarina* but plays only a minor role in

Alonsoa. In *Asarina*, an additional unidentified major component of the phloem sap was indicated in amounts comparable to those of sucrose. This component was characterized by a preparative isolation from the leaves of *Asarina* and its structure was determined by NMR (this thesis, 2.3.2.2, Figure 2.1). It is the iridoid glycoside antirrhinoside. After this, its concentration in the phloem sap of *Asarina* could be determined (Table 1.3).

The minor vein anatomy was studied in both plants by electron microscopy (this thesis, 2.13; Figure 1.6). *Alonsoa meridionalis* possesses minor veins with intermediary cells (Figure 1.6 A, C). In minor veins of *Asarina barclaiana*, two types of companion cells occur. Some minor veins had only TC (data not shown). In others, transversal leaf sections show that two CC-SE complexes of different composition occur in minor veins. In CC-SE complexes of the upper parts of these veins (next to xylem; Figure 1.6, B, D), companion cells with many single plasmodesmata were present. In CC-SE complexes of lower parts of these minor veins, TC were found (Figure 1.6, B, D). This complex type of companion cells is typical for Scrophulariaceae. The most complete characterization of minor vein anatomy of Scrophulariaceae was performed by Batashev on 59 species (1997). Scrophulariaceae plants possess, along with IC, TC and OC, many different structural subtypes where cell wall ingrowths, plasmodesmata and even small plasmodesmal fields can occur simultaneously. Sometimes, plasmodesmal fields are present on the cell wall ingrowths at the mesophyll side (Batashev, 1997). In *Asarina scandens*, similar cells were found and were referred to as “modified intermediary cells” (Turgeon et al., 1993). In *Asarina barclaiana*, symplastic connections are less developed than in *A. scandens*. According to Gamalei’s classification, these cells would correspond to the 1-2a type (Gamalei, 1995), an intermediate between IC and OC. Since no plasmodesmal fields were observed in *A. barclaiana*, its companion cells are referred to as OC in this thesis.

1.7.3. Choice of the model plants

(1) *Alonsoa meridionalis* and *Asarina barclaiana* were chosen for the study on subcellular metabolite concentrations in mesophyll cells and concentration gradients between mesophyll and phloem. These plants represent convenient model systems because they translocate several types of carbohydrates.

(2) For the characterization of stachyose synthase, *Alonsoa meridionalis* was selected because it possesses IC in minor veins and translocates large amounts of stachyose in the phloem.

(3) In addition to these two plants, a number of species from different plant families containing all three types of companion cells (IC, TC, OC) were selected for a comparative study on the apoplastic transport of assimilates. This was necessary to make sure that the observed differences were related to companion cell structure and not specific to a certain species. Plants were selected on the basis of the reported companion cell structure in their minor veins (Gamalei, 1990).

2. MATERIALS AND METHODS

2.1. Materials

2.1.1. Biochemicals

Most chemicals were purchased from Sigma (Sigma-Aldrich, Taufkirchen, Germany), Merck (Darmstadt, Germany) and Carl Roth (Karlsruhe, Germany). Enzymes used for biochemical analyses were obtained from either Sigma or Roche Molecular Biochemicals (Mannheim, Germany) if not otherwise indicated. For chemicals and products from other companies, the sources are listed below:

dNTPs	Roche Molecular Biochemicals, Mannheim, Germany
Digoxigenine-UTP	Roche Molecular Biochemicals, Mannheim, Germany
tRNA	Sigma (Sigma-Aldrich, Taufkirchen, Germany)
DNA size marker (bacteriophage λ DNA)	MBI Fermentas, Vilnius, Lithuania
[α - ³² P]dATP	Hartmann Analytik, Braunschweig, Germany
IPTG (Isopropyl- β -D-thiogalactopyranoside)	AppliChem, Darmstadt, Germany
oligonucleotides	MWG Biotech, Ebersberg, Germany
X-Gal (5-bromo-4-chloro-3-indolyl- β -D-galactopyranoside)	Roche Molecular Biochemicals, Mannheim, Germany
X-Gluc (5-bromo-4-chloro-3-indolyl- β -D-glucuronide)	MWG Biotech, Ebersberg, Germany

Microspin S-300 HR columns	Amersham Pharmacia Biotech, Freiburg, Germany
Sephadex G25 columns	Amersham Pharmacia Biotech, Freiburg, Germany
Hybond N and Hybond N ⁺	Amersham Pharmacia Biotech, Freiburg, Germany
3MM Whatman paper	Biometra Whatman, Germany
Chr 17 Whatman paper	Biometra Whatman, Germany

2.1.2. Enzymes used in molecular biology

Restriction enzymes and buffers were obtained either from MBI Fermentas (Vilnius, Lithuania) or from Gibco BRL (Eggenstein, Germany). For other enzymes, the source is given below:

DNA polymerase I large fragment (Klenow fragment)	MBI Fermentas, Vilnius, Lithuania
Klenow fragment, exonuclease ⁻	MBI Fermentas, Vilnius, Lithuania
MLV Reverse transcriptase	MBI Fermentas, Vilnius, Lithuania
Thermoscript TM RT-PCR system	Gibco BRL, Eggenstein, Germany
T3 RNA polymerase	Gibco BRL, Eggenstein, Germany
T7 RNA polymerase	Gibco BRL, Eggenstein, Germany
T4 DNA ligase	Gibco BRL, Eggenstein, Germany
<i>Taq</i> polymerase	Promega, Mannheim, Germany
RNase A	Sigma-Aldrich, Taufkirchen, Germany

2.1.3. Kits

HexaLabel Kit	MBI Fermentas, Vilnius, Lithuania
Invisorb Spin-Plant RNA Mini Kit	Invitex, Berlin, Germany
Qiaquick Gel Extraction Kit	Qiagen, Hilden, Germany
Qiagen Mini Prep Kit	Qiagen, Hilden, Germany
DNeasy Plant Maxi Kit	Qiagen, Hilden, Germany
E.Z.N.A.Peq Lab Mini Prep Kit	Peq Lab Biotechnologie GmbH, Erlangen, Germany
ABI PRISM dRhodamine Terminator Cycle Sequencing Ready Reaction Kit	PE Applied Biosystems, Weiterstadt, Germany

Genome Walker™ DNA Walking Kit	CLONTECH, Palo Alto, CA. USA
Low molecular weight calibration Kit	Amersham Pharmacia, Freiburg, Germany
RNA ladder, high range	MBI Fermentas, Vilnius, Lithuania
Bacteriophage λ DNA	MBI Fermentas, Vilnius, Lithuania

2.2. Growth conditions

2.2.1. Plants

Alonsoa meridionalis O. Kuntze and *Asarina barclaiana* Pennell (Scrophulariaceae) were grown in a greenhouse on pot soil. The growth conditions were 600 – 700 $\mu\text{mol m}^{-2} \text{s}^{-1}$ photon fluence rate, 14/10 hour light/dark period and 22°C/14°C temperature period. Some experiments were performed at the University of Würzburg where plants were kept in the greenhouse with a similar light regime and slightly different temperature conditions (20°C/15°C). For the experiments carried out at the University of Wales (Bangor, UK), plants were grown on pot soil in a controlled environment chamber (Sanyo Gallenkamp, Loughborough, Leicester UK) at 20°C in a 16 h light/8 h dark cycle and a photon flux of 500 $\mu\text{mol m}^{-2} \text{s}^{-1}$ and 0.035% CO₂.

For the comparative study of apoplastic sugar contents in plants with different minor vein anatomy, several species were selected on the basis of their reported companion cell structure (Gamalei, 1990) in addition to the two species *Alonsoa meridionalis* and *Asarina barclaiana*:

<i>species with transfer/ordinary cells</i>		<i>species with intermediary cells</i>	
<i>Calendula officinalis</i> L.	Asteraceae	<i>Cucurbita pepo</i> L.	Cucurbitaceae
<i>Symphytum officinale</i> L.	Boraginaceae	<i>Coleus blumei</i> Benth.	Lamiaceae
<i>Lepidium sativum</i> L.	Brassicaceae	<i>Mentha</i> sp.	Lamiaceae
<i>Spinacea oleracea</i> L.	Chenopodiaceae	<i>Ligustrum vulgare</i> L.	Oleaceae
<i>Pisum sativum</i> L.	Fabaceae		
<i>Vicia faba</i> L.	Fabaceae		
<i>Atropa belladonna</i> L.	Solanaceae		

These plants were grown outdoors in the Botanical Garden of the University of Würzburg.

All physiological studies, extractions of apoplastic sap and sugar analyses in whole leaves and in single cell samples were performed using mature fully expanded leaves (usually the third leaf from the top of the branch). For the isolation of RNA young leaves (up to 15%

size of the mature fully expanded leaf), mature leaves, stems and flowers were used. DNA was isolated from young leaves and seedlings of *Alonsoa meridionalis*.

For plant transformation experiments, *Arabidopsis thaliana* ecotype Columbia was used. *Arabidopsis* plants were grown in a growth chamber on Mini-tray soil (Baster Einheitserdewerk GmbH, Fröndenberg, Germany) at 22°C with a photon flux of 130 $\mu\text{mol m}^{-2}\text{s}^{-1}$ in a 16 hours light/8 hours dark cycle. For the collection of seeds, the inflorescences of plants were placed in paper bags. The seeds were cleaned from plant debris through a metallic sieve and stored at room temperature.

The transformants of *Arabidopsis* were grown in sterile culture as follows. The seed surfaces were sterilized in a chlorine atmosphere. For this purpose, ca. 50 μl volume of seeds in open 1.5 ml Eppendorf tubes and a glass containing 100 ml of 12-14% sodium hypochlorite solution were placed in a desiccator. After adding 5 ml fuming HCl to the hypochlorite solution and mixing vigorously, the desiccator was rapidly closed, vacuum was applied for about one minute, and the desiccator was left closed for 12 hours for seed sterilization. Then, the desiccator was opened under a clean bench. The plastic tubes with the surface-sterilized seeds were left open under the clean bench for several minutes.

The seeds were resuspended in 0.1% agar and placed on MS2-medium plates containing 50 $\mu\text{g/ml}$ kanamycin. The plates were sealed with tape and incubated for 2 days at 4°C in the dark. Then the plates were transferred into a growth chamber (13/11 hour light/dark period, 24°C, 63 $\mu\text{mol m}^{-2} \text{s}^{-1}$ photon flux). After about two weeks, the transformants were still keeping their green colour and had a developed root system whereas non-transformed seedlings were bleached due to the presence of kanamycin and had very poorly developed roots. The green seedlings were transferred to Mini-Tray soil and cultivated in a growth chamber.

MS2 (Murashige-Skoog) medium according to Murashige and Skoog (1962):

- | | |
|-----------|---|
| 4.405 g/l | Murashige and Skoog medium, micro- and macroelements including vitamins (Duchefa, Haarlem, The Netherlands) |
| 2% (w/v) | sucrose |

The pH was adjusted to 5.8 with KOH, and 0.8% (w/v) Select Agar (Gibco BRL) were added before autoclaving.

2.2.2. Bacteria

Cloning of DNA fragments was performed using the *Escherichia coli* strain DH5 α . For the expression of the stachyose synthase gene from *Alonsoa meridionalis* (2.22), the

E. coli strain BL21 (DE3) was used. For transformation of *Arabidopsis thaliana* (2.24), the *Agrobacterium tumefaciens* strain GV3101 (pMP90) was used.

Liquid cultures of *E. coli* cells were grown overnight at 37°C in a roller or shaker in either LB or TB medium supplemented with antibiotics. For growth on agar plates, 1.5% agar was added to the liquid medium before autoclaving. Antibiotics and other additives were pipetted into the melted agar medium under a clean bench after cooling the medium down to about 70°C.

A. tumefaciens cells were grown in liquid YEB medium or on YEB agar plates supplemented with antibiotics in a roller or shaker at 28°C. Usually, they needed two days to reach the stationary phase.

Bacterial Strain	Relevant Characteristics	Reference
<i>E. coli</i> DH5 α	F ⁻ , ϕ 80 Δ lacZ Δ M15, <i>endA1</i> , <i>recA1</i> , <i>hsdR17</i> (rk ⁻ , mk ⁺), <i>supE44</i> , <i>thi-1</i> , <i>gyrA96</i> , <i>relA1</i> , Δ (<i>lacZYA-argF</i>) U169, λ ⁻	Woodcock et al. (1989)
<i>E. coli</i> BL21 (DE3)	F- <i>ompT</i> [<i>lon</i>] <i>hsdSB</i> (rB ⁻ mB ⁻ ; an <i>E. coli</i> B strain) with DE3, a λ prophage carrying the T7 RNA polymerase gene under the control of the <i>lacUV5</i> promoter.	Studier and Moffat (1985)
<i>A. tumefaciens</i> GV3101 (pMP90)	GV3101 (Chr C58 Rif ^R) harbours the virulence helper plasmid pMP90 Gm ^R (oncogenic parent: pTiC58, nopaline type)	Koncz and Schell (1985)

LB (Luria – Bertani) medium (1 l):

10 g	Select Pepton 140
5 g	yeast extract
10 g	NaCl

TB medium (1 l):

900 ml TB1 and 100 ml TB2 were autoclaved separately and combined under a laminar flow hood afterwards.

TB1:

12 g	Select Pepton 140
24 g	yeast extract
4 ml	glycerol
ad 900 ml	dd H ₂ O

TB2:

2.3 g	KH ₂ PO ₄
16.4 g	K ₂ HPO ₄
ad 100 ml	dd H ₂ O

YEB medium (1l) :

5 g	beef extract (Difco, Becton Dickinson GmbH, Heidelberg, Germany)
1 g	yeast extract
5 g	Select Peptone 140
5 g	sucrose

The pH was adjusted to 7.3 – 7.4 with NaOH before autoclaving.

Agar (Select Agar), agarose, yeast extract and Select Peptone 140 were obtained from Gibco BRL, Eggenstein, Germany. All antibiotics were obtained from Sigma-Aldrich, Taufkirchen, Germany. For other additives, see 2.1.1. Water-soluble additives were filter-sterilized using sterile syringe filters with 0.2 µm pore size from Sarstedt (Nümbrecht, Germany). All additives were stored at –20°C.

Additives	stock solution	concentration in medium
Antibiotics:		
ampicillin	100 mg/ml in dd H ₂ O	100 µg/ml (1:1000)
kanamycin	50 mg/ml in dd H ₂ O	50 µg/ml (1:1000)
rifampicin	33 mg/ml in methanol	33 µg/ml (1:1000)
IPTG	100 mM in dd H ₂ O	200 µM (1:500)
X-Gal	2% (w/v) in DMF	0.004% (1:500)

2.2.3. Plasmids

Plasmid	Used for	Used in Organism/ Strain	Relevant Characteristics	Selection Marker	Source
pGEM®-T Easy	cloning of PCR products	<i>E. coli</i> DH5α	AT-cloning, blue/white selection of transformants	Amp ^R	Promega Madison WI, USA
pBluescript®-IIS ⁺	cloning of templates for <i>in vitro</i> transcription (pAmSTSish, pAmRSish and pAmSUTish)	<i>E. coli</i> DH5α	blue/white selection of transformants	Amp ^R	Stratagene, La Jolla, CA, USA

pET3b	construction of pET*/STS; expression in <i>E. coli</i>	<i>E. coli</i> DH5 α <i>E. coli</i> BL21 (DE3)	gene expression using T7 RNA polymerase expression system	Amp ^R	Rosenberg et al. (1986)
pET*/STS	expression in <i>E. coli</i>	<i>E. coli</i> DH5 α <i>E. coli</i> BL21 (DE3)	the plasmid contains the ORF of <i>Alonsoa</i> stachyose synthase under control of the T7 promoter	Amp ^R	this thesis
pBI101.3	construction of pBIstsA and pBIstsB	<i>E. coli</i> DH5 α	pRK origin, T-DNA region carries a polylinker upstream of the GUS ORF	Km ^R	Jefferson and Hirsch. (1986)
pBIstsA	transformation of plants using <i>A. tumefaciens</i>	<i>E. coli</i> DH5 α , <i>A. tumefaciens</i> GV3101, <i>A. thaliana</i> ecotype Columbia	plasmid carries a 1959 bp fragment of the <i>Alonsoa</i> stachyose synthase promoter (<u>including</u> the 5'-untranslated region) upstream of the GUS ORF	Km ^R (bacteria) Km ^R (plants)	this thesis
pBIstsB	transformation of plants using <i>A. tumefaciens</i>	<i>E. coli</i> DH5 α , <i>A. tumefaciens</i> GV3101, <i>A. thaliana</i> ecotype Columbia	plasmid carries a 1851 bp fragment of the <i>Alonsoa</i> stachyose synthase promoter (<u>without</u> 5'-untranslated region) upstream of the GUS ORF	Km ^R (bacteria) Km ^R (plants)	this thesis

2.3. Extraction of metabolites

2.3.1. Chloroform:methanol extraction

Chloroform:methanol extraction was performed for measurements of sugar and amino acid contents in fresh leaves or in gradient fractions obtained by non-aqueous fractionation (2.6).

Leaves were weighed and ground to a fine powder in liquid nitrogen using a mortar and a pestle. 300 mg of powder were added to 5 ml of a chloroform:methanol mixture (1.5:3.5 v/v) in a plastic tube. When working with gradient fractions, the dried sediments were extracted in 5 ml of a chloroform:methanol mixture. The samples were mixed vigorously for 2 min and kept on ice for 30 min. 3 ml of water were then added to the homogenates, and the separation of two phases (the upper water/methanol phase and the lower chloroform phase) was achieved by centrifugation of the samples at 5000 rpm for 5 min in a Hettich EBA 3 S centrifuge (Hettich, Tuttlingen, Germany). The upper (aqueous) phase was saved, and the rest was extracted once more with 3 ml of water. The aqueous phases were combined and dried completely in a rotary evaporator at 34°C. The dried residues were dissolved in 2 ml ultrapure H₂O (Millipore), filtered through a syringe with a cellulose-nitrate membrane filter (0.45 μ m; Schleicher and Schuell, Germany) and stored at -80°C.

2.3.2. Isolation of galactinol and antirrhinoside from plant material

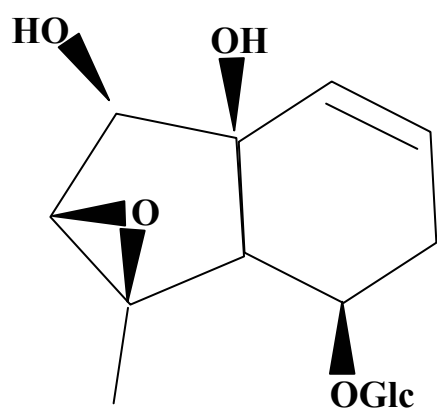
2.3.2.1. Preparative isolation of galactinol

The method of Pharr et al. (1987) was used with some modifications. Plant material with a high content of galactinol had to be used. Leaves from several plant species known to produce galactinol were analysed by HPLC. The analysis showed that leaves of *Buddleja davidii* contained the highest amount of galactinol (up to 0.9 mg per g fresh weight). 450 g of *Buddleja* leaves were ground to a powder in liquid nitrogen and extracted in 1.5 L of a chloroform:methanol mixture on ice for 30 min (see 2.3.1). Then, 500 ml dd H₂O were added, and phases were separated by centrifugation for 20 min at 11 000 g (Sorvall DuPont, Dreieich, Germany; rotor GS3). The upper (aqueous) phase containing the water-soluble metabolites was saved. The rest was extracted once again with 400 ml dd H₂O. The upper phases from both centrifugation steps were combined, and the volume was reduced to 100 ml in a rotary evaporator at 34°C. Then, cations were removed from the extract by adding a cation exchanger Dowex AG 50W-X8 (in H⁺-form) and stirring for 30 min. The supernatant was decanted, and the procedure was repeated with 1/10 volume of Polyclar AT (Sigma) to remove polyphenols and polysaccharides. The extract was filtered through a paper filter to remove the Polyclar AT. Afterwards, the volume of the extract was reduced to 10 ml in the rotary evaporator and the extract was applied to an anion exchange column of 50 cm length and 2.8 cm diameter filled with Dowex 1x8 (OH⁻-form). Passing the extract through the column allowed the removal of anions and at the same time led to a separation of the extract into fractions with different sugar composition. The elution was performed with 0.2 M NaOH at a rate of 2.5 ml/min. 120 Fractions (5 ml per fraction) were collected. The sugar composition of the fractions was determined by HPLC (2.8.1). Galactinol eluted after about 2 hours and was found in the fractions No. 60-80. No other sugars were detectable in these fractions. The galactinol-containing fractions were combined and neutralized using 5 M HCl. This step was necessary because the presence of 0.2 M NaOH in the eluate might lead to the condensation (caramelization) of sugars under alkaline conditions during the following concentration of the combined fractions. Then, the fractions were combined and the volume was reduced to 10 ml in the rotary evaporator at 34°C. In this step, NaCl had been concentrated to up to 2 M which would interfere with the following stachyose synthase activity assay. Therefore, NaCl was removed from galactinol by descending paper chromatography. Two pieces of 18 cm x 45 cm from chromatography paper Whatman Chr 17 were used. The running solution was n-propanol:ethyl acetate:H₂O=7:1:2. For the detection of galactinol, a thin strip was cut off and developed in detection solution (2.5 ml of a saturated

AgNO₃ solution in 500 ml acetone) for 2.5 min. The strips were then transferred to the stop solution (10 g NaOH in 15 ml H₂O added to 500 ml of 96% EtOH). NaCl moved along the chromatogram faster than galactinol, but even after nine hours, the separation was not complete. A large part of the galactinol had not yet been separated from the NaCl and thus was lost. The part of the chromatogram containing galactinol was cut into pieces and galactinol was eluted with 200 ml dd H₂O in an ultrasonication bath for 20 min (Branson Sonifier B 15, Branson Ultrasonics Corp., Geneva, Switzerland). The elution was repeated three times. The eluates (600 ml in total) were combined and the volume was reduced in the rotary evaporator at 34°C to concentrate the galactinol. Then, the concentration of galactinol was determined by HPLC (2.8.1). Altogether, 35 mg of galactinol were isolated from 450 g of leaves.

2.3.2.2. Preparative isolation and confirmation of the chemical structure of antirrhinoside

The isolation of antirrhinoside from leaves of *Asarina* was performed in the same way as that of galactinol (2.3.2.1). 100 g leaves of *Asarina* with an antirrhinoside content of up to 15 mg/g fresh weight were harvested. After elution from paper chromatograms with dd H₂O and concentration in a rotary evaporator, 35 ml of ca. 30 mM antirrhinoside solution were obtained (i.e. ca. 350 mg antirrhinoside). From this solution, 5 ml (ca. 50 mg antirrhinoside dissolved in water) were used for the analysis of the chemical structure of antirrhinoside by NMR at the Institute for anorganic chemistry, University of Göttingen (Figure 2.1).



Antirrhinoside

Figure 2.1. An unknown compound isolated from the leaves of *Asarina barclaiana* was identified by NMR as an iridoid glucoside antirrhinoside. Antirrhinoside was also a major component of the phloem exudate of *Asarina barclaiana*.

2.4. Extraction of apoplastic sap (intercellular washing fluid)

The intercellular washing fluid (IWF) was obtained from leaves according to the method of Speer and Kaiser (1991) and Lohaus et al. (2001). Leaves were detached from the plants and infiltrated with 50 mM CaCl₂ solution using a 60 ml syringe. Prior to the infiltration, the infiltrating solution was cooled on ice. Fully infiltrated leaves were transparent. The leaves were then carefully blotted dry, positioned into a 10 ml vessel located on top of a centrifuge tube and centrifuged for 5 min at 80 – 160g and 4°C (Megafuge 1.0, Heraeus Sepatech, Osterode), the time interval between infiltration and centrifugation being no longer than 5 min. By this procedure, between 50 and 200 µl of apoplastic sap diluted with the infiltration solution were obtained per gram fresh weight.

Apoplastic sugar concentrations in the leaves were determined on the basis of the dilution factor F

$$F = (V_{\text{apoplast}} - V_{\text{gas space}}) / V_{\text{gas space}}$$

The volume of the apoplastic gaseous phase was calculated from the difference of the fresh weight of leaves before and after the infiltration. Apoplastic sugar concentrations were calculated under the assumption that the apoplastic water phase of leaves is about 10% of the leaf volume (Lüttge and Higinbotham, 1979; Speer and Kaiser, 1991). For the leaves of *Alonsoa meridionalis*, a more precise estimation of the volume of the liquid apoplast was made as follows. Leaf discs were floated on water until completely hydrated. Leaf discs were then infiltrated with water containing 0.005 µCi/ml ¹⁴C-sorbitol. After a centrifugation for 5 min at 80 – 160g and 4°C, the radioactivity of the obtained intercellular washing fluid was determined in a liquid scintillation analyser (Packard 1900 TR, Canberra-Packard, Dreieich, Germany). The dilution of the radioactivity of the infiltration solution due to the apoplastic water phase was calculated and its volume was determined:

$$V_{\text{apoplast}} = V_{\text{gas space}} (\text{dpm}_{\text{infiltrated solution}} - \text{dpm}_{\text{IWF}}) / \text{dpm}_{\text{IWF}}$$

The absence of cellular contamination of the apoplastic extracts was proven by measurements of the activity of glucose-6-phosphate dehydrogenase (G6PDH) in the samples (2.5.1). The activities of G6PDH in leaves and apoplastic extracts were compared. For further measurements, only apoplastic extracts were used with less than 0.01% of total leaf G6PDH activity detected in the apoplastic extract.

2.5. Determination of enzyme activities

The activities of the enzymes listed below were measured in leaf extracts (2.5.1, 2.5.6.1), density gradient fractions (2.5.2, 2.5.3, 2.5.4), apoplastic extracts (2.5.1, 2.5.5) and

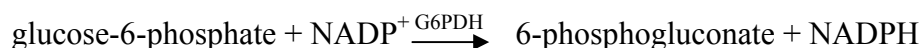
bacterial cells (2.5.6.2). The OD measurements were performed using a double-beam photometer Uvikon 932, Kontron (2.5.1, 2.5.2, 2.5.4) or a two wavelength spectrophotometer Sigma SFP 22 (2.5.3, 2.5.5).

2.5.1. *Glucose-6-phosphate dehydrogenase (G6PDH)*

Leaves (ca. 0.3 g) were homogenized with 0.1 g Polyclar AT, 20 mg Na-ascorbate and 2 ml buffer (0.1 M NaH₂PO₄ : 0.1 M Na₂HPO₄ = 1:2 v/v, pH 7.4). The homogenate was centrifuged and the activity of G6PDH was determined by adding 10 µl supernatant or 10 – 50 µl apoplast extract (IWF) to a 1 ml reaction volume containing

Tricine pH 8.0	0.1 M
NADP	1 mM
MgCl ₂	5 mM
glucose-6-phosphate	10 mM

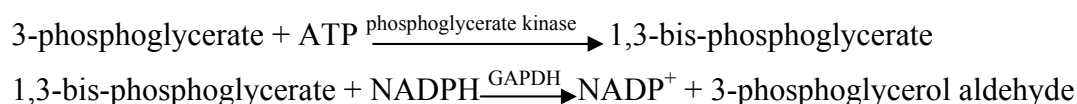
The activity was calculated based on an increase in absorbance at 340 nm due to the formation of NADPH in the reaction



using a molar extinction coefficient for NADPH of 6.22 mM⁻¹cm⁻¹ at 340 nm.

2.5.2. *NADP-dependent Glyceraldehyde 3-phosphate dehydrogenase (GAPDH)*

The activity was measured using 20 µl of density gradient fraction extracts (2.6.3) in a total volume 600 µl. The method is based on a decrease in the absorbance at 340 nm due to the oxidation of NADPH in two coupled reactions (Wirtz et al., 1980):



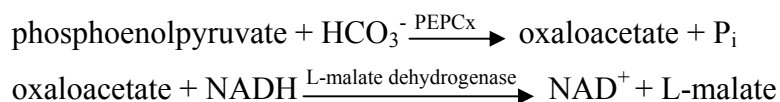
The activity was calculated using a molar extinction coefficient for NADPH of 6.22 mM⁻¹cm⁻¹ at 340 nm.

The reaction mixture contained

HEPES-KOH pH 8.0	0.1 M	
KCl	20 mM	
Na ₂ -EDTA	2 mM	
MgCl ₂	30 mM	
DTT	200 mM	
ATP	200 mM	
NADPH	10 mM	
phosphoglycerate kinase	6 U	
3-phosphoglycerate	200 mM	(start)

2.5.3. *Phosphoenolpyruvate carboxylase (PEPCx)*

70 μ l of extracts of each density gradient fraction (2.6.3) were used for this assay. The assay volume was 600 μ l. The enzyme activity was determined based on a decrease in the absorbance at 334 nm due to the oxidation of NADH in two coupled reactions (Stitt et al., 1978):



The activity was calculated using a molar extinction coefficient for NADPH of $6.18 \text{ mM}^{-1} \text{ cm}^{-1}$ at 334 nm.

The reaction mixture contained

glycylglycine pH 7.9	50 mM	
MgCl ₂	10 mM	
KHCO ₃	4 mM	
NADH	20 mM	
L-malate dehydrogenase	4.8 U	
PEP	8 mM	(start)

2.5.4. α -Mannosidase

The activity of α -mannosidase was determined according to Ye-The (1967) based on an increase in the absorbance at 405 nm due to the formation of p-nitrophenol in the reaction



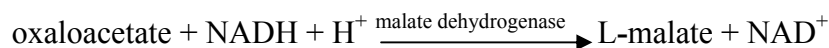
50 μ l of extracts of each density gradient fraction (2.6.3) were used for this enzyme assay which took place in a total volume of 1050 μ l. The reaction mixture contained:

sodium citrate pH 4.5	50 mM
p-nitrophenyl- α -D-mannopyranoside	4.8 mM

The assay mixture was incubated at 37°C for 50 min. Then the reaction was stopped by the addition of 500 μ l 0.8 M boric acid (pH 9.8). The enzyme activity was calculated using a molar extinction coefficient for p-nitrophenol of $18.5 \text{ mM}^{-1} \text{ cm}^{-1}$ at 405 nm.

2.5.5. *Malate dehydrogenase*

The activity was measured based on a decrease in the absorbance at 334 nm due to the oxidation of NADH in the reaction



The reaction mixture contained in a total volume of 1 ml:

25 μ l apoplastic extract (IWF)

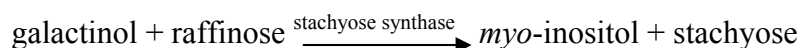
850 µl MOPS pH 7.5	0.1 M	
25 µl NADH	20 mM	
100 µl oxaloacetate in MOPS	20 mM	(start)

2.5.6 Stachyose synthase activity assays

2.5.6.1 Establishment of the *AmSTS* activity assay using leaves of *Alonsoa*

250 – 350 mg of *Alonsoa* leaves were ground on ice in 2 ml of extraction buffer using mortar and pestle. Extraction buffers with four different pH values, 5.5, 6.0, 6.5 and 7.0 were used to determine the pH optimum of *AmSTS*. The extracts were transferred into 2 ml plastic Eppendorf tubes and centrifuged for 5 min at 4°C. The supernatants were desalted on Sephadex G25 columns (Amersham Pharmacia Biotech, Freiburg, Germany). Before desalting, the columns were equilibrated with 25-40 ml Na phosphate buffer by applying buffer on the column and centrifuging at 1800 rpm for 2 min (Megafuge 1.0, Heraeus Sepatech, Osterode, Germany). Before the application of the protein extracts, the columns were emptied by centrifugation for 5 min at 2000 rpm. For desalting, 4 ml of each supernatant were pipetted onto a column and centrifuged for 5 min at 2000 rpm. The recovered desalted extracts were kept on ice until use.

The activity of *Alonsoa* stachyose synthase was determined by measurements of a time-dependent formation of stachyose in the assays according to the reaction:



The assays were performed at 30°C in 1.5 ml Eppendorf tubes in a total volume of 100 µl containing (final concentrations):

sodium phosphate buffer pH 6.5	50 mM
galactinol	1 mM
raffinose	4 mM
DTT	0.6 mM

The reaction was started by the addition of 25 µl of protein extract. To stop the reaction, the tubes were placed at 100°C for 5 min. Aliquots were stopped at 0, 20, 40, 60, 80, 100 and 120 min, to reveal a time course of the reaction. For the first timepoint, the tubes were placed at 100°C immediately after the addition of the extract. After 5 min incubation at 100°C, the tubes were centrifuged for 5 min at 13 000 rpm and the sugar contents of the supernatants were analysed by HPLC (2.8.1). Negative control reactions were performed for 80 min under the same conditions but galactinol was omitted from the assay mixture.

2.5.6.2 *AmSTS* activity assay in protein extracts of *E. coli* BL21 (DE3) (pET*/STS)

The extraction buffer was prepared from Na phosphate stock solution. Other components were added freshly before the extraction. The pelleted cells were resuspended in 10 ml extraction buffer and broken up via four cycles of ultrasonication on ice (15 sec pulse and 45 min pause) in Branson Sonifier B 15 (Branson Ultrasonics Corporation, Geneva, Switzerland). The broken cells were spun down in a Sorvall ultracentrifuge at 4°C and 12 000 g for 20 min. The supernatants were saved and desalted on Sephadex G25 columns as described in 2.5.6.1. The protein extracts recovered from the columns were kept on ice until use for stachyose synthase activity assays.

Extraction buffer:

Na phosphate, pH 6.5	50 mM
DTT	5 mM (freshly added)
Protease inhibitor cocktail	1:200 (freshly added)
(Roche Molecular Biochemicals, Mannheim, Germany)	

The assays were performed at pH 6.5 which has been established as the pH optimum of *AmSTS* from *Alonsoa* leaves. Other conditions were as indicated in 2.5.6.1. The reaction was started by the addition of 49 µl protein extract from BL21 (DE3) (pET*/STS) or BL21 (DE3) (pET3b), respectively. The negative control reactions were performed with extracts from both strains with reaction mixtures lacking galactinol.

2.6 Non-aqueous fractionation of leaves

2.6.1. Preparation of leaf material

Leaves were cut from the plants after 5 hours of the light period. The middle rib was removed, and the samples were ground to a fine powder in liquid nitrogen in a precooled mortar. The leaf tissue powder was then placed in a plastic box and, after the nitrogen had evaporated but before the samples had begun to thaw, transferred into a lyophilizer Lyovac GT3 (Leybold-Heraeus, Köln, Germany). The powder was lyophilized at -25 °C for 5 days. The lyophilizer was opened under nitrogen atmosphere. The plastic box with the leaf tissue powder was placed in a desiccator and stored at -20°C until fractionation on a density gradient.

2.6.2. Non-aqueous fractionation of leaf tissue in a density gradient

The separation of the leaf tissue into fractions enriched with either chloroplastic, cytosolic or vacuolar content was achieved by a centrifugation in an exponential density gradient (Gerhard and Heldt, 1984). The liquid constituents of the gradient were virtually non-

aqueous (heptane and tetrachloroethylene). This prevented the redistribution of the water-soluble metabolites and enzymes during the separation of the plant material within the gradient and therefore made it possible to attribute the amounts of metabolites to the subcellular compartments determined via the activities of specific marker enzymes. Spatial separation of subcellular components within the density gradient occurs due to different density of membranes from cell compartments (Gerhardt and Heldt, 1984).

For the preparation of the density gradient, two solutions of different density (solution A and solution B) were used which were prepared from heptane ($\rho = 0.68 \text{ g/cm}^3$) and tetrachloroethylene ($\rho = 1.62 \text{ g/cm}^3$) at least two days before the fractionation procedure. The densities were for *Alonsoa*:

Solution A: 1.29 g/cm^3

Solution B: 1.58 g/cm^3

and for *Asarina*:

Solution A: 1.34 g/cm^3

Solution B: 1.62 g/cm^3 .

The solutions were stored over a layer of a water adsorbent (Molecular sieve $0.4 \mu\text{m}$, Merck, Darmstadt, Germany) at 4°C . It was important to prepare the solutions A and B from fresh tetrachloroethylene as well as to protect tetrachloroethylene and the solutions from light because the formation of Cl radicals during the storage would have resulted in the complete inhibition of the activities of the marker enzymes in the fractions.

The following steps were performed at 4°C . The exponential density gradient was prepared in a cellulose nitrate centrifuge tube. 1 ml of solution B was pipetted into the tube and carefully underlayered with 0.5 ml of tetrachloroethylene using a Pasteur pipette. This was overlaid with 9.2 ml of a mixture of solutions A and B with exponentially changing density prepared in a gradient mixer. The lyophilized leaf tissue powder (about 200 mg) was suspended in 2 ml of solution A and vortexed. Then the powder was ultrasonicated in a Branson Sonifier B 15 (Branson Ultrasonics Corp., Geneva, Switzerland) while being kept in a heptane bath containing dry ice according to the following scheme:

2 minutes: 5 s pulse / 5 s pause

1 minute: 5 s pulse / 25 s pause

1 minute: 5 s pulse / 5 s pause.

Afterward, the powder was filtered through a metallic sieve and poured into 4 plastic 10 ml-centrifuge tubes which then were filled up with heptane. After centrifugation for 2 min at 3000 rpm (Megafuge 1.0, Heraeus Sepatech, Osterode) the supernatant was discarded, and

the sediments were resuspended in 2 ml of solution A and filtered through a nylon net with 40 μm pore size. From this filtrate, 200 μl were saved for the determination of the activities of the marker enzymes and of metabolites in the leaf tissue before fractionation. 1.5 to 2 ml of the filtrate were carefully pipetted on the top of the gradient. The separation in the gradient was performed by centrifugation at 4°C at 25 000 x g for 130 min (Sorvall Du Pont, Dreieich, Germany) using an HB4 rotor. The separated material was collected in six or seven fractions, of which two aliquots were taken for the determination of activities of the marker enzymes (ca. 600 μl) and metabolites (ca. 800 – 1000 μl). The exact volumes were noted. The aliquots were pipetted into 1.5 ml plastic Eppendorf tubes containing ca. 100 μl quartz sand, filled up with heptane and centrifuged at 13 000 rpm for 15 min. The supernatant was discarded, the sediments were dried in the desiccator and stored at –80 °C until used for the determination of the marker enzyme activities and metabolite contents.

2.6.3. Determination of the activities of marker enzymes in the gradient fractions

The enzymes NADP-dependent glyceraldehyde 3-phosphate dehydrogenase, PEP-carboxylase and α -mannosidase were used as markers for chloroplast, cytosol and vacuole, respectively. Usually, the chloroplastic material was found to be concentrated in the middle region of the gradient, the cytosolic material appeared in the lower region whereas the vacuolar material was mainly found in the fraction of highest density. Dried sediments were resuspended in 500 μl of potassium-phosphate buffer (50 mM pH 7.5) containing 1 mM DTT, vortexed for 1 min and kept on ice for 5 min for extraction of the proteins. Then, another 500 μl buffer were added, and the samples were centrifuged at 13 000 rpm for 2 min at 4°C. The supernatants were used for the measurements of the enzyme activities (2.5.2 – 2.5.4) and for determination of the protein concentration (2.6.6).

2.6.4. Determination of metabolite concentrations in the gradient fractions

For determination of metabolite concentrations in the gradient fractions, a chloroform:methanol extraction of the resuspended fraction was performed (2.3.1). The dried sediments were extracted in 5 ml of the chloroform:methanol mixture. The vacuum-dried extracts were redissolved in 700 μl H₂O (Millipore) and used for HPLC analyses of sugars and amino acids (2.8.1.).

2.6.5. Calculation of the subcellular distribution of metabolites

For the evaluation of the subcellular distribution of sugars and amino acids between the stromal, cytosolic, and vacuolar compartments, a calculation procedure according to Riens et al. (1991) was used. This calculation method is based on the assumption that the

metabolites are confined to the three biggest cellular compartments (chloroplasts, cytosol and vacuole), designated by the corresponding marker enzymes. The evaluation is done by a computer program testing all possible cases for the percentage distribution of a certain metabolite between the three compartments at intervals of 1%. With this interval, 5151 distribution patterns can be analysed. The program calculates which of these 5151 patterns yields the best fit (agreement) with the experimental results. A coefficient Q is taken as the measure for the best agreement:

$$Q = \sqrt{\sum r_i^2 / (n-1)},$$

where r_i is the difference between the measured and the calculated distribution for each fraction and n is the number of the fractions.

To avoid the results being falsified by analytical errors, the calculations are usually based on mean values obtained from measurements from at least three density gradient fractionations. Only the results with the lowest Q value were used.

2.6.6. Determination of the chlorophyll:protein ratio

The chlorophyll:protein ratio was determined for each preparation of leaf tissue powder. A sample of the powder (about 50 mg) was dissolved in 5 ml potassium phosphate buffer (2.6.3), ultrasonicated for 1 min (5 sec pulse and 5 sec pause) and filtered through a nylon net with 40 μm pore size. In the filtrate, the protein concentration was determined according to Lowry et al. (1951) (2.7). Chlorophyll was extracted from the filtrate by the addition of 99% ethanol so that the final ethanol concentration of the extract was adjusted to 80%. The optical density of the extract was measured at 652 nm in a spectrophotometer (Uvikon 932, Kontron) against 80% ethanol. The amount of chlorophyll was calculated using an extinction coefficient of 36 ml mg^{-1} Chl cm^{-1} at 652 nm (Arnon, 1949).

For each density gradient fractionation, the total protein amounts in the fractions were compared with the protein amount in the leaf tissue powder before fractionation. The percentage of recovery characterized the loss of leaf material during the fractionation procedure. For most gradients, the recovery of protein from the fractions was between 85% and 100%, and only the gradients with recovery rates better than 90% were taken for the calculation of the subcellular distribution of metabolites. Based on the known chlorophyll:protein ratio, the amounts of metabolites were recalculated as $\mu\text{mol}/\text{mg}$ Chl which allowed the comparison between several gradients from independent preparations of leaf tissue powder.

2.7. Protein determination

The protein concentrations were measured in gradient fractions from *Alonsoa* and *Asarina* leaves according to Lowry et al. (1951). Before an analysis, a solution containing A:B: C = 99:0.5:0.5 was freshly prepared from the stock solutions:

Solution A = 2% (w/v) Na₂CO₃ in 0.1 M NaOH

Solution B = 1% (w/v) CuSO₄ x 5H₂O

Solution C = 2% (w/v) Na-K-tartrate

130 µl water, 20 µl of the sample and 700 µl ABC mixture were pipetted together, vortexed and incubated for 15 min. Afterwards, 100 µl of Folin-Ciocalteu's phenol reagent (diluted 1:2) were added, and the samples were incubated for 10 min. From each sample, two aliquots were analysed. A third aliquot was used to determine the background absorbance at 578 nm. For this purpose, the 20 µl aliquot was added to the reaction mixture only after both incubations were completed. The samples were centrifuged for 2 min at 13 000 rpm in an Eppendorf centrifuge and the extinction was measured at 578 nm. For each analysis, a calibration curve was made using BSA solutions in the same buffer as used for the sample extraction. The calibration curve points corresponded usually to 9, 18, 27, 36 and 45 µg protein in the sample.

2.8. Sugar analysis

2.8.1. HPLC

Sugars in leaf extracts, density gradient fractions and apoplastic washing fluid samples were assayed by HPLC. An anion exchange column (CarboPAC10; Dionex Corp, Sunnyvale, CA., USA) was used for the determination of mono-, di- and oligosaccharides. Another column, MA1, from the same firm allowed a better resolution in the region of polyols and cyclitols. Both columns were eluted with NaOH using the LC-9A pump from Shimadzu (Kyoto, Japan).

The CarboPAC10 column was eluted isocratically with 80 mM NaOH with a flow rate of 1 ml min⁻¹ and the MA1 column with 600 mM NaOH with a flow rate of 0.4 ml min⁻¹. Both solutions were prepared using Millipore water washed with helium for 15 min to prevent the formation of NaHCO₃. NaOH (50%) of the purest quality commercially available was used (Baker, England), which resulted in a good stability of the base line.

An autosampler # 2157, Pharmacia, LKB was thermostated at 12 °C. Sugars were detected by a thin layer amperometric cell (ESA, Model 5200, Bedford, USA) with a gold

electrode. A Pulse amperometric detector (Coulchem II, Bedford, USA) set a pulse according to the following scheme:

pulse mode	voltage	duration	measure
measurement	50 mV	500 ms	400 ms
clearance	700 mV	540 ms	
regeneration	-800 mV	540 ms	

The calibration was done with 50 μ M, 100 μ M, 250 μ M and 500 μ M sugar concentrations. *Myo*-inositol, galactinol, mannitol, sorbitol, glucose, fructose, sucrose, raffinose, stachyose and verbascose were used as standards and showed a linear range of the detector response between 50 and 500 μ M ($r^2 = 0.99$). Plant samples were diluted before measurements to provide concentrations within this range. The evaluation of chromatograms was performed with the integration program Peaknet 5.1 (Dionex, Idstein, Germany).

2.8.2. Enzymatic measurements of glucose, fructose and sucrose

In some samples of apoplastic washing fluid glucose, fructose and sucrose contents were measured by enzymatic reactions (Bergmeyer, 1983). Glucose was measured by the hexokinase/glucose-6-phosphate dehydrogenase-linked assay. The total volume of the reaction mixture (1 ml) contained:

Sample	10 - 50 μ l
Tricine pH 8.0	0.1 M
NADP	1 mM
MgCl ₂	5 mM
ATP	1 mM
Glucose-6-phosphate dehydrogenase	0.5 U
Hexokinase	0.75 U

Glucose-6-phosphate dehydrogenase was added first, and after the stabilization of the absorbance the reaction was started by the addition of hexokinase to the assay mixture.

After the reaction was completed, fructose was measured by the addition of phosphoglucose isomerase (0.5 U per reaction) to the hexokinase/glucose-6-phosphate dehydrogenase-linked assay.

In parallel, sucrose was measured as glucose released after hydrolysis with invertase. For this purpose, another aliquot of the same sample was pipetted into a cuvette containing in a total volume of 300 μ l:

Na-acetate pH 4.5	0.1 M
-------------------	-------

invertase	2 U
sample	10 – 50 μ l

The reaction proceeded for 10 min. Then, 700 μ l of 0.1 M tricine pH 8.0 were added to the reaction mixture which resulted in a pH shift to 7.5. NADP, ATP and $MgCl_2$ were added up to the concentrations listed for glucose determination. Glucose-6-phosphate dehydrogenase was added as well, and the reaction was started by the addition of hexokinase.

From the increase in the absorbance at 340 nm (see 2.5.1), the amount of NADPH formed in the reactions could be calculated which was stoichiometrically related to the amounts of the oxidized sugars (Bergmeyer, 1983). The amount of sucrose was calculated as the difference between glucose amounts measured after and before the hydrolysis of the sample by invertase.

2.9. Determination of the osmolality of the leaf sap

Discs were cut from the leaves, placed in 1.5 ml Eppendorf tubes and frozen at $-20^{\circ}C$. The thawing resulted in the exudation of cellular sap from the tissue. This sap was used for the determination of the osmolality. The osmometer Wescor 5100B was calibrated using 290 mOsmol kg^{-1} and 1000 mOsmol kg^{-1} standards. An 8 μ l sample of tissue sap was added onto a 5-mm diameter paper disc. The disc was then transferred to the sample holder of the osmometer, and the osmotic pressure was determined according to the instruction provided by the manufacturer.

2.10. Analyses in single cell sap

Single cell sap was extracted from individual epidermal and mesophyll cells by the glass microcapillary technique and analysed for sugar contents as described in Koroleva et al., 1997.

2.10.1. Single cell sampling

For sampling, drawn-out „sampling“ capillaries were used where the exact volume was not important. The capillaries were produced from 1 mm (external diameter) glass capillary tubing (Clark) using a commercial micropipette puller (Harvard Apparatus Ltd., Kent, UK). The very end of each capillary was broken off on a de Fonbrune microforge (Technical Products International Inc., O`Fallon, MI., USA) to produce an aperture of the required diameter. Prior to use, a microcapillary was back-filled with low-viscosity water-saturated paraffin oil (Sigma). It was then connected to a 50 ml plastic syringe and a foot-operated solenoid valve by a series of plastic tubing. The capillary was mounted on a

micromanipulator (Leica, Nussloch, Germany). Use of a stereo microscope (Wild M8, Leica, maximum magnification 160x) allowed the tip of the microcapillary to be precisely aligned with the desired cell. The cell was punctured by moving the tip of the capillary with the micromanipulator. The cell turgor forced the cellular content into the microcapillary. The microcapillary was rapidly removed from the sampled cell and immersed under water-saturated liquid paraffin (previously centrifuged at 1300 g for 10 min). Ejection of the single cell sample under oil allowed the determination of osmotic pressure and sugars (glucose, fructose and sucrose) by enzymatic assay.

2.10.2. Osmolality of single cell sap

The osmotic pressure of single cell sap was measured by freezing point osmometry (Malone et al., 1989; Tomos et al., 1994). A custom-made picoliter osmometer was used to determine the freezing point of single cell saps. The temperature of the Peltier stage of the osmometer was rapidly cooled to -40°C to overcome the effects of supercooling and to induce freezing before returning to about -2°C . Using a stereo microscope, minute ice crystals in each microdroplet were seen to decrease in size as the stage temperature was slowly increased from -2°C to $+1^{\circ}\text{C}$. The melting point of each droplet was then recorded as the approximate temperature displayed at the osmometer hand-set at which the last ice crystal melted and just disappeared. This temperature was then referenced against the melting point of standard solution series of KCl with known osmotic pressure measured in the same way.

2.10.3. Sugar concentrations in single cell sap

Constriction capillaries (constriction pipettes) were used for measuring identical volumes of samples, standards or reagents. Exact volumes are usually unknown and samples were measured by comparison with concentration standards using the same pipette. Constriction pipettes were produced at the microforge. A heated fine-gauge filament was aligned closely with one side of pipette. Upon applying a current to the filament, the glass melted leading to constriction of the lumen as the pipette bent towards the heat. Constriction pipettes of various volumes (from ca. 10 pl to ca 5 nl) could be produced in this way.

Glucose, fructose and sucrose were measured in single cell samples using imidazole buffer containing additives in the following concentrations:

imidazole-HCl buffer pH 7.5	68 mM
MgCl ₂	5.6 mM
ATP	5.6 mM
NADP	23.8 mM

KH ₂ PO ₄	1.2 mM
BSA	0.1 % (w/v)

The enzymes were dissolved in the imidazole buffer containing additives. The following concentrations of the enzymes were used:

G6PDH	43 U/ml
Hexokinase	85 U/ml
Phosphoglucose isomerase	175 U/ml
Invertase	1330 U/ml

(an excess of invertase was necessary because the pH conditions were suboptimal).

Constriction pipettes of ca. 4 nl volume were used for pipetting droplets of buffer under paraffin oil. 100 pl pipettes were used for enzymes and 20 pl pipettes for samples and standards. Using the same pipette for both samples and standards enabled a calibration of the assay.

Four sets of droplets of buffer with cofactors were pipetted to the glass slide inside a 4-mm deep aluminum ring under paraffin oil. The first set was used for the determination of glucose and fructose in the single cell samples, the second for the determination of sucrose in the same samples, and the two other sets were used in the same way to provide a calibration with standards (50, 100 and 200 mM solutions of glucose, fructose and sucrose). Hexokinase and either samples or standards were pipetted into all droplets. Then, invertase was added to those droplets where the sucrose concentration was measured, and the droplets were incubated for 5-10 min to allow the completion of the reaction.

The commonly used principle of enzymatic determination of sugar concentrations based on the different optical densities of the reduced and oxidized forms of NADP(H) at 340 nm was not suitable for single cell samples. The reason is the very small volume of the samples which does not allow single wavelength absorption measurements. Enzymatic assays of the single cell sap, therefore, have to make use of the ability of the reduced cofactors to fluoresce at 460 nm when excited with light at their absorbing wavelength ($\lambda_{\text{max}} = 340 \text{ nm}$).

A fluorescent microscope equipped with a photometer (MPV Compact 2 Fluorovert, Leitz, Wetzlar, Germany) measured the increase in fluorescence in the droplets. The signal was measured against a dark background. The initial fluorescence of the droplets was recorded, and G6PDH was added to all droplets. The measurements of the fluorescence were repeated in intervals of 1 min until the fluorescence stabilized. After that, phosphoglucose

isomerase was pipetted into the droplets. This initiated the fluorescence increase due to fructose oxidation. The increase in fluorescence was plotted against the concentrations of the standards, and the concentrations of glucose and fructose in the single cell samples were calculated from these calibration curves. For the determination of sucrose, the glucose concentration in the invertase-treated samples was calculated from the sucrose standard calibration curve and corrected based on the glucose concentration measured in the samples.

2.11. Inhibition of phloem translocation

In a series of experiments, the accumulation of sugars in the leaf apoplast caused by export inhibition was studied. To prevent assimilate export from the leaves, three experimental procedures were used.

(1) *Cold block*. Ice wrapped in tissue was applied to the petiole of leaves (Webb and Gorham, 1965). Ice lost by melting was replaced. Both control and cold-blocked leaves were harvested after periods of 1, 2, 4 and 6 hours, respectively, after cold jacket application.

(2) *Girdling*. Two shrubs, *Ligustrum* and *Atropa*, were taken for girdling experiments. Leaves were harvested from the plants at 10 a.m. and after that, a ring of bark was removed from several branches. After 3, 9 and 24 hours leaves were harvested from both intact and girdled branches.

(3) *Placement of detached leaves in CaCl₂ or EDTA*. In the experiments with *Alonsoa* and *Asarina*, leaves were cut from these plants, and the petioles were placed in 2 mM CaCl₂ solution for 24 hours. During this time, the leaves were kept under continuous light of 500 $\mu\text{mol photons m}^{-2} \text{ s}^{-1}$. After that, the apoplastic exudate (IWF) was obtained from the leaves as described in 2.4, and the leaves were extracted with chloroform:methanol (2.3.1). The sugar contents were determined in IWF samples and in leaf extracts. In the experiment in which the incubation in CaCl₂ solution was compared with that in 2 mM Na-EDTA, leaves from *Mentha sp.* and *Chrysanthemum sp.* grown outdoors were sampled at 10 a.m., placed in either 2 mM CaCl₂ or 2 mM Na-EDTA (pH 6.5) and exposed to a photon flux density of 1800 $\mu\text{mol m}^{-2} \text{ s}^{-1}$. After 30 min, solutions were replaced with water to prevent wilting, and the incubation was continued for 2 hours. The leaves from both species were taken for the determination of apoplastic sugars (2.4).

2.12. Study of sugar uptake from the apoplast *in vivo*

2.12.1. Feeding experiments

Petioles of leaves were cut under water or, depending on the experiment, under 20 mM EDTA to prevent sealing of the cut phloem, and left in the solution for 30 min (King and

Zeevaart, 1974). Subsequently, the leaves were infiltrated with either pH- or membrane potential-sensitive fluorescent dye solution (2.12.3) and left for 5 min to allow the distribution of the fluorescent dye within the apoplast. Excess infiltrate was removed by centrifugation for 5 min at 450 g at room temperature. Part of a leaf was then enclosed in a sandwich-type cuvette with two windows on the upper and lower side (diameter 2.4 cm). The petiole of the leaf protruded from the cuvette and was kept in water. The leaves were left in darkness, to make sure that the leaf production of CO₂ was of dark respiration origin. Solutes (concentrations 10 mM, 25 mM, 50 mM and 100 mM) were fed to the leaves for 5 min through the petiole.

2.12.2. Gas and H₂O exchange measurements

Leaves were placed in a sandwich-type cuvette and exposed to CO₂-free air which led to stomata opening. This was achieved by passing pressurized air through a soda lime column before it entered the cuvette. The leaves were left in darkness, to make sure that the leaf production of CO₂ was of dark respiration origin. The only light beam reaching the leaf surface was that exiting the fluorescence of fluorescent dyes (2.12.3) which photon flux density ($2 \mu\text{mol m}^{-2} \text{s}^{-1}$) and wavelength (489 nm) excluded photosynthesis and photorespiration. The rate of air flow (0.25 l min^{-1}) was regulated by Tylan flow controllers (Tylan Corp., Carson, CA., USA). Relative humidity was kept at 40% and temperature at 25°C. CO₂ and water exchange were measured by an Infra Red Gas Analysis (IRGA) technique using the Binos instrument of Heraeus (Hanau, Germany).

2.12.3. Recordings of pH- and membrane potential changes

The detection of changes in pH or membrane potential was based on the fluorescence emission of pH- or membrane potential-sensitive probes infiltrated into the apoplast of leaves. The measurement of the fluorescence of the dyes was performed according to Yin et al. (1990) with some modifications. FITC, a dextran conjugate of fluorescein isothiocyanate (MW 4000 dalton; Sigma, St. Louis, MD., USA; 0.25 mM in aqueous solution), or bis-(1,3-dibutylbarbituric acid) trimethine oxonol (BDTO; B-438 of Molecular Probes, Eugene, OR., USA; 0.1 mM in aqueous solution) were infiltrated into the apoplast of leaves. Dextran conjugates of FITC have been used for the investigation of the pH in the apoplast of plant cells because they are not able to penetrate the plasma membrane and stay in the apoplast as long as 17 hours (Hoffmann and Kosegarten, 1995). Furthermore, FITC-dextran exhibits a pK_a value of about 5.92 (Hoffmann and Kosegarten, 1995) that is well suited to the pH ranges in the apoplast (between 5 and 6.5 in most plants studied; Grignon and Sentenac, 1991). B-438 is a lipophilic anionic dye that enters depolarized cells where it binds to intracellular

proteins or membranes and exhibits enhanced fluorescence and red spectral shifts. Increased depolarization results in more influx of the anionic dye and thus in an increase in fluorescence. Fluorescence of the probes was excited by a halogen lamp (24 V; 250 W; Osram, München, Germany) through a 489 nm interference filter from Schott (Mainz, Germany). The half bandwidth of transmission was 11 nm. Additional filters were 9782 and 5030 of Corning Glass Works (Corning, NY., USA). The photon flux density of the exciting beam was $2 \mu\text{mol m}^{-2} \text{s}^{-1}$. Fluorescence emission was collected by fiber optics at an angle of 45° relative to the incident exciting light and measured by a photomultiplier fitted with two filters 9782 from Corning Glass Works, an OG 515 cutoff filter from Schott and a K55 broad band interference filter from Balzers (Liechtenstein). The half bandwidth of transmission was between 518 and 533 nm.

2.13. Electron microscopy and determination of partial volumina of subcellular compartments

Leaf pieces (ca. 4 x 4 mm) were excised, transferred immediately into 3% glutaraldehyde in 50 mM potassium phosphate buffer (pH 7.2) supplemented with sucrose and infiltrated with this solution using a syringe. All following steps were done using glass tubes. The leaf pieces were incubated in a fresh solution of glutaraldehyde fixative for 3 hours. The fixative was then removed and the plant material was washed four to six times with 50 mM potassium phosphate buffer for 10-15 min each and post-fixed in 2% osmium tetroxide in a refrigerator overnight.

The plant material was dehydrated in a graded ethanol series and then gradually saturated with acetone:

ethanol 30% I	wash shortly
ethanol 30% II	20 min
ethanol 50%	20 min
ethanol 70%	wash shortly

The plant material was then contrasted with 1% uranyl acetate in 70% ethanol. The next steps were as follows.

ethanol 80%	15 min
ethanol 85%	15 min
ethanol 96%	15 min
ethanol 100% I	30 min
ethanol 100% II	30 min
ethanol 100%:acetone 100% = 1:1	1 h

acetone 100% I	30 min
acetone 100% II	30 min

The plant material was embedded in Epon epoxy resin (Fluka-Sigma-Aldrich, Taufkirchen, Germany) dissolved in acetone. The epon mixture C (prepared as described below) was used. The embedding of the plant material proceeded stepwise as follows:

Mixture C : acetone = 0.5:9.5	15 min
Mixture C : acetone = 1:9	30 min
Mixture C : acetone = 2 : 8	50 min
Mixture C : acetone = 3 : 7	50 min
Mixture C : acetone = 4 : 6	50 min
Mixture C : acetone = 5 : 5	overnight.

Plastic capsules for the embedding of the plant tissue were also filled with Mixture C : acetone = 5 : 5 and placed in a desiccator containing phosphorus anhydride overnight. The major part of the acetone evaporated from the capsules and from the tubes containing leaf pieces during the night. The leaf pieces were then transferred in the plastic capsules and left for two days in the desiccator at room temperature. The capsules were then transferred into a thermostat and kept at 60°C for 2 days.

Ultrathin sections (40-60 nm) were cut with glass knives on a LKB-III microtome (LKB, Stockholm, Sweden), contrasted on grids by 2% lead citrate, and viewed and photographed at 75 kV (x 2500 – x 4000) with a Hitachi HU-700 electron microscope (Tokyo, Japan).

The partial volumes of the chloroplast, vacuoles and cytosol per mesophyll cell were determined using the micrographs. The determination is based on the principle of Delesse (1874) who found that the volume density of various components making up a rock can be estimated on random sections by measuring the relative areas (A) of their profiles. For the cellular compartments, it is expressed as follows:

$$A_{\text{compartment}}/A_{\text{cell}} = V_{\text{compartment}}/V_{\text{cell}}$$

The relative squares of the subcellular compartments on the sections were determined by an image-analysis technique (Bioscan Optimas, Tokyo, Japan). The calculations were carried out using 15-20 sections of the mesophyll tissue (palisade parenchyme) for both species.

Glutaraldehyde fixative:

3 % (v/v)	glutaraldehyde (Sigma-Aldrich, Taufkirchen, Germany)
50 mM	K-phosphate buffer pH 7.2-7.4
2% (w/v)	sucrose

Contrasting solution:

1.330 g	lead citrate
1.760 g	tri-sodium citrate
30 ml	dd H ₂ O
mix vigorously, then add	
8 ml	NaOH 1 M
ad 50 ml with dd H ₂ O	

Postfixative (OsO₄ 2%):

dd H₂O + potassium phosphate buffer 50 mM + OsO₄ (4% stock sol.) = 1:2:4 (v/v/v)
add sucrose to 2.5% (w/v)

Uranyl acetate:

1.5% (w/v) uranyl acetate in 70% ethanol (place in thermostat at 40°C for dissolving,
store in a refrigerator in darkness)

Epon resins:

Mixture A: 38.3% Epon 812 + 61.7% DDSA, mix for 30 min

Mixture B: 52.9% Epon 812 + 47.1% MNH, mix for 30 min

Mixture C: pour A and B together (3:7), then add a hardener DMP-30 up to 2% (v/v)

2.14. Light microscopy

The sections prepared as described below were used for *in situ* hybridization of RNA probes. Therefore, the material should be preserved from RNases. RNases in the tissue were destroyed by the fixation procedure. To minimize external RNase activity, autoclaved solutions and sterilized glassware were used throughout the procedure.

Plant tissue (leaves and stems of *Alonsoa*) was cut into pieces in a fixative, placed in glass vials with fixative and transferred into a desiccator for infiltration. Vacuum was applied for 20-40 minutes, and the infiltration was repeated several times until the tissue was completely infiltrated. The solution was replaced with new fixative, vacuum was applied for 15 min, and the fixation proceeded at room temperature for 2-6 hours or at 4°C overnight. The fixative was removed, and the following dehydration steps were performed at room temperature, each step for at least 20 min:

1x phosphate buffer

dd H₂O

EtOH series prepared from 96% ethanol and autoclaved dd H₂O, concentrations 10%,
30%, 50%, 70%, 80%, 90% and 96%

100% EtOH 4 times for at least 1 hour

Ethanol was replaced subsequently with chloroform:100% ethanol mixtures (1:3, 1:1, 3:1; 1 hour for each step). Then plant material was incubated two times for at least one hour each in 100% chloroform. To infiltrate the material with embedding paraffin, 4-7 flakes of Paraffin wax (Aldrich, Taufkirchen, Germany) or Paraplast Plus (Sigma-Aldrich, Taufkirchen, Germany) were added to the chloroform. Further addition of paraffin flakes was performed at 37°C during 2 days to facilitate the gradual saturation of material with paraffin. The total volume of added paraffin was about equal to the volume of chloroform in the vials. After that, the vials were incubated at 50°C to enable the evaporation of chloroform. For embedding, a metallic embedding mold was prewarmed to 60°C on a hot plate. Some molten paraffin (filtered through a paper filter) was poured into the mold. The samples were gently stirred and poured into the mold. Plant material was positioned with a pre-warmed needle. For solidification, the mold was quickly dipped into the ice-cold water, incubated for 5 min and transferred into the -20°C freezer for 5 min. This prevented the formation of paraffin crystals which might disrupt the tissue. The embedded material was stored at 4°C for several weeks and could be stored for several years.

For the preparation of slides, precleaned coated glass slides Superfrost® Plus (Roth, Karlsruhe, Germany) were used which electrostatically attract the sections to the slide. The upper right corner of each slide was removed to mark the position of sections on the slide. 8 µm thick sections were cut with a disposable knife on a Microtom (RM 2125RT; Leica, Nussloch, Germany). Paraffin ribbons could be stored at 4°C for one week. 600-800 µl of autoclaved dd H₂O were pipetted onto the slide, and the sections were positioned on the water. To stretch the sections, the slides were incubated at 40°C on a hot plate and then left on the plate at 37°C overnight to allow the water to evaporate. The slides with sections could be stored at -20°C in plastic boxes sealed with tape for several months.

Fixative:

4% (w/v) paraformaldehyde (from 10% stock solution)

0.25% (w/v) glutaraldehyde

1 x sodium phosphate buffer

0.1% Tween 20

10% (v/v) DMSO

10% paraformaldehyde stock solution:

10 g paraformaldehyde were dissolved in 70 ml dd H₂O at 70°C for 30 min in the presence of one pellet of NaOH; the pH was adjusted to 7.0 using 0.1 M HCl

10 x phosphate buffer stock solution:

68.4 ml 0.1 M Na₂HPO₄ + 31.6 ml 0.1 M NaH₂PO₄ + 5.84 g NaCl, pH 6.8

2.15. Isolation of total RNA and genomic DNA from plant tissues

For the isolation of RNA and DNA as well as for all molecular biological methods used in this work, only sterile (autoclaved) glassware and plastic ware (Gilson pipette tips, Eppendorf tubes etc.) were used. The solutions were prepared using sterile (autoclaved) water of MilliQ grade (dd H₂O). The preparations were performed on ice if not indicated otherwise. The centrifugations were mostly done using an Eppendorf table top centrifuge (Schütt, Göttingen, Germany) at 13 000 rpm (16 060 g). RNA samples were stored at -80°C and DNA samples at -20°C.

2.15.1. Isolation of RNA from *Asarina* and *Alonsoa*

To isolate RNA from *Asarina* and *Alonsoa* organs, several different methods were tested: a method from Logemann et al. (1987) using guanidinium chloride; the PeqGOLD RNA Pure™ Kit (Peq Lab, Erlangen, Germany) and the Invisorb Spin Plant-RNA Mini Kit (Invitex, Berlin, Germany). The RNA of the best quality, i.e. with the lowest polysaccharide and DNA content, was obtained using the Invisorb Spin Plant-RNA Mini Kit. The preparation method given in the instruction manual for the kit is described below.

Plant material was harvested and stored at -80°C until use. Ca. 100 mg were ground in liquid nitrogen using mortar and pestle. The fine powder was transferred into a 2 ml plastic Eppendorf tube that contained 450 µl of the lysis solution provided in the kit. After vigorous vortexing, the suspension was incubated for 2 min at room temperature. All following procedures were also performed at room temperature. The lysate was applied to a spin column with a DNA binding filter and incubated for 1 min. Passing of the lysate through the filter during the following centrifugation (2 min, 10 000 rpm) resulted in the removal of DNA. The addition of 0.5 vol. 99.8% ethanol to the RNA-containing lysate provided the conditions for precipitation of RNA from the solution during the following centrifugation. The solution was applied to a spin column with an RNA binding filter, incubated for a minute and centrifuged (30 sec, 10 000 rpm). The filter-bound RNA was washed three times with two different buffers (30 sec, 10 000 rpm), the residual ethanol were removed by an additional centrifugation (2 min, 13 000 rpm), and the RNA was eluted from the filter with dd H₂O (2 min incubation, dd H₂O had to be pipetted directly on the filter membrane; then the columns were centrifuged for 1 min at 13 000 rpm). 20 – 50 µl of dd H₂O were used for elution depending on the desired RNA concentration. The eluted RNA was immediately placed on ice and transferred to -80°C.

2.15.2. Isolation of genomic DNA from *Alonsoa*

Genomic DNA was isolated from young leaves of *Alonsoa* with DNeasy™ Plant Maxi Kit (Qiagen, Hilden, Germany) according to the instructions of the manufacturer. All centrifugations were performed at 4000 g for 5 min at room temperature (Megafuge 1.0, Heraeus Sepatech, Osterode, Germany). Up to 1 g of plant tissue was ground in liquid nitrogen using mortar and pestle. 5 ml lysis buffer (preheated to 65°C) with 10 µl of RNase (100 mg/ml stock solution) were added. The samples were vortexed vigorously and incubated for ten minute at 65°C. The tubes were inverted several times during the incubation. The addition of the 1.8 ml aliquot of a neutralization buffer, followed by 10 min incubation on ice, resulted in the precipitation of detergent, proteins and polysaccharides. The lysates were centrifuged, the supernatant containing floating particles was applied to a spin column with a filter and centrifuged again. After this step, most of the particles either remained on the filter or formed a pellet in the receiver tube. To the supernatant, 1.5 vol. of DNA precipitation buffer were added and immediately mixed by pipetting. The samples were applied to a spin column with a DNA-binding membrane filter and centrifuged. The filter was washed with washing buffer and centrifuged for 10 min to dry the membrane. The DNA was eluted with 0.75 ml elution buffer (preheated to 65°C) in a 5 min incubation at room temperature and a centrifugation for 5 min. The elution was repeated two times, and the eluates were combined. This resulted in isolation of ca. 120 µg DNA from 1 g of *Alonsoa* young leaves.

2.15.3. Isolation of DNA from *Arabidopsis thaliana* F1 transformants

For each *A. thaliana* F1 plant, two leaves were harvested and stored at –80°C until use. 250 µl extraction buffer were pipetted into the Eppendorf tube containing frozen leaves (up to 100 mg fresh weight) and crushed with a small pestle. 400 µl extraction buffer were added, and the tubes were incubated at 60°C for 30 min. Then, 700 µl chloroform:isoamyl alcohol (24:1) were added and mixed gently. The tubes were centrifuged at 8000 rpm (6 080 g) for 10 min and the upper phase was saved. DNA was pelleted by the addition of 700 µl isopropanol and centrifugation for 10 min at 10 000 rpm (9 500 g). The pellets were washed with 500 µl 70% ethanol, followed by 5 min centrifugation at 13 000 rpm, and dried under vacuum. The DNA was resuspended in 50 µl sterile dd H₂O containing 40 µg/ml Rnase, and the amount was checked by running 1 µl sample on an 1% agarose gel. 1-2 µl DNA were used per PCR with either insert-specific primers or, in a control reaction, with ubiquitin primers (ubifor/ubirev; Table 2.1.).

Extraction buffer:

2% (v/v) CTAB (hexadecyltrimethylammonium bromide)

1.4 M NaCl

0.2 mM EDTA

10 mM Tris-HCl pH 8.0

0.2% (v/v) β -mercaptoethanol

2.16. Plasmid DNA isolation from bacteria

2.16.1. Isolation of plasmid DNA from *E. coli* (miniprep and maxiprep)

Plasmid DNA mini preparations were usually performed using a Triton boiling protocol which resulted in a sufficient yield of a plasmid DNA of sufficient quality for most restriction digests and also for transformation. However, for sensitive applications (e.g. sequencing reactions which required a higher purity), the preparations were performed using a Qiagen Miniprep Kit. This kit also was used for plasmid DNA isolation if the Triton boiling procedure had failed to yield enough DNA.

In order to obtain larger amounts of pure plasmid DNA, plasmid DNA preparation was performed using the E.Z.N.A. Plasmid Mini Prep Kit (Peq Lab, Erlangen, Germany).

For mini plasmid preparations, 5 ml LB medium supplemented with the appropriate antibiotics were inoculated with a bacterial colony grown on an agar plate, or from a glycerol culture (2.20.6). The inoculation was performed under a laminar flow hood (LaminAir HLB 2472, Heraeus, Germany). Colonies were picked with sterile (autoclaved) toothpicks. Glycerol cultures were put on ice and scrubbed with a microbiological loop which was then rapidly dipped into the liquid medium. Bacteria were grown overnight at 37°C in a roller. 1.5 ml of the culture were pipetted into a 1.5 ml Eppendorf tube and the cells were spun down for 2 min at 13 000 rpm at room temperature. The supernatant was removed, the centrifugation was repeated and the residual supernatant was removed using a 200 μ l Gilson pipette. The cells were stored at -20°C or used directly for plasmid DNA isolation.

For plasmid DNA preparation with the E.Z.N.A. kit, 50 ml of TB medium (with the appropriate antibiotics) were inoculated from plates or glycerol cultures and the bacteria were grown overnight in a 37°C shaker. The cells were poured into four 15 ml centrifuge tubes (laminar flow hood) and spun down for 10 min at 4300 rpm at 4°C in a Megafuge (Heraeus Sepatech, Osterode, Germany). The supernatant was discarded and the cells were stored at -20°C or directly used for plasmid DNA isolation.

2.16.1.1. Plasmid DNA miniprep isolation using a triton boiling protocol

All centrifugations were performed at room temperature and 13 000 rpm. The pelleted cells were resuspended in 150 µl STEL buffer. The tubes were heated for 30 sec to 100°C and rapidly transferred to ice. This step led to lysis of the cells and denaturation of proteins and DNA. The small plasmid DNA was then able to renature and remained in the supernatant whereas the larger genomic DNA and proteins were pelleted during the following centrifugation for 20 min. The pellet was removed from the tubes using a toothpick, and the plasmid DNA was precipitated by the addition of 180 µl isopropanol to the supernatant. Plasmid DNA was sedimented by a 5 min centrifugation, washed with 500 µl of 70% ethanol (5 min centrifugation), dried for 3 - 15 min at 37°C in open tubes and resuspended in 50 µl dd H₂O containing 200 µg/ml RNase A.

STEL buffer:

Sucrose	8% (w/v)
Triton-X-100	5% (v/v)
Tris-HCl pH 8.0	50 mM
EDTA	50 mM
Lysozyme	0.5 mg/ml

2.16.1.2. Plasmid DNA miniprep isolation with the Qiagen Miniprep Kit

All centrifugations were performed at room temperature and 13 000 rpm. The pelleted cells were resuspended in alkaline lysis buffer containing RNase A and incubated for 5 min at room temperature. Then, the SDS-NaOH solution was added, and the tubes were incubated for another 5 min at room temperature. During this step, the tubes were inverted occasionally. Afterwards, neutralization buffer was added to the lysates and mixed by inverting the tubes. This step led to the precipitation of genomic DNA, polysaccharides and proteins. The precipitates were sedimented by a centrifugation for 10 min. The clear supernatant containing the plasmid DNA was applied onto a spin column with DNA binding filter and centrifuged for 30 sec. The filters were washed with an ethanol-containing washing buffer (30 sec centrifugation) and dried (2 min centrifugation). DNA was eluted by pipetting 50 µl dd H₂O directly onto the filter, incubating for 5 min and centrifuging for 1 min.

2.16.1.3. Plasmid DNA maxiprep isolation with E.Z.N.A. Plasmid Miniprep Kit

The isolation procedure was very similar to that described in 2.16.1.2, the differences being: (1) different kit; (2) larger amount of bacterial cells (¼ of 50 ml TB culture) used for the preparation; (3) filter washing with a special HB buffer before the ethanol washing step; (4) elution with 100 µl water.

2.16.2. Isolation of plasmid DNA from *Agrobacterium tumefaciens*

Cells of *A. tumefaciens* have very stable cell walls which makes a preparative plasmid isolation very difficult. Therefore, only small amounts of plasmid were isolated from *A. tumefaciens* transformed with pBIstsA or pBIstsB (2.2.3) which were then used for *E. coli* transformation for a preparative isolation and characterization of plasmids.

5 ml cultures of *A. tumefaciens* were grown in YEB medium supplemented with kanamycin and rifampicin (2.2.2) for two days at 29°C in a roller. 1.5 ml of the culture was spun down for 5 min, and the cells were resuspended in 100 µl solution I. Then, 200 µl solution II were added. The lysates were supplemented with 200 µl chloroform and incubated for 5 min at room temperature. After that, 150 µl solution III were added, and the lysates were vortexed and centrifuged for 10 min. This resulted in a phase separation, and the upper phase containing the DNA was transferred to a new Eppendorf tube. 1 volume of a phenol:chloroform mixture (1:1) was added to the upper phase and vortexed vigorously. After the next centrifugation, the upper phase was transferred to a new Eppendorf tube, and 2 volumes of cold ethanol (99%) were added. Plasmid DNA was pelleted in a 5 min centrifugation step. The pellet was washed with 150 µl 70% ethanol, dried for 15 min at room temperature and redissolved in 50 µl dd H₂O containing 200 µg/ml RNase A.

Solution I:	glucose	50 mM
	EDTA	10 mM
	Tris-HCl pH 8.0	25 mM
Solution II	NaOH:	0.2 M
	SDS	1 % (w/v)
Solution III:	K acetate pH 4.8	3 M

Solutions I, II and III were either prepared or taken from the Qiagen Miniprep kit.

2.17. Determination of RNA and DNA concentration by spectrophotometry

The concentrations of DNA or RNA in aqueous solution could be determined using a spectrophotometer (Uvikon 932, Kontron). A 1 µl aliquot of the nucleic acid solution was diluted in 600 µl dd H₂O and the extinction was measured at 260 nm and 280 nm, respectively. Double measurements were performed. The E₂₆₀/E₂₈₀ ratio represents a measure for the protein contamination of the nucleic acid sample and should be between 1.8 and 2.0. The concentration of DNA or RNA was then calculated as follows:

$$\text{RNA } [\mu\text{g}/\mu\text{l}] = E_{260} \times 42 \times V_{\text{cuvette}} \times V_{\text{aliquot}}^{-1}$$

$$\text{DNA } [\mu\text{g}/\mu\text{l}] = E_{260} \times 50 \times V_{\text{cuvette}} \times V_{\text{aliquot}}^{-1}$$

The extinction coefficients are valid for double-stranded DNA and single-stranded RNA (Sambrook et al., 1989).

2.18. Purification and precipitation of DNA and RNA

All centrifugations were performed at room temperature at 13 000 rpm (16 060 g). Phenol:chloroform extraction of the nucleic acids was used to remove proteins from the samples (polysaccharides cannot be completely removed by this procedure). The nucleic acids were then precipitated with ethanol and redissolved in dd H₂O. One volume of a phenol:chloroform mixture (1:1, v/v) was added. The samples were vortexed and centrifuged for 5 min to separate the upper aqueous phase (containing the nucleic acids) from the phenol:chloroform phase. Proteins were denatured by phenol and formed a layer between both phases. The water phase was transferred to a new Eppendorf tube, vortexed with 1 volume of chloroform and centrifuged again. The upper phase was transferred to a new Eppendorf tube. 1/10 volume of 3 M Na acetate pH 6.2 and 2.5 volumes of 96% ethanol were added, and nucleic acids were precipitated at -20°C for one hour. The following centrifugation for 10 min resulted in the sedimentation of the nucleic acids. The pellet (usually not visible) was washed with 75% ice-cold ethanol, followed by a centrifugation for 10 min, dried at 37°C for ca. 10 min and dissolved in dd H₂O.

2.19. Agarose gel electrophoresis of DNA and RNA

2.19.1. Separation of DNA

Usually, 1% agarose gels in 1 x TEA buffer were used. An ethidium bromide stock solution (10 mg/ml) was added to a final concentration of 0.25 µg/ml. 0.75% agarose gels were used for better resolution of larger DNA fragments, e.g. for the separation of restriction enzyme-digested genomic DNA, and 1.5% agarose gels were used for the better resolution of smaller fragments. 1/10 volume of loading dye was added to DNA samples before loading them on a gel. Electrophoresis proceeded at 20 - 70 V with 1 x TEA as running buffer. Bacteriophage λ DNA restricted with *Pst*I, to which blue marker had been added, was used as size marker (1 µg per slot). DNA was photographed under UV light using a transilluminator (FLX-20M, Fa. Vilber Lourmat, Marne La-Vallet, France) and a computer program PhotoFinish® 3.0 (WordStar Atlante Technology Center Inc.).

50 x TEA buffer:

Tris-acetate pH 8.3	2 M
EDTA	100 mM

Loading dye:

glycerol	50 % (v/v)
Tris-acetate pH 8.3	40 mM
EDTA	2 mM
Orange G	0.2 % (v/v)

Blue marker:

xylene cyanol	0.1 % (w/v)
sucrose	0.2 g/ml
EDTA	250 mM
bromphenol blue	0.5 g/ml

2.19.2. DNA gel blots (Southern blots)

The principle of this method (Southern, 1975) is the electrophoretical separation of DNA fragments of various sizes on an agarose gel, followed by transfer and immobilization of the DNA on a nylon membrane. The membrane-bound DNA afterwards can be hybridized with labelled DNA probes to identify complementary sequences among the immobilized DNA.

Five samples of genomic DNA from *Alonsoa* (2.15.2) were digested overnight with different restriction enzymes: *EcoRI*, *HindIII*, *PstI*, *SalI* and *BamHI*. For each enzyme, the reaction was performed under the following conditions:

genomic DNA	10 µg
10x buffer (specific for the restriction enzyme)	40 µl
restriction enzyme	50 U
dd H ₂ O	ad 400 µl
incubation at 37°C overnight.	

The completeness of the restriction was checked by electrophoresis of 1/20 volume of each reaction (i.e. 10 µl) at 60 V. The restricted DNA samples were purified by a phenol:chloroform extraction (2.18), precipitated with ethanol at -20°C and redissolved in 15 µl dd H₂O. In some cases, to make sure that the restriction digests were complete, the phenol:chloroform-extracted DNA was subjected to the second restriction overnight and then extracted again with phenol:chloroform. After supplementation with blue loading dye, the DNA samples were loaded on a 0.75% agarose gel (13.5 cm x 14 cm) next to 1 µg λ /*PstI* DNA as size marker. The electrophoresis was started at 80 V and run at 20 V overnight after the DNA had moved out of the slots.

Blotting was performed by alkaline transfer to a Hybond N⁺ nylon membrane (Amersham-Pharmacia, Braunschweig, Germany). First, the gel was photographed and shortly washed in water. The upper part of the gel that contained DNA fragments > 10 kb was washed with depurination solution for 1.5 min. The gel was placed in denaturation (alkaline) buffer and incubated for 20 min under gentle shaking. The incubation was repeated with a fresh portion of the buffer. In the meantime, a piece of Hybond N⁺ membrane of the size of the gel was wetted with water and incubated for 20 min in denaturation buffer. Then, a capillary blot was set up as follows. A plastic tray was half filled with denaturation buffer, a wick of the breadth of the gel was cut from Whatman 3MM paper, wetted with denaturation buffer and placed on a platform on top of the plastic tray with its ends hanging into the buffer. The gel was placed on the wick with the DNA-side upwards, and the membrane was placed on top of the gel. The lower right corners of gel and membrane were cut off to mark the orientation. The membrane was overlaid with three sheets of 3MM paper of membrane size prewetted in denaturation buffer, and a stack of absorbent towels was placed on top of the 3 MM paper. The parts of the wick that were not in contact with the gel were covered with pieces of parafilm to ensure that the suction of the buffer proceeded only through the gel. Finally, a plastic plate and a weight of ca.1 kg were placed on the stack, and the transfer proceeded overnight. Afterwards, the quality of the transfer was briefly checked using a UV transilluminator, the membrane was washed in 2 x SSC for 20 min for neutralization and dried at room temperature on 3MM paper. The membrane was stored in a plastic bag at 4°C until used for DNA hybridization (2.19.5.2).

Depurination solution (can be stored at room temperature for up to 1 month):

HCl 0.125 M

Denaturation (transfer) buffer (made fresh before each blotting):

NaCl 87.66 g

NaOH 20 g

dd H₂O ad 1 l

20 x SSC (can be stored at room temperature up to 3 month):

NaCl 3 M

Na₃ citrate 0.3 M

pH adjusted to 7.0 using NaOH or HCl

2.19.3. Separation of RNA

To test the quality and (roughly) the amount of the isolated RNA, a 1% agarose gel was prepared, and electrophoresis and UV detection were performed as described for DNA

(2.19.1) with the exception that the combs and the gel chamber were incubated in 1% SDS for at least 30 min before use to get rid of RNase activity. In case that RNA was of good quality, the 28 S ribosomal RNA band was thicker than the 18 S rRNA band.

For a more precise estimation of the RNA concentration in the samples for the following Northern blots, small agarose-formaldehyde denaturing gels were prepared as for the RNA separation for Northern blots (2.19.4)

2.19.4. RNA gel blot (Northern blot)

For size-dependent separation of RNA, denaturing conditions are required because single-stranded RNA molecules form secondary structures. Here, agarose-formaldehyde gels were used. 3 g agarose were boiled in 150 ml dd H₂O and cooled down to 70 °C. Then, 20 ml 10 x MEN and 33 ml formaldehyde (37% stock solution) were added and the gel (13.5 cm x 14 cm size) was poured.

10 µg RNA in 9 µl water per slot were used for the separation. A size marker (3 µl of 0.5 mg RNA/ml; MBI Fermentas, Vilnius, Lithuania) was prepared along with the samples. Two master mixes were prepared as follows:

master mix I (amounts for one sample): 3 µl 10 x MEN
 12 µl deionized formamide
 3 µl formaldehyde (37%)

master mix II (total amount): 85 µl blue marker
 15 µl ethidium bromide (10 mg/ml stock solution)

18 µl of the master mix I were added to each Eppendorf tube with RNA sample, and 3 µl of the master mix II were pipetted to the wall of each tube. The tubes were vortexed and briefly centrifuged. The RNA samples were denatured at 65°C for 10 min, cooled down on ice and loaded on the gel. The running buffer (1 x MEN) was added up to the gel surface which was left non-submerged. The slots were filled with the same buffer. Electrophoresis was performed at 120 V for three to four hours.

The gel was photographed and briefly washed with water. The RNA was transferred onto a Hybond N nylon membrane which had been wetted with dd H₂O and incubated for 20 min in 10 x SSC. The blot was built up as described in 2.19.2. using 10 x SSC as transfer buffer. On the next day, the membrane was washed shortly in 2 x SSC, and the quality of the transfer was checked using a UV transilluminator. The membrane was put on 3MM paper and baked for 2 – 3 h at 80°C which resulted in the non-covalent binding of the RNA to the membrane. The membrane was stored at 4°C in a plastic bag until use.

10 x MEN buffer:	MOPS pH 7.0	200 mM
	EDTA	5 mM
	Na acetate	50 mM

2.19.5. Hybridization of DNA and RNA gel blots

2.19.5.1. Labelling of probes

For hybridization of DNA (Southern blot) or RNA (Northern blot) immobilized on a nylon membrane, DNA probes were labelled radioactively using α -³²P-dATP. The probes were prepared using the HexaLabel Kit from MBI Fermentas (Vilnius, Lithuania). 100 ng of DNA template (DNA fragment isolated from an agarose gel) and 10 μ l of a hexanucleotide mixture provided in the kit were denatured in buffer at 100°C for 10 min in a total volume of 40 μ l. Then, 3 μ l of Klenow nucleotide mixture (minus dATP), 3 μ l α -³²P-dATP (10 μ Ci/ μ l; Hartmann Analytik, Braunschweig, Germany) and 1 μ l Klenow exo⁻ polymerase were added. The reaction took place at 37°C for 10 min. After this time, 4 μ l of a mixture of non-labelled dNTPs (0.25 mM of each nucleotide) provided in the kit was added, and the reaction was continued for another 5 min. The reaction was stopped by the addition of 1 μ l 0.5 M EDTA pH 8.0. Free α -³²P-dATP was removed from the probes using a Concert Kit (Gibco BRL, Eggenstein, Germany). The probes were eluted from the DNA-binding spin columns with 100 μ l 1 x TE buffer preheated to 65°C. The incorporation of α -³²P-dATP into the probes was quantified by measuring the radioactivity of 1 μ l of the eluted DNA in a liquid scintillation analyser (Packard 1900 TR, Canberra-Packard, Dreieich, Germany). 2-4 x 10⁷ cpm of labelled DNA were used per hybridization.

5 x buffer with random hexanucleotides:

Tris-HCl	0.25 M
MgCl ₂	25 mM
DTT	5 mM
random hexanucleotides	7.5 U/ μ l pH 8.0

2.19.5.2. Hybridization and washing of blots

The RNA or DNA blots were placed in plastic bags containing ca. 15 ml of hybridization buffer and incubated at 65°C for at least 1 hour in a shaking water bath. The labelled probes (2.19.5.1) were denatured for 5 min at 95 °C and pipetted into the plastic bags with the prehybridized filters. The hybridization proceeded at 65°C in a shaking water bath for 16 – 20 hours. Afterwards, the filters were washed to remove non-hybridized label. The washing was performed either under stringent or non-stringent conditions depending on the

specificity of the probes used. Stringent conditions were provided by washing the filter two times for 20 min each with 2 x SSC, 0.1% SDS (w/v) and once with 0.5 x SSC, 0.1% SDS (w/v). Under non-stringent conditions, filters were washed with 2 x SSC containing 1% SDS (w/v) three times for 20 min each. The filters were then dried on 3MM paper, sealed into plastic bags, and the hybridization signal was detected by phosphoimaging (Fuji BAS-1000, Raytest, Sprockhövel, Germany) for at least three hours. If necessary, longer exposure times of up to one week were applied. The results were evaluated with the computer program Tina 2.0 (Raytest, Sprockhövel, Germany).

Hybridization buffer:	5 x SSC (for the preparation of 20 x SSC see 2.19.2)	
	5 x Denhardt's	
	0.5% (w/v) SDS	
100 x Denhardt's:	Ficoll 400	2% (w/v)
	PVP	2% (w/v)
	BSA (lyophilized)	2% (w/v)

2.20. Gene cloning

Either PCR products or DNA fragments excised from plasmids using restriction enzymes were cloned in *E. coli*. PCR products were ligated into the cloning vector pGEM®-T Easy (Promega, Madison, WI., USA). This vector has 3'-overhanging T-residues on both sides of the insertion site which makes it suitable for the cloning of PCR products because *Taq* polymerase and *Tth* polymerase leave overhanging A residues on the 3'-ends of amplified DNA fragments.

For the production of templates for *in vitro* transcription, cDNA fragments were excised from pGEM®-T Easy and cloned in pBluescript®IIKS⁺ using *EcoRI*. For the construction of binary vectors for plant transformation, inserts whose ends had been filled up with Klenow polymerase were ligated into the vector pBI101.3 which had been restricted with *SmaI* to produce blunt ends.

Both fragments and vectors (except for pGEM®-T Easy which was provided in a kit) were purified via agarose gel electrophoresis using the Qiaquick gel extraction kit before ligation (2.20.1). In case of pBI101.3, the purification of the digested vector via an agarose gel was omitted because due to the large size of the vector, the risk of damage to the DNA during the procedure was too high. Therefore, proteins were removed by phenol:chloroform extraction (2.18) after restriction. The DNA was precipitated with ethanol and resuspended in 10 µl of dd H₂O.

2.20.1. Elution of DNA fragments from agarose gels

DNA fragments deriving from PCRs or restriction enzyme reactions were separated on 1% agarose gels (2.19.1). This step allowed the purification of DNA from proteins/enzymes and the isolation of the DNA fragment of the desired size. The DNA bands were cut from the gel under long-waved UV light. Agarose was removed using the Qiaquick gel extraction kit (Qiagen). After dissolving the agarose at 50°C in a chaotropic reagent, DNA was bound to a silica gel filter in a spin column in the presence of high salt concentrations, washed and eluted from the filter with dd H₂O.

2.20.2. Filling of 5' overhanging ends with Klenow polymerase

When a restriction fragment had to be cloned in a vector, but no compatible restriction site was available, blunt-end cloning was performed. In this case, restriction enzymes producing either blunt or 5' overhanging ends were used. In the latter case, single-stranded DNA ends were filled-in using Klenow DNA polymerase to obtain blunt ends. A fill-in reaction contained:

10 x buffer	4 µl
Klenow fragment 2 U/µl	1 µl (ca. 1 U per µg DNA)
10 mM dNTPs	4 µl
DNA	2 µg
dd H ₂ O	ad 40 µl

The reaction took place at 37°C for no longer than 20 min to prevent that Klenow polymerase, after using up the free dNTPs, acted as a 3'-5' exonuclease. The DNA fragment was purified via an agarose gel using the Qiaquick gel extraction kit (2.20.1).

2.20.3. Ligation

The reaction volume (10 µl) contained 1 µl (1 U/µl) T4-DNA-ligase (Gibco BRL), 2 µl 5 x ligase buffer, 5 – 10 ng vector and the insert in an amount suited to provide a molar vector:insert ratio in the range of 1:3 to 1:30. The reaction took place at 15°C overnight. 5 x ligase buffer contained 10 mM dATP, 50 mM MgCl₂, 10 mM DTT and 660 mM Tris-HCl at pH 7.6.

2.20.4. Preparation of competent cells of *E. coli* strains *DH5α* and *BL21 (DE3)*

Competent cells of *DH5α* were used for transformation with the ligation products and should possess, therefore, a high competence for transformation. *BL21 (DE3)* were only transformed with purified plasmid DNA. Such a transformation does not require the cells to be highly transformation-competent.

2.20.4.1. Competent cells of DH5 α

The method of Inoue et al. (1990) was used with some modifications. To obtain optimal competent cells, the glassware used in the protocol had to be free of any detergents. For this purpose, glassware was first autoclaved filled with dd H₂O to remove traces of detergents, and then autoclaved again empty. 5 ml SOC medium were inoculated with 10 – 20 μ l of a DH5 α glycerol culture and grown overnight (37°C, shaking). This inoculum was then added to 250 ml SOC medium and grown (37°C, shaking) until the cell density reached an OD₆₀₀ of 0.2. After that, the growth was continued at 18°C (shaking) for about an hour until the OD₆₀₀ had reached 0.3. The grown cells were poured into four 50 ml conical centrifuge tubes and sedimented at 4300 rpm at 4°C for 10 min (Megafuge 1.0, Heraeus Sepatech, Osterode). The following steps were performed on ice under a laminar flow hood (LaminAir HLB 2472, Heraeus, Germany). The pelleted cells were resuspended in 15 ml ice-cold transformation buffer per tube and incubated on ice for 15 min. The suspensions were combined pairwise into two centrifuge tubes and centrifuged again at 4300 rpm for 10 min at 4°C. The pellets were resuspended in 10 ml per tube (total 20 ml) of transformation buffer and 350 μ l DMSO were carefully added to each tube under gentle vortexing to avoid a high local DMSO concentration. After 5 min incubation on ice, this step was repeated resulting in a final concentration of DMSO 7% (v/v). 200 μ l aliquots of the competent cells were pipetted into pre-cooled 1.5 ml Eppendorf tubes and shock-frozen in liquid nitrogen. The cells were stored at -80°C.

SOC medium:

Select Pepton 140	2% (w/v)
yeast extract	0.5% (w/v)
NaCl	10 mM
KCl	2.5 mM

The mixture was autoclaved for 10 min, and the filter-sterilized solutions of MgCl₂ (1 M), MgSO₄ (1 M) and glucose (2 M) were added under a clean bench to a final concentrations of 10 mM, 10 mM and 20 mM, respectively.

Transformation buffer:	PIPES	10 mM
	CaCl ₂	15 mM
	KCl	250 mM
	MnCl ₂	55 mM

The pH was adjusted to 6.7 with KOH prior to the addition of MnCl₂, and the solution was filter-sterilized.

2.20.4.2. Competent cells of BL21 (DE3)

2 ml LB medium (2.2.2) were inoculated with a BL21 (DE3) glycerol culture and grown overnight (37°C, shaking). The cells were added to 200 ml LB medium and grown at 37°C up to an OD₆₀₀ of 0.3. The following steps were performed on ice under a laminar flow hood. The culture was cooled down on ice and poured into four 50 ml conical centrifuge tubes. The cells were spun down at 4300 rpm at 4°C for 10 min and carefully resuspended in a total volume of 40 ml transformation buffer I. After 10 min incubation on ice, the cells were pelleted at 4300 rpm at 4°C for 5 min and resuspended in a total volume of 4 ml transformation buffer II. 200 µl aliquots of the competent cells were pipetted into precooled 1.5 ml Eppendorf tubes and shock-frozen in liquid nitrogen. The cells were stored at -80°C.

Transformation buffer I:

K acetate	30 mM
MnCl ₂	50 mM
CaCl ₂	10 mM
RbCl	100 mM
glycerol	15 % (v/v)

pH adjusted to 5.8 with acetic acid

Transformation buffer II:

Na MOPS pH 7.0	10 mM
CaCl ₂	75 mM
RbCl	10 mM
glycerol	15 % (v/v)

2.20.5. Transformation of *E. coli*

The competent cells were thawed on ice. 5 µl ligation reaction or 50 – 200 ng plasmid DNA were added to the competent cell suspension and mixed by pipetting. After an incubation on ice for 20 min, the cells were incubated at 42°C for exactly 30 sec and transferred back to ice for a minute. 800 µl SOC medium were added to the cells under a laminar flow hood and the cells were incubated at 37°C for an hour to allow the expression of antibiotic resistance genes. The cells were pipetted under a clean bench onto LB agar plates supplemented with the appropriate antibiotic(s). If the cells were transformed with a ligation product in pGEM®-T Easy or pBluescript®IIKS⁺, the plates were supplemented with IPTG and X-Gal in addition to the antibiotic(s) (2.2.2). The plates were dried and incubated at 37°C overnight. Single colonies were picked for growth in LB with antibiotic(s) and Miniprep preparation of plasmid DNA (2.16.1.1 and 2.16.1.2) and characterization by either restriction

enzyme digestion with the following separation of DNA fragments by a gel electrophoresis (2.19.1) or PCR (2.21.1). In case of plates containing IPTG and X-Gal, blue colonies contained empty vector and only white colonies were picked for further characterization.

2.20.6. Bacterial glycerol cultures

Original strains of *E. coli* and *A. tumefaciens* as well as strains containing characterized plasmids were grown overnight in 5 ml medium supplemented with antibiotics at appropriate temperature (37°C for *E. coli*, 28-30°C for *Agrobacterium*). 200 µl glycerol were pipetted into plastic tubes with screw tops and autoclaved. 800 µl of bacterial culture were added to 200 µl of sterile glycerol, vortexed, shock-frozen in liquid nitrogen and stored at -80°C.

2.21. Amplification of DNA by the polymerase chain reaction (PCR)

The polymerase chain reaction was used for amplification of fragments of DNA (plasmid or genomic) and cDNA using either specific or degenerate primers. PCRs were performed using a DNA thermal Cycler MJ Research PTC 100 (Biozym, Hess. Oldendorf, Germany) or TGradient (Biometra, Göttingen, Germany). Usually, *Taq* polymerase (Promega, Mannheim, Germany) was used. The reaction mixture contained if not otherwise indicated

DNA template	2-5 µl
10 x PCR buffer (100 mM KCl, 100 mM Tris-HCl pH 9.0)	5 µl
MgCl ₂ (25 mM)	3 µl
dNTP mixture (10 mM of each nucleotide)	1 µl
5'-primer (10 pmol/µl)	1 µl
3'-primer (10 pmol/µl)	1 µl
<i>Taq</i> Polymerase (2 U/µl)	1 µl
ad dd H ₂ O	50 µl.

Usually, a three step cycle program was used except for the amplification of full length *AmSTS* cDNA (2.21.3) and Genome walking PCR (2.21.4). The steps were: (1) 30 sec template denaturation at 94°C; (2) 25-35 cycles of (a) 30 sec template denaturation at 94°C, (b) 30 sec annealing of primers to template at T_{ann} , (c) elongation at the appropriate temperature (72°C for *Taq* polymerase), elongation time depending on the length of expected product (1 min/kb); (3) 10 min extension of unfinished products at 72°C.

2.21.1. Design of specific and degenerate primers

Specific primers were designed based on the known sequences of the cDNA and promoter region of the *Alonsoa* stachyose synthase gene. They were designed to meet the following features: (1) a length of at least 18 nucleotides; (2) no more than three G/C residues

among the six nucleotides at the 3' end of the primer, two of them being in the last two positions; (3) the primers should not form any strong secondary structure or (when using a primer pair) hybridize with each other; (4) the melting temperature (T_m) of the primer should not exceed the amplification temperature. T_m , the melting temperature at which 50% of the primer are bound to template, was calculated using the formula

$$T_m = 69.3 + 41 \times n_{GC} / N - 650 / N$$

where N is the total number of nucleotides and n_{GC} is the number of G/C in the primer.

Another formula can be used also:

$$T_m = 4 \times n_{GC} + 2 \times n_{AT}$$

where n_{AT} is the number of A/T in the primer.

T_m determines the annealing temperature ($T_{ann} = T_m - 3$) of the PCR. Primers used in the same reaction should have similar annealing temperatures.

Degenerate primers were used for amplification of raffinose synthase and stachyose synthase cDNA fragments of total cDNA obtained from *Alonsoa*. They were designed based on a comparison of several known amino acid sequences of raffinose synthases and the only known amino acid sequence of a stachyose synthase (*Vigna angularis*, Peterbauer et al., 1999). The primers were derived from two highly conserved sequence regions (Table 2.1). The PCR with this primer pair resulted in amplification of two cDNA fragments corresponding to raffinose and stachyose synthase, respectively.

2.21.2. cDNA synthesis and Rapid Amplification of cDNA Ends (RACE)

2.21.2.1. cDNA synthesis

Two reverse transcriptases (RT) with different temperature optima were used for the synthesis of first strand cDNA from RNA templates. For cDNA synthesis using the standard oligo-dT₂₀ primer and for 3'RACE, an RT from MBI (RevertAid M-MuLV-RT) with $T_{opt} = 37^\circ\text{C}$ was taken. For 5'RACE that require RT reactions with gene-specific primers, Thermoscript RT from Gibco BRL was chosen which is able to function at temperatures between 50 and 60°C, thus allowing a reaction temperature to match the annealing temperature of the primer.

Reverse transcriptions were performed in a volume of 20 μl . Prior to the reverse transcription reaction, 3 μg of total RNA and 500 ng of primer (100 pmol/ μl ; oligo-dT₂₀ or AP primer in case of 3'RACE, primers *amsts5race1* or *5raceneu1* in case of 5'RACE; Table 2.1) were denatured at 65°C for 5 min in a total volume of 10 μl (adjusted with dd H₂O) and placed on ice. This step leads to binding of the primer to the complementary RNA sequence. Then, the other components of the reaction mixture were added (see 2.21.2.2 and 2.21.2.3), and the reaction proceeded for 60 min at the temperature appropriate for the enzyme.

2.21.2.2. 3' RACE

For reverse transcription, 4 μ l 5 x RT buffer, 2 μ l dNTPs (10 mM) and 0.75 μ l (20 U) RNase inhibitor were added to the 10 μ l RNA/primer sample (see 2.21.2.1) and the total volume was adjusted to 19 μ l with dd H₂O. The mixture was incubated at 37°C for 5 min. After that, 1 μ l RevertAid M-MuLV-RT (200 U/ μ l) was added, and the reaction proceeded at 37°C for 1 h. After the reaction was completed, the cDNA was either incubated at 70°C for 5 min to inactivate the RT or directly used for a PCR.

2 μ l cDNA were used for a PCR with the 1st primer for 3'-RACE and either AP (when oligo-dT₂₀ had been used for reverse transcription) or UAP primer (when AP had been used). The second 3'RACE-PCR was performed with 2 μ l of the 1st PCR mixture, the 2nd 3'RACE primer and UAP. The product of the 2nd PCR was cloned in pGEM®-T Easy (see 2.20) and sequenced from both ends (2.26).

2.21.2.3. 5' RACE

For reverse transcription with Thermoscript RT, the following components were added to the 10 μ l RNA/primer mixture (2.21.2.1):

5 x RT buffer	4 μ l
dNTPs (10 mM each)	2 μ l
RNase Out (MBI Fermentas)	1 μ l
100 mM DTT	1 μ l
RT	1 μ l
H ₂ O	1 μ l

The reaction proceeded at 55°C for 1 h. After the reaction was completed, the free nucleotides were removed using the Concert kit (Gibco BRL, Eggenstein, Germany). Then, terminal desoxynucleotidyl transferase (TdT; Promega, Mannheim, Germany) and dCTP were added to the cDNA for the synthesis of a polyC tail to the 3' end of the cDNA. For this purpose, the cDNA was eluted from the spin column with 50 μ l 1 x TdT buffer prewarmed to 65°C. For the TdT reaction, 1 μ l TdT (15 U/ μ l), 1 μ l 5 x TdT buffer, 1.5 μ l 1 mM dCTP and 1.5 μ l dd H₂O were added to the eluted cDNA and incubated at 37°C for 30 min. 5 μ l of the TdT reaction mixture were then used for a PCR with the sequence-specific primer *amsts5race2* and the 5'*race* anchor primer (Table 2.1). The 5'*race* anchor primer contains an oligoG sequence and therefore can bind to the polyC tail at the 3' end of the first strand cDNA. This allowed the amplification of the cDNA fragment between the priming site of *amsts5race2* and the 5' end of the mRNA. The fragment was then cloned into pGEM®-T Easy (see 2.20) and both ends were sequenced (2.26). For safety, the 5'RACE was repeated with two different gene-specific primers (*5raceneu1* and *5raceneu2*), yielding the same 5' end sequence of the cDNA. This sequence was then used to design the primer *FLCsts5* which binds to the 5' end of *AmSTS* gene, to amplify the full length cDNA (2.21.3).

Table 2.1. Primers used for RT reactions and/or PCR. Ambiguity code: N=A/C/G/T; R=G/A; Y=C/T.

Primer	Sequence (5' → 3')	Used for
<i>degenerate primers</i>		
<i>Sta-5'</i>	GGNTGGTGYACNTGGGAYGC	RT-PCR to search for cDNA fragments of <i>AmSTS</i> and <i>AmRS</i>
<i>Sta-3'</i>	TGRAACATRTCCARTCNGG	
<i>gene-specific primers</i>		
<i>gen5STS</i>	GTAATAACTCAATAGTTCATGCATAAGC	PCR with genomic DNA of <i>Alonsoa</i> to analyse the restriction sites in introns of the stachyose synthase gene
<i>gen5STS1</i>	GTGTGCAAGAGTTTGCTGATGG	
<i>gen5STS2</i>	TCCAGCATGCAGCAATGCAACG	
<i>gen3STS</i>	AAATCCCACCACACTCTTCATAACC	
<i>gen3STS1</i>	CCTCCATCAGCAAACCTCTTGC	
<i>gen3STS2</i>	TCGTTGCATGTGCTGCATGCTGG	
<i>amsts5race1</i>	GTCAGCCCTCCATCAGC	1 st 5'-RACE gene-specific primer for RT
<i>amsts5race2</i>	GCACACCATGGTAAATACCAGC	2 nd 5'-RACE gene-specific primer for RT
<i>5raceneu1</i>	GAGGAGCTCGAAAGAGTTGTCC	1 st 5'-RACE gene-specific primer for PCR
<i>5raceneu2</i>	CAGGAAGTTCAAAATTGCGTTCATGG	2 nd 5'-RACE gene-specific primer for PCR
<i>sts3race1</i>	CTCTGGCAAATCAGATAACTTTGG	3'-RACE gene-specific primer for the 1 st PCR
<i>sts3race2</i>	ATGCATTGGCTGGTGCATGG	3'-RACE gene-specific primer for the 2 nd PCR
<i>FLCsts5</i>	CCAAACTAAGTAATAACTCAATAGTTCATGC	PCR of the full length cDNA of <i>AmSTS</i>
<i>FLCsts3</i>	CAAACACATTTTCATGGCCAATTCTGG	
<i>nhe3site</i>	TGCTAGCTTAGTAAACAAAAGTTACATTAGAAATCC	insertion of <i>NheI</i> sites at the ends of the <i>AmSTS</i> full length cDNA for expression cloning
<i>nhe5site</i>	AGCTAGCGCACCTCCATATGATCCCATC	
<i>gw3GSPa</i>	GGTTGAAAAAACAGAGCAAAAACAGG	PCR to obtain <i>AmSTS</i> promoter fragments, (a) promoter plus 5' UTR and (b) promoter only
<i>gw5GSP</i>	ATCCTCTTGGCCTTGACACCTAGG	
<i>gw3GSPb</i>	AGAAAAATGTGAAGGGGAGGCAGAC	
<i>AmSTSgw1</i>	GACGTGCTCGGGATATCGGTGAGAATCGG	gene-specific primers used for Genome Walking for cloning of the <i>AmSTS</i> promoter
<i>AmSTSgw2</i>	GGATGGGATCATATGGAGGTGCCATGGTTG	
<i>5'race</i>	GGCCACGCGTCGACTAGTACGGGIIGGGIIGGGIIG	5'-RACE anchor primer
<i>AP</i>	GGCCACGCGTCGACTAGTAGTTTTTTTTTTTTTTTTT	3'-RACE adapter primer
<i>UAP</i>	GGCCACGCGTCGACTAGTAG	3'-RACE
<i>dT₂₀</i>	TTTTTTTTTTTTTTTTTTTTTT	RT reactions
<i>ubifor</i>	ATGCAGATYTTTGTGAAGAC	control for traces of DNA in RNA samples or control of quality of cDNA (Heidstra et al., 1994)
<i>ubirev</i>	ACCACCACGRAGACGGGAG	
<i>M13forward</i>	TGACCGGCAGCAAAATG	3'-primer for the determination of the insert orientation in plasmids pBIstsA and pBIstsB used in combination with the 5'-primer <i>pmr5seq3</i> (Table 2.2)

2.21.3. Amplification and cloning of the AmSTS full length cDNA

Two gene-specific primers, *FLCsts5* and *FLCsts3* (Table 2.1), were designed from the 5' and 3' sequences of *AmSTS* obtained by 3' and 5'RACE. PCR was performed with these primers and *AmSTS* cDNA obtained by RT reaction using oligo dT₂₀ (2.21.2.1). For the PCR, an Advantage *Tth* Polymerase mix (Clontech, Palo Alto, CA., USA) with 3'-5' exonuclease („proof-reading“) activity was used to achieve high accuracy of the amplification. Furthermore, the *TthStart*[™] antibody allowed a hot start of the reaction, to prevent premature degradation of primers by the 3'-5' exonuclease activity.

For this reaction, the PCR program and the reaction conditions were based on the requirements of this special polymerase as described below (2.21.4). The PCR product was purified via agarose gel electrophoresis and ligated into pGEM®-T Easy. Cloning and selection of transformants were performed as described in 2.20.5. The first 300 bp of 5' and 3' ends of the insert were sequenced (2.26) and corresponded to the sequences obtained by RACE. After that, both strands of the full length cDNA were sequenced by SEQLAB Sequence Laboratories Göttingen GmbH (Göttingen, Germany). For these reactions, gene-specific primers (Table 2.2) were designed.

2.21.4. Amplification of a promoter fragment by Genome Walker DNA walking

The „Genome walking libraries“ of *Alonsoa meridionalis* genomic DNA were kindly provided by Dr. Christian Knop. They were prepared by separate restriction of *Alonsoa* genomic DNA with 5 different enzymes (*EcoRV*, *ScaI*, *DraI*, *PvuII* and *SspI*) which produce blunt ends. These DNA fragments were then ligated to the „genome walking adapters“ provided in the Genome Walking kit from Clontech (Palo Alto, CA., USA). For each library, two PCR reactions were performed using adapter primers (APs) and two gene-specific primers which were designed on the basis of the 5'RACE results. These primers should have a T_{ann} of about 67°C, i.e. a T_m of about 70°C.

For the first PCR, the adaptor primer AP1 and the gene-specific primer *AmSTSGwl* which binds about 100 nucleotides downstream from the 5' end of the *AmSTS* cDNA were used. The reaction mixtures contained:

Advantage <i>Tth</i> Polymerase mix	1 µl
10x <i>Tth</i> PCR reaction buffer	5 µl
dNTPs (10 mM each)	1 µl
25 mM Mg acetate	2.2 µl
10 pmol primer AP	11 µl
10 pmol primer <i>AmSTSGwl</i>	1 µl
DNA library	1 µl
dd H ₂ O	ad 50 µl

A two-step PCR program was used:

7 cycles	94°C	25 sec
	72°C	3 min
32 cycles	94°C	25 sec
	67°C	3 min
followed by	67°C	7 min

The PCR products were analysed on an agarose gel. For the libraries where DNA bands were observed, a 2nd PCR was performed.

For the second PCR, the adapter primer AP2 which binds downstream of the binding site of AP1, and the gene-specific primer *AmSTSGw2* which binds upstream of the binding site of *AmSTSGw1* were used. The reaction mixtures contained:

Advantage <i>Tth</i> Polymerase mix	1 µl
10x <i>Tth</i> PCR reaction buffer	5 µl
dNTP (10 mM each)	1 µl
25 mM Mg acetate	2.2 µl
10 pmol primer AP2	1 µl
first reaction mixture diluted 1:50	1 µl
10 pmol primer <i>AmSTSGw2</i>	1 µl
dd H ₂ O	ad 50 µl

The same two step program was used as for the first PCR except for the reduced number of cycles (5 instead of 7 for the first set, 20 instead of 32 for the second set). PCR products were analysed on 1% agarose gel. DNA bands of interest were excised from the gel, cloned and sequenced (2.20.1, 2.20.3, 2.20.5, 2.26).

2.21.5. Colony PCR

To identify positive clones of bacteria transformed with pBI101.3 derivatives pBIstsA and pBIstsB where no blue/white selection was possible, colony PCR was performed. 30-40 culture tubes with LB medium containing kanamycin were prepared corresponding to the number of the colonies of transformants to be picked. A PCR master mix was prepared (2.21) and 10 µl dd H₂O were pipetted into 0.5 ml Eppendorf tubes. Each colony was picked with a sterile toothpick. The toothpick was first dabbed into a PCR tube and then placed in a correspondingly labelled culture tube. 15 µl of master mix were added to each tube, and the PCR was performed using an appropriate program as described in 2.21 except that the first step at 94°C was extended (5 min) to break the cells. The cultures were grown overnight at 37°C (shaking). 10 µl of each PCR were run on 1% agarose gel to identify positive clones. The cultures of these clones were used for the isolation of plasmid DNA.

2.22. Expression of *AmSTS* in *E. coli* using pET expression system

2.22.1. Transformation of *E. coli* BL21 (DE3)

The *AmSTS* cDNA was cloned in *E. coli* cells using the pET3b vector and the T7 RNA polymerase expression system (Rosenberg et al., 1986). For this purpose, 2602 bp of the *AmSTS* cDNA were inserted into the *NheI* restriction site of the polylinker of plasmid pET3b under the control of the T7 promoter, yielding pET*/STS.

The construction of pET*/STS was performed as follows. Two *AmSTS* cDNA-specific primers *nhe3site* and *nhe5site* (Table 2.1) were designed that carry *NheI* restriction sites at their 5' ends, and PCR was performed with these primers and the *AmSTS* cDNA cloned in pGEM®-T Easy as the template. The PCR product was cloned in pGEM®-T Easy, yielding pGEM-AmSTSnhe.

Since pET3b also carries an additional *NheI* site, the part of pET3b containing this site was removed by *EcoRV* restriction and religation, yielding pET*3b. Then, the *AmSTS* cDNA was excised from pGEM-AmSTSnhe using *NheI* and ligated into the *NheI* site of pET*3b, yielding pET*/STS. BL21 (DE3) cells transformed with pET*/STS were used to induce the expression of *AmSTS*, and BL21 (DE3) cells transformed with an empty pET3b vector were used to provide a negative control for stachyose synthase activity measurements. The transformants were grown on LB plates containing ampicillin, and the presence and orientation of the insert were confirmed by restriction analysis using *EcoRI*, *HindIII* and *BamHI*.

2.22.2. Induction of the expression of the transgene using IPTG

5 ml LB-ampicillin medium were inoculated with BL21 (DE3) (pET*/STS) and BL21 (DE3) (pET3b), respectively, and grown overnight at 37°C. On the next day, 250 ml of LB medium with ampicillin were inoculated with the overnight cultures and grown at 37°C up to an OD₆₀₀ of 0.6. At this point, IPTG was added up to a final concentration of 0.3 mM and cells were grown for three more hours. During the growth, OD₆₀₀ was measured at time intervals of 30 min and 600 µl aliquots of cells were harvested for the separation of proteins by SDS-PAGE (2.23). At the end of this period the OD₆₀₀ was determined again to make sure that the cultures had continued to grow. The cells were spun down in 50 ml conic sterile centrifuge tubes (4300 rpm, 10 min; Megafuge 1.0, Heraeus Sepatech, Osterode, Germany), and the pellets were resuspended in extraction buffer (2.5.6.2). This was followed by the extraction of proteins which were then used for protein gel analysis and for STS activity measurements.

2.23. SDS - PAGE (Laemmli, 1970)

To check protein formation in *E. coli* in IPTG-induced B121 (DE3) cells, SDS - PAGE (Laemmli, 1970) was used.

2.23.1. Protein extraction from *E. coli* cells

600 µl Aliquots of cell cultures were centrifuged and the cells were resuspended in protein extraction buffer to a similar density based on OD₆₀₀ values measured before harvesting (2.22.2). The samples were solubilized at room temperature for 30 min. Afterwards, the samples were denatured at 95°C for 3 min, centrifuged at 13 000 rpm for 5 min and loaded into the gel slots using a microsyringe. 5 µl of a size marker protein mixture (“Low molecular weight calibration Kit”) were treated in the same way.

Protein extraction buffer:

Tris/HCl pH 6.8	15 mM
SDS	5% (w/v)
β-mercaptoethanol	2% (v/v)
glycerol	5% (v/v)
Bromphenol blue	0.01% (v/v)

Low molecular weight marker:

Phosphorylase b	97 kDa
BSA	66 kDa
Ovalbumine	45 kDa
Carboanhydrase	30 kDa
Trypsin inhibitor	20 kDa
α-Lactalbumine	14 kDa

2.23.2. SDS-Polyacrylamide gel electrophoresis

7.5% polyacrylamide gels were prepared as follows. Glass gel plates, combs and silicon spacer tubes were cleaned with dd H₂O, dried, and the gel cassette was mounted. Solutions for the separating gel and the stacking gel were prepared. TEMED was added to the separating gel solution and the separating gel was poured into the cassette until 1 cm from the ends of comb slots (about 7 cm from the gel bottom). To ensure that the gel was set with a smooth surface, ddH₂O was carefully poured into the cassette using a Pasteur pipette forming a layer of about 2 mm. When the gel was polymerized, a clear refractive index change could be seen between the gel and overlaying water. After that, the water was poured off, TEMED was added to the stacking gel solution, and a stacking gel of about 1 cm was poured. The slot-forming comb was placed into this solution, and the stacking gel was left for

polymerization. 10-20 μ l of the samples (2.23.1) were loaded into the slots. Gel electrophoresis was set at constant current of 30 mA until the blue marker reached the bottom of the gel.

Acrylamide stock solution

Acrylamide	29.2% (w/v)
N,N-methylenbisacrylamide	0.8% (w/v)
dd H ₂ O to 100 ml	

Separating gel solution (38.25 ml for two gels required):

Tris/HCl pH 6.8	0.125 M
SDS	0.1%
Acrylamide	7.5% (w/v)
N,N-methylenbisacrylamide	0.2% (w/v)
Ammonium persulfate	0.05% (w/v)
TEMED (add before pouring the gels)	0.1% (v/v)

Stacking gel solution (15 ml for two gels required):

Tris/HCl pH 6.8	0.125 M
SDS	0.1%
Acrylamide	4% (w/v)
N,N-methylenbisacrylamide	0.11% (w/v)
Ammonium persulfate	0.05% (w/v)
TEMED (add before pouring the gels)	0.1% (v/v)

Electrophoresis buffer:

Tris (no pH adjustment)	0.025 M
Glycine	0.192 M
SDS	0.1% (w/v)

2.23.3. Coomassie staining of the gels

After electrophoresis, the gels were stained for 2 hours in Coomassie staining solution and washed overnight in washing solution containing 10% (v/v) acetic acid and 50% (v/v) methanol. The stained gels were vacuum-dried.

Coomassie staining solution:

Coomassie Brilliant Blue G-250	0.25% (w/v)
Methanol	40% (v/v)
Acetic acid	10 % (v/v)

2.24. Promoter-GUS fusions in transgenic plants

To investigate the expression pattern of *AmSTS* and the possible effect of the 5'UTR of the *AmSTS* cDNA on this expression pattern, *Arabidopsis thaliana* ecotype Columbia plants were transformed with *Agrobacterium tumefaciens* carrying the plasmids pBIstsA or pBIstsB, respectively. These plasmids were obtained by inserting 1.95 kb of the *AmSTS* promoter region into the *Sma*I site of plasmid pBI101.3 upstream of the open reading frame of β -glucuronidase (GUS). The 5'UTR of the *AmSTS* cDNA was added to the promoter in the plasmid pBIstsA but omitted in pBIstsB (2.2.3). Competent cells of *Agrobacterium tumefaciens* strain GV3101 (pMP90) were transformed with pBIstsA and pBIstsB, respectively. Positive transformants were used for the infiltration of *A. thaliana*. Seeds obtained from the infiltrated *A. thaliana* plants were grown on MS2-agar containing kanamycin and then transferred to soil as described in 2.2.1. For determination of GUS activity by staining (2.24.4.1), rosette leaves of first generation transformants (F1) were used while the plants were further grown for seed production. In the second generation of transformants (F2), obtained from F1 seeds, GUS activity staining was performed using whole seedlings, rosette leaves and inflorescences.

2.24.1. Preparation of competent *Agrobacterium tumefaciens* GV3101 cells

5 ml liquid YEB medium supplemented with rifampicin were inoculated with an *A. tumefaciens* GV3101 (pMP90) colony and grown at 28°C overnight. On the next day, 50 ml YEB with rifampicin were inoculated with this culture and grown at 28°C for about 4 h until the cell density in the culture had reached an OD₆₀₀ of 0.5. 10 ml of this culture were used for the preparation of the electroporation-competent cells. The cells were spun down at 4300 rpm (10 min, 4°C; Megafuge 1.0 Heraeus) and resuspended in 10 ml dd H₂O. The cells were then washed eight times by centrifuging and resuspending in 10 ml dd H₂O. This led to the removal of ions from the cell wall and thus rendered the cells suitable for transformation by electroporation. 15-20 μ l aliquots were pipetted into sterile 1.5 ml plastic Eppendorf tubes and stored at -80°C.

2.24.2. Transformation of *Agrobacterium tumefaciens* by electroporation

3 μ l (ca 100 ng) plasmid DNA of pBIstsA or pBIstsB were added to 20 μ l of *Agrobacterium* GV3101 (pMP90) competent cells thawed on ice in a 1.5 ml plastic tube and incubated on ice for 30 min. The electroporation was performed in a 0.2 cm cuvette using the Gene Pulser® Electroporation system (Bio-Rad Laboratories GmbH, Munich, Germany). The pulse parameters were 2.5 kV/25 μ F/ 200 k Ω . The time constant was set automatically and

was 4.6 ms. Immediately after the pulse, 1 ml of ice-cold SOC medium was pipetted into the cuvette and the cell suspension was transferred into a sterile 1.5 ml Eppendorf tube and incubated at 28°C for 1 h. The transformants were selected on YEB plates supplemented with rifampicin and kanamycin at 28°C for 2 days. For purification of transformants, single colonies were streaked onto new plates, and the procedure was repeated two times. For the characterization of transformants, plasmids were isolated (2.16.2) and used for transformation of *E. coli* DH5 α cells. From *E. coli*, plasmids were isolated in preparative amounts and characterized by PCR with gene-specific primers and by restriction analysis.

2.24.3. Transformation of *Arabidopsis thaliana* with *Agrobacterium tumefaciens*

A. thaliana ecotype Columbia plants were grown as described in 2.2.1. Flowering plants were used for transformation with *Agrobacterium* (Clough and Bent, 1998). 100 ml YEB with rifampicin and kanamycin were inoculated with 5 ml overnight cultures of *A. tumefaciens* GV3101 (pMP90) (pBIstsA) or (pBIstsB), respectively, and were grown at 28°C for several hours until the OD₆₀₀ reached 0.5. The cells were spun down and resuspended in about 200 ml of a 5% sucrose solution to final OD₆₀₀ of 0.8. For aeration of cells, the suspensions were kept on a magnetic stirrer until they were used for transformation.

Silwet L-77 was added to the cell suspensions up to a concentration of 0.05% and mixed. The inflorescences of *A. thaliana* plants were then dipped into the *Agrobacterium* suspension for 2-3 sec under gentle agitation. The dipped plants were left under open air for several hours and then placed under a transparent plastic cover to provide a high humidity for two days. Plants were then watered and grown normally until seed production (2.2.1).

2.24.4. Qualitative GUS assay

2.24.4.1. Staining of rosette leaves from F1 plants

The selected kanamycin-resistant F1 plants grown from the seeds of the infiltrated plants were numbered, and from each plant, two leaves were harvested for GUS activity staining and two leaves for DNA isolation (2.15.3). For DNA isolation, leaves were placed in 1.5 ml plastic tubes and stored at -80°C. For GUS activity staining, the leaves were placed in 1.5 ml plastic tubes and covered with washing buffer containing 1 mM X-Gluc. The concentration of K-ferri/ferrocyanide in washing buffer differed dependent on experiment but were at least 3 mM except for one experiment where it was omitted (3.3.6.3, Figure 3.29). The tubes were closed and the covers were perforated with a needle. The tubes were placed in a desiccator and vacuum was applied for 15 min to infiltrate the leaves with X-Gluc solution. The tubes were incubated at 37°C for 16-24 h. After the incubation, the leaves were incubated

for 30 min in 30% ethanol and fixed in FAA fixative for 1 hour at room temperature. Leaves were then incubated in 96% ethanol overnight to remove chlorophyll. Leaves treated in this way were stored in 70% ethanol. On the basis of the GUS activity staining results obtained, F1 plants were selected for further analysis, i.e. F2 seed production.

Washing buffer:

50 mM	Na phosphate pH 7.5
1 mM	EDTA
0,1 % (v/v)	Tween 20
3 – 20 mM	K-ferrocyanide $K_4[Fe(CN)_6] \cdot 3H_2O$
3 – 20 mM	K-ferricyanide $K_3[Fe(CN)_6]$

X-Gluc stock solution:

100 mM X-Gluc (5-bromo-4-chloro-3-indolyl- β -D-glucuronide) in DMF

FAA fixative:

50%	ethanol
10%	acetic acid
5%	formamide

2.24.4.2. Infiltration of seedlings to induce GUS expression

GUS activity staining of seedlings and also of inflorescences and siliques of mature plants was performed as described in 2.24.4.1. For induction experiments, the seedlings were taken directly from plates and were floating for 20 hours in the MS solutions containing additives/no additives. Afterwards, the seedlings were stained for GUS activity.

Incubation solutions:

MS medium (infiltration control)
MS medium with 180 mM sucrose
MS medium with 200 mM glucose

2.25. *in situ* RNA hybridization of thin paraffin sections of *Alonsoa***2.25.1. Preparation of the RNA probes****2.25.1.1. Construction and linearization of plasmids**

RNA antisense probes were produced for *in situ* hybridization with transcripts of *Alonsoa* stachyose synthase (*AmSTS*), raffinose synthase (*AmRS*) and sucrose transporter (*AmSUT1*). cDNA fragments of ca. 1.0 kb for *AmSTS* and of ca. 0.8 kb for *AmRS* had been obtained by RT-PCR using the degenerate primers *Sta-5'* and *Sta-3'* (2.21.2.1; Table 2.1). The fragment of *AmSUT1* was provided by Christian Knop. The fragments had been cloned in

pGEM®-T Easy. From there, they were excised with *EcoRI* and ligated into pBluescript®IIKS⁺ linearized with *EcoRI*, yielding pAmSTSish, pAmRSish and pAmSUTish. The orientation of the inserts was determined by restriction with *HindIII* and *BamHI*.

In all three plasmids, T3 was used for transcription of the antisense RNA. The sense RNA probe was transcribed from AmSUT1ish using T7 RNA Polymerase. Before transcription, the plasmids were linearized with restriction enzymes which should not leave 3'-overhangs which might lead to unspecific initiation of transcription in the wrong direction.

For transcription of antisense RNA probes, the plasmids were linearized with the following enzymes:

PAmSTSish using *XbaI*

PAmRSish using *BamHI*

pAmSUTish using *XbaI*

For transcription of the sense control probes, plasmid AmSUT1ish was linearized with *HindIII*.

For each linearization, 5-10 µg plasmid DNA were restricted for 2 hours at 37°C in a total volume of 200 µl with 30 U of restriction enzyme. The completeness of the restriction was confirmed by agarose gel electrophoresis of a 10 µl aliquot. The linearized plasmids were purified by phenol:chloroform extraction (2.18), then precipitated with ethanol and redissolved in 10 µl dd H₂O. An 1 µl aliquot was used for agarose gel electrophoresis to determine the DNA concentration.

2.25.1.2. *In vitro* transcription

In vitro transcription was performed with T3 (for antisense probes) or T7 (for sense control) RNA polymerase for 2.5 hours at 37°C. The reaction mixtures contained in a total volume of 20 µl:

1 µg linearized plasmid DNA

4 µl 5 x T7 or 5 x T3 buffer

1 µl 100 mM DTT

0.5 µl RNase Out (Gibco BRL, Eggenstein, Germany)

1 µl RNA polymerase (T7 or T3, 50 U/µl, Gibco BRL)

1 µl dNTP + Dig (= 25 mM each of dATP, dCTP, dGTP; 16.25 mM dUTP; 0.175 mM Dig-UTP; Roche Biochemicals, Mannheim, Germany)

After the reaction had proceeded for 2 h, 1 µl was removed from the reaction mixtures, and the RNA concentration was determined by agarose gel electrophoresis (2.19.3). The reaction continued for the next 30 min. The RNA concentration should be at least 40 ng/µl. After the

gel electrophoresis, 1 μ l of 10 μ g/ μ l tRNA and 1 μ l (1 U/ μ l) RNase-free DNase (Promega, Madison, WI., USA) for degradation of the plasmid DNA templates were added to the reaction mixtures, followed by an incubation for 15 min at 37°C. Then, free nucleotides were separated from the RNA by passage through Microspin S-300 HR columns (Amersham Pharmacia Biotech, Freiburg, Germany). If necessary, the RNA was concentrated using LiCl/ethanol-precipitation. For this procedure, 2.5 volumes of 4 M LiCl and 75 μ l of ice-cold 96% ethanol were added to 20 μ l RNA mixtures and RNA was precipitated for 2 hours at –20°C. The precipitated RNA was spun down (13 000 rpm, 10 min), washed with ice-cold 75% ethanol (13 000 rpm, 5 min) and resuspended in dd H₂O by an incubation at 65°C for 5 min.

2.25.1.3. Hydrolysis

The probes longer than 700 nucleotides in size (*AmRS* and *AmSTS*) were subjected to hydrolysis to obtain fragments of maximally 150 nucleotides length. 50 μ l RNA (i.e. half of each probe), 30 μ l of 0.2 M Na₂CO₃ and 20 μ l of 0.2 M NaHCO₃ were incubated at 60°C. The incubation time was calculated as follows:

$$t = (L_0 - L_f) / 0.11 \times L_0 \times L_f,$$

where t = time (min), L_0 = starting length (in kb), L_f = desired final length (in kb).

The reaction was stopped by the addition of 3 μ l 3 M sodium acetate pH 6.0 and 5 μ l 10% acetic acid. Then, 1 μ l of 10 μ g/ μ l tRNA carrier was added, and the RNA was precipitated with 250 μ l ethanol at –20°C for 1 hour and spun down for 15 min at 13 000 rpm. The precipitated RNA was redissolved in dd H₂O at room temperature. The concentration of RNA fragments was checked on an agarose gel. The appropriate probe concentrations were achieved by combining equal amounts of hydrolyzed and non-hydrolyzed probes.

2.25.2. Prehybridization

Paraffin sections were prepared as described in 2.14. The incubations were performed in a glass rack kept in glass boxes filled with 200 ml of the appropriate solution. Paraffin was removed from the sections by incubation of the slides for 30 min each in 100% xylene, 100% ethanol:100% xylene (1:1) and 100% ethanol. This was immediately followed by the prehybridization. The sections were rehydrated in a graded EtOH series for 1 minute each: twice in 100% EtOH, then once in 90%, 70%, 50%, 30% and 10% EtOH. Then the slides were washed three times in dd H₂O for 1 min each. After that, the sections were subjected to Proteinase K treatment which allowed the partial degradation of cellular proteins to make the target RNA more accessible for the probe. The incubation lasted 10 min at 37°C in 2 x SSC, 0.1% SDS (Proteinase buffer) containing 1 μ g/ml Proteinase K (Roche Molecular Biochemicals, Mannheim, Germany). The reaction was stopped by washing the slides for 2

min in 2 mg/ml glycine in 1 x PBS (stirring) and then twice in 1 x PBS for 2 min each (stirring). After that, the sections were refixed for 10 min in a freshly prepared solution of 4% paraformaldehyde in 1 x PBS.

The refixed sections were washed twice with 1 x PBS for 5 min each and then incubated for 10 min in 0.1 M triethanolamine with acetic anhydride pH 8.0 (stirring). This step allowed the saturation of the positive charges within the tissue which might bind the negatively-charged RNA probe. Triethanolamine was removed by washing the sections for 5 min in 2 x SSC. Then, the slides were placed in a plastic box with paper towels wetted with 2 x SSC. 800 µl of prehybridization solution was applied on slides, the box was sealed with tape, and the slides were incubated at 45°C for 30 min.

Prehybridization solution (end concentrations):

formamide (double crystallized)	50 %
NaCl	300 mM
Tris-HCl pH 7.5	10 mM
EDTA	1 mM
Ficoll	0.02 %
PVP	0.02 %
BSA	0.02 %
tRNA	150 µg/ml
DTT	30 mM

10 x PBS:

NaCl	1.3 M
Na ₂ HPO ₄	70 mM
NaH ₂ PO ₄	30 mM
KCl	1.7 mM

Triethanolamine:

dd H ₂ O	200 ml
Triethanolamine (stock solution prewarmed at 80°C for ca. 1 h)	2.66 ml
Acetic anhydride	0.6 ml

2.25.3. Hybridization

Solutions A and B were prepared in amounts corresponding to the number of slides plus two.

Solution A per slide:

double crystallized formamide	50 µl
5 M NaCl	6 µl

100 mM Tris-HCl pH 7.5, 10 mM EDTA	10 μ l
50 x Denhardt's	2 μ l
50% dextran sulfate (prewarmed at 80°C for pipetting)	20 μ l
dd H ₂ O	2 μ l

kept at 37°C until use.

Solution B per slide:

3 M DTT	1 μ l
10 μ g/ μ l tRNA	2.5 μ l
20 μ g/ μ l poly(A) (prewarmed at 80°C for pipetting)	2.5 μ l

kept on ice until use.

The probes (5 μ l of each probe corresponding to 100 ng RNA per slide) were pipetted into 1.5 ml Eppendorf tubes, 5 μ l of solution B were added and 5 min incubation at 80°C followed to dissolve secondary structures of the RNA. Then, 90 μ l of solution A were added by pipetting up and down slowly and carefully to prevent the formation of air bubbles. The mixture was then applied to the slide. The slides were covered by glass coverslips which were pre-cleaned with 96% ethanol and dried with dust-free paper towels. Care was taken to prevent air bubble formation. The slides were placed in a closed moisture chamber with paper towels wetted with 2 x SSC and the hybridization proceeded overnight at 45°C in the dark to keep the ionization of formamide low.

Hybridization solution:

(made up of 90 μ l solution A, 5 μ l solution B and 5 μ l RNA probe in dd H₂O per slide, end concentrations):

formamide (double crystallized)	50%
NaCl	300 mM
Tris-HCl pH 7.5	10 mM
EDTA	1 mM
Ficoll	0.02%
PVP	0.02%
BSA	0.02%
dextran sulfate 500.000	10%
poly(A)	500 μ g/ml
tRNA	150 μ g/ml
DTT	30 mM
RNA probe	40-100 ng/100 μ l

2.25.4. Washing

10 mg/ml RNase A (Sigma-Aldrich, Taufkirchen, Germany) were dissolved in dd H₂O and boiled for 30 min to remove traces of DNases. RNase A was added to RNase buffer to a final concentration of 20 µl/ml and prewarmed at 37°C. The slides were placed in glass racks. Cover slips were removed by placing the racks in 4 x SSC and moving them up and down. The slides were then incubated for 2 min in RNase buffer and treated with prewarmed RNase A for 30 min at 37°C in a shaking water bath. After the RNase treatment, the slides were washed at room temperature three times for 5 min each in RNase buffer (stirring) and for 30 min with 2 x SSC (stirring). This was followed by an incubation in 0.2 x SSC at 56°C in a shaking water bath for 30 min and in 0.2 x SSC at room temperature (stirring) for 10 min.

RNase buffer:

Tris/HCl, pH 7.5	10 mM
EDTA	2 mM
NaCl	500 mM

2.25.5. Detection

The slides were incubated for 1 min at room temperature in 1 x PBS (stirring). At this stage, the slides could be kept in 1 x PBS at 4°C overnight. The slides were prepared for the detection reaction by incubation for 45 min in 1% blocking reagent at room temperature (stirring). This was followed by an incubation in TNT-BSA for 45 min (stirring). For the detection of digoxigenine-labelled RNA, an anti-Dig-antibody solution was prepared. The slides were put in a plastic box with wet paper towels, and 450-500 µl antibody solution were pipetted onto each slide. The box was closed, and the slides were incubated in darkness for 2 h at room temperature.

After incubation with the anti-Dig-antibody, the slides were washed in TNT-BSA four times for 15 min each (stirring) and for 10 min in detection buffer (stirring). For the inhibition of endogenous phosphatases, another 5 min incubation was performed in detection buffer containing 1 mM levamisole (stirring). After that, every slide was dipped in a beaker with detection buffer to make sure that all traces of Triton X-100 were removed. For the detection reaction, the slides were put in a plastic box with wet paper towels, and 150 µl freshly prepared detection solution was pipetted onto each slide. Cover slips were put on the slides, and the slides were incubated for several hours or overnight in a closed moisture chamber sealed with tape.

The coloration of sense control slides was checked regularly during this incubation. When sense control slides started coloring, or when antisense slides showed enough coloring,

the reaction was stopped in 1 x PBS containing 20 mM EDTA. The slides were kept in this solution in the dark before mounting.

For the mounting, the tissue was dehydrated in a graded ethanol series (10%, 30%, 50%, 70%, 90% and twice 100%, 15 sec each). After an incubation for at least 1 min in ethanol:xylene (1:1) and twice in 100% xylene for at least 5 min each, the sections were mounted with Eukit (Kindler, Freiburg, Germany). Several drops of Eukit were pipetted onto the xylene-wet slides, the cover slips were dipped in xylene and then placed on the slides, and the slides were left under the fume hood over night for the evaporation of xylene and the hardening of the resin. Then, photographs could be taken under a microscope.

Blocking reagent (200 ml)

Blocking reagent (Roche Molecular Biochemicals, Mannheim, Germany)	1% (w/v)
Tris/HCl pH 7.5	100 mM
NaCl	50 mM
stir for at least 1 h before use	

TNT-BSA

Tris/HCl pH 7.5	100 mM
NaCl	150 mM
autoclave, then add	
Triton X-100	0.3% (v/v)
BSA	1%

Anti-dig-antibody

dilute 1:1250 in TNT-BSA
preadsorb for at least 30 min before use

Detection buffer

Tris/HCl pH 9.5	100 mM
NaCl	100 mM
MgCl ₂	50 mM

Detection solution (for 10 slides)

5 ml detection buffer

5 µl 100 mM levamisole

22.5 µl 100 mg/ml NBT dissolved in DMF:H₂O = 7 : 3 (= 4-nitro-blue tetrazolium chloride, Roche Molecular Biochemicals, Mannheim, Germany)

16.5 µl 50 mg/ml BCIP dissolved in DMF (= 5-bromo-4 chloro-3-indoyl phosphate, Roche Molecular Biochemicals, Mannheim, Germany)

Stop solution

1 x PBS

add EDTA to a final concentration of 20 mM

2.26. DNA sequencing

The sequencing of DNA was based on the method of Sanger et al. (1977) with some modifications. For sequencing, the ABI PRISMs Rhodamine Terminator Cycle sequencing Ready Reaction Kit was used (Perkin Elmer Applied Biosystems, Weiterstadt, Germany). The kit contains rhodamine derivatives of di-desoxynucleotides which differ in their emission and absorption spectra depending on the ddNTP. The rhodamine-labelled ddNTPs were incorporated into the synthesized DNA during elongation of DNA chains in a sequence-PCR. The reaction mixture contained:

Terminator Ready Reaction Mix	2 μ l
plasmid DNA	200-300 ng
primer	8 pmol
dd H ₂ O ad	10 μ l

For the sequencing, the primers corresponding to sequences present in the vector (T7, T3, for (M13 forward primer), rev (M13 reverse primer)) or gene-specific primers (Table 2.2) were used. The following program was used for sequence-PCR:

96°C	10 sec
50°C	5 sec
60°C	4 min

This cycle was repeated 25 times. After the PCR, the free rhodamine-labelled ddNTPs were removed by an ethanol precipitation of DNA as follows. 1 μ l Na acetate/EDTA buffer (1.5 M Na acetate + 250 mM EDTA, pH >8) and 41 μ l of 96% ethanol were added to 10 μ l reaction mixture. The end concentration of ethanol in the mixture was 75%. The samples were incubated on ice for 15-20 min and centrifuged (13 000 rpm) for 15 min at room temperature. The supernatant was immediately removed quantitatively, and the pellets were washed with 75% ethanol (10 min centrifugation at 13 000 rpm). The pellets were dried for 1 min at 90°C, resuspended in 17 μ l Template Suppression Reagent (Perkin Elmer Applied Biosystems, Weiterstadt, Germany) and denatured at 95°C for 2 min. The samples were kept on ice until sequencing in a ABI PRISM 310 Genetic Analyser (Perkin Elmer Life Sciences Ltd, Cambridge, UK).

To obtain the sequences of the cDNA and promoter of *AmSTS*, the corresponding plasmids and the deduced primers (Table 2.2) were sent to SEQLAB Sequence Laboratories Göttingen GmbH (Göttingen, Germany).

2.27. DNA and amino acid sequence analysis

Amino acid and nucleotide sequences of known cDNAs, proteins and vectors were obtained from Genbank of National Center for Biotechnology Information (Altschul et al., 1990; <http://www.ncbi.nlm.nih.gov>). For alignment of sequences, the programs of the Wisconsin Package from Genetics Computer Group (GCG; Madison, WI., USA) were used which were available through the Gesellschaft für wissenschaftliche Datenverarbeitung Göttingen (GWDG). The programs *seqed*, *map*, *bestfit*, *lineup*, *assemble*, *peptidesort* and *translate* were used.

Table 2.2. Primers used for sequencing.

Primers	Sequence (5'→3')	Used for
<i>T7</i>	TAATACGACTCAATATAGG	sequencing of the ends of PCR products cloned in pGEM®-T Easy or pBluescript®IIS ⁺
<i>T3</i>	TAACCCTCACTAAAGGGA	
<i>for</i>	GTAAAACGACGGCCAGT	
<i>rev</i>	AGCGGATAACAATTTACACAGGA	
<i>pmr5seq3</i>	ATGGCATAAAGGAAGAAGATGG	SEQLAB sequencing of the <i>AmSTS</i> promoter (both directions)
<i>pmr3seq3</i>	ACTTGCATGGTGCATGTAAGC	
<i>pmr5seq2</i>	GTTTGGTTCGAGCTCAATTGG	
<i>pmr3seq2</i>	CAATTTGTGAAGTTAAGATTAGTAGG	
<i>pmr5seq1</i>	TGATGCTTACATGCACCATGC	
<i>pmr3seq1</i>	GGGAAAACAAACCACTAGTTGG	
<i>FLC5seq1</i>	CAACTCTTTTCGAGCTCCTCGACG	SEQLAB sequencing of the full length cDNA of <i>AmSTS</i> (both directions)
<i>FLC3seq1</i>	TAGTACAAGACTTATTTCAAGC	
<i>FLCs5seq2</i>	GATAACGACCCGAATGAGGATGC	
<i>FLCs3seq2</i>	GAGAGCAAAATGGATGCACTTGG	
<i>FLCs5seq3</i>	GAGTGGGTGATGACTTTGG	
<i>FLCs3seq3</i>	TCCACCGAACATTTGATCC	
<i>FLC3seq3</i>	TTTCCAGCATGCAGCAATGC	
<i>FLCs5seq4</i>	TCAAGGTCTGGTGTACAACG	
<i>FLC3seq4</i>	GACCACCAGGTTTTGAACC	
<i>sts3seq3</i>	ATCCTTCGTAAACGCTTTTCATCC	
<i>sts3seq5</i>	CAGAATCGGGACATTTTTTCACG	
<i>sts5seq3</i>	AGGCTGAGAACTATCCTTGG	

3. RESULTS

3.1. Compartmentation of phloem-translocated carbohydrates in leaves and within mesophyll cells in *Alonsoa meridionalis* and *Asarina barclaiana*

3.1.1. Leaves of *Alonsoa* and *Asarina* contain different types of soluble carbohydrates

HPLC analysis (2.8.1) was used to study the composition of soluble carbohydrates in the leaf extracts of *Asarina* and *Alonsoa*. The results showed that the monosaccharides glucose and fructose were present in significant amounts in leaf extracts of *Asarina* and *Alonsoa* (Table 3.1). Galactose was also found in both plants. Sucrose was the only disaccharide detected on HPLC chromatograms for *Asarina* and *Alonsoa*. Two of the raffinose family oligosaccharides, raffinose and stachyose, as well as the precursor of their synthesis, galactinol, and the cyclitol *myo*-inositol, were found in both plants. No significant amounts of other soluble carbohydrates were detected by HPLC in *Alonsoa*. In *Asarina*, a sugar alcohol, mannitol, was found and also an iridoid glycoside, antirrhinoside, the structure of which was confirmed by NMR (2.3.2.2; Figure 2.1). Antirrhinoside made up nearly half of the total content of soluble carbohydrates of *Asarina* leaves.

The opportunity to perform GC-MS analysis of the same samples was kindly provided by Dr. T. Peterbauer, University of Vienna, Austria. The mass spectrometric analysis confirmed the results of the HPLC and also detected four more unknown carbohydrates (Figure 3.1). In *Asarina* leaves, one of them was found in the disaccharide region of the spectrum (Figure 3.1 A). In the leaves of *Alonsoa*, one unknown carbohydrate was found in the monosaccharide region and three others in disaccharide region (Figure 3.1 B). However, these unknown compounds were minor components of the leaf extracts of both plants. No

galactosylated compounds other than galactinol, raffinose and stachyose were detected by GC-MS.

The subcellular compartmentation of soluble carbohydrates was further studied in mesophyll cells of *Alonsoa* and *Asarina* by means of the non-aqueous fractionation technique.

Table 3.1. Sugars, sugar alcohols and oligosaccharides in the leaves of *Alonsoa* and *Asarina* ($\mu\text{mol/g}$ fresh weight). Listed are mean values from four independent measurements \pm SD.

	<i>Asarina</i>	<i>Alonsoa</i>
<i>myo</i> -Inositol	2.0 \pm 1.0	3.4 \pm 0.5
Galactinol	1.4 \pm 0.5	3.5 \pm 1.1
Antirrhinoside	61.4 \pm 10.6	not detected
Mannitol	10.7 \pm 0.9	not detected
Glucose	16.5 \pm 2.6	7.9 \pm 4.0
Fructose	9.2 \pm 2.7	9.7 \pm 4.7
Galactose	0.6 \pm 0.3	1.5 \pm 0.5
Sucrose	14.5 \pm 2.8	6.8 \pm 1.0
Raffinose	0.3 \pm 0.2	1.0 \pm 0.5
Stachyose	0.7 \pm 0.2	1.1 \pm 0.3

3.1.2. Subcellular compartmentation of carbohydrates

3.1.2.1. Distribution of carbohydrates between the subcellular compartments of mesophyll cells

The separation of the leaf tissue into fractions enriched with either chloroplastic, cytoplasmic or vacuolar content was achieved by a centrifugation in an exponential density gradient as described in 2.6. The liquid constituents of the gradient were water-insoluble (heptane and tetrachloroethylene). This prevented the redistribution of the water-soluble metabolites and enzymes during the separation of the plant material within the gradient and therefore made it possible to attribute the amounts of metabolites to the subcellular compartments determined via the activities of specific marker enzymes (Gerhardt and Heldt, 1984; 2.6). The non-aqueous fractionation method does not take into account the tissue heterogeneity of the leaf. That means that subcellular concentrations in the mesophyll cells are calculated as if all the sugars were located exclusively within mesophyll cells. Therefore, the values obtained by using non-aqueous fractionation represent the estimations of the highest possible concentrations in each compartment.

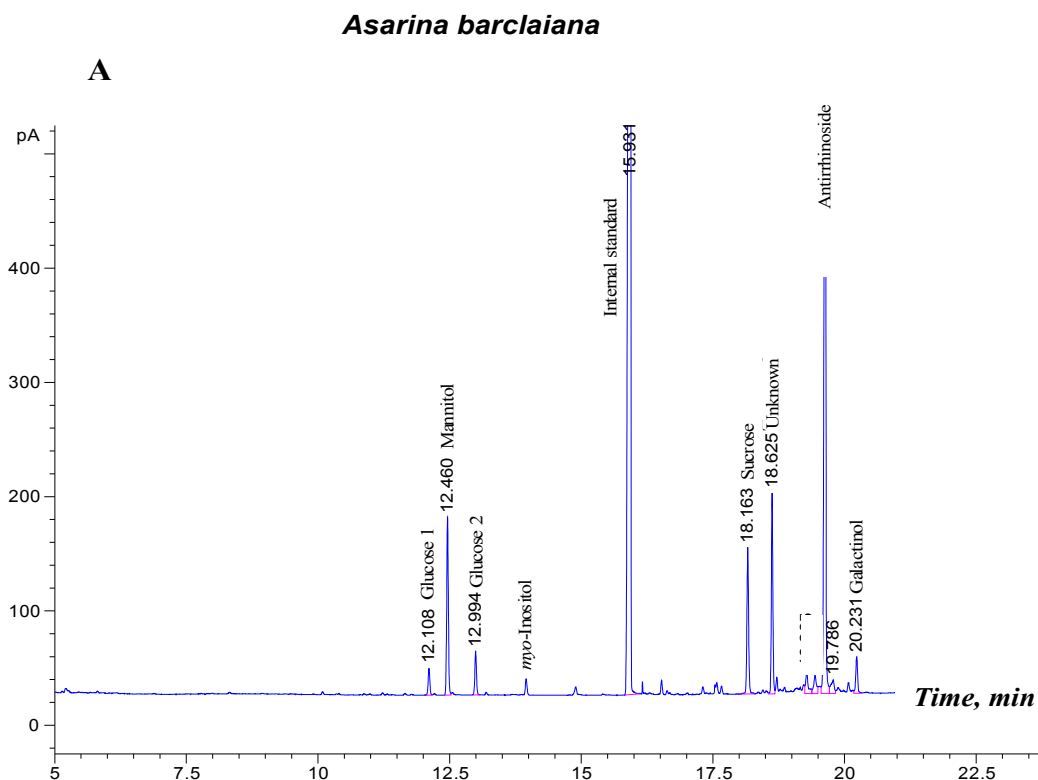


Figure 3.1 A. GC-MS spectrum of leaf extracts from *Asarina*. The sample also contained traces of raffinose and stachyose (not shown).

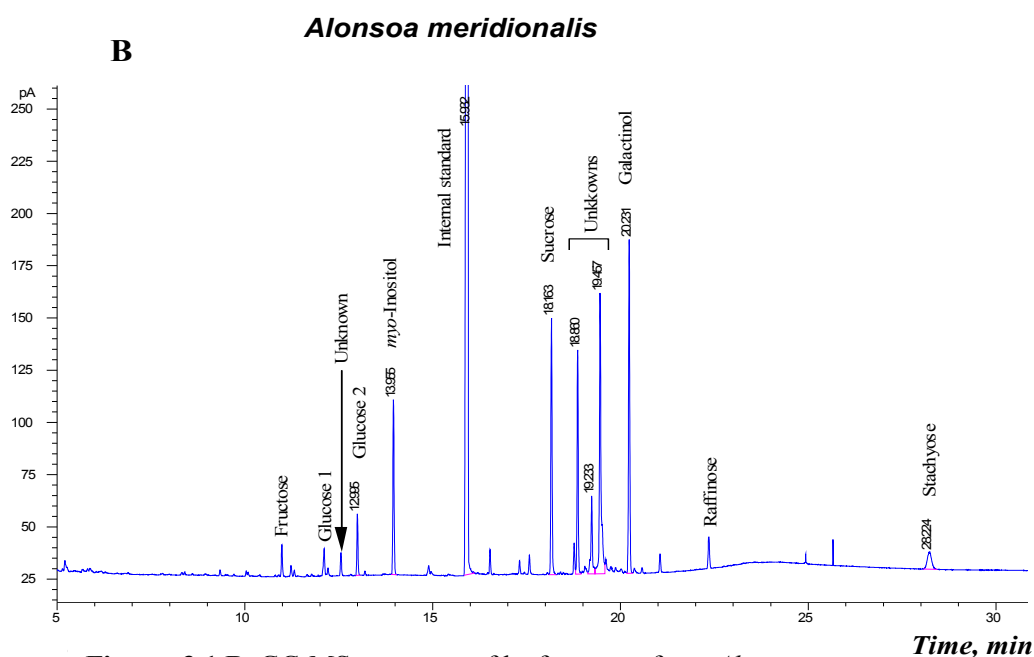


Figure 3.1 B. GC-MS spectrum of leaf extracts from *Alonsoa*.

The gradient fractionations of the powder of *Alonsoa* and *Asarina* leaves resulted in the enrichment of each gradient fraction with the contents of a particular subcellular compartment. The enzymes glyceraldehyde-3-phosphate dehydrogenase (GAPDH),

phosphoenolpyruvate carboxylase (PEPCx) and α -mannosidase were chosen as marker enzymes for chloroplastic, cytoplasmic and vacuolar compartments, respectively (2.6.3). In each fractionation, a good resolution between subcellular compartments can only be achieved if the ratios of activities of the marker enzymes are different for each fraction. A typical

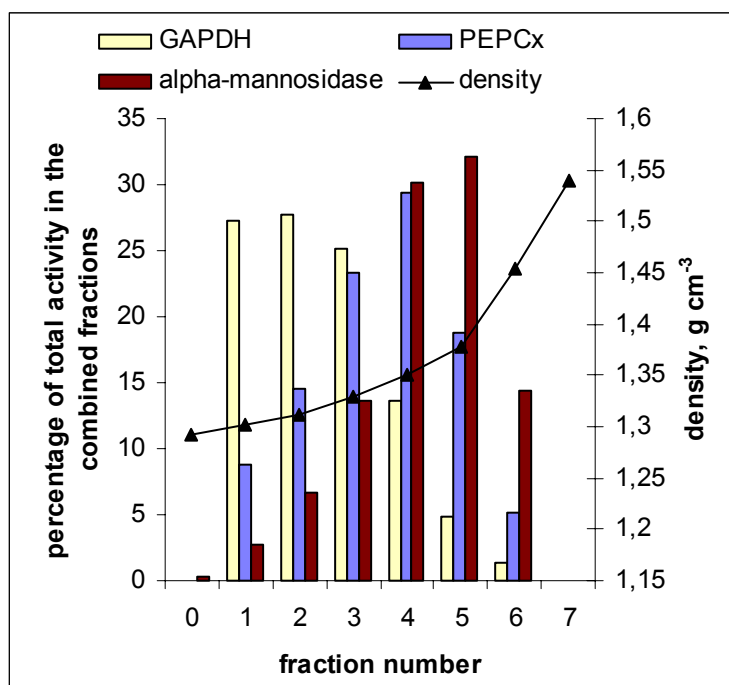


Figure 3.2. Distribution of the activities of marker enzymes between density gradient fractions by one of the fractionations for *Asarina barclaiana*. Marker enzymes are: GAPDH for chloroplasts, PEPCx for cytosol and α -mannosidase for vacuoles.

example is shown in Figure 3.2.

Out of ten gradient fractionations performed for *Asarina*, four resulted in a good separation of marker enzymes and were used for the determination of metabolites in the fractions. For *Alonsoa*, five fractionations were selected from a total of eight fractionations performed. The distributions of sugars between chloroplastic, cytoplasmic and vacuolar compartments are shown in Table 3.2.

The percentages summarized in Table 3.2 showed that in *Asarina* glucose and fructose were entirely confined to the vacuoles. The same was probably true for galactose as well, but since Q values (the measure for deviation of predicted results from the measured ones; 2.6.5) were too high for this sugar, the calculated values are not reliable (data not shown). Antirrhinocide also was mostly present in the vacuoles but a significant part (10%) was distributed between chloroplasts and cytoplasm.

It was not possible to show that raffinose and stachyose are confined to certain compartments in *Asarina* because their concentrations in whole leaves were too low (Table 3.1). After the fractionation procedure, the trace amounts of raffinose and stachyose could only be detected in the largest fractions, namely the vacuole-enriched fractions (data not

shown). Also, the concentration of galactinol was reduced to an undetectable level after fractionation (data not shown).

myo-Inositol and mannitol were present in all three compartments but largest amounts were found in chloroplasts and cytoplasm. Sucrose was also distributed between all three compartments with the highest amounts in vacuoles and cytoplasm.

In *Alonsoa*, the subcellular distribution of metabolites was very similar to that in *Asarina* (Table 3.2). Glucose and fructose were located in the vacuoles. Sucrose was distributed between all compartments with a slight predominance in cytoplasm. In *Alonsoa*, the content of galactinol was higher than in *Asarina*, which made it possible to determine its subcellular distribution. It was mostly found in the vacuoles. The amounts of raffinose and stachyose in gradient fractions were, however, still too low to obtain a reliable values on the subcellular distributions of these sugars (data not shown).

Table 3.2. Distribution of sugars among subcellular compartments of mesophyll cells from *Asarina barclaiana* and *Alonsoa meridionalis* leaves as determined by non-aqueous fractionation (percentages of total sugar content).

Ch: chloroplasts, Cyt: cytoplasm, Vac: vacuoles.

	<i>Asarina barclaiana</i>			<i>Alonsoa meridionalis</i>		
	Ch	Cyt	Vac	Ch	Cyt	Vac
<i>myo</i> -Inositol	53	24	23	81	13	6
Galactinol	not detected			2	2	96
Antirrhinoside	4	6	90	not detected		
Mannitol	36	34	30	not detected		
Glucose	1	1	98	1	1	98
Fructose	1	1	98	1	1	98
Sucrose	14	35	51	21	44	35

3.1.2.2. Estimation of the volumes of subcellular compartments of mesophyll cells in *Alonsoa* and *Asarina*

The estimation of subcellular concentrations from the distribution pattern of the sugars is only possible if the volumes of the subcellular compartments are known. Therefore, an estimation of subcellular volumes of mesophyll cells in *Asarina* and *Alonsoa* was performed. To this aim, the partial volumes of chloroplasts, vacuoles and cytoplasm (including cytosol, nucleus, peroxisomes and mitochondria) were calculated from electron micrographs of mesophyll cells of *Alonsoa* and *Asarina* (2.13).

In Table 3.3, these partial volumes are listed and compared to values found in other plants. The relative volumes of the vacuolar, chloroplastic and cytoplasmic compartments of mesophyll cells made up 72%, 20% and 8% in *Alonsoa* and 70%, 23% and 7% in *Asarina* respectively. These values correspond well to the volumes previously determined in barley, spinach and potato (Winter et al., 1993, Leidreiter et al., 1995; Table 3.3)

Table 3.3. Relative volumes (%) of the subcellular compartments of the total volume of mesophyll cells from *Asarina barclaiana* and *Alonsoa meridionalis* as compared with previously determined volumes occupied by subcellular compartments in leaves of potato, spinach, and barley. The total volume of a mesophyll cell is defined as 100 %. Cytoplasm is defined as cytosol, peroxisomes, nucleus and mitochondria.

	Chloroplast, %	Cytoplasm, %	Vacuole, %
<i>Asarina barclaiana</i>	23	7	70
<i>Alonsoa meridionalis</i>	20	8	72
<i>Solanum tuberosum</i> *	18	6	76
<i>Spinacea oleracea</i> **	16	5	79
<i>Hordeum vulgare</i> ***	19	8	73

* Data from Leidreiter et al., 1995; ** Winter et al., 1994; *** Winter et al., 1993

For the estimation of the real volumes of the compartments on the basis of these relative values, the volume of mesophyll cells has to be known. Such morphometric data are available for three plant species: the dicots potato and spinach and the monocot barley (Leidreiter et al., 1995; Winter et al., 1993, 1994). These volumes are presented in Table 3.4.

Table 3.4. Real ($\mu\text{l mg}^{-1}$ Chl) and partial volumes of mesophyll, epidermis, apoplast and conducting tissue in the leaves of potato, spinach and barley. Data from Winter et al., 1993 (barley), Winter et al., 1994 (spinach) and Leidreiter et al., 1995 (potato).

Aqueous volume	Potato	Spinach	Barley
Leaf	472 \pm 14 100%	810 \pm 119 100%	698 \pm 70 100%
Epidermis	74 \pm 17 14%	36 \pm 3 4%	244 \pm 36 35%
Mesophyll	394 \pm 23 75%	688 \pm 11 85%	379 \pm 27 54%
Apoplast	21 \pm 3 4%	60 \pm 22 7%	41 \pm 4 6%
Conducting tissue	30 \pm 3 6%	12 \pm 3 2%	55 \pm 6 7%

In these three plants, mesophyll cells occupied 54% - 85% of the total leaf aqueous volume. Because the leaf anatomy of the monocot barley differs significantly from the typical

dicot leaf structure, it is reasonable to assume that in the dicots *Asarina* and *Alonsoa* the partial volume occupied by the mesophyll at the whole leaf will be close to that of potato and spinach. If the values for potato are taken as the basis, then in *Asarina* leaves with an average water content of 498 $\mu\text{l mg}^{-1}$ Chl the volume of the mesophyll can be estimated as 374 $\mu\text{l mg}^{-1}$ Chl and in *Alonsoa* with an average water content of 394 $\mu\text{l mg}^{-1}$ Chl the corresponding volume can be estimated as 296 $\mu\text{l mg}^{-1}$ Chl. Then, the volumes of the stromal, cytoplasmic and vacuolar compartment of mesophyll cells would correspond to 85, 26 and 261 $\mu\text{l mg}^{-1}$ Chl for *Asarina* and 59, 24 and 213 $\mu\text{l mg}^{-1}$ Chl for *Alonsoa*.

However, for the calculation of subcellular concentrations on the basis of these volumes, a correction has to be made which takes the volume of epidermis into account. This is because epidermal cells consist of up to 99% vacuoles (Winter, 1993) and thus, by fractionation of the whole leaf tissue, their sugar contents will contribute to the vacuolar fraction of the mesophyll cells and lead to somewhat overestimated vacuolar concentrations. This correction can be made by addition of the volumes of epidermis to the volumes calculated for mesophyll vacuoles. These corrected values for the volumes of mesophyll vacuoles were 331 $\mu\text{l mg}^{-1}$ Chl in *Asarina* and 268 $\mu\text{l mg}^{-1}$ Chl in *Alonsoa*. These values were taken for the calculation of vacuolar concentrations in mesophyll cells of these two species, respectively.

3.1.2.3. Sugar contents and concentrations in subcellular compartments of mesophyll cells in *Alonsoa* and *Asarina*

The subcellular concentrations of sugars in *Alonsoa* and *Asarina* based on estimated volumes of subcellular compartments (3.1.2.2) are shown in Table 3.5. The sugar contents of each subcellular compartment showed that vacuoles contain the highest amounts of soluble carbohydrates (82% in *Asarina* and 69% in *Alonsoa*), while cytoplasm and chloroplasts contain much less. However, because of the very different volumes of these compartments, for most sugars the highest concentrations were found in the cytoplasm. In the vacuoles, hexose levels were the highest in *Alonsoa*. In *Asarina*, the highest vacuolar concentration was that of antirrhinoside followed by glucose and sucrose.

In the cytoplasm, the sucrose level was the highest in *Alonsoa*, followed by *myo*-inositol. In *Asarina*, the highest cytoplasmic level was that of antirrhinoside, followed by mannitol, sucrose and *myo*-inositol. In *Alonsoa* chloroplasts, *myo*-inositol was dominating, and the second concentrated sugar was sucrose. In *Asarina* chloroplasts, the calculated concentrations of mannitol and antirrhinoside were the highest, followed by *myo*-inositol.

A comparison of subcellular concentrations with those in the phloem sap is shown in Figure 3.3. Neither of the subcellular compartments mirrored the phloem with respect to the types of sugars and their concentration ratios. Nevertheless, all metabolites that were transported in the phloem, such as sucrose, antirrhinoside and mannitol were present in the cytoplasm at high concentrations. However, the opposite was not true. For instance, in *Alonsoa* only trace amounts of *myo*-inositol were present in the phloem sap although its cytoplasmic concentration was 26 mM, surpassed only by sucrose.

Table 3.5. Sugar contents (nmol mg⁻¹Chl) and subcellular concentrations (mM) in the chloroplastic, cytoplasmic and vacuolar compartments of mesophyll cells from *Asarina barclaiana* and *Alonsoa meridionalis*.

	Stroma		Cytoplasm		Vacuole	
	nmol mg ⁻¹ Chl	mM	nmol mg ⁻¹ Chl	mM	nmol mg ⁻¹ Chl	mM
<i>Asarina barclaiana</i>						
<i>myo</i> -inositol	1260	15	570	22	546	1.5
mannitol	2080	24	2400	92	1250	4
antirrhinoside	2128	25	3193	123	47903	144
glucose	40	0.5	86	3	5680	17
fructose	48	0.5	48	2	1676	5
sucrose	588	7	1112	43	3200	9
<i>total per compartment</i>	6144 (8%)	72	7409 (10%)	285	60255 (82%)	180
<i>Alonsoa meridionalis</i>						
<i>myo</i> -inositol	3821	65	613	26	282	0.8
galactinol	32	0.5	32	1	1570	5.5
glucose	52	1	52	2	5120	19
fructose	65	2	65	3	6320	23
sucrose	818	14	1715	71	1365	5
raffinose and stachyose	4	0	70	3	1030	3
<i>total per compartment</i>	4792 (20%)	82	2547 (11%)	106	15687 (69%)	56

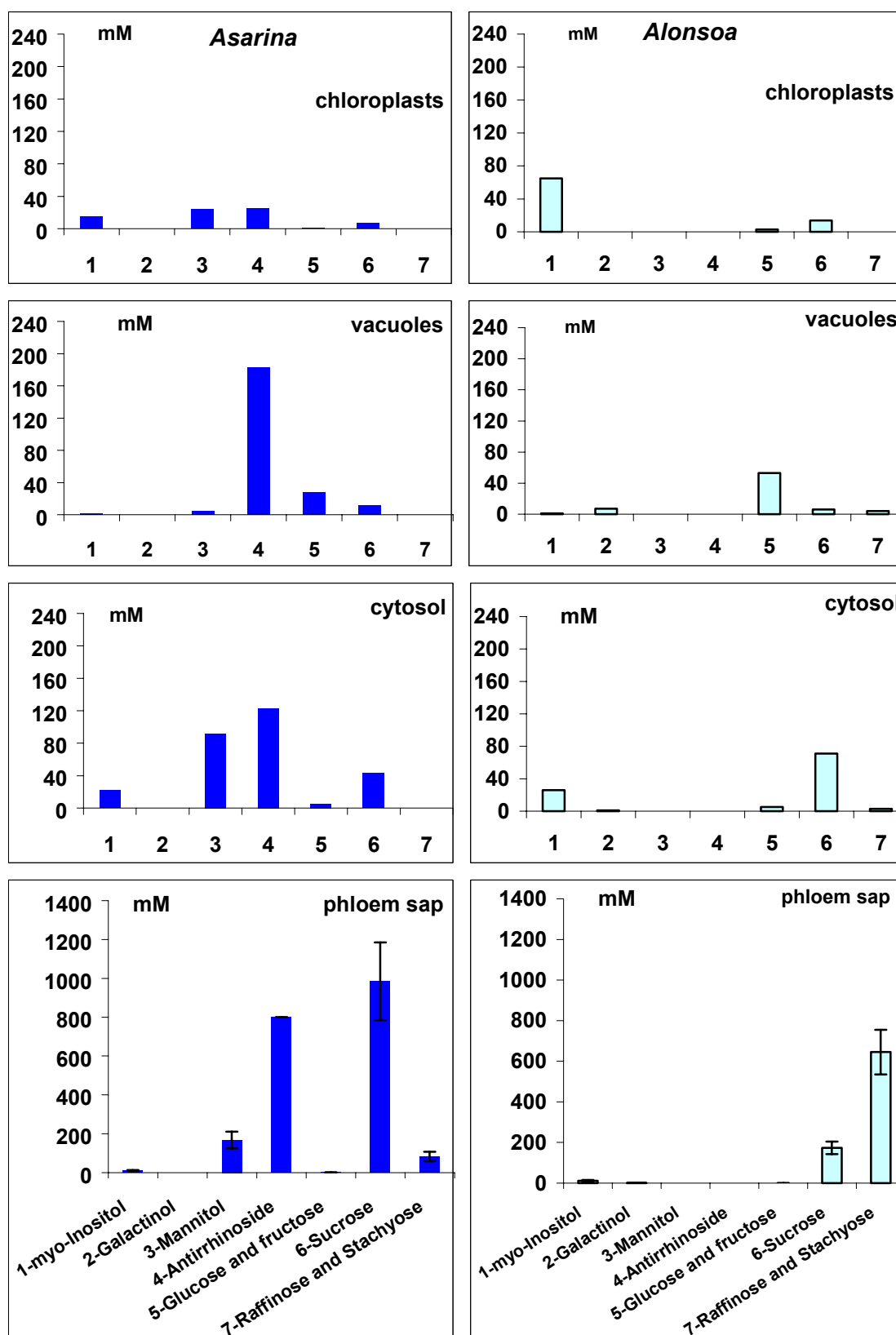


Figure 3.3. Sugar concentrations (mM) in subcellular compartments of mesophyll cells and in phloem sap of *Asarina barclaiana* (left column) and *Alonsoa meridionalis* (right column). Data for phloem concentrations are taken from Table 1.1. 1-myo-inositol, 2-galactinol, 3-mannitol, 4-antirrhinoside, 5-glucose + fructose, 6-sucrose, 7-raffinose + stachyose

3.1.3. Concentrations of sucrose, glucose and fructose in mesophyll cells measured by single cell sampling technique agree well with the non-aqueous fractionation data

As already mentioned, the disadvantage of the non-aqueous fractionation method is that it does not take into account the tissue heterogeneity of the leaf. Subcellular concentrations are calculated assuming all the sugars in the leaf to be located exclusively within mesophyll cells, ignoring the fact that some of these sugars are actually located outside of these cells. This assumption can lead to an overestimation of subcellular concentrations because also phloem, epidermis and apoplast contain sugars. Another source of error could be the fact that the partial volumes of leaf tissues in leaves of *Asarina* and *Alonsoa* were not determined by morphometry, but estimated from those in potato assuming that the differences between these dicot species may not be significant.

Therefore, direct measurements of sugar concentrations in mesophyll cells of *Alonsoa* and *Asarina* leaves are necessary for the proper interpretation of non-aqueous fractionation results. A technique that directly measures the concentrations of metabolites in a single cell is the so-called single cell sampling. It distinguishes between different types of leaf tissues. The single cell sampling technique does not distinguish between subcellular compartments, but results in metabolite concentrations close to those in the vacuole because the vacuole represents the overwhelming portion of a cell (Fricke et al., 1994a).

Before the measurements in the single cell samples from *Alonsoa* and *Asarina* were performed, the quantification method had to be calibrated using standards (2.10.3; Figure 3.4). Figure 3.4 shows the high reliability of the measurements in a concentration range between 2

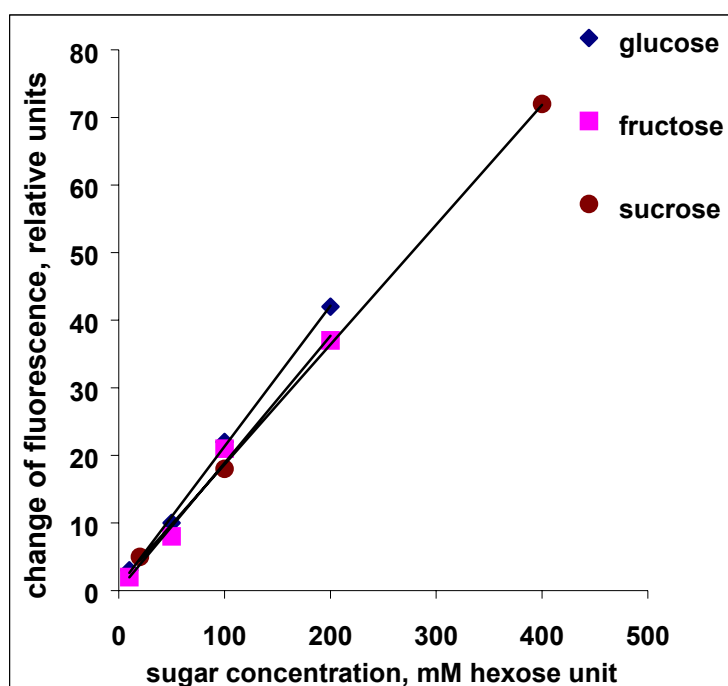


Figure 3.4. Calibration of the single cell sugar assay. The increase of fluorescence was measured against dark background in sets of droplets containing solutions of glucose, fructose or sucrose of known concentration using self-made constriction pipettes of unknown volume. The same pipettes were then used for measurements of sugar concentrations in the single cell samples obtained from epidermis and mesophyll of leaves of *Asarina* and *Alonsoa*. The concentrations were calculated using the shown calibration curves.

and 200 mM. Mesophyll cells of *Alonsoa* and *Asarina* were sampled in the morning at 10:00 after 3 hours of light and the contents of glucose, fructose and sucrose were determined. The results are compared with the values calculated on the basis of non-aqueous fractionation (Table 3.6). Both methods showed a good agreement not only for hexoses which are entirely vacuolar and do not occur in the phloem sap, but also for sucrose which is present at high concentrations in the phloem (Table 1.1). Hence, the values determined by single cell sampling supported the assumptions made for the calculation of subcellular concentrations in *Alonsoa* and *Asarina* by non-aqueous fractionation, and confirmed the results of the subcellular fractionation experiments.

	glucose (mM)	fructose (mM)	sucrose (mM)
<i>Asarina barclaiana</i> non-aqueous fractionation	17	5	9
single cell sampling	19 ± 8	7 ± 3	6 ± 3
<i>Alonsoa meridionalis</i> non-aqueous fractionation	9	23	5
single cell sampling	11 ± 11	21 ± 10	4 ± 4

Table 3.6. Vacuolar concentrations (mM) of glucose, fructose and sucrose in mesophyll cells of *Alonsoa* and *Asarina* as estimated by non-aqueous fractionation and determined by single cell sampling. For single cell sampling, mean values of 5 independent measurements ± SD are shown.

3.1.4. Epidermal concentrations of sucrose and hexoses in *Alonsoa* and *Asarina* were similar to those in mesophyll cells

The single cell sampling technique provides an opportunity to determine sugar concentrations not only in mesophyll cells but also in epidermal cells and thus to evaluate the role of the epidermis in carbon compartmentation in the leaves of *Alonsoa* and *Asarina*. The concentrations of glucose, fructose and sucrose in epidermal cells were compared with those in mesophyll cells in the morning (10:00) and in the evening (18:00) in plants receiving light from 7:00 to 23:00.

At both timepoints, the concentrations of glucose, fructose and sucrose in mesophyll did not differ significantly from those in epidermis (Figure 3.5). To see whether this would be also the case when leaves were forced to accumulate sugars, the translocation from the leaves was blocked. To this aim, the leaves of *Alonsoa* and *Asarina* were detached from the plants and placed in continuous light for 24 hours while the petioles were kept in 2 mM CaCl₂ solution to favour sealing of the phloem with callose. This caused an increase of the total sugar content of the leaves (3.1.6). Afterwards, the concentrations of sucrose and hexoses were measured in single cell samples from mesophyll and epidermis (Figure 3.6).

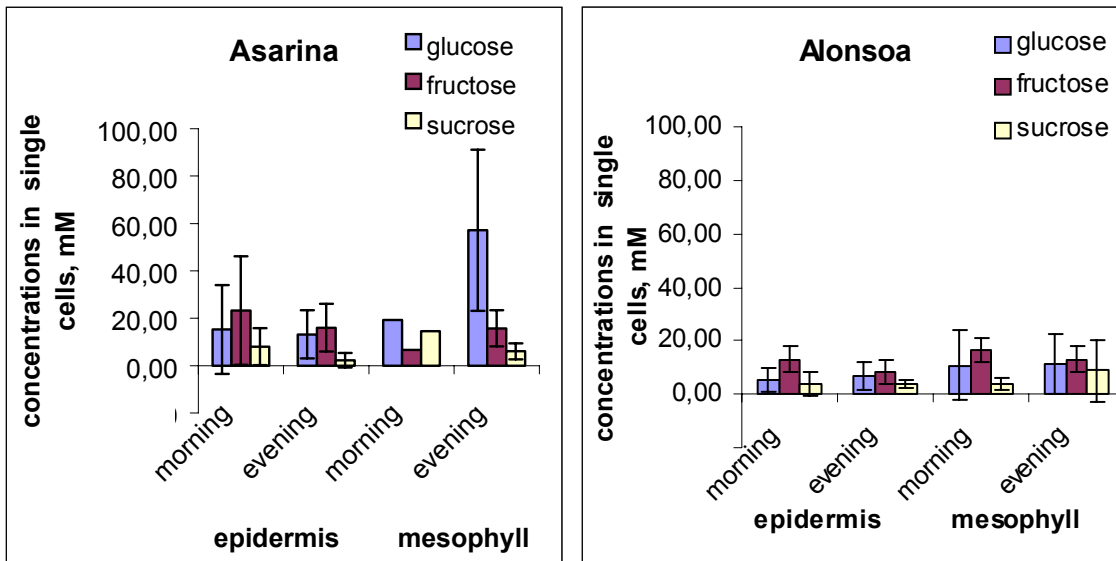


Figure 3.5. Sugar levels in single cell samples of epidermis and mesophyll cells of *Asarina barclaiana* and *Alonsoa meridionalis* after 3 hours of light ("morning") and after 11 hours of light ("evening"). Mean values of 5 independent measurements \pm SD are shown.

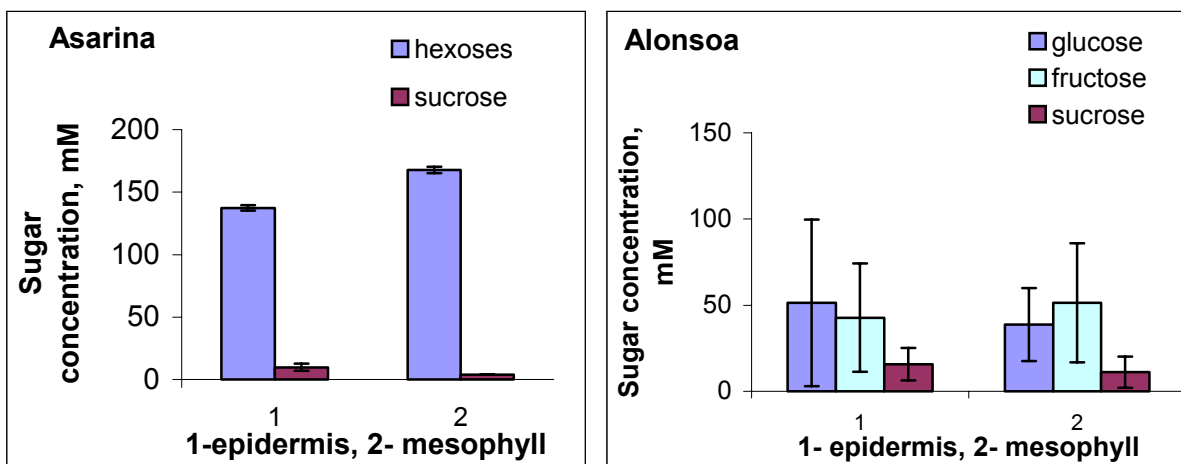


Figure 3.6. Sugar contents in mesophyll and epidermis cells sampled from the detached leaves of *Alonsoa meridionalis* and *Asarina barclaiana* after exposure of the leaves to continuous light (photon flux of $500 \mu\text{mol m}^{-2} \text{s}^{-1}$) during 24 hours. Mean values of 5 independent measurements \pm SD are shown.

The results showed that epidermal and mesophyll cells of both plants accumulated similar levels of soluble carbohydrates. In the epidermal cells of *Alonsoa*, hexose levels were five times higher and sucrose levels were three times higher than in control plants („morning“ timepoint). In the mesophyll cells of *Alonsoa*, hexose and sucrose levels increased by a factor of three. In the epidermal cells of *Asarina*, hexose levels increased by a factor of 3.5 and sucrose levels by a factor of 1.5. In mesophyll cells of *Asarina*, a sixfold accumulation of hexoses was observed whereas sucrose levels did not increase significantly. The pronounced increase of cellular sugar concentrations not only in the mesophyll but also in the epidermis

indicated that in *Alonsoa* and *Asarina*, the epidermis can serve as a transient reservoir for soluble carbohydrates.

3.1.5. Soluble carbohydrates in *Alonsoa* and *Asarina* essentially contributed to the osmolality of the cytosol in mesophyll cells

The osmolality of the whole leaf sap and of single cell samples taken from mesophyll and epidermis was determined for *Alonsoa* and *Asarina* (2.9, 2.10.2; Figure 3.7). For both plants, the values measured in the single cells were higher than those in the whole leaves. This situation has already been observed in several plant species and is supposed to be due to the dilution of the cellular content in whole leaf sap with water from other tissues like the xylem (Fricke et al., 1994b).

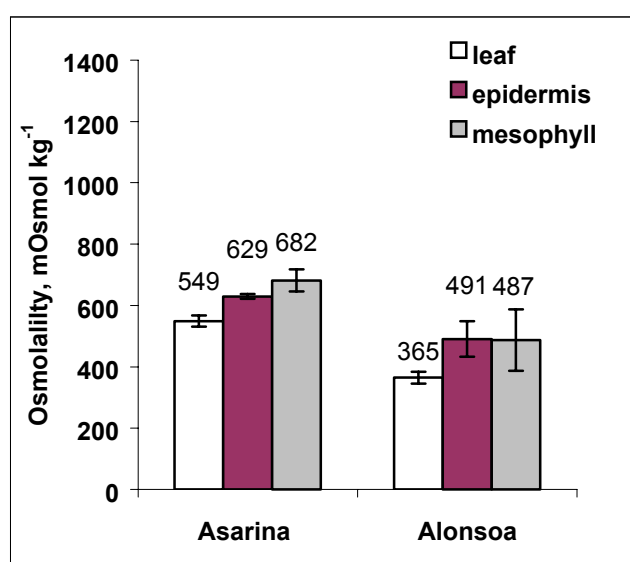


Figure 3.7. Osmolalities of leaf extracts and single cells of epidermis and mesophyll in *Asarina barclaiana* and *Alonsoa meridionalis*. Samples were taken from plants after a 3 hour light period. Mean values from 5 independent measurements \pm SD are shown.

As can be estimated from the data of Figures 3.5 and 3.7, glucose, fructose and sucrose in the single cell samples taken from epidermal cells only contributed 7% to the osmolality in *Asarina* and 5% in *Alonsoa*. This means that in vacuoles of epidermal cells, other solutes accounted for the bulk osmolalities. These could be inorganic ions and organic acids (Fricke et al., 1994b) as well as those carbohydrates which were not analysed in the epidermal cells by single cell technique in these experiments, for instance, antirrhinoside in *Asarina*.

Water exchange between subcellular compartments is not limited in the cell. That means that the same osmotic pressure that was measured in single cell samples representing mostly vacuolar sap will be also found in the cytosol of these cells. From the data of Figure 3.7 and Table 3.5, the contribution of soluble carbohydrates to osmolality of subcellular compartments of mesophyll cells in *Asarina* and *Alonsoa* can be estimated (to calculate exact

values, the osmolality coefficients are necessary which are not available for all carbohydrates). For vacuoles of mesophyll cells, total soluble carbohydrates without antirrhinoside accounted for 5% of osmolality in *Asarina*, antirrhinoside alone for about 21%. In *Alonsoa*, soluble carbohydrates accounted for 11% of vacuolar osmolality. In the cytosol, however, sugars without antirrhinoside accounted for about 26% osmolality in *Asarina* and antirrhinoside alone for another 18%. In *Alonsoa*, sugars accounted for about 22% osmolality. With the exception of antirrhinoside, the main osmotica in the cytosol of *Asarina* mesophyll cells were mannitol, sucrose and *myo*-inositol. In *Alonsoa*, these were sucrose and *myo*-inositol.

In the whole leaves of *Asarina*, the sum of soluble carbohydrates without antirrhinoside contributed to about 10% of the osmolality of the whole leaf sap and antirrhinoside alone accounted for 11%. In *Alonsoa*, total soluble carbohydrates made up 9.6% of the osmolality of whole leaf sap.

3.1.6. Levels of phloem-translocated carbohydrates other than raffinose and stachyose increased in the leaves with blocked translocation

The study of the subcellular compartmentation of phloem-translocated sugars within mesophyll cells of *Asarina* and *Alonsoa* has revealed that sucrose, antirrhinoside and mannitol in *Asarina* and sucrose in *Alonsoa* were present in the cytoplasmic, chloroplastic and vacuolar compartments. However, a re-compartmentation of metabolites within cells can take place under certain conditions. Excess amounts of soluble sugars can enter the vacuoles whose storage function allows the levels of sugars in the leaves to increase severalfold temporarily (Kaiser and Heber, 1984). *Asarina* and *Alonsoa* translocate several types of sugars in the phloem. In order to find out whether all these sugars will accumulate in the leaves when assimilate export is prevented, the following experiment was performed.

The leaves of *Alonsoa* and *Asarina* were detached from the plants and placed in continuous light (photon flux of $500 \mu\text{mol m}^{-2} \text{s}^{-1}$) while the petioles were kept in 2 mM CaCl_2 solution to favour the sealing of the phloem with callose. Sugar concentrations were determined in the leaves after 24 and 96 hours of exposure, respectively (Figure 3.8).

When translocation was blocked in *Asarina* leaves, the concentrations of the main transport carbohydrates, sucrose and antirrhinoside, increased. These carbohydrates contribute up to 48 and 39% of total transported carbon, respectively (calculated from Table 1.1). The increase was observed also for one minor transported component, mannitol, which accounted for 3% of total transported carbon in *Asarina*. The concentration of other minor transported components, raffinose and stachyose, did not show a significant increase. Glucose and

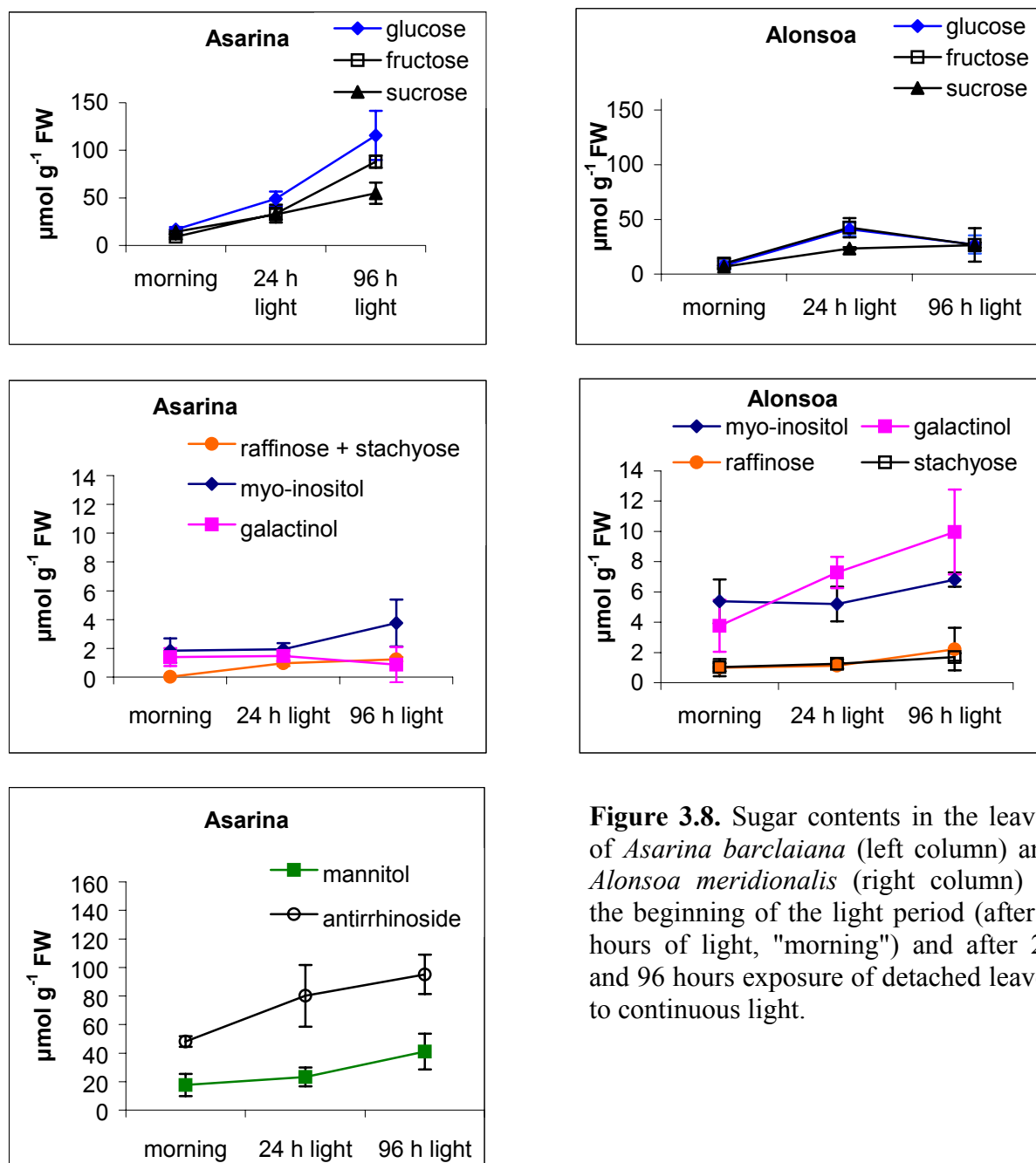


Figure 3.8. Sugar contents in the leaves of *Asarina barclaiana* (left column) and *Alonsoa meridionalis* (right column) at the beginning of the light period (after 3 hours of light, "morning") and after 24 and 96 hours exposure of detached leaves to continuous light.

fructose accumulated also, probably due to hydrolysis of sucrose by vacuolar invertase. The slight domination of glucose over fructose may be due to a partial hydrolysis of glucosyl from antirrhinoside during the accumulation of the latter in the vacuoles.

In *Alonsoa*, glucose, fructose, sucrose and galactinol accumulated in the leaves when phloem translocation was blocked. The contents of glucose and fructose were very similar which suggested their production by hydrolysis of sucrose by invertase. The main transport carbohydrates raffinose and stachyose which contribute 28% and 59%, respectively, of total transported carbon, did not show significant accumulation. However, their precursor galactinol, and also a minor transported component, sucrose, (13% of total transported

carbon) accumulated when translocation was blocked. These results might suggest that the activity of galactinol synthase was not changed but the rate of the galactinol-consuming reactions catalysed by raffinose and stachyose synthases decreased in *Alonsoa* under blockage of translocation.

It was impossible to determine the subcellular localization of raffinose and stachyose in mesophyll cells, since their overall concentration was too low (3.1.2.1). One possible reason for this may be that raffinose and stachyose synthases are localized outside the mesophyll cells. According to the polymerization trap model (Turgeon, 1991), the most likely location for the synthesis of raffinose and stachyose would be within companion cells. This might also explain the lack of accumulation of raffinose and stachyose in leaves during translocation blockage, assuming that they cannot diffuse into mesophyll cells.

3.2. Sugar concentrations in the apoplast of leaves in putative symplastic and apoplastic phloem loaders

The participation of the apoplast in sugar transfer from mesophyll to phloem in plants with different companion cells can be studied by measurements of sugar levels in the apoplast. Apoplastic sugar levels were determined in several plant species with transfer or ordinary companion cells (*Vicia faba*, Ntsika and Delrot, 1986; *Spinacea oleracea* and *Hordeum vulgare*, Lohaus et al., 1995). However, no comparison was made with plants with intermediary cells and presumably symplastic phloem loading. For this study, a number of species with either transfer or ordinary or intermediary companion cells from several plant families had to be selected, to make sure that the observed differences were related to companion cell structure.

The aim of the following experiments was to compare plants with different phloem loading mode with respect to (i) sugar composition and content in the apoplast of source leaves with normal and with inhibited phloem translocation, respectively, and (ii) types of sugars that are taken up from the apoplast into the symplast.

For the comparative study of apoplastic sugar contents in plants with different minor vein anatomy, several species were selected on the basis of the reported companion cell structure in their minor veins (Gamalei, 1990):

3.2.1. Diurnal levels of the translocated carbohydrates in the apoplast

Diurnal changes in apoplastic glucose, fructose and sucrose levels in the leaves were compared in two species, a putative symplastic phloem loader *Alonsoa meridionalis* and an apoplastic phloem loader with transfer cells in minor veins, *Vicia faba*. Plants were grown in

a greenhouse (2.2.1). The leaves were sampled, infiltrated with ice-cold 50 mM CaCl₂ solution and centrifuged at low speed (2.4). The presence of Ca²⁺ ions in the infiltration solution was important for the determination of apoplastic sugar concentrations, as Ca²⁺ favours the sealing of the damaged phloem cells with callose and thus prevents the contamination of the apoplast with phloem contents during the isolation of intercellular washing fluid (W. Kaiser, personal communication). The fluid obtained by centrifugation represented a diluted apoplastic solution. To check for symplastic contamination, the activity of glucose-6-phosphate dehydrogenase was determined (2.5.1). Glucose, fructose and sucrose concentrations in pure samples were measured by enzymatic analyses (2.8.2) and the concentrations of other carbohydrates were determined by HPLC.

<i>species with transfer/ordinary cells</i>		<i>species with intermediary cells</i>	
<i>Calendula officinalis</i> L.	Asteraceae	<i>Cucurbita pepo</i> L.	Cucurbitaceae
<i>Chrysanthemum</i> sp.	Asteraceae	<i>Coleus blumei</i> Benth.	Lamiaceae
<i>Symphytum officinale</i> L.	Boraginaceae	<i>Mentha</i> sp.	Lamiaceae
<i>Lepidium sativum</i> L.	Brassicaceae	<i>Ligustrum vulgare</i> L.	Oleaceae
<i>Spinacea oleracea</i> L.	Chenopodiaceae	<i>Alonsoa meridionalis</i> O. Kuntze	Scrophulariaceae
<i>Pisum sativum</i> L.	Fabaceae		
<i>Vicia faba</i> L.	Fabaceae		
<i>Atropa belladonna</i> L.	Solanaceae		

Apoplastic glucose and fructose levels were somewhat higher than those of sucrose in *Alonsoa* (Figure 3.9). Importantly, no other carbohydrates were detected by HPLC in the apoplast of this species. In *Vicia*, similarly, glucose, fructose and sucrose were the only sugars found in the apoplast. However, in this species, sucrose levels were much higher than those of hexoses during the period of observation. The levels of sucrose in *Vicia* were about three times higher than in *Alonsoa*.

3.2.2. Levels of the translocated carbohydrates in the apoplast increased in apoplastic but not in symplastic phloem loaders when phloem translocation was blocked

The export of assimilates from the leaves of these two species was blocked by application of an ice jacket to the leaf petiole ("cold girdling"; Webb and Gorham, 1965) for several hours (2.11). Ice lost by melting was replaced. Figure 3.10 compares the effects of cold girdling on apoplastic concentrations of glucose, fructose and sucrose in *Vicia faba* and *Alonsoa meridionalis*. Neither hexoses nor sucrose levels increased in the apoplast of *Alonsoa* during the blockage of translocation. Contrarily, in *Vicia* sucrose levels increased fivefold when compared to non-girdled leaves already after two hours of petiole chilling and remained

high throughout the experiment. No other sugars were detected in the apoplast of these species by HPLC.

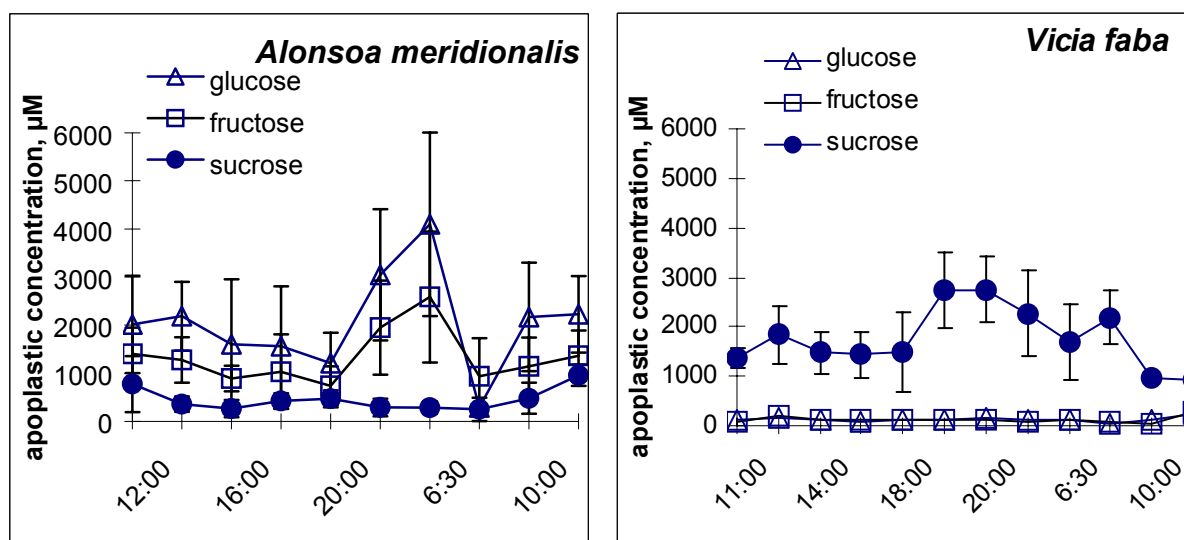


Figure 3.9. Time course of glucose, fructose and sucrose concentrations in the apoplast of leaves of *Alonsoa meridionalis* and *Vicia faba*. Mean values of 5 independent measurements \pm SD are shown.

Figure 3.11 shows a similar experiment performed on *Spinacea oleracea*, a putative apoplastic phloem loader with ordinary cells in minor veins and the putative symplastic phloem loader *Coleus blumei*. In the non-girdled controls, levels of all measured apoplastic sugars were in the same range in both plant species. In spinach, the cold jacket increased the apoplastic sucrose concentration above that measured in control leaves within 1 h of its application. After 4 h of cold girdling, the apoplastic sucrose levels exceeded those measured in ungirdled controls by a factor of more than four. Apoplastic glucose and fructose levels did not increase significantly. Even their highest levels were far below the apoplastic sucrose concentration in cold-girdled leaves.

In *Coleus*, no marked changes were observed in apoplastic sucrose and hexose levels under cold girdling. No other sugars were detected in the apoplast of *Coleus* by HPLC.

In a similar experiment performed with *Symphytum officinale* (an apoplastic loader with transfer cells in minor veins) and *Cucurbita pepo* (a putative symplastic loader), the cold jackets around the leaf petioles were maintained for about 3 h. As has already been shown for the apoplastic loaders *Spinacea* and *Vicia* (Figures 3.9 and 3.10), the application of the cold jacket increased the apoplastic sucrose levels in leaves of *Symphytum*. As in case of the symplastic loaders *Coleus* and *Alonsoa* (Figures 3.9, 3.10), no increase in either sucrose or hexose levels in the leaf apoplast was observed in cold-blocked leaves of *Cucurbita* (data not shown).

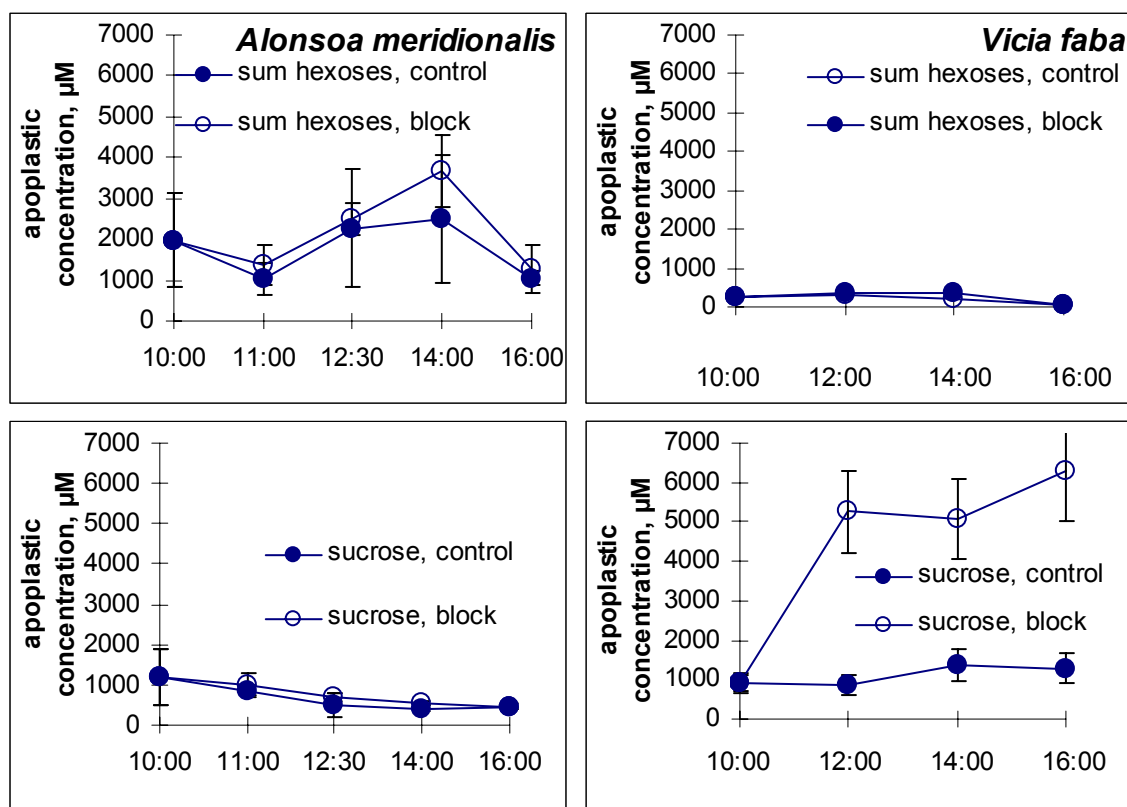


Figure 3.10. Apoplastic concentrations of hexoses (glucose + fructose) and sucrose in leaves of *Alonsoa meridionalis* (left column) and *Vicia faba* during the day (filled circles) and after the application of a cold jacket on the petiole at 10:00 for 1, 2, 4 and 6 hours (open circles). Mean values of 5 independent measurements \pm SD are shown.

The inhibition of phloem translocation can be achieved not only by application of a cold jacket, but also by other procedures like cutting or removal of the phloem ring from the branches of trees. Figure 3.12 compares the effects of some of these treatments on apoplastic sugar levels in several putative apoplastic and symplastic phloem loaders.

The cut ends of the shoots of *Chrysanthemum* (apoplastic phloem loader) and *Mentha* (symplastic phloem loader) were placed in CaCl_2 solution to inhibit export of assimilates. Alternatively, EDTA solution was fed to the petioles in order to chelate Ca^{2+} ions and thus to prevent callose sealing of sieve tubes and to allow the export to continue (King and Zeevaart, 1974). In this experiment, no significant differences between the two treatments could be seen for apoplastic sugar concentrations in either species (Figure 3.12). The apoplastic concentrations of all sugars measured in *Mentha* were lower than those in *Chrysanthemum*.

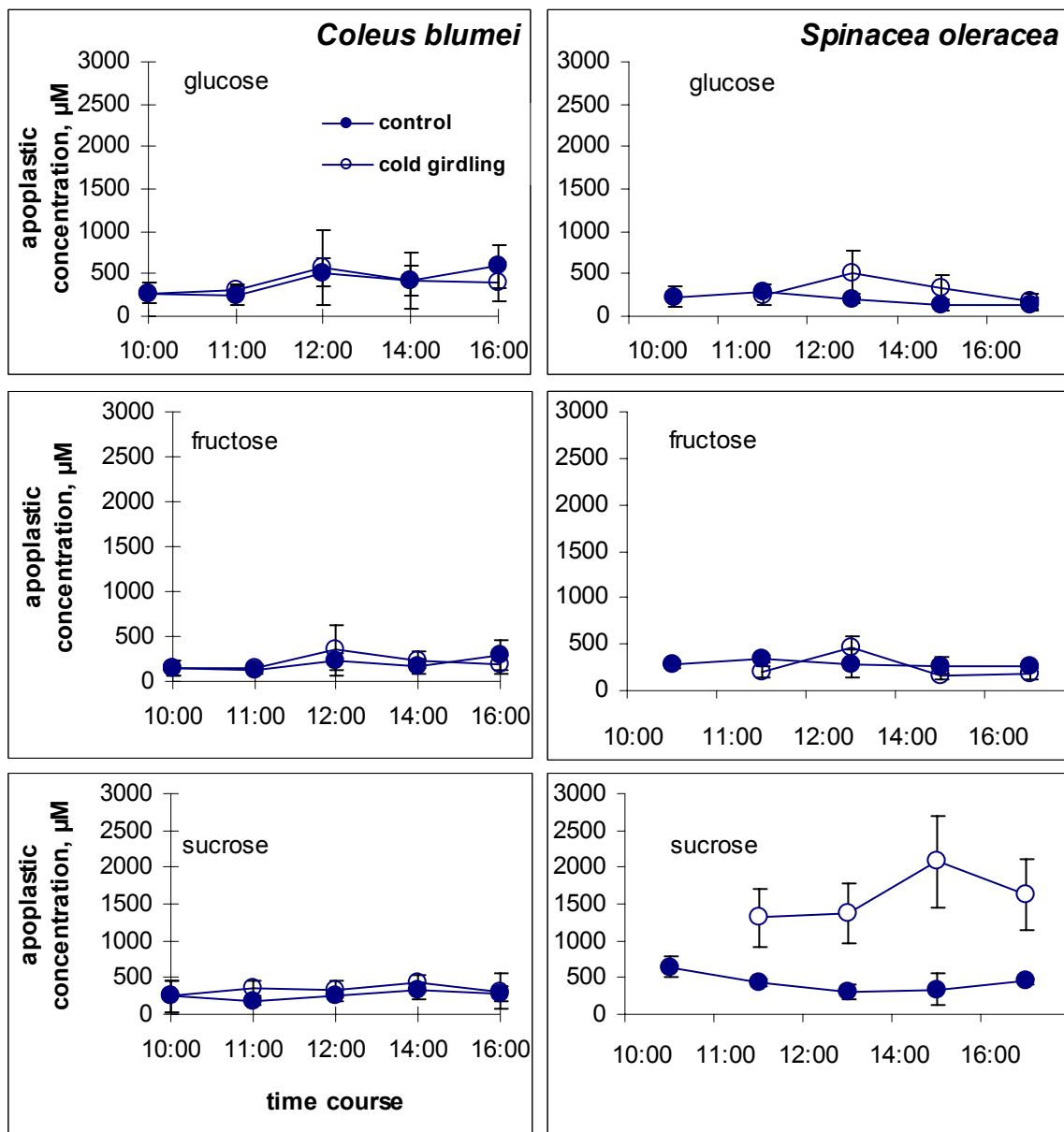


Figure 3.11. Apoplastic glucose, fructose and sucrose concentrations in *Coleus blumei* (left column) and *Spinacea oleracea* (right column) in untreated leaves (filled circles) and after application of a cold jacket on the petiole at 10:00 for 1, 2, 4 and 6 hours (open circles). Mean values of 5 independent measurements \pm SD are shown.

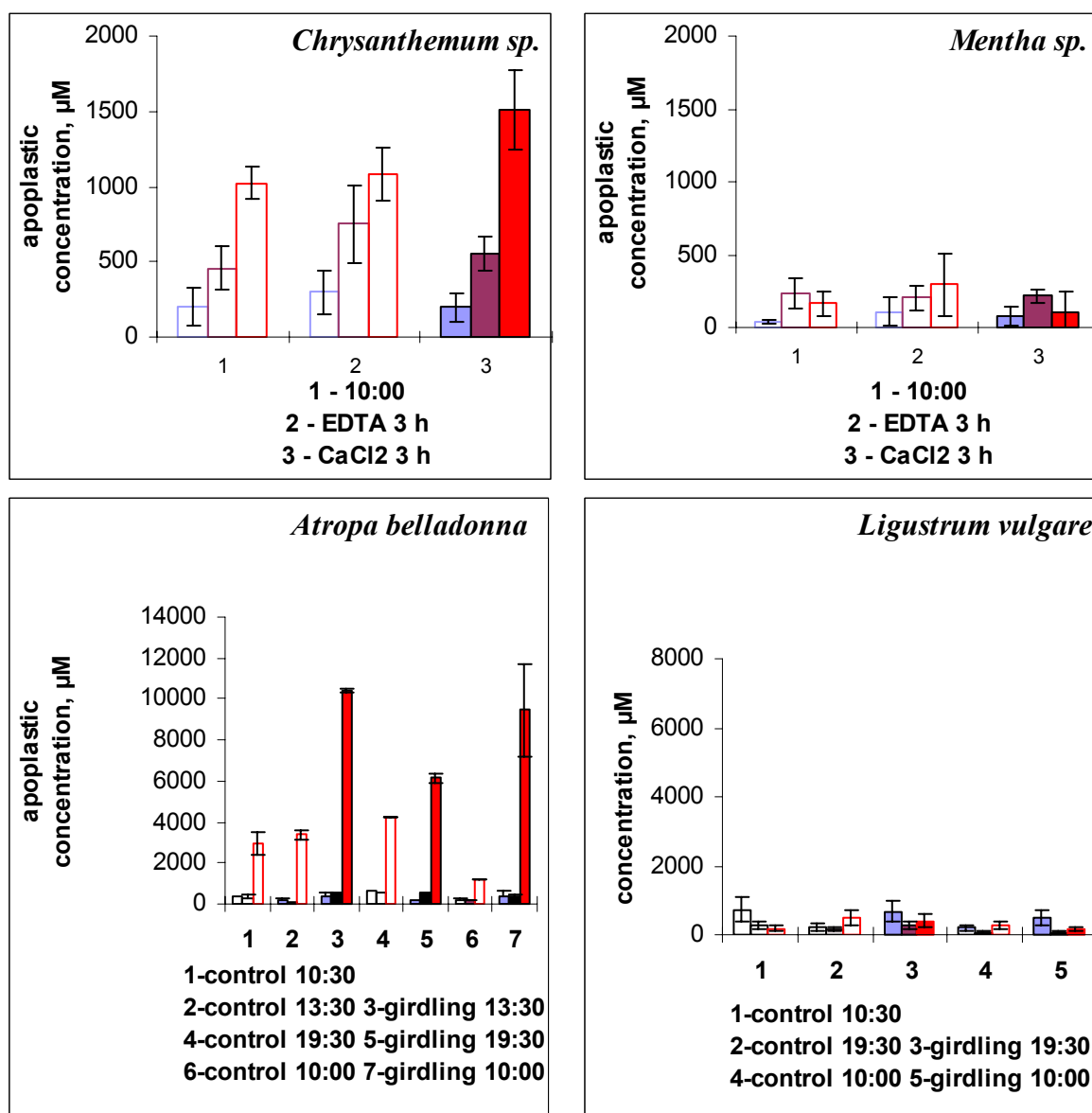


Figure 3.12. Apoplastic sugar concentrations in leaves of putative apoplastic phloem loaders *Chrysanthemum sp.* and *Atropa belladonna* and putative symplastic phloem loaders *Mentha sp.* and *Ligustrum vulgare* as influenced by phloem translocation blockage by cutting (*Chrysanthemum*, *Mentha*) and removal of a phloem ring from the branches (*Atropa*, *Ligustrum*). Open bars: samples from control plants. Filled bars: samples from experimental plants. Sugars are (right to left): glucose, fructose, sucrose. Mean values of 5 independent measurements \pm SD are shown.

A ring of bark was removed from branches of *Atropa belladonna* (apoplastic phloem loader) and *Ligustrum vulgare* (symplastic phloem loader) at 10:00 and the effect on apoplastic leaf sugar concentrations was examined. In *Atropa*, after 3 h the apoplastic sucrose levels in leaves from treated branches had increased considerably above the levels measured in the control and remained above that level until the evening (timepoint 19:30) and into the next morning (measured at 10:00). Apoplastic hexose levels were far below sucrose levels. In

Ligustrum, apoplastic levels of sucrose did not respond to bark removal. No significant changes in hexose levels were observed.

In these experiments, different procedures were used to decrease translocation to exclude method-related artefactual results. A cold jacket may lower transport only temporarily (Geiger and Sovonick, 1970; Krapp and Stitt, 1995), while cutting and removal of the phloem around the branch were intended to block translocation entirely. However, whether transport was inhibited by cold girdling, by mechanical removal of phloem tissue or by callose blockage of sieve tubes, the inhibition always resulted in the increase of sucrose levels in the apoplast of leaves of the apoplastic phloem loaders (*Spinacea*, *Symphytum*, *Chrysanthemum* and *Atropa*) but not in leaves of the putative symplastic phloem loaders (*Cucurbita*, *Coleus*, *Ligustrum* and *Mentha*). These data suggest a difference in the extent of apoplast involvement in sugar transfer into the phloem in both groups of plants.

For all studied species, sucrose was the dominant sugar in the apoplast only in apoplastic phloem loaders, while in putative symplastic phloem loaders hexose levels were sometimes higher than sucrose levels (Figures 3.9 - 3.12). Neither raffinose nor stachyose were detected in the apoplast of leaves of *Alonsoa* and other symplastic phloem loaders that translocate these sugars in the phloem (*Coleus*, *Cucurbita*) even when phloem transport was blocked.

3.2.3. Uptake of sugars including non-metabolizable isomers fed exogenously into the apoplast was driven by proton-motive force in both symplastic and apoplastic phloem loaders.

In order to find out whether there are persistent differences in the mode of sugar uptake from the apoplast into the leaf tissue in apoplastic versus symplastic phloem loaders, a selected number of symplastic and apoplastic phloem loaders was examined. The capacity and energetics of uptake of different carbohydrates fed into the apoplast were compared in the leaves of these plants. One symplastic loader, *Alonsoa*, and one apoplastic loader, *Calendula*, were analysed in more detail.

The experiments were performed as described by Hedrich et al. (2001) (2.12.1). Different sugars (concentrations 10, 25, 50 or 100 mM, dissolved in dd H₂O) were fed to the cut petioles of leaves during short time intervals (5 min). During the experiments, the respiratory CO₂ release from the leaves and the leaf transpiration were recorded. To monitor changes in the apoplastic pH, the pH-sensitive fluorescent dye FITC was introduced into the leaf apoplast just before the beginning of the experiments. In the parallel experiments, a membrane-potential sensitive fluorescent dye BDTO was used instead of FITC which allowed the recording of membrane potential changes.

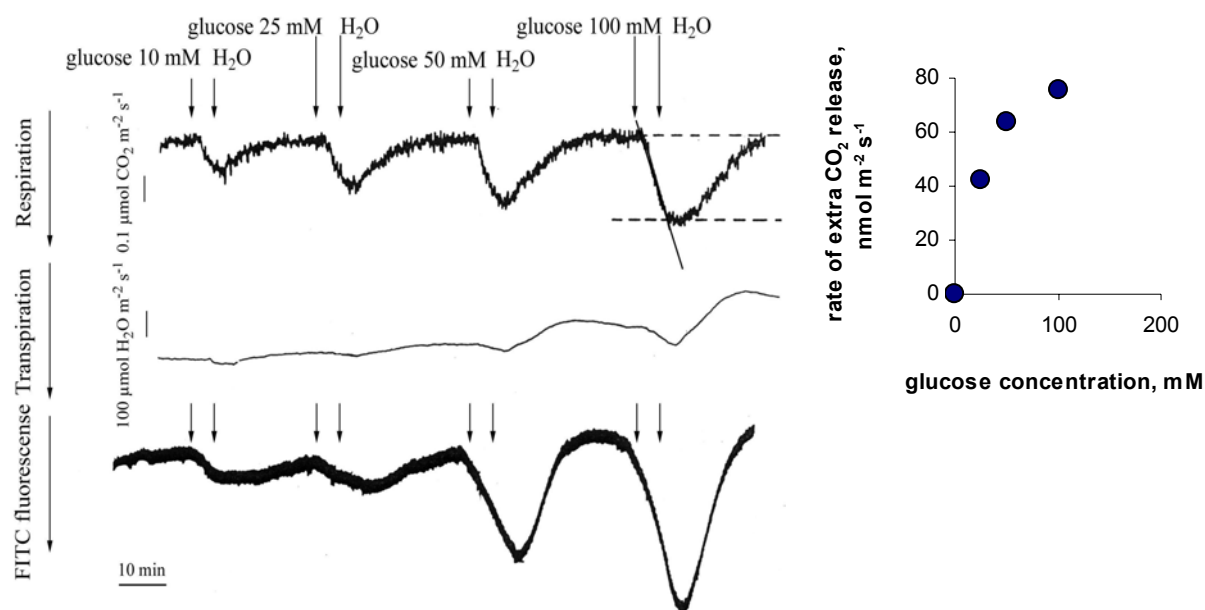


Figure 3.13. Respiration, transpiration and apoplastic pH of a leaf of *Alonsoa meridionalis* as influenced by 5 min feeding of glucose solutions (10 mM, 25 mM, 50 mM or 100 mM). Increase of FITC fluorescence indicates apoplastic alkalinization. Initial rate of the leaf transpiration was $1750 \mu\text{mol H}_2\text{O m}^{-2} \text{s}^{-1}$. The insert shows calculated glucose-stimulated CO₂ release as a function of glucose concentration in the solution fed to the cut petiole (for 25, 50 and 100 mM).

A close relationship was established between the sugar concentration in the feeding solution and the apoplastic alkalinization and stimulation of respiration recorded during the experiments. This is shown in Figure 3.13. Glucose was fed to the cut petiole for 5 min at a time as indicated by arrows. It was transported into the leaf with the transpiration stream. As it arrived in the leaf blade, respiration was stimulated. An example of the calculation of the extent of glucose-stimulated respiration from the maxima of stimulated CO₂ release is shown in the insert. After glucose had arrived in the apoplast stimulating respiration, the apoplastic pH increased. After feeding was discontinued, respiration started to decline and, subsequently, alkalinization was slowly reversed.

In similar experiments, the effects of different sugars were compared at a constant feeding concentration of 50 mM. Glucose, sucrose, raffinose and stachyose were fed into the apoplast of a leaf of *Alonsoa meridionalis*. This led to an increase in respiratory CO₂ production and to a transient alkalinization of the apoplast as indicated by FITC fluorescence (Figure 3.14, A – D). Both respiration and pH returned slowly to initial levels after the feeding had been discontinued. In a similar experiment with another *Alonsoa* leaf, the membrane potential-sensitive dye BDTO was infiltrated into the leaf instead of FITC. When sugars were fed, the membrane potential first depolarized and then repolarized even exhibiting some hyperpolarization (Figure 3.14, A - D).

In experiments with the apoplastic phloem loader *Calendula officinalis*, this sequence of events was more clearly resolved (Figure 3.15, A - D). Here, a small acidification preceded apoplastic alkalization. It was accompanied by the depolarization of the membrane potential which continued as long as this small initial acidification lasted. The beginning of the repolarization of the membrane potential as indicated by the increase of BDTO fluorescence coincided with the beginning of the apoplastic alkalization as indicated by the increase of FITC fluorescence (Figure 3.15, A-D). This sequence of events was clearly observed with fed glucose and fructose but was less pronounced with raffinose and stachyose.

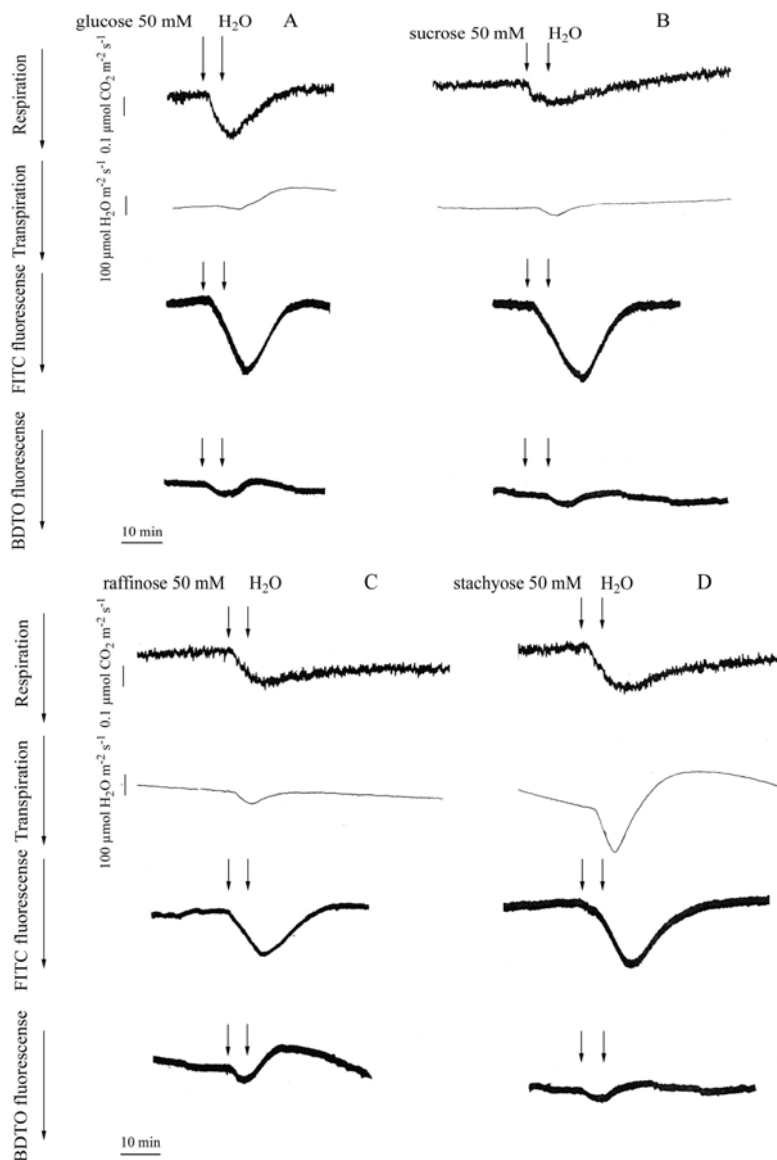


Figure 3.14. Respiration, transpiration, apoplastic pH and membrane potential of a leaf of *Alonsoa meridionalis* as influenced by 5 min feeding of 50 mM solution of **A**, glucose, **B**, sucrose, **C**, raffinose and **D**, stachyose. Increasing FITC fluorescence indicates alkalization of apoplast. Increase of BDTO fluorescence indicates a depolarization of membrane potential. Initial rates of leaf transpiration were: **A**, $1750 \mu\text{mol H}_2\text{O m}^{-2} \text{s}^{-1}$; **B**, $1820 \mu\text{mol H}_2\text{O m}^{-2} \text{s}^{-1}$; **C**, $1840 \mu\text{mol H}_2\text{O m}^{-2} \text{s}^{-1}$; **D**, $1550 \mu\text{mol H}_2\text{O m}^{-2} \text{s}^{-1}$.

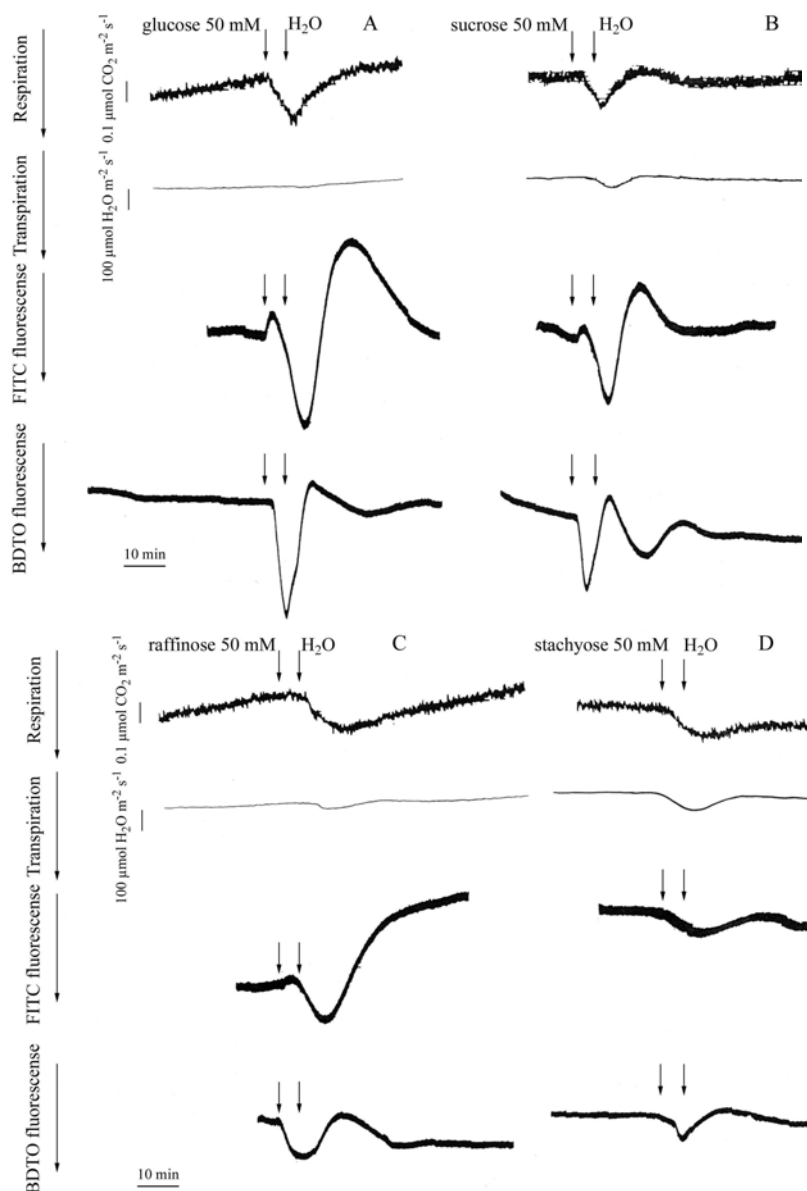


Figure 3.15. Respiration, transpiration, apoplastic pH and membrane potential of a leaf of *Calendula officinalis* as influenced by 5 min feeding of 50 mM solution of **A**, glucose, **B**, sucrose, **C**, raffinose and **D**, stachyose. Increase of FITC fluorescence indicates an alkalinization of the apoplast. Increase of BDTO fluorescence indicates a depolarization of membrane potential. Initial rates of leaf transpiration rates were: **A**, $1860 \mu\text{mol H}_2\text{O m}^{-2}\text{s}^{-1}$; **B**, $1575 \mu\text{mol H}_2\text{O m}^{-2}\text{s}^{-1}$; **C**, $1815 \mu\text{mol H}_2\text{O m}^{-2}\text{s}^{-1}$; **D**, $1680 \mu\text{mol H}_2\text{O m}^{-2}\text{s}^{-1}$.

Increases of respiration, apoplastic alkalinization and depolarization of the membrane potential similar to those in the leaves of *Alonsoa* and *Calendula* were also observed when 50 mM sugar solutions were fed to the petioles of detached leaves of the symplastic phloem loaders *Mentha sp.*, *Coleus blumei* and *Cucurbita pepo* or to the apoplastic phloem loaders *Helianthus tuberosus*, *Lepidium sativum* and *Pisum sativum* (data not shown).

In general, sugars fed to leaves can be respired. To find out whether this was the reason for the increase of basal respiration in the experiments described thus far, non-

metabolizable sugars such as 2-deoxy-D-glucose or turanose (3-O- α -D-glucopyranosyl-D-fructofuranose, a non-metabolizable isomer of sucrose) were fed to leaves. In Figure 3.16, it can be seen that the increases in respiratory CO₂ production in response to the feeding of 2-deoxy-D-glucose or turanose to the apoplast are comparable to those observed with metabolizable sugars. Similar results were obtained with palatinose, another non-metabolizable sucrose isomer (6-O- α -D-glucopyranosyl-D-fructofuranose; data not shown). Apparently, the basal respiration of the leaves used in these experiments was limited not by the lack of respiratory substrates, but by a low demand for energy. However, unlike deoxyglucose and the metabolizable sugars, turanose and palatinose were efficient not in all species tested. Thus, in *Calendula*, palatinose was readily taken up as indicated by pH and membrane potential changes (Figure 3.16) but turanose caused no effects in respiration, apoplastic pH and membrane potential (not shown). Contrarily, in *Lepidium*, turanose was readily taken up (Figure 3.16).

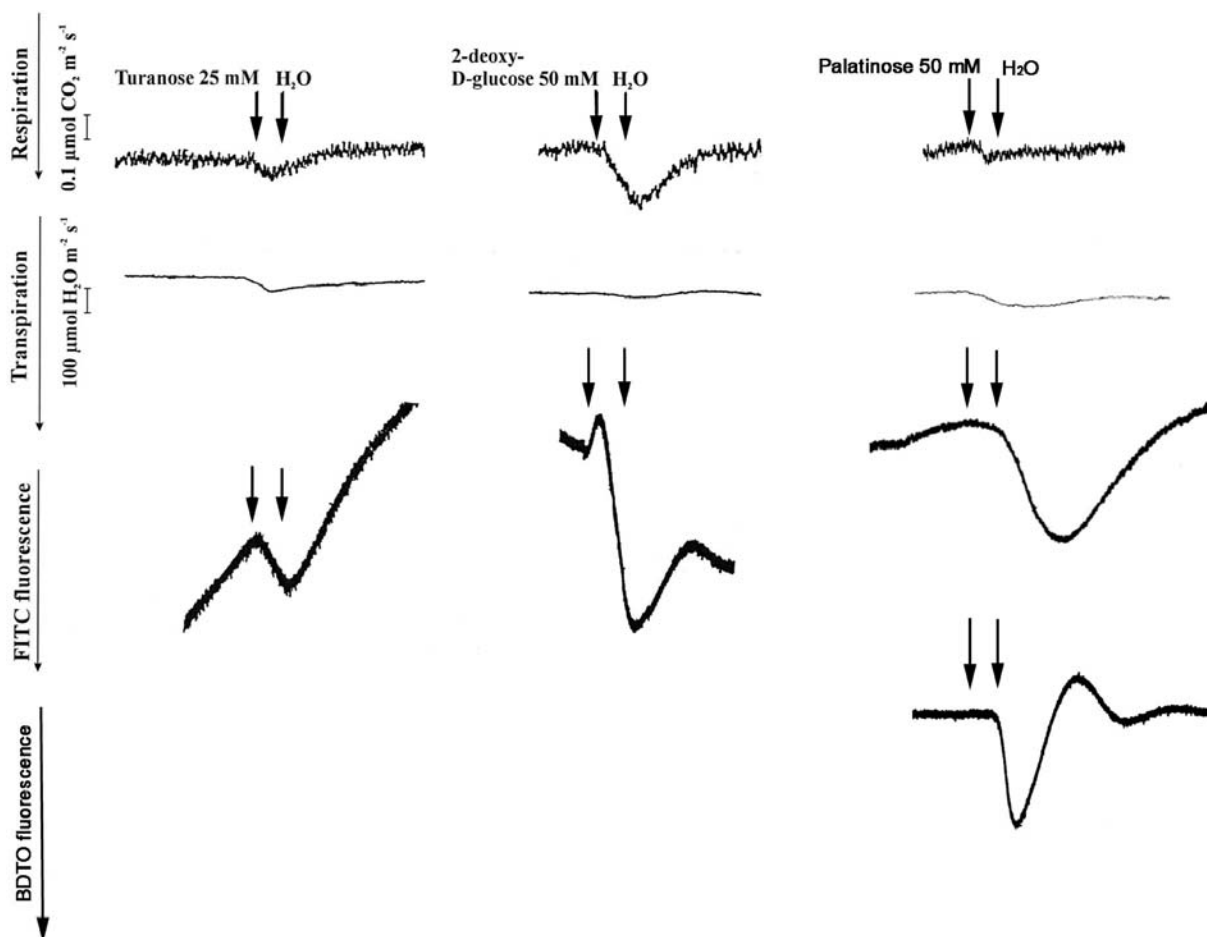
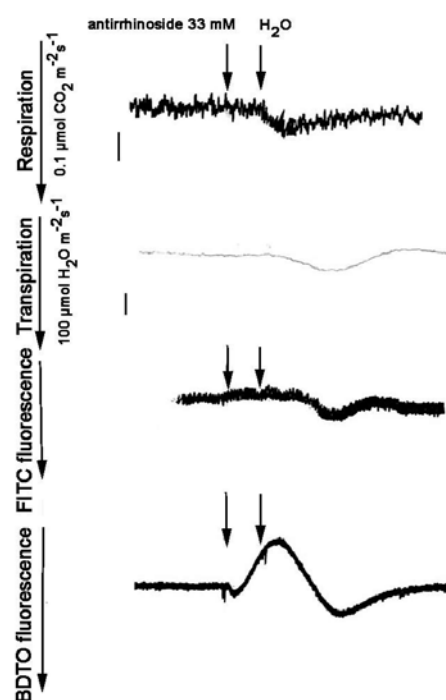


Figure 3.16. Uptake of non-metabolizable isomers 2-deoxy-D-glucose, turanose and palatinose fed to leaves of *Lepidium sativum* (turanose) and *Calendula officinalis* (2-deoxy-D-glucose and palatinose). The increase of the FITC fluorescence indicates an alkalinization of the apoplast and the increase in BDTO fluorescence (not shown for 2-deoxy-D-glucose and turanose) indicates a depolarization of membrane potential.

Since non-metabolizable isomers could also be taken up by leaf tissues that do not normally contain these sugars, the analysis was extended to include another molecule species, namely an iridoid glycoside, antirrhinoside. Antirrhinoside had been isolated from leaves of *Asarina barclaiana* (2.3.2.2). It consists of an aglycon and a glucose residue (Figure 2.1). It has been shown that transmembrane transfer of glycosides can occur against their concentration gradient, most probably through hexose transporters which recognize a glycoside residue as substrate (Christmann et al., 1993). Unfortunately, the leaves of *Asarina barclaiana*, the plant which does transport antirrhinoside in its phloem (1.7.2, Table 1.3) were not suitable for experiments involving the feeding of sugars to the apoplast. Therefore, leaves of *Calendula* were used. This plant produces a number of glycosides, but not iridoid glycosides and not antirrhinoside (Jensen, 1991).

When antirrhinoside was fed to *Calendula* leaves, stimulation of respiration, apoplastic alkalization and the depolarization of membrane potential were observed which indicated that this glucoside is taken up into leaf cells like all other sugar molecules tested (Figure 3.17). However, the hyperpolarization phase was prolonged and the pH changes were weak when compared to those observed with glucose of the same concentration (33 mM; not shown). This indicates that, in *Calendula*, antirrhinoside is taken up either via another transporter or the affinity to this glucoside is much weaker than that to glucose.

Figure 3.17. Respiration, transpiration, apoplastic pH and membrane potential of a leaf of *Calendula officinalis* as influenced by 5 min feeding of 33 mM solution of antirrhinoside. Increase of FITC fluorescence indicates an alkalization of the apoplast. Increase of BDTO fluorescence indicates a depolarization of membrane potential.



An attempt to compare the uptake rates for different sugars was made using leaves of *Alonsoa* and *Calendula*. Both for sucrose, raffinose and stachyose which are phloem-translocated, and for glucose which is unlikely normally to be taken up by companion cells since no hexoses have been found in the phloem sap of plants to date, the maximum extent of the sugar-dependent increase in respiration were calculated. Representative examples are shown in Table 3.7, both as a rate of CO₂ release and as a percentage increase of basal respiration. The values presented in Table 3.7 are typical examples. As a rule, the monosaccharide glucose showed the strongest stimulation of respiration but the trisaccharide raffinose and the tetrasaccharide stachyose were also effective in stimulating respiration in both plants. The amplitudes of respiration responses and changes of apoplastic pH and of membrane potential were in the same range for all sugars.

For glucose, sucrose and raffinose, sugar-dependent changes in the rate of CO₂ release were plotted against sugar concentration (as it is shown in the insert in Figure 3.13) for leaves of *Alonsoa* (Figure 3.18, A). The leaves showed a high capacity for the uptake of sugars from the apoplast as can be seen from the respiration curves which showed a half-maximum saturation at feeding concentrations of 19 – 25 mM. Figure 3.18, B compares the quantifications of respiration responses caused by feeding raffinose to leaves of three different species, a raffinose-translocating *Alonsoa* and sucrose-translocating *Calendula* and *Helianthus*. The respiration responses were concentration-dependent in all three species and amplitudes were of the same range, although *Alonsoa* showed somewhat higher capacity for raffinose uptake. Similar comparison was also made for glucose and sucrose fed to leaves of these species. No pronounced differences in uptake capacity has been revealed (data not shown).

Table 3.7. Maximal increase in basal respiration of leaves as observed by sugar feeding into the leaf apoplast. Listed values are typical examples.

<i>feeding solution</i>	<i>Alonsoa</i>			<i>Calendula</i>		
	<i>basal respiration rate</i> ¹	<i>maximum of stimulated respiration rate</i> ¹	<i>stimulation by sugar feeding</i>	<i>basal respiration rate</i> ¹	<i>maximum of stimulated respiration rate</i> ¹	<i>stimulation by sugar feeding</i>
glucose 50 mM	504	767	52%	719	1059	45%
sucrose 50 mM	505	631	25%	796	990	24%
raffinose 50 mM	583	768	32%	680	825	21%
stachyose 50 mM	728	971	33%	544	690	27%

¹ nmol CO₂ m⁻² s⁻¹

The observations made in these experiments can be summarized as follows. First, all carbohydrates introduced into the leaf apoplast were taken up into the symplast, the uptake being powered by proton motive force. Indeed, not only glucose and sucrose, but also raffinose and stachyose were transported together with protons at the expense of the proton motive force across the plasma membrane. Energized uptake from the apoplast into the leaf cells was also observed for the foreign iridoid glycoside antirrhinoside in *Calendula*. Even the unmetabolizable sucrose analogs palatinose and turanose were readily taken up when fed into the apoplast although it had been assumed that these sugars cannot be transported into the plant cells because they are not recognized by the known sugar transporters (e.g. M'Batchi and Delrot, 1988).

Second, no persistent differences in the mode of uptake of sugars introduced into a leaf apoplast could be seen between apoplastic and putative symplastic phloem loaders. Uptake of raffinose and stachyose from the apoplast indeed occurred both in species that are known to synthesize these sugars in leaves and translocate them (*Cucurbita*, *Coleus*, *Alonsoa*) and in species with transfer/ordinary companion cells in their minor veins which belong to plant families translocating (almost) exclusively sucrose in the phloem (*Helianthus*, *Calendula*, *Lepidium*, *Pisum*). It can be concluded that, in the described experiments, leaves of symplastic phloem loaders translocating raffinose and stachyose along with sucrose, as well as leaves of apoplastic phloem loaders translocating only sucrose, did not differ in the capacity and specificity of uptake of the three sugars fed exogenously into the apoplast. The mechanism of uptake was similar for the three sugars in that the PMF was the driving

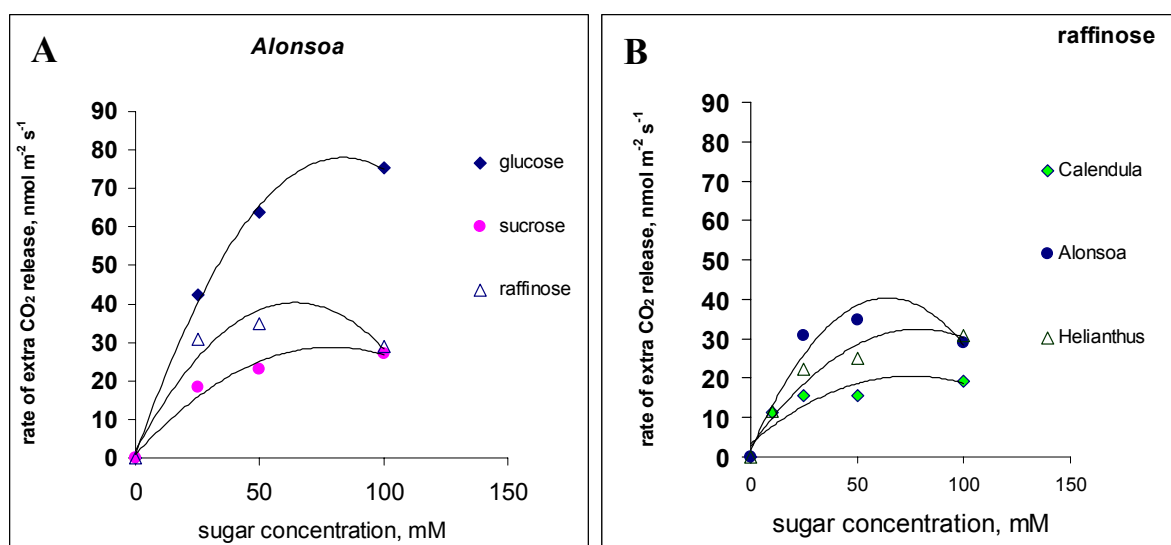


Figure 3.18. Maximum changes in the rate of CO₂ release caused in leaves by feeding sugars at concentrations of 25, 50 and 100 mM. Comparison is made: **A**, among different sugars fed to leaves of *Alonsoa*; **B**, among different species when feeding raffinose.

force and that the observed apoplastic alkalization suggested the uptake to proceed via H^+ /sugar-symporters. The amplitudes of respiration responses and changes of apoplastic pH and of membrane potential were in the same range for glucose, which is very unlikely to be taken up by companion cells since no hexoses have been found in the phloem sap of plants to date, and for phloem-translocated sugars such as sucrose in apoplastic plants and sucrose, raffinose and stachyose in symplastic plants.

Altogether, the results obtained in the sugar feeding experiments also suggest that in the leaf cells of the plant species examined – apoplastic and symplastic phloem loaders alike – the exchange of sugars between symplast and apoplast may not be limited by the presence of specific transporters in the plasma membranes. The concurrent alkalization of the apoplast suggests that the sugars and an iridoid glycoside were taken up in a proton symport mechanism as is known for sugar transporters. The efficient uptake of non-metabolizable foreign sucrose analogs argues either for an uptake mechanism with broad specificity that involves the PMF or for participation of transporters (H^+ -symporters) which are not characterized as yet.

3.3. Characterization of *AmSTS*, a stachyose synthase from *Alonsoa meridionalis*

3.3.1. Cloning of cDNA fragments of *Alonsoa meridionalis* raffinose synthase and stachyose synthase

To obtain cDNA fragments of stachyose synthase (*AmSTS*) and raffinose synthase (*AmRS*) from *Alonsoa meridionalis* by RT-PCR, degenerate primers were deduced from conserved motifs of the STS and RS amino acid sequences from *Vigna angularis* (STS; Peterbauer et al., 1999), *Cucumis sativum* (RS; Accession No. AAD02832) and *Arabidopsis thaliana* (RS; Accession No. BAB11595; Figure 3.19). Since STS and RS amino acid sequences are homologous with the exception of a 70 amino acid insertion in the STS sequence, the degenerate primers were deduced from amino acid stretches which were highly conserved in both enzymes (Figure 3.19). The 70 amino acid insertion in the stachyose synthase sequence was located between the two primers, thus allowing to distinguish between RT-PCR products from raffinose and stachyose synthases.

The deduced degenerate primers *sta-5'* and *sta-3'* (Table 2.1) were used for RT-PCR on cDNA prepared from leaf RNA (2.21.2.1) with the following PCR program:

94°C	60 sec	
94°C	30 sec	} 35 cycles
55°C	30 sec	
72°C	90 sec	
72°C	10 min	

This resulted in two PCR products, one of ca 0.8 kb length and another one of ca 1.1 kb. The fragments were cloned in pGEM®-T Easy and sequenced. The comparison of the encoded amino acid sequences with the two previously known raffinose synthases and the stachyose synthase revealed homologies of 80%, thus confirming that the obtained fragments represented RS (the 0.8 kb fragment) and STS (the 1.1 kb fragment) from *Alonsoa*.

3.3.2. The full length cDNA of stachyose synthase from Alonsoa (AmSTS) was cloned

In order to amplify the 3'- and 5' end of the *AmSTS* cDNA by RACE (2.21.2.2, 2.21.2.3), gene-specific primers were deduced from the sequence of the *AmSTS* cDNA fragment obtained by RT-PCR (3.3.1). 5' RACE was performed two times independently, first with primers *amsts5race1* and *amsts5race2*, and the second time with another pair of primers, *5raceneu1* and *5raceneu2* (Table 2.1). Both amplifications resulted in the same 5' end sequence of the *AmSTS* cDNA. After the 3'-end and 5'-end sequences of *AmSTS* cDNA had been obtained, two specific primers *FLCsts5* and *FLCsts3* (Table 2.1) were deduced and used in an RT-PCR for the amplification of the full length *AmSTS* cDNA (2.21.3).

The nucleotide sequence and deduced amino acid sequence of the full length *AmSTS* cDNA clone are shown in Figure 3.20. The nucleotide sequence is 2889 bp in length, including a 5'-untranslated region of 108 bp and a 3'-untranslated region of 172 bp. The ORF of stachyose synthase encodes a protein of 868 amino acids with a molecular weight of 95.6 kDa. Interestingly, the 5'-UTR contains two small uORFs, one encoding four and the other eleven amino acids, both in-frame with the *AmSTS* ORF (Figure 3.20).

To date, two complete cDNA sequences of stachyose synthases are available, one from *Vigna angularis* (Peterbauer et al., 1999) and another from *Pisum sativum* (Peterbauer et al., direct submission; Accession No. CAC38094). The comparison of the *AmSTS* sequence with these two STS sequences is shown in Figure 3.21. *AmSTS* shows 71% similarity (63% identity) with *VaSTS* and 74% similarity (66% identity) with *PsSTS* at the amino acid level.

VaSTS	MAPNDP VNATIGLEPSE -----KVFDLSDGKLTVKG-VVLL	36
AtRS	MAPLHESLSSINDVIESKPLFVPIKPKILQPN SFNLS EGSLCAKDSPTLL	50
CsRS	MAPSFKNGGSNVV SFDGLN -----DMSSPFATDGSDFTVNGHSFL	40
VaSTS	SHVPE NVTFSSFSSICVPRDAPSSIIQRVTAASHKGGFLGF SHVSPSDRL	86
AtRS	FDV PQNVTFTPFSSHS STDAFLPILRLVQANAHKGGFLGFTKESPSDRL	100
CsRS	SDVPE NVIVAS -----PSPYTSIDKSPVSVGCFVGFDASEPDSRH	79
VaSTS	INSLG SFRGRNFLSIFRFKTTWSTOWVGN SGSDLOEFTOWILLIEVPE TE S	136
AtRS	TN SLGRFEDREFLSLFRFKMWWSTAWIGK SGSDLOAETQWVMLKIPEDS	150
CsRS	VV SIGRLKDIRFMSIFRFKVVWTT HVGRNGGDLESETQIVILEKSDSGR	129
VaSTS	-YVVIIP TIEKSF RSALHPGSDDHVKTCAESGSTQVRS SFGAIAYVHVA	185
AtRS	-YVAIIP TIECAF RSALHPGEGKGNVICAESGSTKVES SFKSIAYIHIC	199
CsRS	PYVFL LPIVEGPERISTIQPGDDFVDVGV ESGSSKVVDA SFRSMILYLHAG	179
VaSTS	ET PYNLMREAYSALRVHLD SFRLL EETVPRIVDKF GWCTWDAFYLT VNP	235
AtRS	DN PYNLMKEAFSALRVHMNTFKLLEEK LPKIVDKF GWCTWDA CYLT VDP	249
CsRS	DD PALVKEAMKIVRTHL GTFRLL EETVPRIVDKF GWCTWDAFYLT VHP	229
VaSTS	VG VHGLKDFSEGGVAPRFVVIDDGWQSVNF DDDPNE DAKNLVLGGEOM	285
AtRS	ATI WTGVKEFEDGGVCPKFVIIDDGWQSI NFDGDEL DKDAENLVLGGEOM	299
CsRS	QG VTEGVRHLVDGGCP GLVLIDDGWQSI GHDSPTTKEGMNQTVAGEOM	279
VaSTS	TAR LHRFEEGDKFRKYOKGLLLGNAP SFNPETIKELISKGIEAHLGKQ	335
AtRS	TAR LTSFKECKKFRNYKEESL GSDDVSGS-----	328
CsRS	PCR LLKFOENYKERD VVNP KATGR RGQK-----	308
VaSTS	AA AISAGGSDLAEI ELMIVK VREEIDDL FGGK GKESNESGGCCCKAAECG	385
AtRS	-----	-
CsRS	-----	-
VaSTS	GM KDFITDLRTEFKGLDDVYVWHALCGG WGVRE G-TTHDSKIIECKLS	434
AtRS	GM AFTKDLRLRFKSLDDIYVWHALCGA WNGVR PE-TMMDLKAKVAF FELS	378
CsRS	GM KAFIDELKGEFKIV EHVYVWHALCGY WGLLRQVPLPEARVITQPVLS	358
VaSTS	PGL VGTMKDLAVDKIVEGS IGLV HPHOANDLYDSMHSYLAQTGVIGVKID	484
AtRS	PS LGATMADLAVDKVVEAG IGLV HPSKAHEFYDSMHSYLASVGVIGAKID	428
CsRS	PGL QMTMEDLAVDKIVLHKVGLVPE PKAE EMYEGLHAHLEKVGIDG VKID	408
VaSTS	VI HSLLEYVCEEYGGRVE IAKAY YDGLTNSITKFN SGS TIASMQCNDFF	534
AtRS	VF QLES SLAEEH GGRVEIAKAYYDGLTESMIKFN SGD VIASMQCNEFF	478
CsRS	VI LLEMLCEDYGGRVD IAKAY YKAMTKSINKHFKGN GV IASMEHCNDEM	458
VaSTS	FL GTKQIPFGRVGDDEFWQD DPNG DPMGVFWLQGVHMIHCSYNSLWMGQIT	584
AtRS	FL ATKQISIGRVGDDEFWQD DPY GDPQGVYWLQGVHMIHCSYNSIWMGOMI	528
CsRS	FL GTEALISLGRVGDDEFWCT DPS GDPNGTFWLQGHMVHCANDSLWMGNFT	508
VaSTS	QP DWMFQSDH ECAK FHAGSRAICGGPVYVSDSVG --SHDFDLIKKL VFP	632
AtRS	QP DWMFQSDH VCAE YHAASRAICGGPVYLS DHLG KASHNFDL IKKL AEF	578
CsRS	HP DWMFQSTH PCA AFHAASRAIS GG PIYVSDSVG --KH NFDLLK KL VLE	556
VaSTS	DGT VFKCIYFPLP TRD CLFRNPLFDQK T VLKIWNFNKYGGVIGAF NCOGA	682
AtRS	DGT IPRCVHYALP TRD SLFKNPLFDK E SILKIFNFNKEGGVIGT F NCOGA	628
CsRS	DGS ILRSEYYALP TRD CLFEDPLHNG E TMLKIWNLNKETGVIGAF NCOGG	606
VaSTS	GWD PKGKPKFKGFPE CYKA ISCTVHVTEVEWDQ --KKEA EHMGKAEFYVY	730
AtRS	GWS PEHRFKGYKECYT TVSG TVHVS DI EWDONPEAAGSQVTYTGDYLVY	678
CsRS	GWC RTERNQCF S QYSKRVTSKTNP DI EWH S--GEN PISIEGVKTEALY	654
VaSTS	IN QAEVLHIMTEVSE PT LTIOPSTFELYNFV PVE KLGSSN IK FAPIGT	780
AtRS	KQ SEELIFMNSK SE AMKITLEPSAFD LL SFVPVTELVSSG VR FAPLGLL	728
CsRS	LY QAKLLLSKP -SOD LDIALDPFE F ELLTVSPVTKL L QTS L HFAPIGLV	703
VaSTS	NM ENS GG TIOELE Y IEKD --V KVKVKGGR FL AYSTQSPKKF OL N GS DAA	828
AtRS	NM ENC VI QDMKVTG DNS-IR VDVKEGR F MAYSSAPV K CYLNDKEAE	777
CsRS	NM LN SG ALQSV DD LSSVEIGVK CG EMRVFAS KK FRACRID GE V	753
VaSTS	FQ WLPD -G KLT LN AWTE END GVS DT AIF F- 857	
AtRS	FK WE ET GKLS FF VWVE ES SG IS HLS FT F - 807	
CsRS	FK YD Q QMVV VQ VPWF IDS SSG IS VIE Y LF 784	

Figure 3.19. The deduction of degenerate primers for amplification of cDNA fragments of *Alonsoa meridionalis* stachyose synthase and raffinose synthase. *VaSTS*, *Vigna angularis* stachyose synthase; *AtRS*, *A. thaliana* raffinose synthase; *CsRS*, *Cucumis sativum* raffinose synthase. Amino acid residues conserved in all three sequences are labelled in black and chemically similar amino acid residues are labelled in grey. The two amino acid sequence fragments which were used for the deduction of the primers are indicated by pink colour.

3.3.3. Stachyose synthase activity assay with protein extracts of *Alonsoa meridionalis* leaves and of *E. coli* cells containing an expression vector carrying the *AmSTS* ORF

The function of stachyose synthesis was assigned to the cloned *AmSTS* cDNA on the basis of amino acid sequence homology of the encoded protein with *Vigna angularis* STS, which has been shown to perform stachyose synthesis when expressed in a Baculovirus system (Peterbauer et al., 1999). To test whether the protein encoded by the *AmSTS* cDNA is also able to perform stachyose synthesis, the full length *AmSTS* cDNA was inserted into the *E. coli* expression vector pET3b (Rosenberg et al., 1986) under the control of an inducible promoter, yielding the plasmid pET*/STS (2.22.1). This plasmid was transformed into the *E. coli* strain BL21 (DE3).

To establish the conditions for the test of enzymatic activity of *AmSTS*, a stachyose synthase assay was performed using leaves of *Alonsoa meridionalis*. Galactinol isolated from the leaves of *Buddleja davidii* (2.3.2.1) was used as a substrate.

3.3.3.1. Stachyose synthase activity assay using leaves of *Alonsoa*

Determination of the activity of stachyose synthase was performed with crude extracts from *Alonsoa* leaves (2.5.6.1). Different concentrations of raffinose were tested in the assay. Concentrations higher than 10 mM had an inhibitory effect on STS activity with complete inhibition occurring at a raffinose concentration of 20 mM (data not shown). The assays were performed with 4 mM raffinose at different pH values ranging from 5.5 to 7.0. The highest activity ($1.98 \mu\text{mol stachyose g}^{-1} \text{FW h}^{-1}$) was measured at pH 6.5 (Figure 3.22 B).

3.3.3.2. The induction of *AmSTS* expression did not function in *E. coli* cells

The *E. coli* strain BL21 (DE3) was transformed with the expression vector containing the *AmSTS* cDNA (pET*/STS), and with the empty expression vector pET3b as a control (2.22.1). After the induction of T7 RNA polymerase expression by the addition of IPTG (2.22.2), the cells were harvested in 30 min intervals to monitor the formation of the protein on a polyacrylamide gel (2.23). Three hours after induction, the cells were harvested for the extraction of total proteins for the STS activity assay (2.5.6.2). Although the 99 kDa protein corresponding to the T7 RNA polymerase appeared in SDS-PAGE of the crude extract on the gel already one hour after the addition of IPTG, no additional protein in the region of 95 kDa, the expected size of *AmSTS*, was detected at any timepoint examined (data not shown).

To test if the protein was formed in *E. coli* cells in amounts too small to detect by SDS-PAGE, the assay of STS activity was performed with the cell extracts harvested three hours after induction (2.5.6.2). No activity could be detected (data not shown). Both

observations indicated that the *E. coli* expression system is not suitable for the functional expression of plant stachyose synthase cDNA.

```

1 ATGTGTCCAACTAAGTAATAACTCAATAGTTCATGCATAAGCTTTTCTACAAAAAAAT 60
  M C P N * V I T Q * F M H K L F Y K K N
61 AATAACTGATTTTTAGCCTTCCCCTGTTTTTGCTCTGTTTTTCAACCATGGCACCTCCA 120
  N N * F L A F P C F C S V F S T M A P P
121 TATGATCCCATCCCCATCCCCATCCCCATGAGCGCAATTTTGAACCTCCTGAGCTCCACC 180
   5 Y D P I P I P I P M S A I L N F L S S T
181 GTAAAGGACAACCTCTTCGAGCTCCTCGACGGAACACTCTCCGTGAAAAATGTCCCGATT 240
   25 V K D N S F E L L D G T L S V K N V P I
241 CTGACCGATATCCCAGCAACGTGAGTTTCTCCAGCTTCTCTCCATAGTCCAATCCTCT 300
   45 L T D I P S N V S F S S F S S I V Q S S
301 GAAGCTCCAGTTCCTGTTCCAGCGCTCAATCACTCTCCTCCAGCGGGGTTTCTCTC 360
   65 E A P V P L F Q R A Q S L S S S G G F L
361 GGGTTCAGCCAGAATGAACCTCTTCTCGCCTGATGAATTCCTGGGAAAATTCACCGAT 420
   85 G F S Q N E P S S R L M N S L G K F T D
421 AGGGACTTCGTCAGCATTTTCAGGTTCAAAACCTGGTGGTCTACTCAATGGGTCGGGACA 480
  105 R D F V S I F R F K T W W S T Q W V G T
481 ACAGGTTCCAGACATACAAATGGAGACACAGTGGATAATGCTAGACGTGCCGGAGATCAAG 540
  125 T G S D I Q M E T Q W I M L D V P E I K
541 TCCTACGCTGTCGTTGGTCCCAATAGTTGAAGGGAAAATTCAGGTCGGCACTTTTCCCTGGG 600
  145 S Y A V V V P I V E G K F R S A L F P G
601 AAAGACGGTCATATCTTGATCGGTGCAGAAAGTGGTCTACCAAAGTGAAGACATCAAAC 660
  165 K D G H I L I G A E S G S T K V K T S N
661 TTCGACGCGATCGCGTATGTGCACGTGTCTGAAAATCCTTACACCTTGATGAGAGACGCT 720
  185 F D A I A Y V H V S E N P Y T L M R D A
721 TACTGCTGTAAGAGTTCATCTCAACACGTTCAAGCTTATCGAAGAGAAAATCCGCGCCG 780
  205 Y T A V R V H L N T F K L I E E K S A P
781 CCCCTGGTGAATAAGTTCGGGTGGTGGACTTGGGATGCTTTTTACTTGACCGTGGAGCCA 840
  225 P L V N K F G W W T W D A F Y L T V E P
841 GCTGGTATTTACCATGGTGTGCAAGAGTTTGGTGTGAGAGGGGTCACCCCGAGGTTTCTG 900
  245 A G I Y H G V Q E F A D G G L T P R F L
901 ATTATAGACGACGGGTGGCAAAGCATTAAATAACGATGATAACGACCCGAATGAGGATGCG 960
  265 I I D D G W Q S I N N D D N D P N E D A
961 AAGAATCTCGTACTCGGGGGGACTCAAATGACTGCCAGGCTTCACAGGCTTGATGAATGT 1020
  285 K N L V L G G T Q M T A R L H R L D E C
1021 GAGAAAATTTAGGAAAATACAAAGGTGGATCGATGTCGGGACCTAATCGTCCACCGTTTGAT 1080
  305 E K F R K Y K G G S M S G P N R P P F D
1081 CCTAAGAAGCCGAAGTTGTTGATTTCTAAGGCTATTGAGATCGAAGTTGCTGAAAAAGCA 1140
  325 P K K P K L L I S K A I E I E V A E K A
1141 CGTGACAAGGCGGCTCAATCGGGTGTCACTGATTTGGCTAGATACGAAGCTGAGATTGAG 1200
  345 R D K A A Q S G V T D L A R Y E A E I E
1201 AAAGTGCACAAAAGAAATGGATCAAAATGTTTCGGTGGAGGTGGAGAAGAAAACGAGTTCGGGT 1260
  365 K L T K E L D Q M F G G G G E E T S S G
1261 AAAAGCTGTTTCGAGTTGCTCTTGCAAAATCAGATAAATTTGGGATGAAAGCGTTTACGAAG 1320
  385 K S C S S C S C K S D N F G M K A F T K
1321 GATTTAAGGACGAATTTCAAAGGTTTGGATGATATATATGTTTGGCATGCATTGGCTGGT 1380
  405 D L R T N F K G L D D I Y V W H A L A G
1381 GCATGGGGAGGAGTTAGGCCCGGTGCGACTCATTTGAATGCCAAGATTGTCCCGACCAAC 1440
  425 A W G G V R P G A T H L N A K I V P T N
1441 CTGTCACCCGACTGGATGGAACAATGACTGATCTGGCAGTTGTGAAGATTATCGAGGGT 1500
  445 L S P G L D G T M T D L A V V K I I E G
1501 TCAACCGGGCTCGTGGATCCTGATCAGGCGGAGGACTTCTACGACTCCATGCACCTCGTAT 1560
  465 S T G L V D P D Q A E D F Y D S M H S Y
1561 CTCTCTAGTGTGGAATTAAGTGGAGTTAAAGTGGATGTTATCCATACGCTTGAATACATA 1620
  485 L S S V G I T G V K V D V I H T L E Y I

```



```

1621 TCCGAAGATTACGGAGGTCGGGTCGAGCTTGC GAAAGCTTACTACAAGGGGTTGTCGAAA 1680
505 S E D Y G G R V E L A K A Y Y K G L S K
1681 TCCCTTGCTAAGAACTTCAACGGAAC TGGACTTATTTCCAGCATGCAGCAATGCAACGAC 1740
525 S L A K N F N G T G L I S S M Q Q C N D
1741 TTCTTTTACTTGGAACTGAGCAGATATCCATGGGACGAGTGGGTGATGACTTCTGGTTC 1800
545 F F L L G T E Q I S M G R V G D D F W F
1801 CAAGATCCTAATGGTGATCCGATGGGAGTTTATTGGCTACAAGGGGTGCACATGATCCAC 1860
565 Q D P N G D P M G V Y W L Q G V H M I H
1861 TGTGCCTACAACAGCATGTGGATGGGT CAGTTCATCCAACCCGATTGGGACATGTTTCAA 1920
585 C A Y N S M W M G Q F I Q P D W D M F Q
1921 TCCGATCACCCGGGGGGTACTTTT CACGCGGGATCAAGGGCTATCTGTGGGGTCCGGTG 1980
605 S D H P G G Y F H A G S R A I C G G P V
1981 TACGTGAGTGATTCCCTCGGTGGCCATAATTT CGATCTTCTGAAGAACTTGTGTTCAAT 2040
625 Y V S D S L G G H N F D L L K K L V F N
2041 GATGGTACAATCCCAAGTGCATCCATTTTGCTCTCCCGACTAGAGATTGCCTCTTTAAG 2100
645 D G T I P K C I H F A L P T R D C L F K
2101 AACCCCTGTGTTTGACAGCAAAACCATTTCTCAA AATTTGGAAC TCAACAAGTATGGAGGT 2160
665 N P L F D S K T I L K I W N F N K Y G G
2161 GTGATCGGAGCTTTCAACTGCCAAGGCGCCGGGTGGGACCCGAAGGAGCAAAGGATCAAG 2220
685 V I G A F N C Q G A G W D P K E Q R I K
2221 GGGTACTCTCAGTGTTACAAACCACTCTCGGGTTCGGTCCATGTTAGTGGCATCGAATTT 2280
705 G Y S Q C Y K P L S G S V H V S G I E F
2281 GATCAGAAAAAGGAAGCGTCTGAAATGGGAGAGGCAGAGGAATACGCGGTTTATCTTAGC 2340
725 D Q K K E A S E M G E A E E Y A V Y L S
2341 GAGGCTGAGAACTATCCTTGGCAACCCGCGACTCTGATCCCATCAAGATTACCATT CAG 2400
745 E A E K L S L A T R D S D P I K I T I Q
2401 TCCTCCACATTCGAGATTTTTCAGCTTCGTC CCGATCAAGAACTCGGTGAGGGTGTCAA 2460
765 S S T F E I F S F V P I K K L G E G V K
2461 TTCGCGCCTATTGGGCTAACCAACTTGTTTAACGCGGGAGGGACCATTCAAGGTCTGGTG 2520
785 F A P I G L T N L F N A G G T I Q G L V
2521 TACAACGAGGGTATAGCGAAGATTGAAGTGAAGGGTGACGGGAAATTCTTGGCTTACTCG 2580
805 Y N E G I A K I E V K G D G K F L A Y S
2581 AGCGTCGTGCCTAAGAAAGCGTACGTGAATGGAGCCGAGAAGGTGTTTGCTTGGTCTGGA 2640
825 S V V P K K A Y V N G A E K V F A W S G
2641 AATGGGAAGCTGGAGTTGGACATAACTTGGTATGAAGAGTGTGGTGGGATTTCTAATGTA 2700
845 N G K L E L D I T W Y E E C G G I S N V
2701 ACTTTTGTGTTACTAAGGATGATAATGTGTGATGCATATGATAATAAGTGTGCCTGATAAA 2760
865 T F V Y *
2761 CATGGCTCTAAAATGGTACTTAGTTTTTTGTGTTGTACTAATATTTTGATTTTCAGTGCT 2820
2821 TGAAATAAGTCTGTACTATTGTATGATGATTATGCCAGAATTGGCCATGAAAATGTGT 2880
2881 TTTGTTTGA 2889

```

Figure 3.20. The nucleotide and deduced amino acid sequences of the *AmSTS* cDNA full length clone. The 5'-untranslated region of 108 nucleotides is underlined and the two 5'-uORFs within it are shadowed. The methionine at the start of the STS protein sequence is labelled by inverse printing.

VaSTS	MAPPNDE-----VNATIGLEPSEKVFDSLSDGKLTVKGVVLLSHVPEENVTFSSFSSTCVPR--DAPS	59
PsSTS	MAPPIN-----STTSNLIKTESIFDLSEKFKVKGFPLFHVPEENVSFRSFSSICKPSESNAFP	59
AmSTS	MAPPYDFIPIPIPSAALNFLSSTVKDNSFELLDGTLSVKNVPIILTDIENSVSFSSFSSTVQSS--EAPV	68
	* * * * *	
VaSTS	SILQRMVTAASHKGGFLGFSHVSPSRLINSLGSEFRGRNFLSIFRFTWWSTQWVGNNSGSDLQMETQWILLI	129
PsSTS	SLLQKVLAYSHKGGFLGFSHETPSRLMNSIGSEFNKDFLSIFRFTWWSTQWIGKSGSDLQMETQWILLI	129
AmSTS	PLFORAQSLSSSGGFLGFSQNEPSSRLMNSLCKFTDRDFVSIFRFTWWSTQWVGTGSDIQMETQWIML	138
	* * * * *	
VaSTS	EVPETESYVVIPIIEKSFRSALHPGSDDHVKICAESGSTQVRASSEGAIAIVHVAETPYNLMREAYSAL	199
PsSTS	EVPETKSYVVIPIIEKCFRSALFPGFNDHVKIIAESGSTKVKESTFNSTIAYVHFSENPYDLMKEAYSAL	199
AmSTS	DVPEIKSYAVVVPIVVGKFRSALFPKGDGHILIGAESGSTKVKKTSNFDIAYVHVSENPYTLMRDAYTAV	208
	* * * * *	
VaSTS	RVHLDSFRLLLEKTVPRIVDKFGWCTWDAFYLTVPVGVWHGLKDFSEGGVAAPRFVVIDDGWQSVNFDDE	269
PsSTS	RVHLNSFRLLLEKTIENLVDKFGWCTWDAFYLTVPPIGIFHGLDDFKGGVEPRFVIIDDGWQSISFDGY	269
AmSTS	RVHLNFKLLEEKSAEPLVNKFGWCTWDAFYLTVEPAGIYHGVQEFADGGITPRFLIIDDGWQSINNDEN	278
	* * * * *	
VaSTS	DPNEDAKNLVLGGEQMTARLHRFEEDGDKFRKYQKGLLLGNAPSFNPETIKELISKGIEAEHLG-KQAAA	338
PsSTS	DPNEDAKNLVLGGEQMSGRLHRFDECYKFRKYESGLLLGNPSPPYDNNFTDLILKGIHEKLRKKREBA	339
AmSTS	DPNEDAKNLVLGGTQMTARLHRLEDEKFRKYKGGSMGSPNRPFPDKPKPKLLISKALIEIYVAEKARDKA	348
	* * * * *	
VaSTS	ISAGSSDLAEIELMIVKVRREEIDDLFGG--KGKESNEGGCCCKAAECGGMKDFTTDLRTEFKGLDDVVV	406
PsSTS	ISSKSSDLAEIESKIKKVVKEIDDLFGG--EQFSSGKKS---EMKSEYGLKAFTKDLRTKFKGLDDVVV	403
AmSTS	AQSGVTDLARYEAEIEKLTKELDQMFGGGEETSCKSCSSCCKSDNEGMKAFTKDLRTNFKGLDDIYV	418
	* * * * *	
VaSTS	WHALCGGWGGVVRPETHLDSKIIIPCKLSPGLVGTMDLAVDKIVEGSLGLVHPHQANDIYDSMHSYLAQT	476
PsSTS	WHALCGAWGGVVRPETHLDTKIVPCKLSPGLDGTMDLAVVEISKASLGLVHPSQANELYDSMHSYLAES	473
AmSTS	WHALCAGWGGVVRPETHLNAKIVPTNLSPLDGTMTDLAVVKIIEGSTGLVDPDQAEELYDSMHSYLSV	488
	* * * * *	
VaSTS	GVTGVKIDVIHSLEYVCEEYGGRVIAKAYYDGLTNSIINKFNFGSGIIASMQQCNDFFFLGTKQIIPFGRV	546
PsSTS	GITGVKVDVIHSLEYVDEYGGRVDLAKVYYEGLTKSIVKNFNFGNGMIASMQHCNDFFFLGTKQISMGRV	543
AmSTS	GITGVKVDVIHTLEYISEDYGGRVIAKAYYKGLSKLAKNFNGTGLISSMQQCNDFFFLGTEQISMGRV	558
	* * * * *	
VaSTS	GDDFWFQDPNGDPMGVFWLQGVHMIHCSYNSLWMGQTIQPDWDMFQSDHECAKFHAGSRAICGGPVYVSD	616
PsSTS	GDDFWFQDPNGDPMGSFWLQGVHMIHCSYNSLWMGQTIQPDWDMFQSDHVC AKFHAGSRAICGGPIYVSD	613
AmSTS	GDDFWFQDPNGDPMGVYWLQGVHMIHCAYNMWMGQFIQPDWDMFQSDHPGGYFHAGSRAICGGPVYVSD	628
	* * * * *	
VaSTS	SVGSHDFDLIKKLVFDGTVPKCIYFELPTRDCLFRNPLFDQKTVLKIWNFNKYGGVIGAFNCQGAGWDP	686
PsSTS	NVGSHTDFDLIKKLVFDGTIPKCIYFELPTRDCLFKNPLFDHTTVLKIWNFNKYGGVIGAFNCQGAGWDP	683
AmSTS	SLGCHNFDLLKKLVFNDGTIPKCIHFAELPTRDCLFKNPLFDSKTIILKIWNFNKYGGVIGAFNCQGAGWDP	698
	* * * * *	
VaSTS	KGKKEKGFPECYKATISCTVHVTEVEWDQKKEAEHMGKAAEYVVYLNQAEVLHLMTVPVSEPLQITIQPSTF	756
PsSTS	IMQKERGFPECYKPIPGTVHVTEVEWDQKEETSHLKGAAEYVVYLNQAEELSLMTLKSSEPIQFTIQPSTF	753
AmSTS	KEQRTKGYSQCYKPLSGSVHVSGLIEFDQKKEASEMGEAAEYAVYLSAEKLSLATRDSDEPIKITIQSSTF	768
	* * * * *	
VaSTS	ELYNFVPEKELGSSNIKFAPIGLTNMENS GGTIQELLEYIEKDVKVKVKGGRFLAYSTQSPKKFQLNQSD	826
PsSTS	ELYSFVPTKLCG--IKFAPIGLTNMENS GGTVIDLLEYVNGAKIKVKGGGSFLAYSSSPKKFQLNQCE	822
AmSTS	EIFSFPVPIKKGEC-VKFAPIGLTNLENA GGTIQGLVYNEGIAKIEVKGDGKFLAYSSVVPKKAYVNGAE	837
	* * * * *	
VaSTS	AAFOWLFDGKLTLLNAWIEENDGVSDLAIFF	857
PsSTS	VDFEVLGDGKLCVNVPEWIEEACGVSDMEIFF	853
AmSTS	KVFAWVSGNGKLELDITWYEECGGISNVTFVY	868

Figure 3.21. A comparison of the deduced amino acid sequence of *AmSTS* with two known sequences of stachyose synthases: *VaSTS* from *Vigna angularis* (Peterbauer et al., 1999) and *PsSTS* from *Pisum sativum* (T. Peterbauer, Accession No. CAC38094). *AmSTS* shows 71% similarity (63% identity) with *VaSTS* and 74% similarity (66% identity) with *PsSTS*.

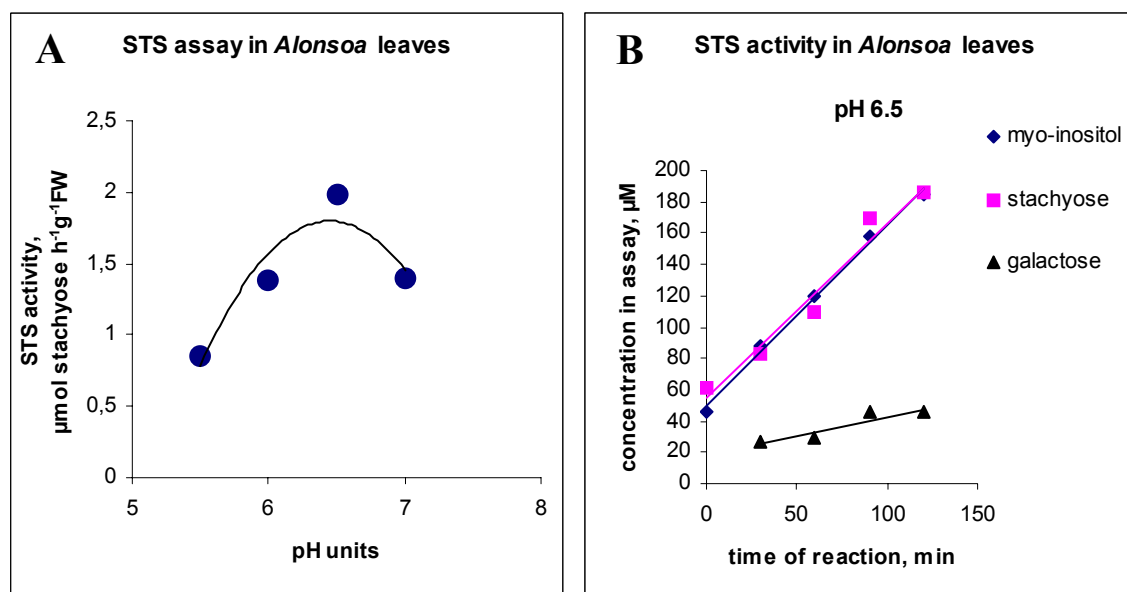


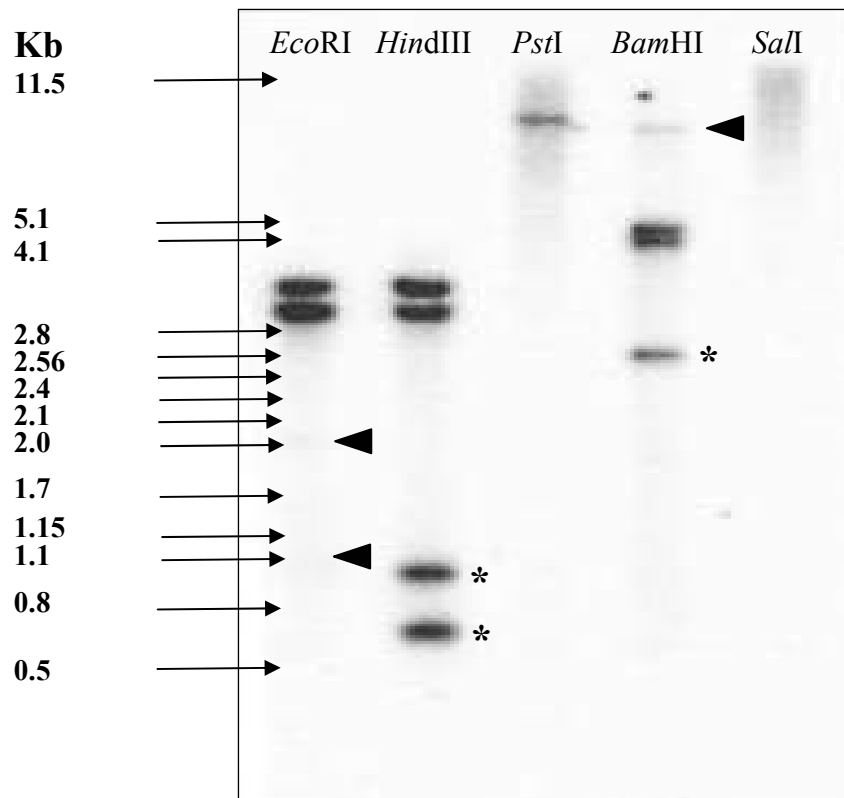
Figure 3.22. Determination of the activity of stachyose synthase in crude extracts of leaves of *Alonsoa meridionalis*. **A**, time-dependent increase of stachyose and *myo*-inositol concentrations in the assay; **B**, activity measured at different pH values.

3.3.4. *AmSTS* is encoded by a small gene family containing most probably two members

To obtain information about the gene family situation of *AmSTS*, a Southern blot with total genomic DNA of *Alonsoa meridionalis* was hybridized with the full size cDNA of *AmSTS* (2.19.2).

Total DNA from *Alonsoa* leaves was restricted by five different endonucleases which have different numbers of restriction sites within the *AmSTS* cDNA sequence: *EcoRI* (1 site), *HindIII* (2 sites), *BamHI* (1 site), *PstI* (none) and *SalI* (none) and transferred to a nylon membrane. After hybridization, the membrane was washed under stringent conditions (2.19.5.2).

The hybridization was performed twice with independent preparations of total genomic DNA from *Alonsoa*. Both blots showed the same hybridization pattern (Figure 3.23). The expected numbers of the hybridizing DNA bands are listed below the image of the blot. In both cases, one additional labelled hybridizing fragment for *HindIII*-restricted DNA and one additional labelled fragment for *BamHI*-restricted DNA were present. That means that either, at least one additional restriction site for *HindIII* and *BamHI*, respectively, is present within the *AmSTS* introns, or that the *AmSTS* gene family includes more than one member.



Expected number of bands	2	3	1	2	1
Observed number of bands	2	4	1	3	?

Figure 3.23. Hybridization of a Southern blot containing genomic DNA of *Alonsoa meridionalis* with the *AmSTS* full size cDNA. Filled arrow heads point at weak bands. Stars mark internal *AmSTS* gene fragments. The numbers of hybridizing fragments as expected from the known restriction sites within the *AmSTS* cDNA and its introns are compared with the numbers of hybridizing fragments observed.

To check whether additional restriction sites are present within *AmSTS* introns, PCR was performed with genomic DNA isolated from *Alonsoa* leaves. Primers were designed to obtain three DNA fragments covering the whole length of *AmSTS* transcribed region. The positions of the specific primers on the *AmSTS* cDNA sequence are shown in Figure 3.24. The three PCR products obtained were about 50 - 200 bp longer than the corresponding *AmSTS* cDNA fragments, indicating that the ORF of the *AmSTS* gene does not contain large introns (data not shown). The PCR products were cloned in pGEM®-T Easy and subjected to restriction analysis which showed that the amplified DNA fragments contained no restriction sites for *EcoRI*, *HindIII*, *BamHI* and *PstI* in addition to those already known for the *AmSTS* cDNA (data not shown). The size of the introns was estimated as 50, 100 and 180 bp (Figure 3.24).

Mapping of the restriction sites for *EcoRI*, *HindIII* and *BamHI* on the *AmSTS* gene sequence including its 1850 bp 5' promoter region (for the isolation of promoter see 3.3.6.1)

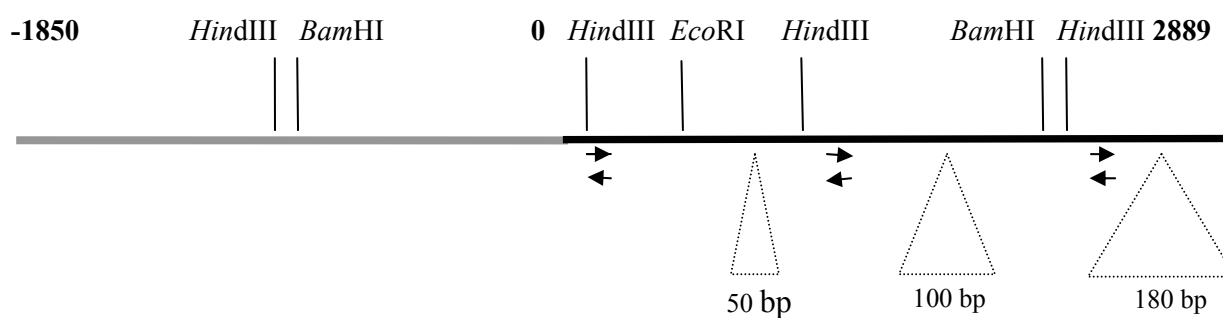


Figure 3.24. The positions of restriction sites for *EcoRI*, *HindIII* and *BamHI* on the *AmSTS* gene. The promoter region is presented in grey and the transcribed region is given in black. The size and (approximate) positions of the three introns found within the *AmSTS* ORF are shown as triangles. Arrows indicate the position of primers used to obtain DNA fragments with introns.

allowed to estimate the expected size of several DNA fragments hybridizing on the Southern blot. These were a 890 bp and a 960 bp fragment for DNA restricted with *HindIII* and a 2565 bp fragment for DNA restricted with *BamHI* (Figure 3.23). The appearance of two larger DNA fragments (*HindIII* and *BamHI*) cannot be explained by additional restriction sites in introns and indicates the presence of (an)other gene family member(s). It is unlikely that these additional fragments are due to cross-hybridization between *AmSTS* and *AmRS* sequences, since the hybridization of additional fragments was of similar strength as that of the identified fragments. Rather, this cross-hybridization might explain the appearance of three weak bands found. The presence of only one hybridizing fragment in case of *PstI* restriction might indicate that the number of gene family members is small; there are probably only two gene copies situated not far from each other.

3.3.5. Localization of *AmSTS* mRNA in leaves of *Alonsoa meridionalis* by in situ RNA hybridization: *AmSTS* expression is confined to intermediary cells

The *in situ* antisense RNA hybridization method allows to localize the expression of a gene to specific cells or tissues within plant organs. Since the washing conditions are not stringent, *in situ* probes do not distinguish between different members of a gene family. Thus, with antisense RNA corresponding to the *AmSTS* cDNA fragment (3.3.1), the expression of all *AmSTS* genes can be detected.

The localization of the expression of the genes of stachyose synthase, raffinose synthase and of the sucrose transporter gene (*AmSUT*) should be compared to each other in *Alonsoa meridionalis* by the *in situ* antisense RNA hybridization studies. For this analysis, information about the expression levels of the selected genes in different plant organs was

necessary. *AmSUT* expression levels were very low and could only be detected by RT-PCR (Knop et al., 2001). *AmSUT* expression levels were highest in stems, followed by flowers, mature leaves and roots. To obtain data about the expression levels of *AmSTS* and *AmRS*,

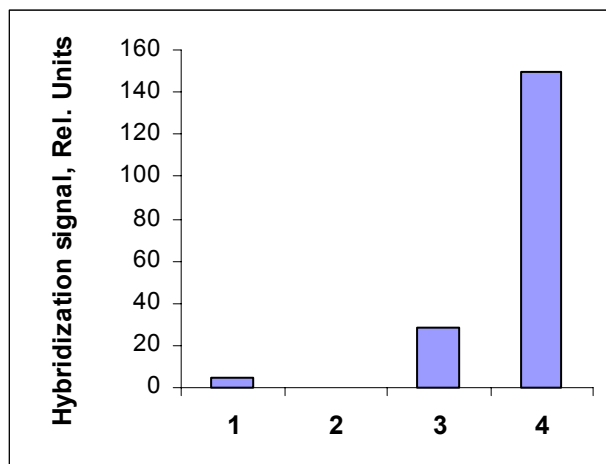


Figure 3.25. Relative expression levels of *AmSTS* in different organs of *Alonsoa meridionalis*. **1**, flowers; **2**, stems; **3**, young leaves; **4**, mature leaves.

RNA gel blot hybridisation analysis was performed with RNA isolated from source leaves, sink leaves, stems and flowers (2.19.4). However, even after long-term exposure of the hybridized blots, no hybridizing bands were observed for *AmRS* which indicates that this gene has very low expression levels. In case of *AmSTS*, expression levels (quantified on the basis of RNA amounts as indicated by the strength of the 28S rRNA band) was strongest in source leaves, followed by sink leaves and flowers, while no hybridization was found for RNA from stem (Figure 3.25).

For the *in situ* hybridisation, pieces of stems and leaves of *Alonsoa* were fixed and embedded in paraffin, and 8 μm thick sections were put on slides (2.14). RNA probes were prepared as described in 2.25.1.2 The cloning of the cDNA fragments of both *AmRS* and *AmSTS* has been described (3.3.1). In order to obtain templates for *in vitro* transcription, the *EcoRI* inserts of the pGEM®-T Easy clones of *AmRS* and *AmSTS*, as well as a cDNA fragment of *AmSUT* provided by Christian Knop, were subcloned in pBluescript®-IIS⁺. The *in situ* hybridisations were performed as described in 2.25.2-5. To preserve the quality of the leaf sections, it was essential not to dry the slides during the whole procedure. Staining of intermediary cells of *Alonsoa* leaves hybridised with *AmSTS* antisense RNA was observed after 15 hours incubation in detection reagent (Figure 3.26) in two independent experiments. With the other probes, no staining was detected in sections of both leaves and stems even after 36 hours of incubation in detection reagent (not shown).

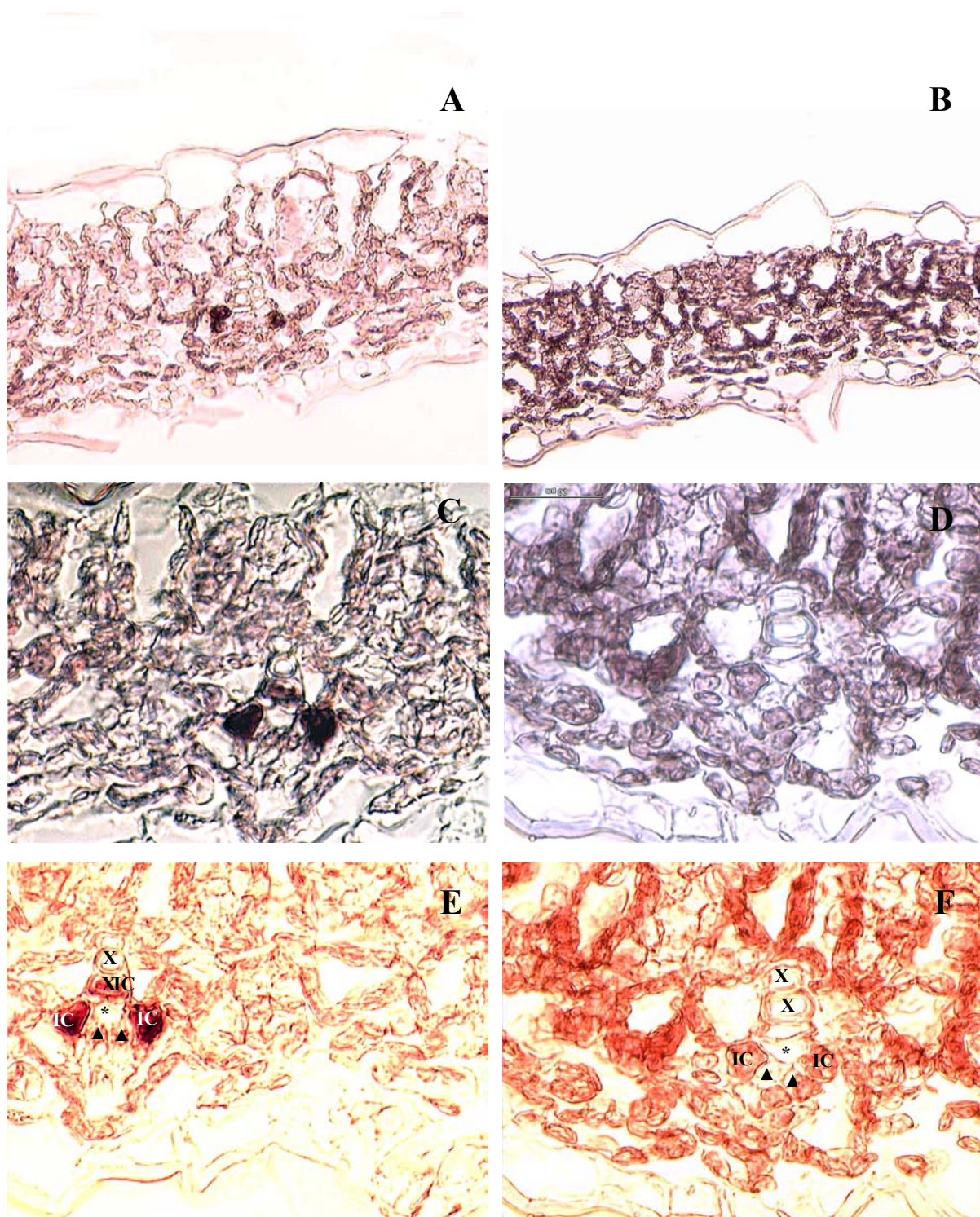


Figure 3.26. *In situ* hybridization of 8 μm thin sections of leaves of *Alonsoa meridionalis* with a digoxigenine-labelled *AmSTS* antisense RNA probe. **A, C, E** – hybridization with the antisense probe; **B, D, F** – hybridization with the sense control. **A, B** – an overview of a transverse section through a leaf (magnification x100), arrowheads point at a minor vein; **C, D, E, F** – a minor vein, magnification x600. **C, D** – staining of intermediary cells with the *AmSTS* antisense probe, no staining in control (arrows); **E, F** – the same minor vein photographed with another filter combination. **IC**, intermediary cell; **X**, xylem vessel; *****, phloem parenchyma cell; **▲** point at sieve elements.

3.3.6. Expression of *AmSTS* promoter-GUS fusion constructs in *Arabidopsis*

Since expression levels of *AmSTS* were low overall, they might well be below the detection limit of *in situ* hybridisation in some cells/organs. In such a case, the expression pattern can be studied by using a promoter-reporter gene fusion in transgenic plants. However, no method for transformation of *Alonsoa* has been established yet. Yet promoter activities are often conserved in other plant species. Therefore a *AmSTS* promoter- β -glucuronidase (GUS) fusion construct was prepared in a binary vector in order to study the regulation of the *AmSTS* promoter in *Arabidopsis*. To find out whether the 5' untranslated region has a function in the regulation of transcription levels or patterns, two constructs were prepared, one containing only the promoter and one also the 5' UTR.

3.3.6.1. Cloning of the *AmSTS* promoter

1.85 Kb of the *AmSTS* 5'-upstream sequence were obtained by the Genome Walking method (2.21.4) and cloned in pGEM®-T Easy. The sequence is shown in Figure 3.27. No known *cis*-elements for the interaction with plant transcription factors could be found in this sequence in either of two databases as it was checked by two database searches (<http://transfac.gbf.de/TRANSFAC>; <http://pdap1.trc.rwcp.or.jp/research/db/TFSEARCH.html>).

3.3.6.2. Promoter-GUS fusion constructs and 5' uORF

The cloning strategy for the promoter-GUS fusion construct in the binary vector pBI101.3 is shown in Figure 3.28. Two constructs were prepared, one that contained only the promoter (PmrB) and another one that contained also the 5' untranslated region of the *AmSTS* cDNA with the two small uORFs (PmrA; 3.3.2; Figure 3.28).

3.3.6.3. The *AmSTS* promoter directed GUS activity in minor veins in transgenic F1 lines of *Arabidopsis* containing either *AmSTS* promoter-GUS fusion construct

Arabidopsis thaliana ecotype Columbia was transformed via infiltration (2.24.3) and seeds of the transformed plants were germinated on MS medium containing 2% sucrose and kanamycin. For each construct, 15 F1 plantlets were transferred to pot soil and grown for seeds. When the F1 plants were in the rosette stage, two rosette leaves of each plant were used for GUS activity staining (2.24.4.1). All leaves analysed showed GUS activity staining in the vascular tissue (Figure 3.29). Interestingly, the PmrA and PmrB constructs differed in GUS expression levels. Although among lines transformed with the same construct, various levels of GUS expression were observed, most PmrA transformants showed an essentially higher level of GUS activity than the PmrB transformants. For each construct, eleven transgenic F1 plants were selected for further analysis, ten of which showed high and one of which showed low levels of GUS activity. The seeds from these plants were harvested, and 100 F2 seeds per


```

-1850 ATCCTCTTGG CCTTGACACC TAGGGCAAAT CCCCCGAGGT ACTGTCGGGC GCTGAAAGCG
-1790 GAGACCTCTA CCAAGGGACT TTGCTGCGTA CACAAAATTC AAACCTCGAGA CCTCTTGGTT
-1730 AAGCGACTAA AGCCTCTTCT GCTTAAGTCA GCTCTTTGGT TATGTAAGGC AATTATATTC
-1670 AATTATTATT TCTTTCAATT TTAGTCCAAT GGACAAAGAT TCATAAGAAT CTTATCACAA
-1610 TTCACACGTA CAAGTACAAC CCAGGAAATA TTTGCCCTAT GATGCTTACA TGCACCATGC
-1550 AAGTGCATGG GCTAAAGCCT TCAAAGCCTA ATTCATAATA TAATTACAAG TTTATAATGT
-1490 TTATCTGTTT AGGCCCTTAA AAACCAAAGG AAATTTTTTAT TTAGGCCCAT GTAAGTCCAC
-1430 CCAGTTATCA TTTTATCGTC TTATAAAAAT AGTAGGGCCC TCGGCTCCAT GCTTAACCGC
-1370 AACACAACC ACGACGACAA CAATAATAAT AATATTTGTT AGCAAATAAT CATATACGCA
-1310 TATAATATA TACTAGCGAT AGTAGAACAC TCGAGCACGT GCTTAAATGC ATAAGTCATA
-1250 ACATAATAGA TTGAATGATT TTTTTTTTGT ATTTGTTTGA AATTTATTTG AAAGAAGTCT
-1190 TCTAATATAT ATTGTATTTT CTTTTTTTCC CTTTGTGTAG TAAATGGGAT TAATTTTGAA
-1130 TAATTAATGT CATCAACAAA CTATGAAATG CATCCTTTTG CAAGCTTACA AGTGTCAATA
-1070 AAGTGATAAC TATCGTATTT AATTCGCCAA ATCAGAGCTG ATTCAACCAC CCTCCCAGCC
-1010 TACTAATCTT AACTTCACAA ATTGTATTTA ATTTTGGGCC TATTAATTCA TAAACATTAG
-950 TTAAATGTAG GTTTGTCAAG GTTAACAGTG ATCAAAGATT ATCAACGTAC ATCAAAAAGTC
-890 GGATCCCCAT GTCGGTCTGA ATGAATCGTT ATTTCCGCGT AATTACATGT TTGTCTAGGT
-830 AAAAGTAGAG GCGCACACGA ACCACCTGAA CTGCACTTGA AAAAGTTTGG TCGAGCTCAA
-770 TTGGAGCCCC GTTCATATAT GCTCGGGAGC TCACGAGCTC CATTTCCTAAT ATAATATTTA
-710 TTACGTATTA TATATATTGC TTGAGCACGA GCTCGAGCCA ATTTGAAACC TAAAGAGTTC
-650 GAGCTCAAAA TTCCTAAAAG TGGCTCTTTG GCTCGAGCCC AACACTTATT ACTCAAGTTC
-590 AAGCTCAGAT TTTTGTGCGA GTTCGGTCCG TGTGCCTCGA TCGCGAGAGG ACAGAAATTA
-530 CAAATTTTGG ATCAAGCAAT AAATTAACAA AGAAGTTTCC ACACTCCCAA TCATTTTCGG
-470 CCATTTGTGT GTTCATCAAC AGTTAGGCTC CTCTGATAAG ACAGTTGAGA TTCATAACAC
-410 ACAAAACAAA TGGAGCTAAA TTTGCTATTC AAAACTTAAC AAGAAACAAA AGAAAATTCA
-350 AACCAAAAA TAAAGAATAA ATTAATATAT TTGCTAAATA AAATGGCATC AGAGACCATG
-290 CATGGATAAA TAAAATCTGT TTTACGATTC AATACGCGGT CGTTTTCGTT TTCCATTGGAC
-230 GCCAACTAGT GGTTTGTTTT CCCCCTCGCA AAAATGGCAT AAAGGAAGAA GAATGGAAGC
-170 ATAAACCGCC CGAACCTTTA TCTATACACC TTTCTTTTTT TTTATTCTTT CTACTTTCTA
-110 AATAATTCAT TTTCCCACTT TCTTTATTTT TTTATTCCTC TGTTTTTATT TTCATTCTCC
+1
-50 CCACACTCTC TCTCTCTATA TATATGTCTG CCTCCCCTTC ACATTTTTTCT ATGTGTCCAA
11 ACTAAGTAAT AACTCAATAG TTCATGCATA AGCTTTTCTA CAAAAAAAT AATAACTGAT
71 TTTAGCCTT CGCCCTGTT TTGCTCTGTT TTTTCAACC ATG

```

Figure 3.27. The sequence of the *AmSTS* promoter region. The sequence corresponding to the 5'-untranslated region of *AmSTS* mRNA is underlined and the ATG start codon of the *AmSTS* ORF is labelled by inverse printing.

plant were germinated on MS medium with 2% sucrose and kanamycin (50 seeds/plate). The germination rate was protocolled. Germinated seedlings represented either homozygous (33%) or heterozygous (67%) transformants. For GUS activity staining, six seedlings from each line were used in the primary leaf stage (3.3.6.5). The other seedlings were transferred to soil. For each line, 12 plants were grown for seed production, and 20 plants were grown under 12 hours light/12 hours dark for further GUS activity staining. From eight lines for each construct, two rosette leaves were taken for a quick isolation of total DNA (2.15.3) for PCR analysis with the *AmSTS* promoter-specific primer *pmr5seq3* and the *M13 forward* primer (Figure 3.28). PCRs were performed with 5 µl of total DNA, an annealing temperature of 54°C, an amplification time of 150 seconds and 35 cycles. In each case, a PCR product of the expected size (2480 bp for PmrA, 2370 bp for PmrB) was obtained (data not shown).

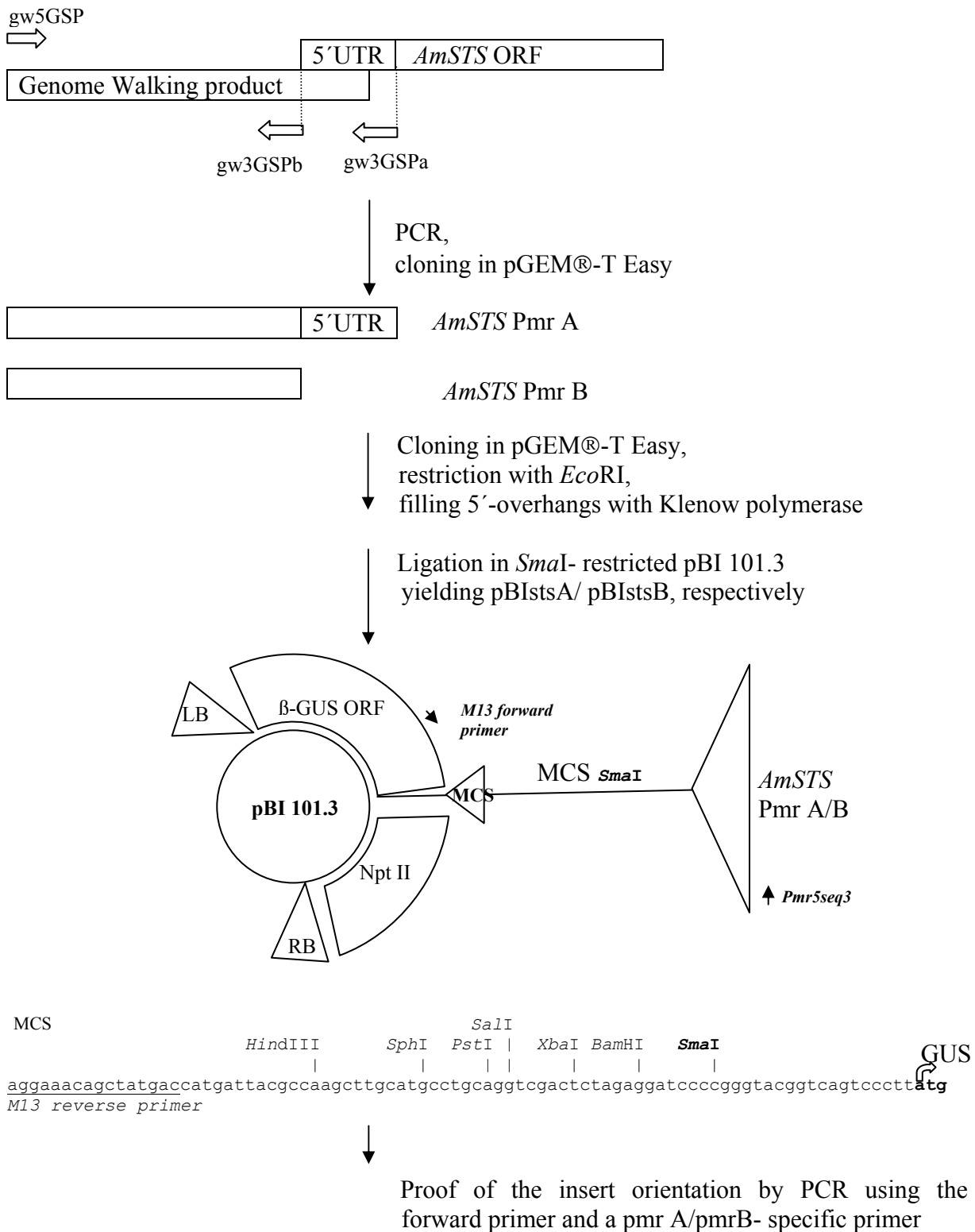


Figure 3.28. Construction of pBIstsA/pBIstsB plasmids carrying either 1.85 Kb of *AmSTS* 5'upstream region plus 109 bp 5'UTR (pBIstsA) or only 1.85 Kb (pBIstsB) upstream of the β-glucuronidase (GUS) ORF. The ligation site (*Sma*I) and the first codon of GUS ORF are labelled by bold print. NptII, neomycin phosphotransferase; RB, LB – right and left borders of pBI101.3 T-DNA region. PCR with the *M13 forward* primer and *pmr5seq3* primer was used to identify the positive clones.

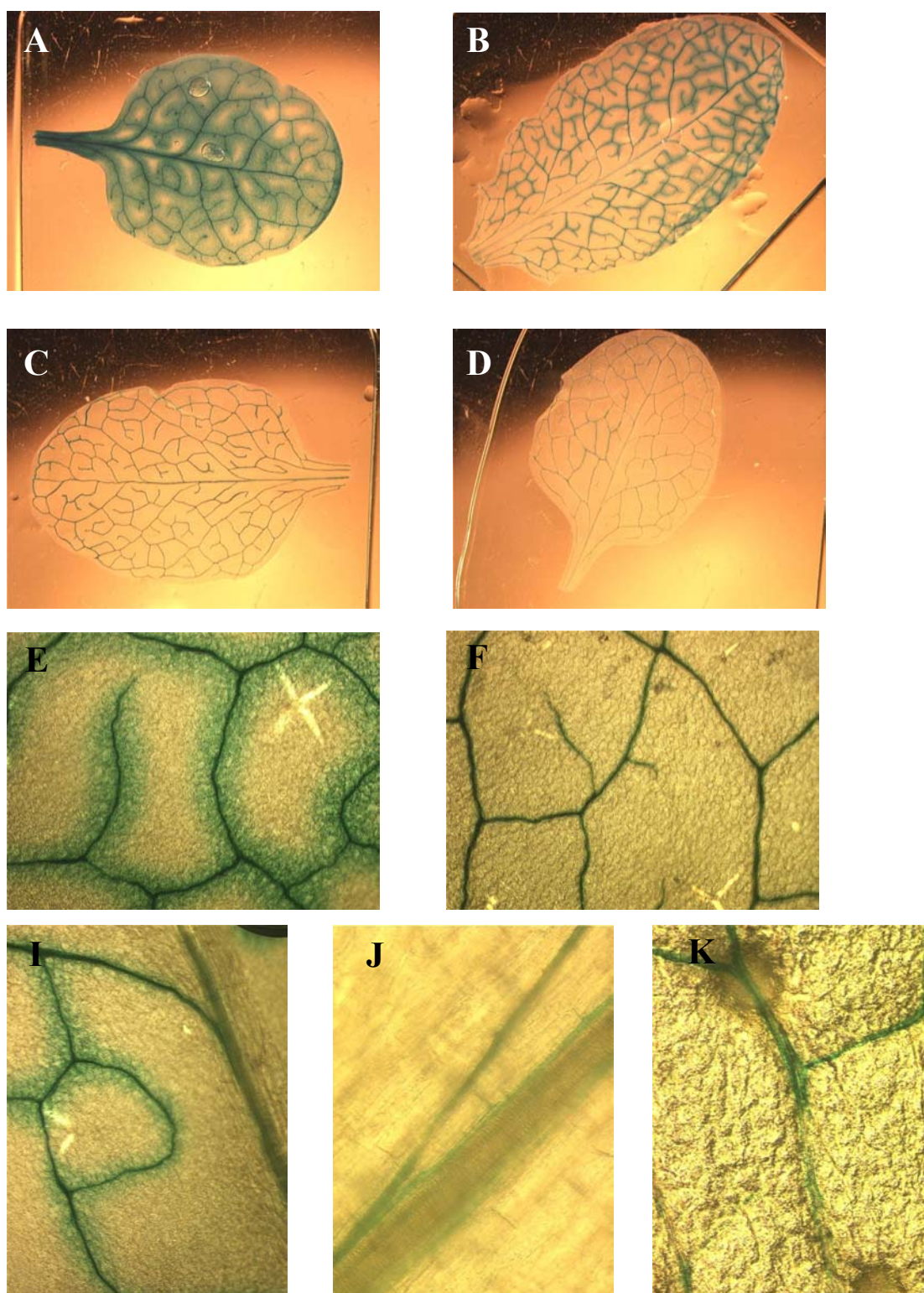


Figure 3.29. Localization of GUS activity in leaves of F1 *A. thaliana* plants transformed with the *AmSTS PmrA-GUS* or the *AmSTS PmrB-GUS* construct, respectively. From 36 lines of F1 transformants analysed, representative lines for both constructs are shown. **A, B, E, I - K** - ferro/ferricyanide not added into the incubation medium; **C, D, F, J, K** - incubation of leaves of the same lines in the presence of 3 mM K-ferro/ferricyanide. **A**, PmrA, line 5; **B**, PmrB, line 13; **C**, PmrA, line 16; **D**, PmrB, line 22; **E**, PmrB, line 13, diffusion of the GUS reaction product from the veins into the mesophyll can be observed; **F**, PmrB line 22, no diffusion of the dye in the presence of K-ferro/ferricyanide; **I**, PmrB, line 13, diffusion of the dye is stronger in lower order veins; **J, K** - in higher order veins, the dye is localized in the phloem part of the vein (**J** - PmrB, line 22; **K** - PmrA, line 9).

3.3.6.4. GUS activity was also found in the vascular tissue of sepals and siliques of F2 plants

When the F2 plants were flowering, flowers, inflorescence shoots and developing siliques were harvested for GUS activity staining. The results are shown in Figure 3.30. GUS activity was found in vascular tissue of sepals and siliques, but not in petals and not in inflorescence shoots. It should be pointed out that this staining was observed in pieces of inflorescences which were cut from the plants before the GUS activity test was performed. Therefore, the staining could not be due to the diffusion of the product of the GUS reaction from the source leaves to the sink tissues. As already mentioned, the source leaves show a very high GUS activity resulting in some diffusion of the dye into the mesophyll even in the presence of 3 mM K-ferri/ferrocyanide in the reaction buffer.

3.3.6.5. The expression of the *AmSTS* promoter-*GUS* fusion was strongly enhanced by sucrose and glucose in *Arabidopsis*

F2 seedlings in the primary leaf stage from all lines for both constructs were taken from MS agar plates containing 2% sucrose and kanamycin and used directly for GUS activity staining. In all cases, staining was confined to the vascular system of primary leaves and cotyledons (Figure 3.31 A-C, E). In some plantlets of lines displaying very high GUS activity, weak staining of roots could also be observed, which was probably due to diffusion of the dye (Figure 3.31 D). In some plantlets, hydrotodes were also stained (Figure 3.31 F). From four lines for each construct (PmrA: lines 3, 4, 6, 8; PmrB: lines 13, 17, 20, 25) 18 seedlings were used to examine the inducibility of the promoter by exogenously added sugars. Plantlets were transferred to liquid MS medium containing either (a) no additives, (b) 180 mM sucrose or (c) 200 mM glucose, and incubated for 20 hrs at a light/dark cycle. They were harvested after 10 hours of light and stained for GUS activity. The results are shown in Figure 3.32 A-F. *AmSTS-GUS* expression was still confined to the vascular system in all cases. For each construct, in three out of four lines, expression levels after incubation in MS medium without sugar essentially lower than after incubation in MS medium with either sucrose or glucose (Figure 3.31, A-F). The GUS activity in seedlings incubated in MS medium without additives was significantly lower than in seedlings taken from agar plates and stained directly, while seedlings incubated in MS medium with 180 mM sucrose or 200 mM glucose showed significantly higher GUS activity than seedlings directly taken from plates (data not shown).

The question arises whether the induction of the *AmSTS* promoter observed in seedlings incubated in MS medium containing 180 mM sucrose or 200 mM glucose as compared to MS medium without additives was related to the specific action of sugars, or was caused by the osmotic action of sugars on the turgor of the leaf cells. This question needs

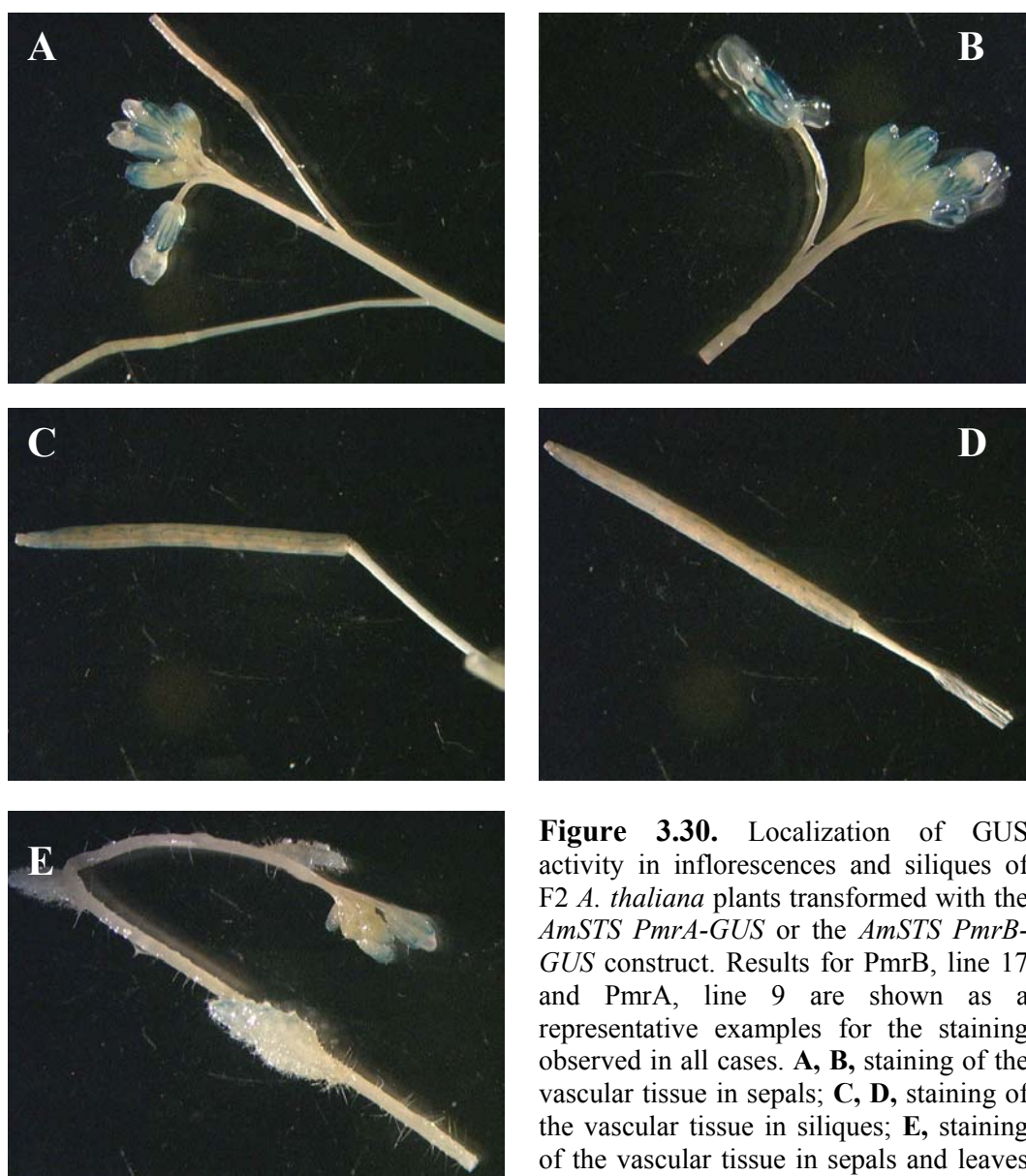


Figure 3.30. Localization of GUS activity in inflorescences and siliques of F2 *A. thaliana* plants transformed with the *AmSTS PmrA-GUS* or the *AmSTS PmrB-GUS* construct. Results for PmrB, line 17 and PmrA, line 9 are shown as a representative examples for the staining observed in all cases. **A, B**, staining of the vascular tissue in sepals; **C, D**, staining of the vascular tissue in siliques; **E**, staining of the vascular tissue in sepals and leaves of inflorescence shoots. Note that no staining can be seen in inflorescence shoots (**A, B, E**).

to be investigated by further experiments as soon as homozygous transformants will be obtained. However, the following experiments suggest that the induction was rather osmotically caused than sugar-specific. In one experiment, six seedlings from two lines were taken from agar plates and incubated in water for one hour, whereas six other seedlings were left in air for the same period to induce drought stress. After incubation, GUS activity staining was performed with all seedlings. The seedlings that were kept in air showed a stronger staining than the seedlings incubated in water (Figure 3.32, G, H). In another experiment, sorbitol showed the same effect on *AmSTS-GUS* expression as glucose and sucrose. This suggests that *AmSTS* expression is enhanced rather by an osmotical mechanism than by specific sensing of sugars.

It should be taken into account that these results were obtained with a mixture of homozygous and heterozygous plants. However, since they were consistent in several independent lines tested, they can be considered to be significant.

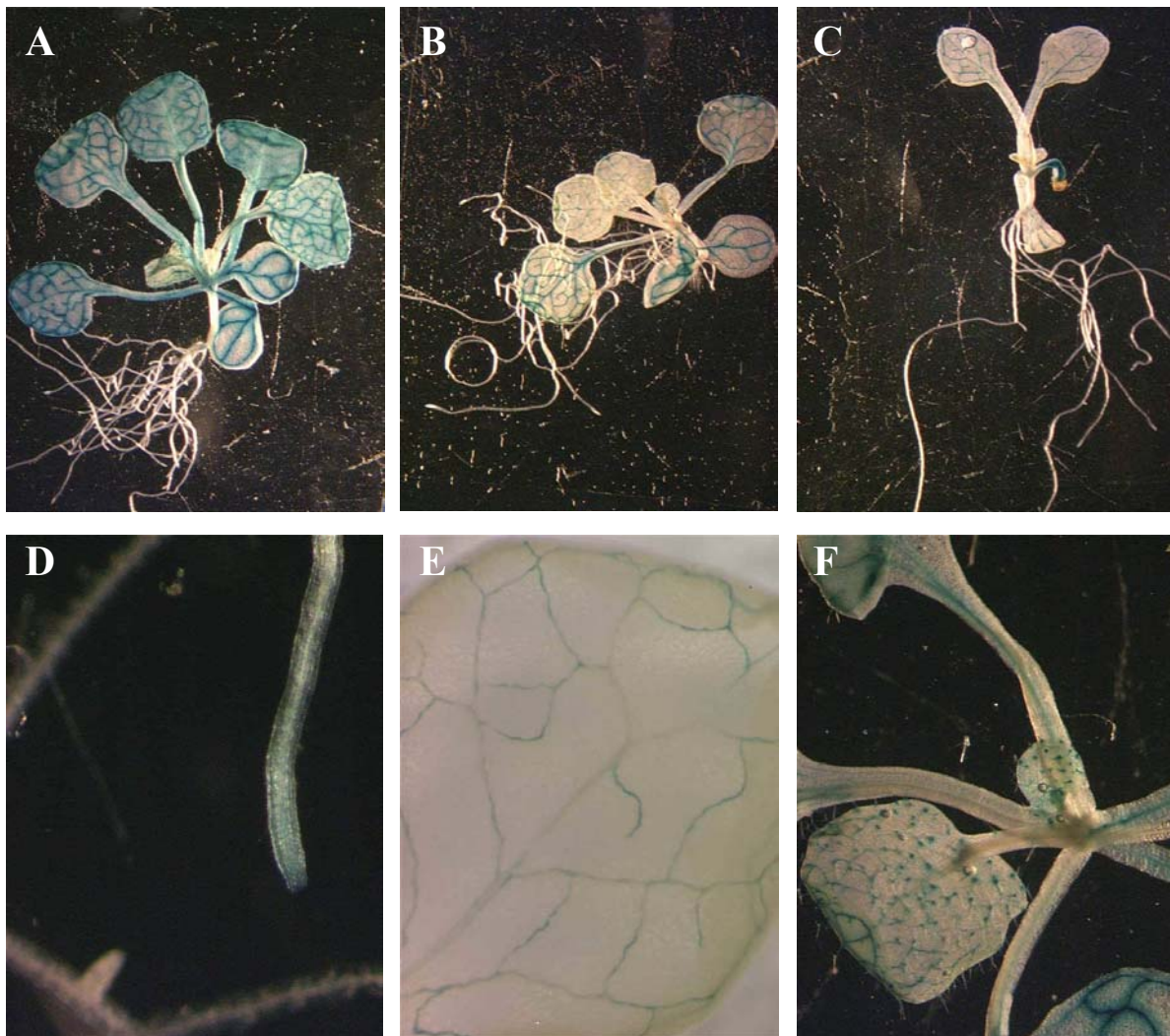


Figure 3.31. Localization of GUS activity in seedlings of *A. thaliana* F2 plants transformed with the *AmSTS PmrA-GUS* or the *AmSTS PmrB-GUS* construct. **A, B**, staining of whole seedlings of PmrA, line 8 (**A**) and PmrB, line 13 (**B**); **C**, staining of the cotyledons in a seedling of PmrB, line 13; **D**, root staining due to the diffusion of the GUS reaction product in PmrB, line 17; **E**, minor veins stained in the leaf of a seedling of PmrB, line 20; **F**, hydatodes stained in PmrB, line 17.

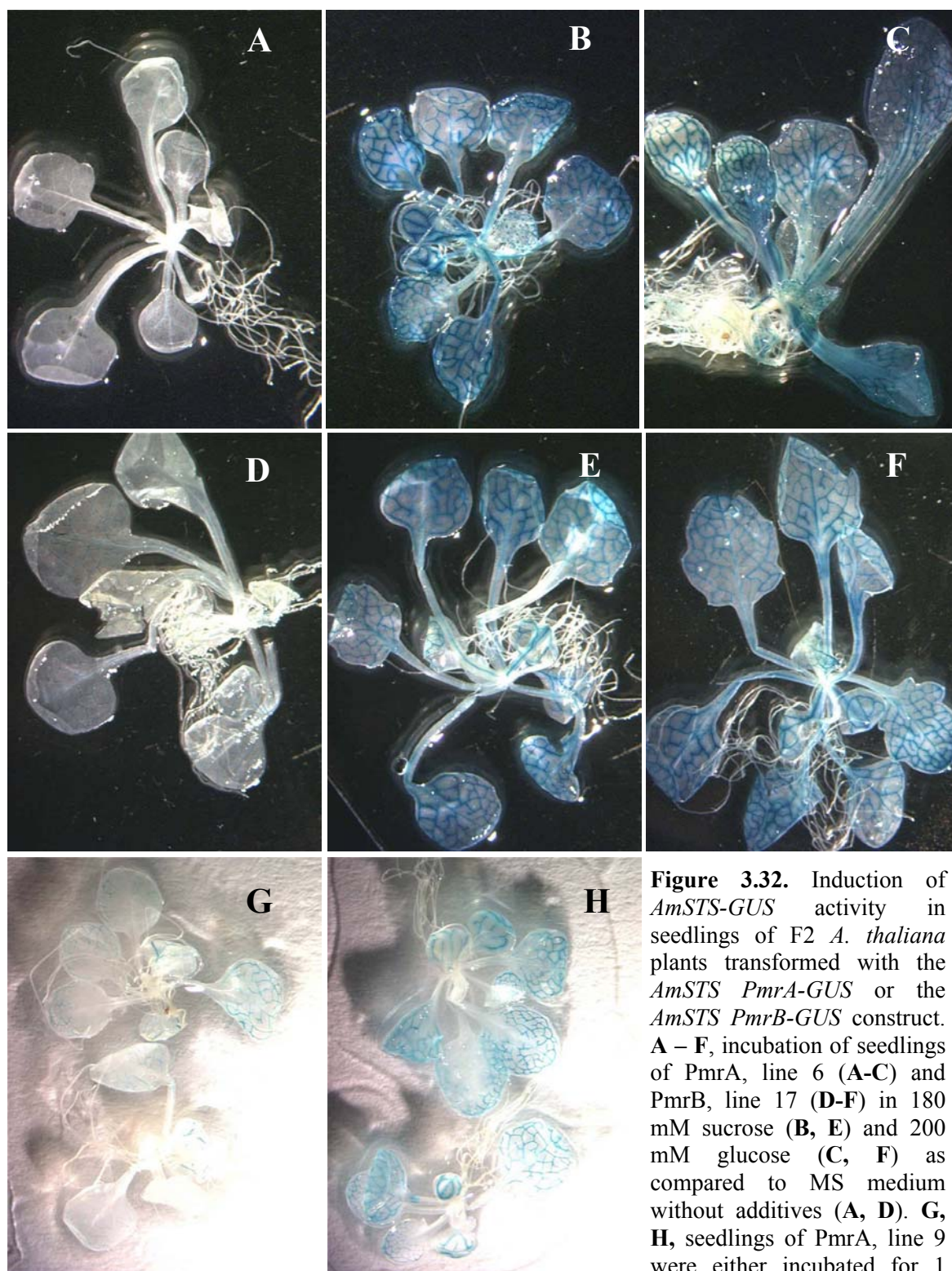


Figure 3.32. Induction of *AmSTS-GUS* activity in seedlings of F2 *A. thaliana* plants transformed with the *AmSTS PmrA-GUS* or the *AmSTS PmrB-GUS* construct. **A – F**, incubation of seedlings of PmrA, line 6 (**A-C**) and PmrB, line 17 (**D-F**) in 180 mM sucrose (**B, E**) and 200 mM glucose (**C, F**) as compared to MS medium without additives (**A, D**). **G, H**, seedlings of PmrA, line 9 were either incubated for 1 hour in water (**G**) or left for 1 hour in air (**H**) before GUS activity staining.

4. DISCUSSION

This study was focused on the following aspects of the phloem loading:

- Are there sugar concentration gradients between the phloem and the cytoplasm of mesophyll cells in a symplastic phloem loader?
- How does the inhibition of phloem translocation affect sugar compartmentation in leaves of *Alonsoa meridionalis* and *Asarina barclaiana* ?
- Is the leaf apoplast similarly involved in sugar compartmentation in both symplastic and apoplastic loaders?
- In which cells of a leaf is stachyose synthase expressed in the symplastic phloem loader *Alonsoa meridionalis*? How is this expression regulated?

4.1. Subcellular compartmentation of carbohydrates and estimation of phloem:mesophyll concentration ratios: implications for the phloem loading mode of different carbohydrates in *Asarina* and *Alonsoa*

4.1.1. Subcellular distributions of carbohydrates in the symplastic phloem loader Alonsoa meridionalis do not differ from those in apoplastic phloem loaders

A comparison of the distribution of carbohydrates among subcellular compartments of leaf cells in *Alonsoa* and *Asarina*, including data for other plant species, is shown in Table 4.1. For all species listed, the data have been obtained by non-aqueous fractionation of leaves. The data show that the distribution of metabolites between subcellular compartments is similar in different plant species. Hexoses are confined exclusively to vacuoles. Sucrose and mannitol were found in all three subcellular compartments, but in most species the highest amounts of these carbohydrates were found in the cytoplasm. *Myo*-Inositol was the only substance of which the largest pool was observed in chloroplasts. The subcellular distribution

of galactinol had previously been determined only in one species, *Antirrhinum majus* (Moore et al., 1997). Now, the data for *Alonsoa meridionalis* are available which show that galactinol is confined to the vacuole in both species. The subcellular distribution of the iridoid glucoside antirrhinoside synthesized in *Asarina barclaiana* was studied for the first time. Antirrhinoside was mostly confined to the vacuoles.

Table 4.1. Percentage distribution of carbohydrates among the stromal (Ch), cytoplasmic (Cyt) and vacuolar (Vac) compartments of leaf cells in different plant species.

	<i>Hexoses</i>			<i>Sucrose</i>			<i>Mannitol</i>			<i>myo-Inositol</i>			<i>Galactinol</i>			<i>Antirrhinoside</i>		
	Ch	Cyt	Vac	Ch	Cyt	Vac	Ch	Cyt	Vac	Ch	Cyt	Vac	Ch	Cyt	Vac	Ch	Cyt	Vac
¹ <i>Asarina barclaiana</i>	1	1	98	14	35	51	36	34	30	53	24	23				4	6	90
¹ <i>Alonsoa meridionalis</i>	1	1	98	21	44	35				81	13	6	2	2	96			
² <i>Antirrhinum majus</i>	0	0	100	1	84	15	36	41	24	55	27	18	4	0	96			
³ <i>Nicotiana tabacum</i>	1	1	98	9	52	38												
² <i>Petroselinum hortense</i>	3	0	97	5	57	38	19	43	38	43	23	34						
⁴ <i>Solanum tuberosum</i>	1	1	98	27	40	33												

¹ This thesis; ² data from Moore et al. (1997); ³ data from Heineke et al. (1994); ⁴ data from Leidreiter et al. (1995)

The fact that in all the species studied so far, the patterns of subcellular distribution for each carbohydrate were similar may imply that these substances preferentially accumulate in the compartments where they are synthesized. However, Table 4.2 shows that the subcellular distributions of sugars and of the key enzymes of their biosynthesis do not coincide in most cases. One group of carbohydrates including hexoses, galactinol and antirrhinoside was located mostly in vacuoles. For hexoses, this probably means that they derive mostly from the hydrolysis of sucrose by vacuolar invertase. No exact information is available on the compartmentation of the synthesis of antirrhinoside and other iridoid glucosides within plant cells. For most secondary metabolites, the pathway of their synthesis is distributed among multiple subcellular compartments (e.g. Burbulis and Winkel-Shirley, 1999). Most findings for galactinol synthase indicate that it may be located in the cytosol because of its pH optimum (about 7.0; Bachmann et al., 1994) although in some cases a galactinol synthase

with a pH optimum of about 5 has been found which might imply that one of the isoforms is associated with vacuoles (Keller and Pharr, 1996). However, in mesophyll cells, galactinol was nearly exclusively confined to vacuoles.

Another group of carbohydrates, which includes sucrose, *myo*-inositol and mannitol, showed more or less equal distribution between all the three subcellular compartments, although they are synthesized in the cytosol (sucrose, mannitol) or in cytosol and plastids (*myo*-inositol). This might be related to the function of these compounds as compatible solutes (Wyn Jones and Gorham, 1983; Stoop et al., 1996; Nelson et al., 1999) which may require that the distribution of these compounds between cellular compartments is not restricted. These sugars were indeed shown to account for 22-26% of the cytosolic osmolality in *Asarina* and *Alonsoa* (3.1.5). Their relatively large chloroplastic pools might also include a fraction bound to the chloroplastic outer envelope which would be co-isolated with chloroplasts. Relatively large pools of carbohydrates including sucrose were found in the fraction of wheat chloroplasts during their isolation by non-aqueous fractionation (Heber, 1957). This chloroplastic fraction was small in greenhouse-grown plants but increased when chloroplasts were isolated from cold-grown plants. The accumulation of carbohydrates including sucrose in the chloroplastic fraction of such plants was interpreted as a part of the cold acclimation process to protect chloroplastic membranes.

Table 4.2. Comparison of the subcellular localization of carbohydrates as determined by non-aqueous fractionation with the localization of the key enzymes of their biosynthesis in plant cells.

Carbohydrates and their preferential localization	Localization of their key biosynthetic enzymes	Reference
Hexoses (<i>vacuole</i>)	Cytosol (phosphatases, neutral invertase); vacuole and apoplast (acidic invertase); chloroplasts (starch hydrolysis)	Heldt (1996)
Sucrose (<i>chloroplasts, cytosol, vacuole</i>)	Cytosol (sucrose phosphate synthase and sucrose phosphate phosphatase)	Bird et al. (1974)
<i>myo</i>-Inositol (<i>chloroplasts, cytosol, vacuole</i>)	Plastids and cytosol	Adhikari et al. (1987)
Galactinol (<i>vacuole</i>)	Cytosol and vacuoles	Pharr et al. (1981)
Mannitol (<i>chloroplasts, cytosol, vacuole</i>)	Cytosol and nuclei	Everard et al. (1993) Yamamoto et al. (1997)
Antirrhinoside (<i>vacuole</i>)	? Mevalonate kinase, the key enzyme for isoprenyl synthesis, is localized in cytosol and plastids	Newman and Chappell (1999) for mevalonate kinase

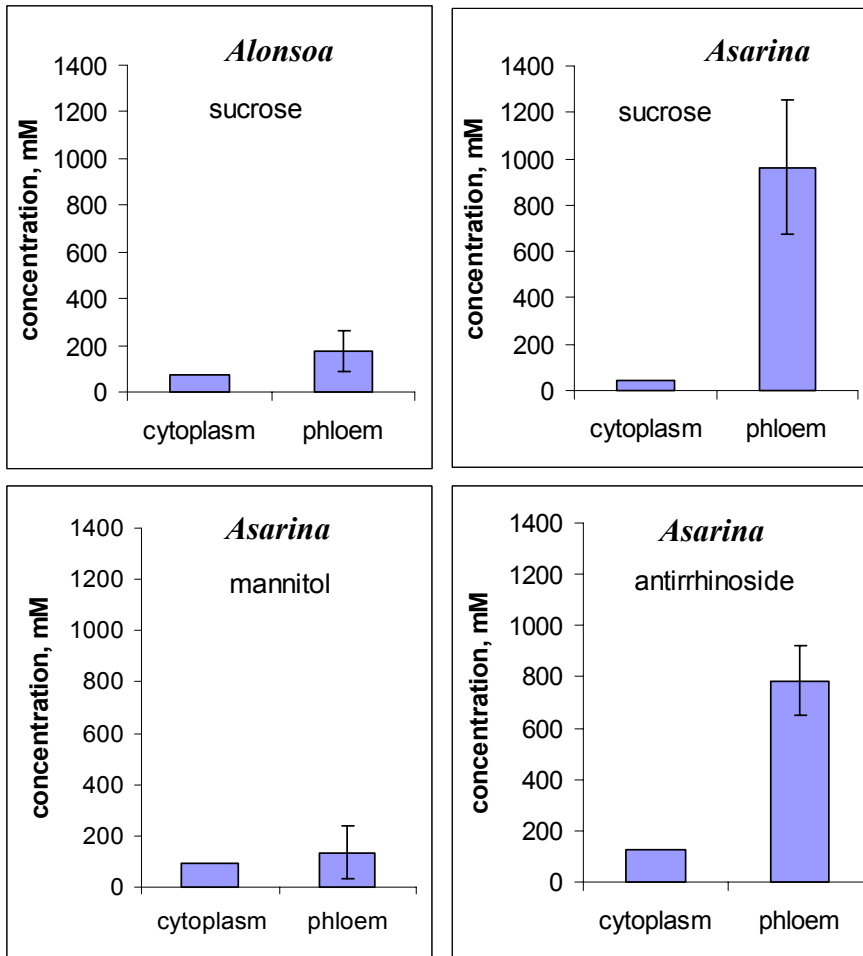


Figure 4.1. Concentrations of the translocated carbohydrates in the cytoplasm of the mesophyll cells and in the phloem sap of *Alonsoa meridionalis* and *Asarina barclaiana*. Data are derived from results of non-aqueous fractionations (cytoplasmic concentrations; 3.1) and of phloem sap analysis by the laser aphid stylet technique (n=9; Table 1.3).

From the species listed in Table 4.1, only *Alonsoa meridionalis* is a symplastic phloem loader. Other plants have been classified as apoplastic phloem loaders according to their minor vein anatomy (transfer cells in minor veins of *Antirrhinum*, ordinary cells in minor veins of *Nicotiana*, *Solanum* and *Petroselinum*; data from Gamalei (1990) for *Antirrhinum*, *Nicotiana* and *Solanum*, and from Flora and Madore (1996) for *Petroselinum*). One might expect that in the symplastic phloem loader *Alonsoa*, some concentrating mechanisms for sucrose and galactinol exist which would favour the symplastic loading of carbohydrates into the phloem as predicted by the polymerization trap model. However, no differences in the distribution patterns of translocated carbohydrates among subcellular compartments of mesophyll cells were found in *Alonsoa* as compared with the apoplastic phloem loaders *Asarina*, *Antirrhinum*, *Nicotiana*, *Petroselinum* and *Solanum*.

4.1.2. Concentration ratios between the cytoplasm of mesophyll cells and the phloem sap indicate the presence of an active loading step for sucrose and antirrhinoside, the major transported carbohydrates in *Asarina*

In *Asarina*, the ratio of sucrose concentrations between phloem and cytoplasm was as high as 22. This is in the range of the ratios previously estimated for the apoplastic phloem loaders spinach (16; Lohaus et al., 1995), barley (5; Lohaus et al., 1995) and maize (5; Lohaus

et al., 1998). These data indicate unequivocally that there must be an active step for the loading of sucrose into the phloem against a concentration gradient in *Asarina*.

The concentration of antirrhinoside in the phloem sap of *Asarina* was as high as that of sucrose, and six times higher than its concentration in the cytoplasm of mesophyll cells. This means that the loading of antirrhinoside into the phloem also requires an energization. The increase of dark respiration, the depolarization of the membrane potential and the alkalization of the apoplast observed when antirrhinoside was introduced into the leaf apoplast, indicate an energizing role of the proton motive force for the uptake of antirrhinoside (3.2.2). Whether this apoplastic transport is the only mechanism for the loading of antirrhinoside into the phloem remains to be established.

In general, the method of non-aqueous fractionation tends to overestimate subcellular concentrations for metabolites which are not exclusively located in the mesophyll (Gerhardt and Heldt, 1984; Riens et al., 1991). However, even the rough estimates made in this thesis show that in *Asarina*, the transfer of sucrose and antirrhinoside into the phloem requires an active energizing step, for it occurs against at least 22 and 6 times higher concentrations, respectively (Figure 4.1). This is in accordance with the presence of transfer cells and ordinary cells in the minor veins of *Asarina* (Figure 1.6 B, D). Transfer cells and ordinary cells were shown to be specialized for the apoplastic loading of sucrose against a concentration gradient using the proton motive force as the energizing power. H⁺/sucrose symporter *PmSUT2* was immunolocalized on the plasma membrane of ordinary cells in *Plantago major* (Stadler et al., 1995) and H⁺-ATPase was immunolocalized on the cell wall ingrowths of transfer cells in *Vicia faba* (Bentwood and Cronshaw, 1978). H⁺/sucrose symporters were also found in *Asarina* and their function in sucrose uptake was confirmed by functional expression and complementation in yeast (Knop, 2001). Thus, in *Asarina*, sucrose and antirrhinoside are probably actively loaded into the phloem via the apoplast.

4.1.3. Concentration ratios between the cytoplasm of mesophyll cells and the phloem sap indicate that the minor transported sugars, mannitol in Asarina and sucrose in Alonsoa, may be symplastically loaded into the phloem

The concentrations of mannitol in the phloem sap (136 ± 101 mM; Knop, 1998) and in the cytoplasm of mesophyll cells in *Asarina* (92 mM, this thesis) did not differ significantly when the standard deviation value for the phloem sap is taken into account (Figure 4.1). This would imply that there may be no concentration barrier for the diffusion of mannitol from mesophyll cells into the phloem via the symplastic pathway. However, it should be kept in mind that the method of non-aqueous fractionation tends to overestimate subcellular concentrations since it does not account for the non-mesophyll parts of the leaves. That means

that the actual metabolic situation in the cells might still necessitate an active loading of mannitol into the phloem in *Asarina*.

The study of the minor vein anatomy of this plant has shown that ordinary companion cells in minor veins possess single plasmodesmal connections with the bundle sheath cells (Figure 1.6 B and D). Thus, a symplastic transfer of carbohydrates, namely of mannitol which accounts for 3% of total translocated carbon from the mesophyll into the phloem (Table 1.3) could occur in *Asarina*. This, however, does not preclude the possibility that additionally, apoplastic loading of mannitol may take place in this plant. The kinetics of the uptake of ^{14}C -mannitol introduced into the apoplast of the Apiaceae *Petroselinum crispum*, a plant with ordinary companion cells in minor veins (Flora and Madore, 1996), has revealed two components, a linear one and a saturable one. The latter indicates a participation of transporters in the process. H^+ /mannitol transporters were found in celery (Noiraud et al., 2001), an Apiaceae that contains ordinary cells with single plasmodesmal connections with the bundle sheath (Gamalei, 1990).

Alonsoa is the only symplastic phloem loader which has been studied by the non-aqueous fractionation technique with respect to the ratio of sucrose concentrations in the phloem sap and in the cytosol of mesophyll cells. In *Alonsoa*, this ratio was only two. This value is much lower than those determined for apoplastic phloem loaders but is rather similar to values estimated for peach (1.7; Moing et al., 1997) and *Cucumis melo* (0.7; Haritatos et al., 1996). The lower concentration gradient is due to the lower sucrose concentration in the phloem sap of *Alonsoa* as compared to apoplastic phloem loaders. For instance, the sucrose concentration in the phloem of *Asarina* (963 ± 280 mM) is five times higher than that in *Alonsoa* (174 ± 85 mM), whereas the cytoplasmic concentrations of sucrose in both plants differ only by a factor of about two (43 mM in *Asarina* and 71 mM in *Alonsoa*). For *Alonsoa*, an active uptake of sucrose against a concentration gradient should be also assumed, although the twofold concentration gradient found in this plant is obviously easier to overcome or even reverse, depending on the metabolic situation, than the much steeper gradients found in apoplastic phloem loaders. Most importantly, a H^+ /sucrose transporter *AmSUT1* was shown to be present in plasma membrane of the phloem cells and companion cells of *Alonsoa* which should participate in the apoplastic loading of sucrose (Knop, 2001).

The real concentration barriers for the movement of sugars from the mesophyll into the phloem via plasmodesmata could essentially differ from the estimated ones for several reasons. First, it is only mesophyll bundle sheath cells which are in close symplastic contact with intermediary cells. It is not impossible that sugar concentrations in these cells differ from

those in other mesophyll cells, as could be shown for the monocotyledonous plant barley using a single cell sampling technique (Koroleva et al., 1998). In barley, bundle sheath cells differ drastically in sucrose and fructane concentrations from other mesophyll cells. Unfortunately, it was not possible in this thesis to distinguish between mesophyll bundle sheath cells of *Asarina* and *Alonsoa* when using the single cell method (data not shown).

Second, the actual concentration barriers would depend on the sugar concentrations in that subcellular compartment which provides the route for the symplastic transfer through the plasmodesmata. There are two possible compartments within a plasmodesma, the cytosolic sleeve and the lumen of the ER desmotubule (1.3). The non-aqueous fractionation technique does not resolve between these compartments. For instance, non-aqueous fractionation of leaves expressing a single chain antibody which was anchored to the ER by the KDEL sequence showed that it was entirely confined to the cytoplasm (Strauß et al., 2001). The additional sub-compartmentation of sugars within the cytoplasm could render their higher concentrations on the “mesophyll side” of plasmodesmata irrelevant for the transport process.

4.2. Inhibition of the export of sugars from the leaves results in the re-compartmentation of translocated carbohydrates in leaves of *Asarina* and *Alonsoa*

Sugar export from the leaves was blocked but photosynthesis continued when detached leaves of *Asarina* and *Alonsoa* were placed under continuous light for 24 to 96 hours. The effects of this treatment on sugar compartmentation in the leaves were studied, in that sugar levels in the two largest tissues of a leaf, epidermis and mesophyll, were determined. Taking into account the very high phloem concentrations of carbohydrates as compared to other plant tissues, it is unlikely that the phloem tissue itself has a sufficient capacity for further accumulation of carbohydrates when their export is inhibited. Therefore, other tissues like mesophyll and epidermis should allow transient accumulation of carbohydrates. The aim of these experiments was to find out whether both tissues are involved in the transient accumulation of carbohydrates in leaves of *Alonsoa* and *Asarina*. Also, as these plants translocate five different carbohydrates in the phloem, it was of interest to see whether the inhibition of translocation would affect the accumulation of these carbohydrates differentially.

The results of single cell sampling showed that in both *Asarina* and *Alonsoa*, the epidermis significantly contributes to the accumulation of hexoses and sucrose (3.1.4). This corresponds to results obtained with leaves of transgenic potato (Kehr et al., 1999) but

contradicts results obtained with barley (Koroleva et al., 1998). In transgenic potato, the leaf epidermis took part in the accumulation of excess sugars resulting from the antisense repression of the expression of sucrose transporter in the phloem. In barley, no accumulation of sugars was observed in the leaf epidermis when the export of sugars from the leaves was inhibited by sink cooling. However, in contrast to the situation in both potato and barley, the concentrations of sucrose and hexoses were similar in mesophyll and epidermis of *Asarina* and *Alonsoa* also in the absence of phloem translocation blockage (3.1.4). This can indicate that epidermis and mesophyll in both *Asarina* and *Alonsoa* are symplastically connected.

Unfortunately, it was not possible to determine whether other carbohydrates also accumulated in the epidermis of these plants. Not distinguishing between epidermis and mesophyll, it could be shown that the inhibition of the phloem translocation resulted in the accumulation of sucrose, antirrhinoside and, to a lesser extent, mannitol in the leaves of *Asarina* (3.1.5). This indicates that when photosynthesis is not inhibited, the synthesis of these compounds proceeds also in the absence of their export from the leaves. The same situation was observed for sucrose in leaves of *Alonsoa*. However, the levels of raffinose and stachyose behaved differently. Although the precursor of their synthesis, galactinol, accumulated in the leaves of *Alonsoa*, no increase in the amounts of raffinose and stachyose was observed. Simultaneously, the *myo*-inositol level decreased (3.1.6). The concentration of *myo*-inositol in the leaf represents a balance between its consumption during the synthesis of galactinol and its production during the synthesis of raffinose and stachyose. Thus, the synthesis of RFOs in the leaves of *Alonsoa* seems to be inhibited by the blockage of phloem translocation. Since the levels of raffinose and stachyose did not increase, it can be concluded that no re-compartmentation of these sugars occurred within *Alonsoa* leaves during the inhibition of phloem translocation. The sequence of events in this phenomenon may be as follows. Either, the ceased phloem transport may have caused a rapid inhibition of the RFO synthesis by some unknown mechanism, thus preventing the further accumulation of these sugars and, therefore, making their exit from the phloem and redistribution in the leaves unnecessary. Alternatively, the overaccumulation of these sugars in the phloem may itself be a result of the inability of raffinose and stachyose to escape from the phloem and thus lead to the end product inhibition of RFO synthesis when a critical concentration is achieved. Which process is most probably taking place will be discussed below (4.3.4) after the results of the study on membrane transport of raffinose and stachyose will have been considered.

4.3. Apoplastic compartmentation of translocated sugars in symplastic and apoplastic phloem loaders

4.3.1. *Inhibition of phloem translocation leads to the accumulation of sucrose in the apoplast of leaves in apoplastic, but not in symplastic phloem loaders*

The studies on apoplastic sugar concentrations in this thesis were performed on two groups of species taken from different plant families. A common feature for each group was the type of companion cells present in minor veins (intermediary cells *versus* transfer cells/ordinary cells). This was necessary to minimize the possibility that the observed characteristics were species- or family-specific, and to base the comparison on the type of companion cells (Voitsekhovskaja et al., 2000). The two following questions had to be studied. (1) Which sugars can be found in the leaf apoplast of plants translocating different types of carbohydrates in the phloem? (2) Are the sugar levels in the apoplast of these plants correlated with their presumable phloem loading mode?

The method employed was the inhibition of the phloem translocation with the aim to cause a re-compartmentation of the sugars (originally destined for export) within the leaves and to compare the participation of the apoplast in this re-compartmentation in both plant groups. The export of assimilates from the leaves was blocked in groups of apoplastic and symplastic phloem loaders either by removal of a phloem ring or by application of an ice jacket to the leaf petiole ("cold girdling"; Webb and Gorham, 1965). While the former procedure blocks phloem translocation entirely, the latter treatment has been shown to result only in its retardation (Webb and Gorham, 1965; Geiger and Sovonick, 1970; Faucher et al., 1982; Krapp and Stitt, 1995). The mechanism of this phenomenon is not completely understood but presumably is related to the inhibiting effect of low temperature on cytoskeleton motility (Geiger and Sovonick, 1970; Boevink et al., 1999).

The only sugars which could be detected in the apoplast of all plants studied were sucrose, glucose and fructose (3.2.1). The comparison of apoplastic sugar levels in leaves with normal and inhibited translocation has revealed one difference between apoplastic and symplastic phloem loaders. Sucrose accumulated in the leaf apoplast in apoplastic but not in symplastic loaders when phloem translocation was inhibited (3.2.1). This would be in accordance with the consideration of the apoplast as the main route for sugar loading in apoplastic but not in symplastic loaders. Indeed, neither sucrose nor raffinose and stachyose accumulated in the apoplast of symplastic loaders translocating these sugars in the phloem. However, the question arises which mechanism prevents the exit of sugars into the apoplast of these species. To understand this, the origin of sucrose accumulated in the apoplast of

apoplastic loaders has to be considered. This sucrose might represent a pool which has been released from the mesophyll cells into the apoplast but has not yet entered the phloem due to a retardation of phloem loading. On the other hand, sucrose may leak back out of the phloem by an inversion of the sucrose transporter reaction due to the overaccumulation of sucrose in these cells as a consequence of retarded phloem translocation.

The assumption that most sugars found in the apoplast come from the mesophyll would explain the failure to find raffinose and stachyose in the apoplast in significant concentrations (this thesis; Madore and Webb, 1981; Schmitz et al., 1987). In a number of symplastic phloem loaders, raffinose and stachyose do not occur in the mesophyll, but are synthesized in the intermediary cells (Holthaus and Schmitz, 1991b; Büchi et al., 1998; Haritatos et al., 1996; this thesis). However, a cytoplasmic sucrose pool comparable to that in apoplastic phloem loaders was found in the symplastic phloem loader *Alonsoa* (3.1.2), putting forward the question why this sucrose could not be released into the apoplast. Thus, the assumption that the apoplastic sucrose which accumulated during the inhibition of phloem translocation originated from the mesophyll, is unlikely.

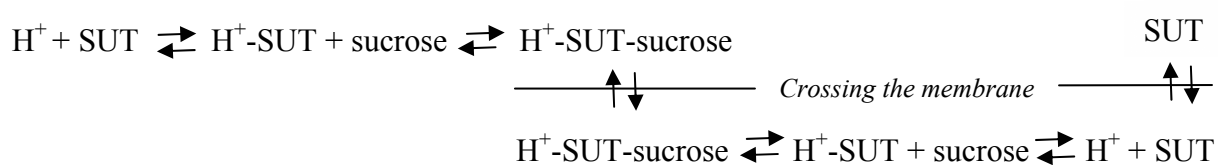
The assumption that the sucrose accumulating in the apoplast of apoplastic phloem loaders during transport blockage is mostly of phloem origin, would explain why no increase in apoplastic sucrose was observed in symplastic phloem loaders in similar experiments. In apoplastic phloem loaders, sucrose concentrations in the phloem sap are several times higher than in symplastic phloem loaders (Table 1.3 for *Alonsoa*; Moing et al., 1997; Ohshima et al., 1999; Knop et al., 2001; Lohaus and Fischer, 2001). Therefore, when phloem translocation is inhibited, sucrose concentration in the phloem of apoplastic loaders can easily exceed a critical level leading to the reversion of the sucrose transporters reaction (see 4.3.2). In this case, the question arises again why no raffinose and stachyose leak out of the phloem into the apoplast in similar experiments performed on symplastic phloem loaders such as *Alonsoa*, for the phloem concentrations of these sugars are as high as that of sucrose in apoplastic loaders (Table 1.3). One possible explanation for this could be the different equipment of the plasma membrane of leaf cells with specific sugar transporters in symplastic and apoplastic phloem loaders or the different mode of the operation of these transporters. This point will be discussed in 4.3.2.

4.3.2. The exchange of sucrose, raffinose and stachyose through plasma membrane in both symplastic and apoplastic phloem loaders is not limited by the lack of specific transporters

A simple approach to estimate the abundance of H⁺/sugar transporters in the plasma membrane of leaf cells *in vivo* is based on the energization of the sugar uptake by the H⁺-

cotransport (Hedrich et al., 2001; Heber et al., 2002, in press; Voitsekhovskaja et al., 2002, in press). H^+ /sugar-cotransport is tightly coupled with ATP hydrolysis in the cytosol of the cells via the H^+ -pumping plasma membrane ATPase the activity of which restores the pH gradient across the plasma membrane (Sze et al., 1999). That means that the active proton-dependent uptake of sugars from the apoplast into cells can be detected by monitoring apoplastic pH and dark respiration which is the source of ATP in the absence of photosynthesis.

It should be considered that the transmembrane transfer of sugars catalyzed by H^+ /sugar symporters represents an enzymatic reaction which is reversible. An example is shown below for the reaction of a H^+ /sucrose symporter, SUT:



The mechanism of H^+ /sucrose symport consists of several reversible steps (Boorer et al., 1996). The direction of each reaction depends on the concentration of substrates on both sides of the membrane. The active proton-dependent uptake of sucrose can be detected when monitoring the pH in the apoplast. Simultaneously, an increase in the dark respiration will indicate the restoration of the proton motive force by H^+ -ATPase activity.

In this way, not only the transporters performing the uptake of sugars from the apoplast should be detected but also the activities of transporters which normally enable the export of sugars from the cells into the apoplast. This is because of the reversibility of the reaction of the transporters. The introduction of the exogenous sugars in unusually high concentrations into the leaf apoplast will reverse the reaction and the active proton-dependent uptake can be detected when monitoring apoplastic pH and respiration.

Sucrose, raffinose, stachyose and glucose were introduced for a short time into the apoplast of leaves from symplastic and apoplastic loaders in concentrations of 50 – 100 mM, i.e. 1 – 3 orders higher than the apoplastic concentrations of sucrose and hexoses (0.1 – 5 mM; 3.2.1). In all cases, the proton motive force-dependent uptake was indicated by a transient increase in respiration, a transient alkalinization of the apoplast and oscillations of the membrane potential. This is the first time that proton-dependent transport could be shown unequivocally for raffinose and stachyose. Changes in membrane potential caused by exogenously applied raffinose (van Bel et al., 1995), as well as PCMBs sensitivity of raffinose and stachyose uptake from the apoplast (Madore, 1990; Turgeon and Gowan, 1990;

Flora and Madore, 1993), had previously suggested the proton motive force-dependent uptake of these sugars. Recently, the plasma membrane depolarization was shown for a variety of sugars (including raffinose and stachyose) exogenously applied to lactifier protoplasts of *Hevea brasiliensis* (Bouteau et al., 1999). However, no simultaneous measurements of both components of proton motive force, pH and membrane potential have been performed before.

The introduction of sugars in high concentrations into the leaf apoplast changes the osmotic environment of leaf cells and might induce a “bulk” uptake of any transportable substances present in the apoplast into the cells, to balance the osmotic pressure. However, Figure 4.2 shows that the responses of respiration and proton motive force observed during sugar feeding into the apoplast in the discussed experiments cannot be related to such changes. Mannitol and sucrose introduced into the apoplast of a potato leaf caused strikingly different responses of respiration and apoplastic pH, although both solutes were fed in the same concentration, 200 mM.

The experimental approach used in this thesis provides a sensitive and convenient tool to assess the equipment of the plasma membrane of leaf cells with sugar-specific transporters. Although this method actually does not determine whether the uptake is mediated by different systems or by one system with different affinity to single sugars, it does detect the uptake events occurring *in vivo*. This method has been used for the study of malate and KCl uptake from the apoplast (Hedrich et al., 2001). Later, it was used for the assessment of the uptake of different classes of compounds from the apoplast including inorganic salts, organic ions, heavy metal cations and even nucleotides (Heber et al., 2002, in press). In most cases, uptake could be shown and was driven by the proton motive force. This has been interpreted to imply

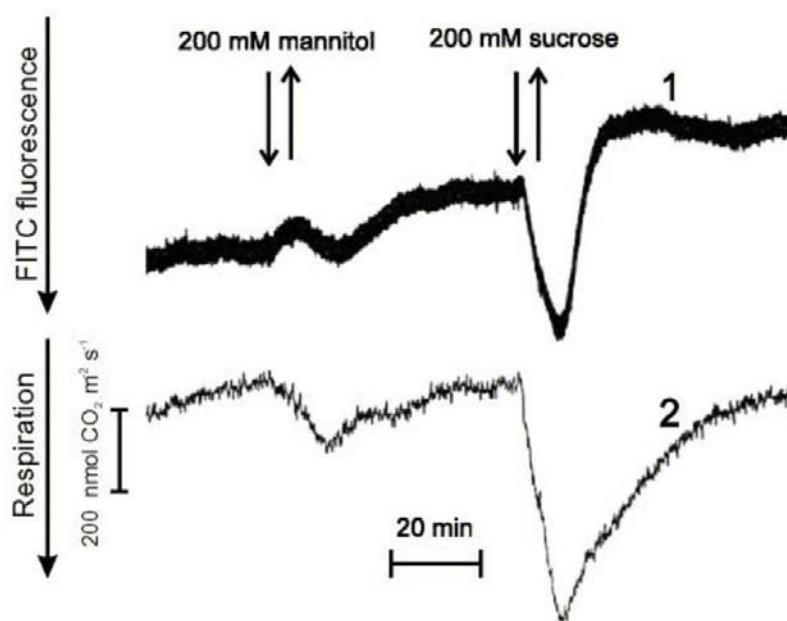


Figure 4.2. Respiratory CO_2 release and apoplastic pH as influenced by 5 min feeding of mannitol and sucrose in concentrations of 200 mM to the petiole of a potato leaf. Increase in FITC fluorescence indicates an alkalization of the apoplast. Courtesy of N. Bukhov and U. Heber (unpublished).

an obvious necessity for the plant to keep the apoplast free of any osmotic solutes which otherwise could lead to the breakdown of turgor control (Heber et al., 2002, in press).

All species studied in these experiments were able to take up not only glucose and sucrose, but also raffinose and stachyose. The symplastic species studied are known to synthesize RFOs in leaves and translocate them (Madore, 1990 for *Coleus*; Mitchell et al., 1992 for *Cucurbita*; Knop et al., 2001 for *Alonsoa*) whereas the apoplastic phloem loaders *Helianthus*, *Calendula* and *Pisum* are sucrose-translocating plants the leaves of which very unlikely contain RFOs (Table 1.3). However, RFOs are commonly synthesized in all plants at least at some developmental stages like seeds (Peterbauer and Richter, 2001).

No drastic differences between symplastic and apoplastic phloem loaders could be observed in the mode of uptake of phloem-translocated carbohydrates. One reason for this could be that it was not possible in these experiments to distinguish between the uptake of sugars into the mesophyll and into the phloem. The extent of the stimulation of respiration (increases by 20 – 50 %) suggests the participation of a large portion of the leaf tissue in the uptake. Winter (1993) reported for spinach leaves that mesophyll tissue and companion cell/sieve element complexes occupied about 85 % and 0.5 %, respectively, of the leaf volume. However, the partial volume of the mitochondria is reported to be as high as 25% of the cell volume in companion cells and only 0.5 % in mesophyll cells (Gamalei, 1990). If the availability of mitochondria is taken as a basis, then about 1/3 of the observed sugar-dependent respiration increase could originate from the CC/SE complexes.

There are also results from previous studies that indicate that the phloem contributes significantly to the uptake of sugars exogenously introduced into the apoplast. When ¹⁴C-labelled glucose was applied to leaf discs of *Coleus blumei* in millimolar concentrations, the label directly entered the veins within 30 seconds to two minutes (Turgeon and Gowan, 1992). The labelling of the mesophyll was much weaker. Also in leaf discs of *Coleus* incubated in ¹⁴C-labelled stachyose, the veins were labelled preferentially, and the label entered the veins directly (Madore, 1990). Glucose does not occur in the phloem sap. Therefore, the fact that ¹⁴C-labelled glucose was taken up directly into the veins of *Coleus* leaf discs indicates that the observed uptake may not represent the part of the phloem loading mechanism of sugars endogenously generated *in vivo*. This is probably true also for the observed uptake of ¹⁴C-labelled stachyose into the leaves of *Cucurbita* (Madore and Webb, 1981) where no further translocation of the labelled stachyose could be observed. In the experiments described in 3.2.3, the high capacity for the uptake of different sugars from the apoplast could be demonstrated by high levels of the uptake-related increases in respiration

(20% - 50% of basal respiration, 3.2.3) for several plant species. This indicated that the leaves are able to remove exogenously applied osmotica (sugars) from the apoplast which otherwise could lead to a breakdown of the turgor. However, the mechanism employed for this process is not necessarily related to phloem loading as indicated by the uptake of ^{14}C -labelled sugars in the experiments of Turgeon and Gowan (1992) and Madore and Webb (1981), described above. Which transporters are involved in this uptake mechanism characterized by low affinity and high capacity (3.2.3), remains to be clarified.

In summary, the observations made in these experiments indicate that the exchange of sucrose, raffinose and stachyose between symplast and apoplast via the plasma membrane in both symplastic and apoplastic phloem loaders cannot be limited by a lack of specific transporters.

4.3.3. The non-metabolizable sucrose isomeres palatinose and turanose can be taken up from the apoplast into the leaf cells in a proton motive force-dependent manner

The non-metabolizable sucrose isomeres turanose and palatinose were shown to cause a transient increase in respiration, a transient alkalization of the apoplast and the depolarization of the plasma membrane, thus indicating the presence of a H^+ -symport system which can recognize these sugars (3.2.3). Palatinose and turanose are considered to be unable to enter plant cells because they are not recognized as the substrates for known sugar transporters (e.g. M'Batchi and Delrot, 1988; Li et al., 1994; Meyer et al., 2000). In *Hevea* protoplasts, the depolarization of the plasma membrane was shown in response to turanose, but no H^+ uptake was monitored in this experiment (Bouteau et al., 1999). Palatinose did not cause the depolarization of the plasma membrane of *Hevea* protoplasts. In this thesis, species-specific differences in the uptake of non-metabolizable sucrose isomeres were also observed. *Calendula* leaf cells readily took up palatinose but not turanose, in contrast to *Lepidium* leaves which were able to perform the uptake of turanose (3.2.3). This fact is especially of interest because palatinose is used in studies of plasma membrane-associated systems of sugar sensing that are based on the assumption that this sugar cannot cross the plasma membrane of plant cells (e.g. Loreti et al., 2000). Recently, the uptake of palatinose from the apoplast into leaf cells was suggested in transgenic tobacco expressing *pall*, the gene for sucrose isomerase from the bacterium *Erwinia rhapontici* which performs palatinose synthesis (Börnke et al., 2001). The data obtained in this thesis provide evidence for transmembrane transfer of palatinose in plants, and, at the same time, indicate that plant species may differ in their ability to take up palatinose into leaf cells.

4.3.4. Sugar exchange between apoplast and phloem is limited in symplastic but not in apoplastic phloem loaders

The data on the composition of the apoplastic sugars indicate that sugar exchange between apoplast and phloem is limited in symplastic but not in apoplastic phloem loaders (3.2.2; 4.3.2). This limitation is not due to the lack of specific sugar transporters in the plasma membrane of symplastic loaders (4.3.2, 4.3.3). One possible explanation for the observed difference could be an additional sub-compartmentation of raffinose and stachyose in the intermediary cells of symplastic loaders. This also might explain the observed inhibition of stachyose and raffinose synthesis in the leaves of *Alonsoa meridionalis* in response to the inhibition of phloem export (4.2). If stachyose and raffinose could not escape from the phloem into the apoplast, nor into the mesophyll via plasmodesmata, then their levels would increase in the phloem itself when translocation is blocked. Raffinose was shown to inhibit stachyose synthesis in *Cucumis* leaves in a competitive manner at concentrations higher than 5 mM (Holthaus and Schmitz, 1991a). Also, in this thesis it was observed that the STS activity in partially purified extracts from *Alonsoa* leaves could not be detected at raffinose concentrations about 20 mM (3.3.3.1). However, the inhibitory effect of raffinose on STS was not observed in *Ajuga reptans* nor in *Ocimum basilicum* where STS activity was examined at a raffinose concentration of 40 mM (Bachmann et al., 1994; Büchi et al., 1998). If the increased levels of raffinose in the phloem of *Alonsoa* would inhibit the synthesis of stachyose, this might result in a negative feedback regulation of stachyose synthesis by the retardation or inhibition of phloem translocation.

4.4. Molecular characterization of *AmSTS*, a stachyose synthase from the symplastic phloem loader *Alonsoa meridionalis*.

4.4.1. *AmSTS* is expressed in intermediary cells of *Alonsoa meridionalis*

In this study, a full length cDNA clone of stachyose synthase was isolated from the leaves of the symplastic phloem loader *Alonsoa meridionalis* (3.3.2). The analysis of the *AmSTS* expression pattern was performed first by hybridization of RNA gel blots containing RNA from flowers, stems, sink leaves and source leaves of *Alonsoa* (3.3.5). Highest expression levels were observed in source leaves, followed by sink leaves and flowers. No expression could be detected in stems of *Alonsoa* by this method. This last finding was confusing, for one of the main functions of the stems in plants is phloem translocation. Therefore, a more precise analysis was performed by *in situ* antisense RNA hybridization using thin sections prepared from source leaves and from stems of *Alonsoa*.

The results demonstrate that in leaves of *Alonsoa*, *AmSTS* expression is confined to the intermediary cells of the minor veins. This is the first time that the expression pattern of stachyose synthase was determined at the cellular level. Interestingly, no hybridization signal could be obtained in companion cells of *Alonsoa* stems, thus confirming the results of the RNA gel blot analyses.

The *in situ* RNA hybridization technique does not distinguish between transcripts of the different gene family members because of the low stringency of the washing steps. The results of DNA gel blot hybridization analysis of *Alonsoa* genomic DNA indicated that *AmSTS* is encoded by a small gene family with most probably two members (3.3.4). Hence, from the *in situ* hybridization results (3.3.5) together with the results of the expression of the *AmSTS* promoter-GUS construct in *Arabidopsis* (3.3.6), it could only be concluded that either both members of the gene family have a similar expression pattern, or that the second gene is not expressed in leaves, or its expression level in the leaves is too low to be detected by *in situ* hybridization. The gene family of STS was analysed in *Vigna angularis* and the results also indicated the presence of at least two isoforms (Peterbauer et al., 1999).

The localization of *AmSTS* expression in intermediary cells of *Alonsoa meridionalis* provides a further confirmation of the specialization of intermediary cells for stachyose synthesis in addition to the immunolocalization of stachyose synthase in intermediary cells of *Cucumis melo* by Holthaus and Schmitz (1991b). Although *Alonsoa meridionalis* and *Cucumis melo* belong to different plant families, their intermediary cells have a similar biochemical specialization confirming the similar function of these cells in both symplastic phloem loaders.

4.4.2. The *AmSTS* promoter directs GUS expression into the phloem in *Arabidopsis*

The cell-specific expression of *AmSTS* in intermediary cells of *Alonsoa meridionalis* puts forward the question which transcription factors may be responsible for this specificity and whether companion cells of other structural types also possess these transcription factors. Furthermore, information on the regulation of the expression of STS in intermediary cells is important for the understanding of the functioning of symplastic phloem loading in general. To further investigate these points, a 1.85 kb fragment of the promoter region of *AmSTS* was cloned and its sequence was identified (3.6.3.1).

No known regulatory elements could be shown within the *AmSTS* promoter region (3.6.3.1). For the further study, the *AmSTS* promoter was fused to the β -glucuronidase reporter gene in the pBI101.3 plant transformation vector. The transcription start for *AmSTS* was identified (3.3.2) and the results showed that two small uORFs are present in the 108 bp

5'UTR of the *AmSTS* mRNA, both in-frame with the *AmSTS* ORF (3.3.2). The translation start codons of both uORFs are in a poor nucleotide context whereas the first codon of *AmSTS* ORF is in a strong context as indicated by the presence of the Kozak consensus sequence around it (RNNatgG; Kozak, 1996). Two uORFs were also found in 5'UTR of mRNA of stachyose synthase from *Vigna angularis* (Peterbauer et al., 1999). Although mRNAs containing uORFs in 5'UTR are rather rare in eucaryots, representing e.g. less than 10% of the known mRNAs in vertebrates, they are found with higher frequency in gene families with regulatory importance including transcriptional factors and genes encoding components of signal transduction pathways (Geballe and Morris, 1994). The presence of additional start codons upstream of the translational start was shown to lower the translation efficiency (e.g. for plants: Chang et al., 2000; Kwak and Lee, 2001). *In vitro* translation studies have shown that this can be due to the stalling of ribosomes at the stop codons of the uORF(s) (Raney et al., 2000). Other regulatory mechanisms depend on the amino acid sequences encoded by uORF(s).

To examine whether the presense of *AmSTS* uORFs affected the GUS level in *Arabidopsis*, two types of *AmSTS* promoter-GUS fusion constructs were made, one with and one without the 5'UTR. For both constructs it was shown that the *AmSTS* promoter directs the expression of GUS into the phloem in *Arabidopsis* (3.3.6.3). The activity of GUS was high as indicated by the very strong production and diffusion of the indigo dye within the entire conducting tissue of *Arabidopsis*. However, when diffusion was prevented by detachment of the inflorescence shoots from the plants before staining, no dye appeared in the vascular tissue of inflorescence shoots indicating that in whole plants, the staining was derived from dye diffusion via the phloem (3.3.6.4). Not only leaves but also sepals and siliques showed staining in the conducting tissue. In roots, only a slight staining was observed in some cases, associated with conducting tissues and areas around it. Thus, the *AmSTS* promoter directs the expression of *GUS* into the phloem of leaves, sepals and green siliques but not into the phloem of inflorescence shoots.

Leaves are the carbon source organs for the whole plant. However, also sepals and siliques can be local source organs for the sinks located nearby like flowers and seeds. For instance, in apple, sepals showed the ability to perform photosynthesis comparable to that in leaves and accounted for 35% of the carbohydrate balance in flowers (Vemmos and Goldwin, 1994). In siliques of rapeseed, virtually 100% of the seed dry matter was found to come from photosynthesis activity of the pod (Singh, 1993). As the inflorescence shoots are unlikely to contribute to the carbohydrate balance of reproductive organs by net assimilation, they are

equivalent to the stems of *Alonsoa* the main function of which seems to be to ensure the transport of carbohydrates from sources to sinks. In summary, the activity of the *AmSTS* promoter was presumably associated with organs of *Arabidopsis* with source function requiring an effective phloem loading.

Both *AmSTS* promoter constructs, the one including the 5'UTR of *AmSTS* mRNA (PmrA) and the one without this region (PmrB) were similar in the tissue specificity of *GUS* activity in *Arabidopsis* (3.3.6.3, 3.3.6.4). However, the expression levels of *GUS* differed between lines expressing these two constructs as was shown by the comparison of altogether 14 lines transformed with PmrA and 16 lines transformed with PmrB. This difference was opposite to what would have been predicted on the basis of the known mechanism of translation repression by uORFs. The presence of the two uORFs from the 5'UTR of *AmSTS* upstream of the *GUS* ORF did not lower the levels of *GUS* activity but rather led to an increase in the *GUS* expression. This preliminary observation has yet to be confirmed by the analysis of the copy number of T-DNAs in all transgenic lines. At present, it is still possible that the difference in *GUS* activity levels is due to differences in T-DNA copy numbers.

The pattern of *GUS* expression under the control of the *AmSTS* promoter in *Arabidopsis* seems to resemble the expression pattern of a *GUS* fusion of the promoter region of a galactinol synthase gene from *Cucumis melo* (*CmGASI*; Haritatos et al., 2000b). The *CmGASI* promoter directed the expression of *GUS* into minor veins of *A. thaliana* and *N. tabacum*. The expression patterns for *AmSTS-GUS* and *CmGASI-GUS* constructs in *Arabidopsis* are compared in Table 4.3. The differences between both patterns were that siliques showed staining in the veins of *AmSTS-GUS* transgenic plants but not of *CmGASI-GUS* transgenic plants, and that petals (heterotrophic organs) were stained in *CmGASI-GUS* but not in *AmSTS-GUS* transgenic plants. Also, the staining of inflorescence shoots was not analysed in *CmGASI-GUS* plants (Haritatos et al., 2000b).

Arabidopsis contains ordinary companion cells in minor veins and is able to synthesize and translocate trace amounts of galactinol and raffinose but not stachyose (Haritatos et al., 2000a). Nevertheless, the expression patterns of *AmSTS* in *Alonsoa* and of *GUS* under control of the *AmSTS* promoter in *Arabidopsis* seem to coincide. This indicates that the regulatory factors activating *AmSTS* expression are present in companion cells of *Arabidopsis*. The same conclusion was made for the expression of *CmGASI-GUS* in *Arabidopsis* and tobacco (Haritatos et al., 2000b). Tobacco does not synthesize galactinol and RFOs; nevertheless, *CmGASI-GUS* was expressed also in this plant in the minor veins. However, this comparison is incomplete because it does not include the analysis of expression of *CmGASI* in melon, and

both tobacco and *Arabidopsis* differ from melon in their carbohydrate metabolism and minor vein anatomy.

The study of *AmSTS* expression has shown that expression patterns seem to be conserved between *Arabidopsis* and *Alonsoa*, in spite of their different companion cell structure.

Table 4.3. GUS activity in organs of *Arabidopsis* as shown by staining of plants expressing either a *AmSTS-GUS* (this thesis) or a *CmGAS1-GUS* (Haritatos et al., 2000b) construct.

Plant organs	GUS staining observed in		Material taken for staining
	<i>AmSTS-GUS</i>	<i>CmGAS1-GUS</i>	
veins of cotyledones	stained	stained	seedlings
veins of mature leaves	strongest staining in minor veins	strongest staining in minor veins	seedlings, detached rosette leaves
hydatodes	stained	stained	“
midrib at short staining times	no	no	“
midrib at longer staining time	stained	stained	“
minor veins at short staining time	stained	stained	leaves, leaf pieces
mesophyll	no (stained by diffusion in the absence of FeII/III)	stained in high copy number lines	leaves
damaged organs	stained	stained	
veins of sepals and petals	sepals only	both sepals and petals	inflorescences
conducting tissue in siliques	stained	no	detached siliques
inflorescence shoots	no	not tested	cut pieces of inflorescence shoots
roots	no (or faint staining due to diffusion)	patchy staining	seedlings

4.4.3. Preliminary results indicate that the *AmSTS* promoter is inducible by sugars but also by osmotically active solutes

The involvement of *AmSTS* in carbohydrate metabolism and phloem loading made it interesting to investigate the influence of sugars on its expression. In this thesis, only preliminary results could be obtained because no homozygous lines are available yet and transgene copy numbers have not yet been determined. However, the same results were obtained with all F2 plants from 20 independent lines (10 PmrA lines and 10 PmrB lines) indicating that the observations are significant. The data show that the incubation of seedlings

of transgenic plants on MS medium containing either 5% sucrose (180 mM) or 4% glucose (200 mM) for 20 hours led to a strong increase of GUS activity in seedlings as compared with GUS levels after incubation on MS medium without additives or in seedlings taken directly from MS plates with 2% sucrose (3.3.6.5). However, this induction may be due to a breakdown of the turgor control in the cells. Preliminary results show that a similar increase of GUS activity as caused by sucrose and glucose can also be caused by raffinose and sorbitol. Furthermore, GUS activity increased in seedlings subjected to one hour of drought stress, compared to a watered control (3.3.6.5). Once homozygous lines are available, further studies will reveal which factors affect the expression of *AmSTS-GUS* in *Arabidopsis*.

4.5. Reformulation of the model of symplastic phloem loading

The current model of symplastic phloem loading, the polymerization trap model, is based on two postulates (1.6). First, the synthesis of stachyose is assumed to take place in intermediary cells. Second, plasmodesmal connections between the intermediary cells and the mesophyll bundle sheath cells represent a mechanical barrier for the diffusion of stachyose into the mesophyll cells because of their size exclusion limit. Thus, stachyose is trapped in intermediary cells and can only diffuse into sieve elements via much larger plasmodesmata.

The first postulate has been directly confirmed by the immunolocalization of stachyose synthase in intermediary cells of *Cucumis melo* (Holthaus and Schmitz, 1991b) and now by the localization of the expression of *AmSTS* in intermediary cells of *Alonsoa meridionalis* in this thesis. The second postulate, however, about the diameter of plasmodesmata limiting the diffusion of stachyose into the mesophyll, is contradicted by the accumulating information on the transport of large proteins and riboprotein complexes via plasmodesmata from mesophyll cells into intermediary cells. This contradiction arises when the cytosol is considered as the transport compartment for the protein transfer through plasmodesmata and also as the site of stachyose synthesis in intermediary cells (1.6).

Some observations made in this thesis are not consistent with the presumed compartmentation of stachyose in the cytosol of intermediary cells. First, it could be shown that the transfer of stachyose across the plasma membranes of leaf cells takes place with a capacity similar to that for the transfer of other sugars like sucrose (3.2.3). The boundary between apoplast and cytosol is represented by the plasma membrane. Thus, if stachyose is synthesized in the cytosol of intermediary cells, it should be able to escape from the cytosol into the apoplast at least when its release into sieve elements is inhibited. Second, stachyose does not accumulate in the apoplast when phloem translocation is blocked (3.2.2). Altogether,

stachyose has not yet been found in the apoplast in concentrations higher than trace amounts. These data indicate that it is rather unlikely for stachyose to be localized in the cytosol.

An interesting suggestion about an alternative intracellular compartmentation of stachyose and its synthesis within intermediary cells comes from the studies on lactose biosynthesis that occurs in milk-secreting cells of mammary glands. Lactose is a β -galactosyl-1,4-D-glucose, synthesized from UDP-galactose and glucose by lactose synthase. The biosynthesis of lactose occurs exclusively in cells of mammary glands and was shown to be the key process in milk secretion. This is due to the fact that lactose is synthesized within the lumen of Golgi vesicles and it is not able to escape into the cytosol (White et al., 1980). Thus, lactose synthesis draws water into the vesicles by osmosis. Therefore, lactose synthesis activity determines the volume of the secreted milk. Recently, this mechanism was confirmed by the construction of transgenic mice whose enhanced or reduced lactose synthesis activity resulted in either increased or decreased secretion of milk, respectively, and also determined the composition of the secreted milk (Boston et al., 2001).

A comparison of structural and functional characteristics of intermediary cells and milk-secreting cells shows some similarities. In both cell types, endomembrane vesicles, rough endoplasmic reticulum and mitochondria are highly developed (Figure 4.3 A and B). Both cell types are specialized for the synthesis of galactosylated compounds, β -galactosyls in milk-secreting cells and α -galactosyls in intermediary cells, respectively. Interestingly, the pH optimum for lactose synthase is about 6.8-7.0, a value similar to that of stachyose synthase and which is considered as an argument for the location of stachyose synthase in the cytosol. However, lactose synthase is confined to the Golgi lumen of milk-secreting cells of mammary glands. This compartmentation of lactose synthesis makes it impossible for lactose to escape into the cytosol which would inhibit milk secretion. In contrast, if lactose were synthesized in the cytosol, it would have to enter the Golgi vesicles via a reversible membrane transporter-catalyzed reaction and hence could accumulate in the cytosol. Recently, two different vacuolar compartments were shown to be present in mesophyll protoplasts, a large acidic one and a population of smaller pH-neutral vacuoles (Paris et al., 1996). These compartments require different peptide signals for protein targeting (Di Sansebastiano et al., 1998; 2001). Thus, also in plant cells, the neutral pH optimum cannot be considered as a feature of the cytosolic enzymes alone.

The mechanism of phloem loading in plants with intermediary cells can be re-evaluated if it is postulated that stachyose synthesis occurs within the endomembrane system of these cells. In such a model, stachyose is trapped not in the cytosol but in the

endomembrane system of intermediary cells. This could draw the water flux into the endomembrane compartment, analogous to the process of milk secretion. In plant cells, the rigid cell wall prevents the release of the contents of endomembrane vesicles into the extracellular space but does not affect the release into sieve elements through plasmodesmata. If the data discussed above are taken into account, it seems unlikely that any re-compartmentation of stachyose takes place within the sieve elements. A three-dimensional reconstruction of the endomembrane systems in intermediary cells of *Fraxinus excelsior* and *Lycopus europaeus* from serial sections performed by Gamalei and Pakhomova (1981) showed that here, the ER represents a single large endomembrane compartment rather than a population of vesicles and is continuous between intermediary cells and sieve elements. Thus, stachyose could be synthesized and translocated within the endomembrane system.

In this model, the mechanism of symplastic phloem loading would not represent the simple diffusion of stachyose into the phloem. Instead, the osmotically drawn water flux which would be created by the localization of stachyose synthesis in the endomembrane system would draw stachyose from the intermediary cells into the sieve elements. Furthermore, the water flux would allow other compounds to enter the endomembrane system via specific transporters. These molecules could come from the apoplast or arrive in intermediary cells from mesophyll cells via plasmodesmata. It is known that due to the presence of aquaporines there are no limitations to the water exchange between subcellular compartments (Johansson et al., 2000). Thus, intermediary cells can be considered as osmotic “pumps”.

A similar function could also be assumed for raffinose and stachyose in seeds which is common in plants. The synthesis of stachyose and raffinose could help to establish the transport water flux in a developing seedling in a similar way, i.e. by creation of an osmotic “starting point” for this process. Interestingly, many “seed imbibition proteins” represent raffinose synthases based on their amino acid sequences.

Gamalei et al. (2000) have examined the ultrastructural changes of intermediary cells in leaves during inhibition of phloem export. Inhibition of phloem translocation led to complete disappearance of the endomembrane system of intermediary cells (shown in Figure 4.3 C, D). Gamalei postulated in 1994 that the endoplasmic reticulum is the main channel for sugar transport (1.3; Gamalei, 1994; Gamalei et al., 1994) and interpreted the disappearance of endomembranes as a cessation of sugar loading into the ER (Gamalei et al., 2000). It is possible that the cessation of stachyose synthesis in the ER, e.g. due to feedback inhibition (see above), led to a drop of the osmotic pressure within the ER.

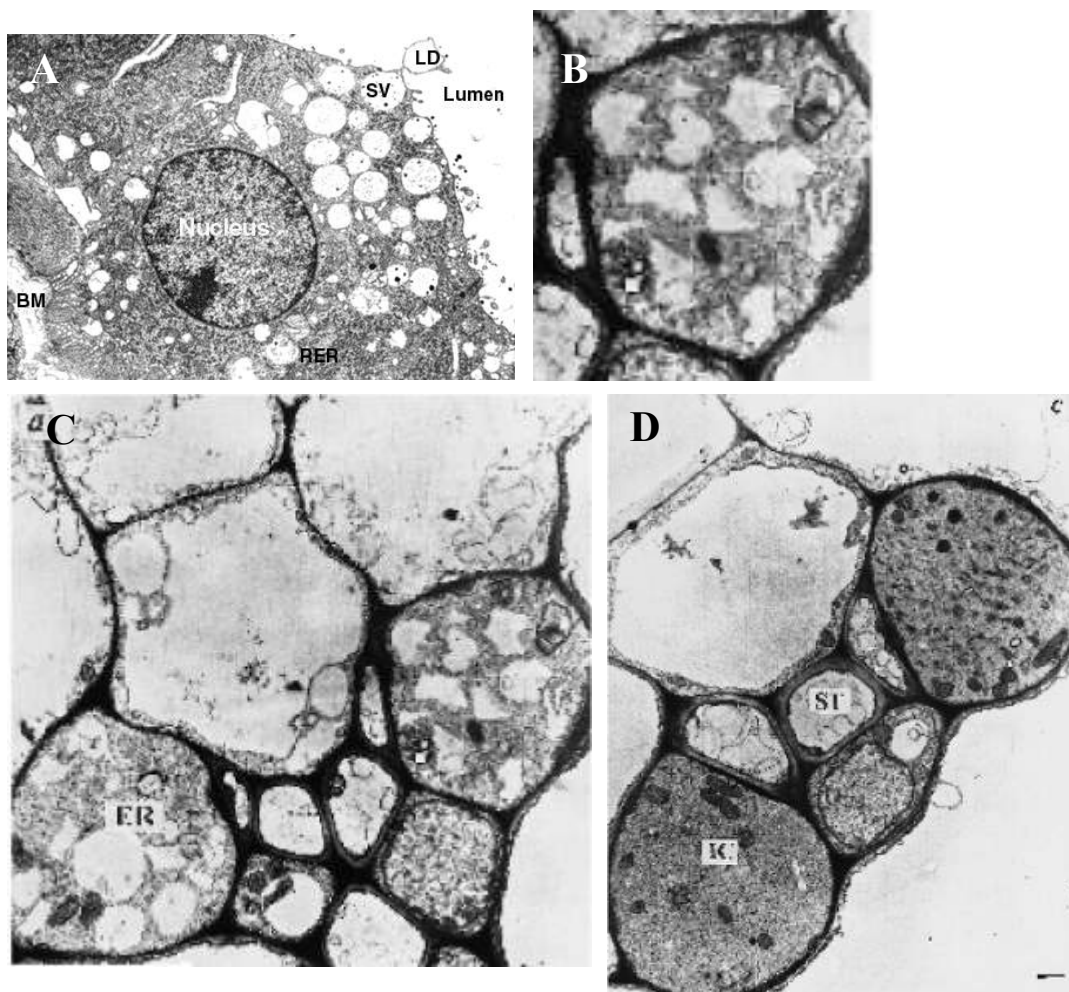


Figure 4.3. Ultrastructure of **A**, a milk-secreting cell of a cow mammary gland; **B**, an intermediary cells of *Cucumis melo*; **C** and **D**, a minor vein of *Coleus blumei* at normal (**C**) and inhibited (**D**) phloem translocation. Data taken from: **A**, lactation biology homepage (<http://classes.aces.uiuc.edu/AnSci308/mamultrastruct.html>); **B**, **C** and **D**, Gamalei et al., 2000.

Based on this model, *AmSTS* should be localized in the ER. However, no putative transmembrane domains could be identified within the amino acid sequence of *AmSTS*. This finding might contradict the proposed model, but it has to be taken into account that the mechanisms of protein targeting in plants have not yet been studied sufficiently. Interestingly, the only immunolocalization study of stachyose synthase in intermediary cells performed by Holthaus and Schmitz (1991b) has shown that the protein was often associated with the endomembrane vesicles.

The reformulation of the model of symplastic phloem loading made in this thesis would serve to explain some inconsistencies in the polymerization trap model and relate both structural and functional characteristics of intermediary cells. The model postulates that stachyose synthesis occurs within the endomembrane system of intermediary cells and that stachyose cannot escape from the endomembrane system, thus leading to the increase of

osmotic pressure within this compartment. These postulates could be tested by an examination of the permeability of endomembranes for stachyose. Another approach could be the targeting of a stachyose cleaving enzyme into the endomembrane system in a plant species with intermediary cells in its minor veins. The latter could be achieved by transformation of *Cucumis melo* (Guis et al., 2000) with a construct containing the ORF of a modified alkaline α -galactosidase (Gao and Schaffer, 1999) with a signal peptide for uptake into the endomembrane system under control of a strong IC-specific promoter, e.g. the *AmSTS* promoter.

5. SUMMARY

This thesis aimed to investigate the role of compartmentation of phloem-translocated carbohydrates and of the synthesis of one specific transport form, the stachyose, in the process of phloem loading in leaves of symplastic phloem loaders. These plants are characterized by (1) the presence of a special type of companion cells in the minor veins, the intermediary cells, and (2) the translocation of raffinose family oligosaccharides, mainly stachyose, in the phloem. The intermediary cells are characterized by highly developed plasmodesmata connecting mesophyll and phloem. This symplastic continuity between the two tissues provides an additional route for sugars entering the phloem as compared to apoplastic phloem loaders where plasmodesmal connections between companion cells and mesophyll are missing. At the same time, the presence of symplastic connections makes it necessary for a plant, in order to keep the sugar concentrations in the phloem high, to develop an effective mechanism to sustain a concentration gradient between mesophyll and phloem in spite of their symplastic continuity.

To elucidate how the compartmentation of translocated carbohydrates can be used by a plant to establish such a mechanism, this compartmentation between subcellular compartments of mesophyll cells was analysed in one model plant species with intermediary cells in minor veins, *Alonsoa meridionalis*. A related species, *Asarina barclaina*, which differs in the minor vein anatomy from *Alonsoa* was included as a comparison. Furthermore, the capacity to exchange translocated carbohydrates between symplastic and apoplastic compartments was compared in leaves of symplastic and apoplastic phloem loaders. The third part of this study was the characterization of the gene encoding stachyose synthase from leaves of *Alonsoa meridionalis* (*AmSTS*). This characterization included the determination of the expression pattern of *AmSTS* at the cellular level in leaves of *Alonsoa* and the isolation

and characterization of the *AmSTS* promoter by the construction of transgenic *Arabidopsis* plants expressing a *AmSTS-GUS* fusion.

The results obtained can be summarized as follows.

- Distribution patterns of carbohydrates among subcellular compartments of mesophyll cells are similar in different plant species.
- Sugar concentrations in subcellular compartments of mesophyll cells of the symplastic phloem loader *Alonsoa meridionalis* do not differ from those in apoplastic phloem loaders.
- The concentration gradient between cytosol of mesophyll cells and phloem in *Alonsoa meridionalis* was 10 times lower than in apoplastic phloem loaders. However, this was due to the lower sucrose concentration in the phloem as compared to apoplastic loaders.
- Evidence was obtained for a proton motive force-dependent transport of raffinose and stachyose, as well as of turanose and palatinose from the apoplast into leaf cells indicating the presence of as yet unidentified plasma membrane transporters.
- The capacity for the uptake of exogenously added sugars from the apoplast into the leaf cells does not differ between symplastic and apoplastic phloem loaders.
- The sugar composition in the apoplast of symplastic and apoplastic phloem loaders is related to phloem transport in apoplastic but not in symplastic phloem loaders, indicating that exchange of sugars between apoplast and phloem occurs only in apoplastic phloem loaders. As shown above, this cannot be due to the lack of specific plasma membrane transporters in symplastic phloem loaders.
- *AmSTS* is expressed in leaves and flowers, but not in stems of *Alonsoa*. The expression of *AmSTS* in leaves is confined to intermediary cells.
- The isolation of the *AmSTS* promoter and the construction of transgenic *Arabidopsis* plants containing a *AmSTS-GUS* fusion showed that the expression pattern of the *AmSTS* promoter is conserved in *Arabidopsis*. *AmSTS* expression is confined to the phloem of source organs.
- The expression of *AmSTS-GUS* in *Arabidopsis* seems to be regulated depending on changes in osmotic pressure.
- The availability of the *AmSTS-GUS* *Arabidopsis* plants provides a tool for further studies on the mechanism and the regulation of the phloem loading.

6. ABBREVIATIONS

Amp	ampicillin
Amp ^R	ampicilin resistance
<i>AmSTS</i>	<i>Alonsoa meridionalis</i> stachyose synthase
AP	adapter primer
ATP	adenosine 5' triphosphate
BCIP	5-bromo-4 chloro-3-indolyl phosphate
BDTO	bis-(1,3-dibutylbarbituric acid) trimethine oxonol
bp	base pair
BS	bundle sheath cell
BSA	bovine serum albumin
CC	companion cell
cDNA	complementary DNA
Ch	chloroplasts
Chl	chlorophyll
CMV	cucumber mosaic virus
CTAB	hexadecyltrimethylammonium bromide
CW	cell wall
Cyt	cytoplasm
dCTP	deoxycytosine 5' triphosphate
dd H ₂ O	double distilled water
DDSA	Dodeceny Succinic Anhydride hardener for epoxy resin
DIG	digoxigenine
DMF	dimethylformatide
DMP-30	2,4,6-tris (dimethylaminomethyl) phenol, a tertiary amine epoxy accelerator
DMSO	dimethylsulfoxide
DNA	desoxyribonucleic acid
dNTPs	deoxyribonucleotides
dpm	decays per minute
DTT	dithiothreitol
EDTA	ethylenediamine tetraacetic acid

ER	endoplasmic reticulum
EtOH	ethanol
F1	transformants of the first generation
F2	transformants of the second generation
FITC	fluorescein isothiocyanate
FW	fresh weight
G6PDH	glucose-6-phosphate dehydrogenase
GAPDH	glyceraldehyde 3-phosphate dehydrogenase
GC-MS	Gas Chromatography-Mass Spectrometry
GS	galactinol synthase (UDP-galactose: <i>myo</i> -Inositol galactosyltransferase)
GUS	β -glucuronidase
GWDG	Gesellschaft für wissenschaftliche Datenverarbeitung Göttingen
HEPES	hydroxyethyl-piperazinethane sulfonic acid
HPLC	high pressure liquid chromatography
IC	intermediary cells
IPTG	isopropyl- β -D-thiogalactopyranoside
IRGA	Infra Red Gas Analysis
IWF	intercellular washing fluid or apoplastic extract
K_m	Michaelis-Menten constant
kb	kilobase pair
kDa	kilodalton
Km	kanamycin
Km^R	kanamycin resistance
MC	mesophyll cell
MCS	multiple cloning site
MEN	MOPS-sodium acetate-EDTA buffer
MES	morpholinoethane sulfonic acid
MOPS	morpholinopropane sulfonic acid
MS medium	Murashige-Skoog medium
MS2	Murashige-Skoog medium with 2% (w/v) sucrose
NAD	nicotinamide adenine dinucleotide (oxidized)
NADH	nicotinamide adenine dinucleotide (reduced)
NADP	nicotinamide adenine dinucleotide phosphate (oxidized)
NADPH	nicotinamide adenine dinucleotide phosphate (reduced)
NBT	4-nitro-blue tetrazolium chloride
NMR	nuclear magnetic resonance
OC	ordinary cells
OD	optical density
ORF	open reading frame
PAGE	polyacrylamid-gel electrophoresis
PBS	phosphate buffer saline
PCMBS	<i>para</i> -chloro-mercuribenzenesulphonate
PCR	polymerase chain reaction
PEP	phosphoenolpyruvate
PEPCx	phosphoenolpyruvate carboxylase
pf	plasmodesmal field

PIPES	1, 4-piperazinediethane sulfonic acid
PM	plasma membrane
PMF	proton motive force
PP	phloem parenchyma
rpm	rounds per minute
PVP	polyvinylpyrrolidon
RACE	rapid amplification of cDNA ends
RFOs	raffinose family oligosaccharides
RNA	ribonucleic acid
RS	raffinose synthase (galactinol:sucrose 6- α -D-galactosyltransferase)
RT	reverse transcriptase
SD	standard deviation
SDS	sodium dodecylsulfate
SE	sieve element
SE-CC complex	sieve element-companion cell complex
SEL	size exclusion limit
sp	single plasmodesma
SSC	saline-sodium citrate buffer
STEL	sucrose – Triton-X-100 – Tris– EDTA –lysozyme buffer
STS	stachyose synthase (galactinol:raffinose 6- α -D-galactosyltransferase)
SUT	sucrose transporter
T _{ann}	annealing temperature
<i>Taq</i>	<i>Thermus aquaticus</i>
TC	transfer cells
TdT	terminal desoxynucleotidyl transferase
TEMED	N,N,N',N'-tetramethylene diamine
T _m	melting temperature
T _{op}	temperature optimum
Tricine	N-Tris-(hydroxymethyl)-methyl glycine
Tris	tris-(hydroxymethyl)-aminomethane
<i>Tth</i>	<i>Thermus thermophilus</i>
U	enzyme activity unit (1 unit corresponds to the conversion of 1 μ mol substrate min ⁻¹)
uORF	upstream open reading frame
UTP	uridine 5' triphosphate
UV	ultraviolet light
Vac	vacuoles
v/v	volume/volume
w/v	weight/volume
X-Gal	5-bromo-4-chloro-3-indolyl- β -D-galactopyranoside
X-Gluc	5-bromo-4-chloro-3-indolyl- β -D-glucuronide
XV	xylem vessel

7. REFERENCES

- Adhikari, J., Bhaduri, T. J., DasGupta, S. and Majumder, A. L. (1987) Chloroplast as a locale of L-*myo*-inositol-1-phosphate synthase. *Plant Physiol* **85**, 611-164.
- Altschul, S. F., Gish, W., Miller, W., Myers, E. W. and Lipman, D. J. (1990) Basic local alignment search tool. *J Mol Biol* **215**, 403-410.
- Arnon, D. I. (1949) Copper enzymes in isolated chloroplasts. Polyphenoloxidase in *Beta vulgaris*. *Plant Physiol* **24**, 1-15.
- Bachmann, M. and Keller, F. (1995) Metabolism of the raffinose family oligosaccharides in leaves of *Ajuga reptans* L. Inter- and intracellular compartmentation. *Plant Physiol* **109**, 991-998.
- Bachmann, M., Matile, P. and Keller, F. (1994) Metabolism of the raffinose family oligosaccharides in leaves of *Ajuga reptans* L. Cold acclimation, translocation, and sink to source transition: discovery of chain elongation enzyme. *Plant Physiol* **105**, 1335-1345.
- Batashev, D. (1997) Comparative Anatomy of Leaf Terminal Phloem in Subclasses Lamiidae and Asteridae. In *Dissertation*, St.-Petersburg.
- Batashev, D. and Gamalei, Y. V. (1996) Diurnal changes in cell structures related to assimilate accumulation and export from leaves of *Acanthus* and *Phlomis* with and without blocking phloem transport. *Russ J Plant Physiol* **43**, 344-351.
- Bentwood, B. J. and Cronshaw, J. (1978) Cytochemical localization of adenosine triphosphatase in the phloem of *Pisum sativum* and its relation to the function of transfer cells. *Planta* **140**, 111-120.
- Bergmeyer, H. U. (1974) Methods of enzymatic analysis, (ed. H. U. Bergmeyer), Verlag Chemie, Weinheim, Academic Press Inc., New York, London.
- Bird, I. F., Cornelius, M. J., Keys, A. J. and Whittingham, C. P. (1974) Intracellular site of sucrose synthesis in leaves. *Phytochemistry* **13**, 59-64.
- Blackman, L. M. and Overall, R. L. (2001) Structure and function of plasmodesmata. *Aust J Plant Physiol* **28**, 709-721.

- Boevink, P., Martin, B., Oparka, K., Santa Cruz, S. and Hawes, C. (1999) Transport of virally expressed green fluorescent protein through the secretory pathway in tobacco leaves is inhibited by cold shock and brefeldin A. *Planta* **208**, 392-400.
- Boorer, K. J., Loo, D. D. F., Frommer, W. B. and Wright, E. M. (1996) Transport mechanism of the cloned potato H⁺/sucrose cotransporter *StSUT1*. *J Biol Chem* **271**, 25139-25144.
- Boston, W. S., Bleck, G. T., Conroy, J. C., Wheeler, M. B. and Miller, D. J. (2001) Short communications: Effect of increased expression of alpha-lactalbumin in transgenic mice on milk yield and pup growth. *J Dairy Sci* **84**, 620-622.
- Bouteau, F., Dellis, O., Bousquet, U. and Rona, J. P. (1999) Evidence of multiple sugar uptake across the plasma membrane of laticifer protoplasts from *Hevea*. *Bioelectrochem Bioenerg* **48**, 135-139.
- Burbulis, I. E. and Winkel-Shirley, B. (1999) Interactions among enzymes of the *Arabidopsis* flavonoid biosynthetic pathway. *Proc Natl Acad Sci USA* **96**, 12929-12934.
- Börnke, F., Hajirezaei, M., Heineke, D., Melzer, M., Herbers, K. and Sonnewald, U. (submitted) High level production of the non-cariogenic sucrose isomer palatinose in transgenic tobacco plants strongly impairs development. *Planta*.
- Büchi, R., Bachmann, M. and Keller, F. (1998) Carbohydrate metabolism in source leaves of sweet basil (*Ocimum basilicum* L.), a starch-sorting and stachyose-translocating labiate. *J Plant Physiol* **153**, 308-315.
- Cantril, L. C., Overall, R. L. and Goodwin, P. B. (2002, in press) Changes in symplastic permeability during adventitious shoot regeneration in tobacco thin cell layers in *planta*.
- Cantrill, L. C., Overall, R. L. and Goodwin, P. B. (1999) Cell-to-cell communication via plasma membrane. *Cell Biology International* **23**, 653-661.
- Chang, K. S., Lee, S. H., Hwang, S. B. and Park, K. Y. (2000) Characterization and translational regulation of the arginine decarboxylase gene in carnation (*Dianthus caryophyllus* L.). *Plant J* **24**, 45-56.
- Christmann, J., Kreis, W. and E., R. (1993) Uptake, transport and storage of cardenolides in foxglove: Cardenolide sinks and occurrence of cardenolides in the sieve tubes of *Digitalis lanata*. *Botanica Acta* **106**, 419-427.
- Clough, S. J. and Bent, A. F. (1998) Floral dip: a simplified method for *Agrobacterium*-mediated transformation of *Arabidopsis thaliana*. *Plant J* **16**, 735-743.
- Delesse, M. A. (1847) Procéde mécanique pour déterminer la composition des roches. *CR Acad Sci Paris* **25**, 544-559.
- Di Sansebastiano, G.-P., Paris, N., Marc-Martin, S. and Neuhaus, J.-M. (1998) Specific accumulation of GFP in a non-acidic vacuolar compartment via a C-terminal propeptide-mediated sorting pathway. *Plant J* **15**, 449-457.
- Di Sansebastiano, G.-P., Paris, N., Marc-Martin, S. and Neuhaus, J.-M. (2001) Regeneration of a lytic central vacuole and of neutral peripheral vacuoles can be visualized by green fluorescent proteins targeted to either type of vacuoles. *Plant Physiol* **126**, 78-86.
- Esau, K. (1967) Minor veins in *Beta* leaves: structure related to function. *Proc Amer Phil Soc* **11**, 219-233.
- Everard, J. D., Franceschi, V. R. and Loescher, W. H. (1993) Mannose-6-phosphate reductase, a key enzyme in photoassimilate partitioning, is abundant and located in the

- cytosol of photosynthetically active cells of celery (*Apium graveolens* L.) source leaves. *Plant Physiol* **102**, 345-356.
- Faucher, M., Bonnemain, J.-L. and Doffin, M. (1982) Effets de refroidissements localises sur la circulation liberienne chez quelques especes avec on sans proteines-P et influence du mode de refroidissement. *Physiol Veg* **20**, 395-405.
- Fischer, D. G. (1986) Ultrastructure, plasmodesmatal frequency and solute concentration in green areas of variegated *Coleus blumei* Benth. leaves. *Planta* **169**, 141-152.
- Flora, L. L. and Madore, M. A. (1993) Stachyose and mannitol transport in olive (*Olea europaea* L.). *Planta* **189**, 484-490.
- Flora, L. L. and Madore, M. A. (1996) Significance of minor-vein anatomy to carbohydrate transport. *Planta* **198**, 171 - 178.
- Fricke, W., Leigh, R. A. and Tomos, A. D. (1994a) Concentrations of inorganic and organic solutes in extracts from individual epidermal, mesophyll and bundle-sheath cells of barley leaves. *Planta* **192**, 310-316.
- Fricke, W., Leigh, R. A. and Tomos, A. D. (1994b) Epidermal solute concentrations and osmolality in barley leaves studied at the single-cell level. *Planta* **192**, 317-323.
- Gamalei, Y. V. (1984) The structure of leaf minor veins and the types of translocated carbohydrates. *Dokl Akad Nauk (in russ.)* **277**, 1513-1516.
- Gamalei, Y. V. (1990) Leaf Phloem, Nauka, Leningrad.
- Gamalei, Y. V. (1994) The endoplasmic reticulum of plants: its origin, structure and functions, BIN RAN, St.-Petersburg.
- Gamalei, Y. V. (1995) Comparative biology of trees and herbs intercellular communication. In *L'Arbre. Biologie et Development - 3ème colloque*, (ed. C. Edelin), pp. 1-11, Montpellier.
- Gamalei, Y. V. (2000) Comparative anatomy and physiology of leaf minor veins and bundle sheath parenchyma in leaves of dicotyledonous plants. *Botan Zhurnal (in russ.)* **85**, 34-49.
- Gamalei, Y. V. and Pakhomova, M. V. (1981) Structure of the companion cells of leaf phloem: the results of a three-dimensional reconstruction from serial sections. *Cytologija (in Russian)* **23**, 117-129.
- Gamalei, Y. V. and Pakhomova, M. V. (2000) The time course of carbohydrate transport and storage in the leaves of the plant species with symplastic and apoplastic phloem loaded under the normal and experimentally modified conditions. *Russ J Plant Physiol* **47**, 109-128.
- Gamalei, Y. V., Pakhomova, M. V., Syutkina, A. V. and Voitsekhovskaja, O. (2000) Compartmentation of assimilate fluxes in leaves. I. Ultrastructural responses of mesophyll and companion cells to the alteration of assimilate export. *Plant biol* **2**, 98-106.
- Gamalei, Y. V. and Sjutkina, A. V. (1999) Structural types and ecophysiology of terminal phloem in plant species of steppes and deserts. In *International Conference on Assimilate Transport and Partitioning, Book of Abstracts*, Newcastle, Australia.
- Gamalei, Y. V., van Bel, A. J. E., Pakhomova, M. V. and Sjutkina, A. V. (1994) Effects of temperature on the conformation of the endoplasmic reticulum and on starch

- accumulation in leaves with the symplasmic minor-vein configuration. *Planta* **494**, 443-453.
- Gao, Z. and Schaffer, A. A. (1999) A novel alkaline α -galactosidase from melon fruit with a substrate preference for raffinose. *Plant Physiol* **119**, 979-987.
- Geballe, A. P. and Morris, D. R. (1994) Initiation codons within 5'-leaders of mRNAs as regulators of translation. *Trend Biochem Sci* **19**, 159-164.
- Geiger, D. (1975) Phloem loading. In *Transport in Plants*, Springer Verlag, Berlin.
- Geiger, D. R. and Sovonick, S. A. (1970) Temporary inhibition of translocation velocity and mass transfer rate by petiole cooling. *Plant Physiol* **46**, 847-849.
- Gerhardt, R. and Heldt, H. W. (1984) Measurement of subcellular metabolite levels by fractionation of freeze-stopped material in nonaqueous media. *Plant Physiol* **75**, 542-547.
- Ghoshroy, S., Lartey, R., Sheng, J. and Citovsky, V. (1997) Transport of proteins and nucleic acids through plasmodesmata. *Annu Rev Plant Physiol Plant Mol Biol* **48**, 27-50.
- Giaquinta, R. (1980) Mechanism and control of phloem loading of sucrose. *Ber Dtsch bot Ges* **93**, 187-201.
- Grignon, C. and Sentenac, H. (1991) pH and ionic conditions in the apoplast. *Annu Rev Plant Physiol Plant Mol Biol* **42**, 103-128.
- Guis, M., Ben Amor, M., Latché, A., Pech, J.-C. and Roustan, J.-P. (2000) A reliable system for the transformation of cantaloupe charentais melon (*Cucumis melo* L. var. *cantalupensis*) leading to a majority of diploid regenerants. *Scientia Horticulturae* **84**, 91-99.
- Gunning, B. E. S. and Pate, J. S. (1969) "Transfer cells". Plant cells with wall ingrowths, specialized in relation to short distance transport of solutes - their occurrence, structure, and development. *Protoplasma* **68**, 107-133.
- Haritatos, E., Ayre, B. G. and Turgeon, R. (2000b) Identification of phloem involved in assimilate loading in leaves by the activity of galactinol synthase promoter. *Plant Physiol* **123**, 929-937.
- Haritatos, E., Keller, F. and Turgeon, R. (1996) Raffinose oligosaccharide concentrations measured in individual cell and tissue types in *Cucumis melo* L. leaves: implications for phloem loading. *Planta* **198**, 614-622.
- Haritatos, E., Medville, R. and Turgeon, R. (2000a) Minor vein structure and sugar transport in *Arabidopsis thaliana*. *Planta* **211**, 105-111.
- Heber, U. (1957) Zur Frage der Lokalisation von löslichen Zuckern in der Pflanzenzelle. *Ber. Dtsch. Bot. Ges.* **70**, 371-382.
- Heber, U., Wiese, C., Neimanis, S., Savchenko, G., Bukhov, N. and Hedrich, R. (2002, in press) Energy-dependent solute transport from the apoplast into the symplast of leaves during transpiration. *Russ J Plant Physiol* **49**.
- Hedrich, R., Neimanis, S., Savchenko, G., Felle, H. H., Kaiser, W. M. and Heber, U. (2001) Changes in apoplastic pH and membrane potential in leaves in relation to stomal responses to CO₂, malate, abscisic acid or interruption of water supply. *Planta* **213**, 594-601.

- Heidstra, R., Geurts, R., Franssen, H., Spalink, H. P., van Kammen, A. and Bisseling, T. (1994) Root hair deformation activity of nodulation factors and their fate on *Vicia sativa*. *Plant Physiol* **105**, 787-797.
- Heineke, D., Wildenberger, K., Sonnewald, U., Willmitzer, L. and Heldt, H. W. (1994) Accumulation of hexoses in leaf vacuoles: Studies with transgenic tobacco plants expressing yeast-derived invertase in the cytosol, vacuole or apoplast. *Planta* **194**, 29-33.
- Heldt, H. W. (1996) Pflanzenbiochemie, Spektrum Verlag, Heidelberg.
- Hendrix, J. E. (1982) Sugar translocation in two members of the Cucurbitaceae. *Plant Sci Lett* **25**, 1-7.
- Hoffmann, B. and Kosegarten, H. (1995) FITC-dextran for measuring apoplast pH and apoplastic pH gradients between various cell types in sunflower leaves. *Physiol Plant* **95**, 327-335.
- Hoffmann-Thoma, G., van Bel, A. J. E. and Ehlers, K. (2001) Ultrastructure of minor-vein phloem and assimilate export in summer and winter leaves of the symplasmically loading evergreens *Ajuga reptans* L., *Aucuba japonica* Thunb., and *Hedera helix* L. *Planta* **212**, 231-242.
- Holthaus, U. and Schmitz, K. (1991a) Stachyose synthesis in mature leaves of *Cucumis melo*. Purification and characterization of stachyose synthase (EC 2.4.1.67). *Planta* **184**, 525-231.
- Holthaus, U. and Schmitz, K. (1991b) Distribution and immunolocalization of stachyose synthase in *Cucumis melo* L. *Planta* **185**, 479-486.
- Häfliger, B., Kindhauser, E. and Keller, F. (1999) Metabolism of D-glycero-D-mannoheptidol, volemitol, in *Polyanthus*. Discovery of a novel ketose reductase. *Plant Physiol* **119**, 191-197.
- Inoue, H., Nojima, H. and Okayama, H. (1990) High efficiency transformation of *Escherichia coli* with plasmids. *Gene* **96**, 23-28.
- Jefferson, R. A. B., S.M. Hirsh, D. (1986) β -glucuronidase from *Escherichia coli* as a gene-fusion marker. *Proc Natl Acad Sci USA* **83**, 8447-8451.
- Jensen, S. R. (1991) Plant iridoids, their biosynthesis and distribution in angiosperms. In *Ecological Chemistry and Biochemistry of Plant Terpenoids*, (eds. J. B. Harborne and F. A. Tomas-Barbaran), pp. 133-158, Clarendon Press, Oxford.
- Johansson, I., Karlsson, M., Johanson, U., Larsson, C. and Kjellbom, P. (2000) The role of aquaporins in cellular and whole plant water balance. *Biochim Biophys Acta* **1465**, 324-342.
- Kaiser, G. and Heber, U. (1984) Sucrose transport into vacuoles isolated from barley mesophyll protoplasts. *Planta* **161**, 562-568.
- Kehr, J., Wagner, U., Willmitzer, L. and Fisahn, J. (1999) Effect of modified carbon allocation on turgor, osmolality, sugar and potassium content, and membrane potential in the epidermis of transgenic potato (*Solanum tuberosum* L.) plants. *J Exp Bot* **50**, 565-571.
- Keller, F. and Pharr, D. M. (1996) Metabolism of Carbohydrates in Sinks and Sources: Galactosyl-Sucrose Oligosaccharides. In *Photoassimilate Distribution in Plants and Crops: Source-Sink Relationships*, (eds. E. Zamski and A. A. Schaffer), pp. 157-183, Marcel Dekker, Inc., New York-Basel-Hong Kong.

- King, R. W. and Zeevaart, J. A. D. (1974) Enhancement of phloem exudation from cut petioles by chelating agents. *Plant Physiol* **53**, 96-103.
- Knop, C. (1998) Untersuchungen zum Zucker- und Aminosäuretransport bei der symplastischen Phloembeladung, Diplomarbeit, Math. Nat. Fakultät, Universität Göttingen, Göttingen.
- Knop, C. (2001) Zur Bedeutung von Saccharose-Transportern in Pflanzen mit offener Phloemanatomie, Universität Göttingen, Dissertation.
- Knop, C., Voitsekhovskaja, O. and Lohaus, G. (2001) Sucrose transporters in two members of the Scrophulariaceae with different types of transport sugar. *Planta* **213**, 80-91.
- Koncz, C. and Schell, J. (1985) The promoter of the TL-DNA gene 5 controls the tissue specific expression of chimeric genes carried by a novel type of *Agrobacterium* binary vector. *Mol Gen Genet* **204**, 383-396.
- Koroleva, O. A., Farrar, J. F., Tomos, A. D. and Pollock, C. J. (1997) Patterns of solute in individual mesophyll, bundle sheath and epidermal cells of barley leaves induced to accumulate carbohydrate. *New Phytol* **136**, 97-104.
- Koroleva, O. A., Farrar, J. F., Tomos, A. D. and Pollock, C. J. (1998) Carbohydrates in individual cells of epidermis, mesophyll, and bundle sheath in barley leaves with changed export or photosynthetic rate. *Plant Physiol* **118**, 1525-1532.
- Kozak, M. (1996) Interpreting cDNA sequences: some insights from studies on translation. *Mammalian Genome* **7**, 536-574.
- Kragler, F., Monzer, J., Xoconostle-Cázares, B. and Lucas, W. J. (2000) Peptide antagonists of the plasmodesmal macromolecular trafficking pathway. *EMBO J* **19**, 2856-2868.
- Krapp, A. and Stitt, M. (1995) An evaluation of direct and indirect mechanisms for the "sink-regulation" of photosynthesis in spinach: changes in gas exchange, carbohydrates, metabolites enzyme activities and steady-state transcript levels after cold-girdling source leaves. *Planta* **195**, 313-323.
- Kursanov, A. L. (1984) Assimilate transport in plants, Elsevier, Amsterdam.
- Kwak, S. H. and Lee, S. H. (2001) The regulation of ornithine decarboxylase gene expression by sucrose and small upstream open reading frame in tomato (*Lycopersicon esculentum* Mill). *Plant Cell Physiol* **42**, 314-323.
- Laemmli, U. K. (1970) Cleavage of structural proteins during the assembly of the head of bacteriophage T4. *Nature* **227**, 680-685.
- Leidreiter, K., Kruse, A., Heineke, D., Robinson, D. G. and Heldt, H. W. (1995) Subcellular volumes and metabolite concentrations in potato (*Solanum tuberosum* cv. Désirée) leaves. *Bot Acta* **108**, 439-444.
- Lemoine, R. (2000) Sucrose transporters in plants: update on function and structure. *Biochim Biophys Acta* **1465**, 246-262.
- Lemoine, R., Kühn, C., Thiele, N., Delrot, S. and Frommer, W. B. (1996) Antisense inhibition of the sucrose transporter in potato: effects on amount and activity. *Plant Cell Environ* **19**, 1124-1131.
- Li, Z. S., Noubhani, A. M., Bourbonloux, A. and Delrot, S. (1994) Affinity preparation of sucrose binding proteins from the plasma membrane. *Biochem Biophys Acta* **1219**, 389-397.

- Logemann, J., Schell, J. and Willmitzer, L. (1987) Improved method for the isolation of RNA from plant tissues. *Anal Biochem* **163**, 16-20.
- Lohaus, G., Burba, M. and Heldt, H. W. (1994) Comparison of the contents of sucrose and amino acids in leaves, phloem sap and taproots of high and low sugar-producing hybrids of sugar beet (*Beta vulgaris* L.). *J Exp Bot* **45**, 1097-1101.
- Lohaus, G., Büker, M., Hußmann, M., Soave, C. and Heldt, H. W. (1998) Transport of amino acids with special emphasis on the synthesis and transport of asparagine in the Illinois Low Protein and Illinois High Protein strains of maize. *Planta* **205**, 181-188.
- Lohaus, G. and Fischer, K. (2001, in press) Intracellular and intercellular transport of nitrogen and carbon In: *Advances in Photosynthesis: Photosynthetic nitrogen assimilation and associated carbon metabolism*, (eds. C. H. Foyer and G. Noctor), Chapter 11 Kluwer Acad Publishers, Dordrecht.
- Lohaus, G., Pennewiss, K., Sattelmacher, B., Hussmann, M. and Muehling, K. H. (2001) Is the infiltration technique appropriate for the isolation of apoplastic fluid? A critical evaluation with different plant species. *Physiol Plant* **111**, 457-465.
- Lohaus, G., Winter, H., Riens, B. and Heldt, H. W. (1995) Further studies of the phloem loading process in leaves of barley and spinach. The comparison of metabolite concentrations in the apoplastic compartment with those in the cytosolic compartment and in the sieve tubes. *Bot Acta* **108**, 270-275.
- Loreti, E., Alpi, A. and Perata, P. (2000) Glucose and disaccharide-sensing mechanisms modulate the expression of α -amylase in barley embryos. *Plant Physiol* **123**, 939-948.
- Lowry, O. H., Rosebrough, N. J., Farr, A. L. and Randall, R. J. (1951) 1951 Protein measurement with the Folin phenol reagent. *J Biol Chem* **193**, 265-275.
- Luttge, U. and Higinbotham, N. (1979) *Transport in plants*, Springer Verlag, New York.
- Madore, M. A. (1990) Carbohydrate metabolism in photosynthetic and nonphotosynthetic tissues of variegated leaves of *Coleus blumei* Benth. *Plant Physiol* **93**, 617-622.
- Madore, M. A. and Webb, J. A. (1981) 1981 Leaf free space analysis and vein loading in *Cucurbita pepo*. *Can J Bot* **59**, 2550-2557.
- Malone, M., Leigh, R. A. and Tomos, A. D. (1989) Extraction and analysis of sap from individual wheat leaf cells: the effect of sampling speed on the osmotic pressure of the extracted sap. *Plant Cell Environ* **12**, 919-926.
- Meyer, S., Meltzer, M., Truernit, E., Hümmer, C., Besenbeck, R., Stadler, R. and Sauer, N. (2000) *AtSUC3*, a gene encoding a new *Arabidopsis* sucrose transporter, is expressed in cells adjacent to the vascular tissues and in a carpel cell layer. *Plant J* **24**, 869-882.
- Mitchell, D. E., Gadus, M. V. and Madore, M. A. (1992) Patterns of assimilate production and translocation in muskmelon (*Cucumis melo* L.). *Plant Physiol* **99**, 959-965.
- Moing, A., Carbonne, F., Zipperlin, B., Svanella, L. and Gaudillère, J.-P. (1997) Phloem loading in peach: symplastic or apoplastic? *Physiol Plant* **101**, 489-496.
- Moore, B. D., Palmquist, D. E. and Seemann, J. R. (1997) Influence of plant growth at high CO₂ concentrations on leaf content of ribulose-1,5-biphosphate carboxylase/oxygenase and intracellular distribution of soluble carbohydrates in tobacco, snapdragon, and parsley. *Plant Physiol* **115**, 241-248.
- Murashige, T. and Skoog, F. (1962) A revised medium for rapid growth and bioassays with tobacco tissue culture. *Physiol Plant* **15**, 473-497.

- M'Batchi, B. and Delrot, S. (1988) Stimulation of sugar exit from leaf tissues of *Vicia faba*. *Planta* **174**, 340-348.
- Münch, E. (1930) Die Stoffwechselbewegungen in der Pflanze, Fischer Verlag, Jena.
- Nelson, D. E., Koukoumanos, M. and Bohnert, H. J. (1999) Myo-inositol-dependent sodium uptake in ice plant. *Plant Physiol* **119**, 165-172.
- Newman, J. D. and Chappell, J. (1999) Isoprenoid biosynthesis in plants: carbon partitioning within cytoplasmic pathway. *Crit Rev Biochem Mol Biol* **34**, 95-106.
- Noiraud, N., Maurousset, L. and Lemoine, R. (2001) Identification of a mannitol transporter, AgMaT1, in celery phloem. *Plant Cell* **13**, 695-705.
- Ntsika, G. and Delrot, S. (1986) Changes in apoplastic and intracellular leaf sugars induced by the blocking of export in *Vicia faba*. *Physiol Plant* **68**, 145-153.
- Ohshima, T., Hayashi, H. and Chino, M. (1990) Collection and chemical composition of pure phloem sap from *Zea mays* L. *Plant Cell Physiol* **31**, 695-705.
- Paris, N., Stanley, C. M., Jones, R. L. and Rogers, J. C. (1996) Plant cells contain two functionally distinct vacuolar compartments. *Cell* **85**, 563-572.
- Pate, J. S. and Gunning, B. E. S. (1969) Vascular transfer cells in angiosperm leaves. A taxonomic and morphological survey. *Protoplasma* **68**, 135-156.
- Peterbauer, T., Mucha, J., Mayer, U., Popp, M., Glössl, J. and Richter, A. (1999) Stachyose synthesis in seeds of adzuki bean (*Vigna angularis*): molecular cloning and functional expression of stachyose synthase. *Plant J* **20**, 509-518.
- Peterbauer, T. and Richter, A. (2001) Biochemistry and physiology of raffinose family oligosaccharides and galactosyl cyclitols in seeds. *Seed Science Research* **11**, 185-197.
- Pharr, D. M., Hendrix, J. E., Robbins, N. S., Gross, K. C. and Sox, H. N. (1987) Isolation of galactinol from leaves of *Cucumis sativus*. *Plant Science* **50**, 21-26.
- Pharr, D. M., Sox, H. N., Locy, R. D. and Huber, S. C. (1981) Partial characterization of the galactinol forming enzyme from leaves of *Cucumis sativus* L. *Plant Sci Lett* **23**, 25-33.
- Raney, A., Baron, A. C., Mize, G. J., Law, G. L. and Morris, D. R. (2000) In vitro translation of the upstream open reading frame in the mammalian mRNA encoding S-Adenosylmethionine decarboxylase. *J Biol Chem* **275**, 24444-24450.
- Riens, B., Lohaus, G., Heineke, D. and Heldt, H. W. (1991) Amino acid and sucrose content determined in the cytosolic, chloroplastic, and vacuolar compartments and in the phloem sap of spinach leaves. *Plant Physiol* **97**, 227-233.
- Riesmeier, J. W., Willmitzer, L. and Frommer, W. B. (1994) Evidence for an essential role of the sucrose transporter in phloem loading and assimilate partitioning. *EMBO J* **13**, 1-7.
- Robards, A. W. and Lucas, W. J. (1990) Plasmodesmata. *Annu Rev Plant Physiol Plant Mol Biol* **41**, 369-419.
- Rosenberg, A. H., Lade, B. N., Chui, D. S., Lin, S.-W., Dunn, J. J. and Studier, F. W. (1986) Vectors for selective expression of cloned DNAs by T7 RNA polymerase. *Gene* **56**, 125-135.
- Sambrook, J., Fritsch, E. F. and Maniatis, T. (1989) Molecular cloning: A laboratory manual, Cold Spring Harbor, New York.
- Sanger, F., Nickler, S. and Coulson, A. R. (1977) DNA sequencing with chain-terminating inhibitors. *Proc Natl Acad Sci USA* **74**, 5463-5467.

- Schmitz, K., Cuypers, B. and Moll, M. (1987) Pathway of assimilate transfer between mesophyll cells and minor veins in leaves of *Cucumis melo* L. *Planta* **171**, 19-29.
- Schulz, A. (1997) Phloem. Structure related to function. In *Progress in Botany, Vol. 59*, pp. 429-475, Springer-Verlag, Berlin, Heidelberg, New York.
- Schulz, A., Kühn, C., Riesmeier, J. W. and Frommer, W. B. (1998) Ultrastructural effects in potato leaves due to antisense-inhibition of the sucrose transporter indicate an apoplasmic mode of phloem loading. *Planta* **206**, 533-543.
- Senser, M. and Kandler, O. (1967) Vorkommen und Verbreitung von Galactinol in Blättern Höherer Pflanzen. *Phytochemistry* **7**, 1533-1540.
- Shalitin, D. and Wolf, S. (2000) Cucumber mosaic virus infection affects sugar transport in melon plants. *Plant Physiol* **123**.
- Singh, R. (1993) Photosynthesis characteristics of fruiting structures of cultivated crops. In *Photosynthesis: Photoreactions to Plant Productivity*, (eds. Y. P. Abrol, P. Mohanty and E. E. Govindi), pp. 390-415, Kluwer Academic Publishers, Dordrecht.
- Southern, E. M. (1975) Detection of specific sequences among DNA fragments separated by gel electrophoresis. *J Mol Biol* **98**, 479-483.
- Speer, M. and Kaiser, W. M. (1991) Ion relations of symplastic and apoplasmic space in leaves from *Spinacea oleracea* L. and *Pisum sativum* L. under salinity. *Plant Physiol* **97**, 990-997.
- Sprenger, N. and Keller, F. (2000) Allocation of raffinose family oligosaccharides to transport and storage pools in *Ajuga reptans*: the roles of two distinct galactinol synthases. *Plant J* **21**, 249-258.
- Stadler, R., Brandner, J., Schulz, A., Gahrtz, C. and Sauer, N. (1995) Phloem loading by the *PmSUC2* sucrose carrier from *Plantago major* occurs into companion cells. *The Plant Cell* **7**, 1545-1554.
- Stitt, M., Bulpin, T. and Rees, T. (1978) Pathways of starch breakdown in photosynthetic tissues of *Pisum sativum*. *Biochem Biophys Acta* **544**, 200-214.
- Stoop, J. M. N., Williamson, J. D. and Pharr, D. M. (1996) Mannitol metabolism in plants: a method for coping with stress. *Trend Plant Sci* **1**, 139-144.
- Strauß, M., Kauder, F., Peisker, M., Sonnewald, U., Conrad, U. and Heineke, D. (2001) Expression of an abscisic acid-binding single chain antibody influences the subcellular distribution of abscisic acid and leads to developmental changes in transgenic potato plants. *Planta* **213**, 361-369.
- Studier, F. W. and Moffatt, B. A. (1985) Use of bacteriophage T7 RNA polymerase to direct selective high-level expression of cloned genes. *J Mol Biol* **189**, 113-130.
- Sze, H., Li, X. and Palmgren, M. G. (1999) Energization of plant cell membranes by H⁺-pumping ATPases: regulation and biosynthesis. *Plant cell* **11**, 677-689.
- Tomos, A. D., Hinde, P., Richardson, P., Pritchard, J. and Fricke, W. (1994) Microsampling and measurement of solutes in single cells. In *Plant Cell Biology - a Practical Approach*, (eds. N. Harris and K. J. Oparika), pp. 297-314, IRL Press, Oxford UK.
- Turgeon, R. (1991) Symplastic phloem loading and the sink-source transition in leaves: a model. In *Recent Advances in Phloem Transport and Assimilate Partitioning*, (eds. J. L. Bonnemain, S. Delrot and W. J. Lucas), Ouest Edition, Nantes.

- Turgeon, R., Beebe, D. U. and Gowan, E. (1993) The intermediary cell: minor-vein anatomy and raffinose oligosaccharide synthesis in the Scrophulariaceae. *Planta* **191**, 446-456.
- Turgeon, R. and Gowan, E. (1990) Phloem loading in *Coleus blumei* in the absence of carrier-mediated uptake. *Plant Physiol* **94**, 1244-1249.
- Turgeon, R. and Gowan, E. (1992) Sugar synthesis and phloem loading in *Coleus blumei* leaves. *Planta* **187**, 388-394.
- Turgeon, R. and Webb, J. A. (1973) Leaf development and phloem transport in *Cucurbita pepo*: transition from import to export. *Planta* **113**, 179-191.
- Turgeon, R. and Webb, J. A. (1975) Leaf development and phloem transport in *Cucurbita pepo*: carbon economy. *Planta* **123**, 53-62.
- Turgeon, R. and Wimmers, L. E. (1988) Different patterns of vein loading of exogenous [^{14}C]sucrose in leaves of *Pisum sativum* and *Coleus blumei*. *Plant Physiol* **87**, 179-182.
- van Bel, A. J. E., Hendriks, J. H. M., Boon, E. J. M. C., Gamalei, Y. V. and van de Merwe, A. P. (1996) Different ratios of sucrose/raffinose-induced membrane depolarizations in the mesophyll of species with symplastic (*Catharanthus roseus*, *Ocimum basilicum*) or apoplastic (*Impatiens walleriana*, *Vicia faba*) minor-vein configurations. *Planta* **199**, 185-192.
- Vaquero, C., Turner, A. P., Demangeat, G., Sanz, A., Serra, M. T., Roberts, K. and Garcia-Luque, I. (1994) The 3a protein from cucumber mosaic virus increases the gating capacity of plasmodesmata in transgenic tobacco plants. *J Gen Virol* **75**, 3193-3197.
- Vemmos, S. N. and Glodwin, G. K. (1994) The photosynthetic activity of Cox's orange pippin apple flowers in relation to fruit setting. *Ann Bot* **73**, 385-391.
- Voitsekhovskaja, O., Heber, U., Wiese, C., Lohaus, G., Heldt, H. W. and Gamalei, Y. V. (2002, in press) Energized uptake of sugars from the apoplast of leaves: a study of some plants possessing different minor vein anatomy. *Russ J Plant Physiol* **49**.
- Voitsekhovskaja, O. V., Pakhomova, M. V., Syutkina, A. V., Gamalei, Y. V. and Heber, U. (2000) Compartmentation of assimilate fluxes in leaves. II. Apoplastic sugar levels in leaves of plants with different companion cell types. *Plant Biol* **2**, 107-112.
- Waigmann, E., Lucas, W. J., Citovsky, V. and Zambryski, P. C. (1994) Direct functional assay for tobacco mosaic virus cell-to-cell movement protein and identification of a domain involved in increasing plasmodesmal permeability. *Proc Natl Acad Sci USA* **91**, 1433-1437.
- Webb, J. A. and Gorham, P. R. (1965) The effect of node temperature on assimilation and translocation of ^{14}C in squash. *Can J Bot* **43**, 1009-1017.
- White, M. D., Kuhn, J. and Ward, S. (1980) Permeability of lactating-rat mammary gland Golgi membranes to monosaccharides. *Biochem J* **190**, 621-624.
- Winter, H. (1993) Untersuchung zur Akkumulation und Translokation von Assimilaten: Subzelluläre Volumina und Metabolitkonzentrationen in Blättern von Gerste und Spinat, pp. 144, Georg-August-Universität, Göttingen.
- Winter, H., Robinson, D. G. and Heldt, H. W. (1993) Subcellular volumes and metabolite concentrations in barley leaves. *Planta* **191**, 180-190.
- Winter, H., Robinson, D. G. and Heldt, H. W. (1994) Subcellular concentrations and metabolite concentrations in spinach leaves. *Planta* **193**, 530-535.

- Winzer, T., Lohaus, G. and Heldt, H. W. (1996) Influence of phloem transport, N-fertilization and ion accumulation on sucrose storage in the taproots of fodder beet and sugar beet. *J Exp Bot* **47**, 863-870.
- Wirtz, W., Stitt, M. and Heldt, H. W. (1980) Enzymatic determination of metabolites in the subcellular compartments of spinach chloroplasts. *Plant Physiol* **106**, 661-671.
- Wolf, S. and Lucas, W. J. (1994) Virus movement proteins and other molecular probes of plasmodesmal function. *Plant Cell Environ* **17**, 573-585.
- Woodcock, D. M., Crowther, P. J., Doherty, J., Jefferson, S., Decruz, E., Noyer Weidner, M., Smith, S. S., Michael, M. Z. and Graham, M. W. (1989) Quantitative evaluation of *Escherichia coli* host stains for tolerance to cytosine methylation in the plasmid and phage recombinants. *Nucl Acids Res* **17**, 3469-3478.
- Wyn Jones, R. G. and Gorham, J. (1983) Osmoregulation. *Encyclopedia of Plant Physiology*. 12C Physiological Plant Ecology, pp. 35-98, Springer Verlag, Berlin.
- Xoconostle-Cázares, B., Ruiz-Medrano, R. and Lucas, W. J. (2000) Proteolytic processing of CmPP36, a protein from the cytochrome b₅ reductase family, is required for entry into the phloem translocation pathway. *Plant J* **24**, 735-747.
- Yamamoto, Y. T., Zamski, E., Williamson, J. D., Conkling, M. A. and Pharr, D. M. (1997) Subcellular localization of celery mannitol dehydrogenase. *Plant Physiol* **115**, 1397-1403.
- Ye-The, L. I. (1967) Studies on the glycosidase in Jack bean meal. I. Isolation and properties of α -mannosidase. *J Biol Chem* **242**, 5474-5480.
- Yin, Z.-H., Neimanis, S., Wagner, U. and Heber, U. (1990) Light-dependent pH changes in leaves of C₃ plants. *Planta* **182**, 244-252.
- Zhang, W. H. and Tyerman, S. D. (1997) Effect of low oxygen concentration on the electrical properties of cortical cells of wheat roots. *Plant Physiol* **150**, 567-572.
- Zimmermann, M. H. and Ziegler, H. (1975) Transport in plants. I. - Phloem transport. Appendix III: list of sugars and sugar alcohols in sieve-tube exudates. In *Encyclopedia of Plant Physiology - new series, Vol. 1*, (eds. M. H. Zimmermann and J. A. Milburn), pp. 480-503, Springer-Verlag, Berlin, Heidelberg, New York.

VIELEN DANK AN...

Herrn Prof. Hans-Walter Heldt für die mir gewährte Möglichkeit, zuerst als DAAD-Stipendiatin und dann als Doktorandin an der von ihm geleiteten Abteilung diese Doktorarbeit durchzuführen, sowie für jede Unterstützung und Interesse seinerseits;

Frau PD Dr. Gertrud Lohaus für die Möglichkeit, in ihrer Arbeitsgruppe am Thema Phloemtransport zu arbeiten, für ihre Unterstützung bei allen wissenschaftlichen und bürokratischen Problemen und für ihr Verständnis, die das Gelingen dieser Arbeit ermöglichten;

Herrn Prof. Yuri Gamalei für die Anregung, biochemische Untersuchungen im Zusammenhang mit der Struktur der pflanzlichen Zellen zu setzen, für sein Interesse am Verlauf und sein Glauben an den Erfolg dieser Arbeit sowie häufige Diskussionen zu Fragen des Phloemtransports.

Mein besonderer Dank gilt Frau Dr. Katharina Pawlowski für ihre Anregung, meine Arbeit auf der Stachyose-Synthese zu fokussieren, und für die Einführung in die faszinierende Welt der Molekularbiologie; für ihr ständiges Interesse an meinen Fortschritten; unsere Diskussionen und permanenten Austausch der Meinungen, die als „tägliches Brot“ für meine Ausbildung als Doktorandin dienten; und für das rechtzeitig erledigte Lesen und die Korrektur dieser Arbeit.

Herrn Prof. Em. Dr. Ulrich Heber (Universität Würzburg) danke ich besonders herzlich für die Möglichkeit, Versuche zum Thema Apoplast in seinem Labor durchzuführen und mehr über die Pflanzenphysiologie zu lernen, für sein Interesse an meiner Arbeit und die einfach unvergeßliche Atmosphäre brisanter Diskussionen in einer internationalen wissenschaftlichen Umgebung.

I would like to thank Dr. Olga Koroleva (University of Wales, Bangor) for her generous hospitality in Wales, for the introduction to the Single Cell Sampling and Analysis Technique and for the experiments we did together.

Dr. Thomas Peterbauer (Universität Wien) danke ich für die freundlicherweise gewährte Möglichkeit, die GC-MS Analyse meiner Versuchspflanzen durchzuführen.

Dr. Marina Pakhomova (Botanisches Institut, Sankt-Petersburg) bin ich sehr verbunden für die Einführung in die Elektronmikroskopie und die Erklärung von Hunderten von Photos, die mir eine Vorstellung über die Vielfalt der Zellstruktur von Pflanzen vermittelt haben.

Dr. Kirill Demchenko danke ich für die exzellente fachliche Einführung in die Einbettung von Pflanzenmaterial für Lichtmikroskopie und für seine großzügige und unersetzliche Hilfe bei allen Computerproblemen inklusive des Ausdrucks dieser Arbeit.

Jens Tilsner bin ich dankbar für sein außerordentlich sorgfältiges Lesen und die Korrektur dieser Arbeit und für seinen nie vergessenen "Guten Morgen"-Gruß bei meiner etwas verspäteten Ankunft im Labor nach produktiver Nachtarbeit (trotz unserer deutlichen Meinungsunterschiede zum oft angesprochenen Thema „Kompatibilität von Rockmusik und Arbeitsproduktivität im Labor“).

Dr. Sigrun Reumann danke ich für die bereitwillige Korrektur meiner Arbeit und ihre Hilfsbereitschaft bei allen Problemen im Labor.

Dr. Christian Knop danke ich für die Daten zum Phloemsaft von *Asarina* und *Alonsoa* und für die Bereitschaft, alle sporadischen Fragen zum Thema meiner Doktorarbeit sachkundig und ausführlich zu beantworten.

Marion Taube danke ich für ihre liebevolle Hilfe bei den Kältегürtel-Versuchen.

Allen Kollegen aus Göttingen, Esteban Antonicelli, Lavanya Babujee, Dr. Mareike Böddeker, Anne Brandeck, Dr. Dieter Heineke, Dr. K.-P. Heise, Melanie Hußmann, Gerd Mader, Andrea Nickel, Dr. Anke Sirrenberg, Maria Schubert, Anita Stottmeister, Michaela Strauß, Dr. Thilo Winzer und Dr. Zewen Zhou danke ich für jegliche Hilfestellung und jedes gutes Wort und vor allem für die einmalige und unvergeßliche warme, herzliche Atmosphäre in der Abteilung, die ich immer vermissen werde...

Herrn Wedemeyer, unseren Gärtner, danke ich für seine besonders freundliche und nette Art und für seine liebevolle Fürsorge um meine Pflanzen.

Dr. Meike Lorenz bin ich dankbar für ihre Hilfe bei der Handhabung der digitalen Kamera ihrer Abteilung.

Der Abteilung von Frau Prof. Dr. Christiane Gatz danke ich für die mir für diese Doktorarbeit freundlicherweise zur Verfügung gestellten Materialien und Geräte. Mein besonderer Dank gilt Wolfram Brenner für seine Hilfe im Umgang mit Arabidopsis und Dr. Corinna Thurow für ihre Unterstützung bei der Handhabung von pET3b.

Jan Nadwodnik danke ich für die gemeinsam überlebte Galaktinol-Isolierung während des Großpraktikums II.

Allen meinen Kollegen aus St.-Peterburg, die mich in Erinnerung behalten haben, danke ich für ihre Briefe, Emails und für ihre Unterstützung aus der Ferne.

Meiner Freundin Anna Boulankina bin ich dankbar für die nächtelangen Diskussionen über mysteriöse Aspekte von *Protein Sorting* und die Regulation der *AmSTS* Expression. Meiner Freundin Irina Bulanowa danke ich für ihre ausgezeichneten Übersetzungen mehrerer Dokumente (Russisch-Englisch-Deutsch in allen Richtungen). Meiner Freundin Ekaterina Vorobieva danke ich für ihre liebevolle Unterstützung in allen Dingen. Den anderen Mitglieder der „friedlichen russischen Mafia“ danke für ihre treue Hilfsbereitschaft.

Meinen Eltern danke ich für ihr Warten, ihren Glauben, ihre Verständnis und all ihre Hilfe.

LEBENS LAUF

- 18.05.1973 geboren in St. Petersburg (Leningrad), Rußland.
Staatsangehörigkeit: russisch
- 1980-1990 Besuch der Allgemeinen Mittelschule in St. Petersburg
- Juli 1990 Schulabschluß: Abitur
- 1990-1995 Studium an der Staatlichen Universität St. Petersburg,
Fakultät für Biologie und Bodenkunde
- 1994-1995 Diplomarbeit über „Untersuchungen zur Beziehung zwischen
Photosynthese und Dunkelatmung in C₃-Pflanzen mit
unterschiedlichen Vegetationsrhythmen“ unter Anleitung von
Dr. N. S. Mamuschina
- Juli 1995 Studiumsabschluß: Diplom mit Auszeichnung
- August 1995 –
August 1998 Wissenschaftliche Mitarbeiterin am Botanischen Institut der
Russischen Akademie der Wissenschaften, St. Petersburg, unter
Leitung von Prof. Dr. Y. V. Gamalei
- August 1998 –
September 1998 Deutschkurs am Goethe-Institut Göttingen
- Oktober 1998 –
März 2000 DAAD-Stipendiatin an der Abteilung für Biochemie der Pflanze
des Albrecht-von-Haller-Instituts für Pflanzenwissenschaften
der Universität zu Göttingen, Projekt: „Phloemtransport und
Assimilatverteilung in source-Blättern“
- Seit April 2000 Doktorandin an der Abteilung für Biochemie der Pflanze des
Albrecht-von-Haller-Instituts für Pflanzenwissenschaften der
Universität zu Göttingen,
unter der Anleitung von Prof. Dr. H.-W. Heldt